

# Dissertation

submitted to the  
Combined Faculties for the Natural Sciences and Mathematics  
of the Ruperto-Carola University of Heidelberg, Germany  
for the degree of  
Doctor of Natural Sciences

Put forward by:

**Martin Holthausen**

born in: Stuttgart-Bad Cannstatt  
Oral Examination: December 21th 2012



# **Towards Testable Theories with Discrete Flavour Symmetries**

Referees:

Prof. Dr. Manfred Lindner  
Prof. Dr. Tilman Plehn



## Abstract

The leptonic mixing matrix may be understood as a consequence of remnant symmetries of the mass matrices, which emerge from the spontaneous breakdown of a larger symmetry into smaller non-commuting subgroups. The mixing patterns that may be obtained from groups of order smaller than 1556 are presented. To dynamically realize this symmetry breaking pattern an additional mechanism is needed. Here a minimal solution to this problem is provided, based on non-trivial extensions of the flavour group. A scan over possible extensions of popular flavour groups is presented and the smallest semidirect product extension of the group  $A_4$  is discussed. A model based on this symmetry group is constructed and it is shown to naturally give the required vacuum structure. Modifications that can account for the deviation from the predicted value for the mixing angle  $\theta_{13}$  are presented. The vacuum alignment mechanism is applied in a model at the electroweak scale, which contains a dark matter candidate, and its phenomenology is studied. Consistency conditions for CP transformations in the context of discrete flavour groups are developed and they are shown to have non-trivial implications for existing models. Finally, we give an outlook about how the Standard Model may be viewed from a Planck scale perspective.

## Zusammenfassung

Die leptonische Mischungsmatrix kann als Resultat übrigbleibender Symmetrien der Massenmatrizen verstanden werden, die aus der spontanen Brechung einer größeren Symmetriegruppe in kleinere nicht-vertauschende Untergruppen hervorgehen. Die Mischungsmatrizen, die auf diese Weise aus Gruppen mit Ordnung kleiner als 1556 folgen, werden präsentiert. Um diese Art der Symmetriebrechung dynamisch zu realisieren ist ein zusätzlicher Mechanismus von Nöten. Hier wird eine minimale Lösung dieses Problems präsentiert, basierend auf nicht-trivialen Erweiterungen der Flavourgruppe. Eine systematische Suche nach solch möglichen Erweiterungen wird präsentiert und die kleinste Erweiterung der Gruppe  $A_4$ , die sich als semidirektes Produkt schreiben lässt, wird diskutiert. Ein Model basierend auf dieser Symmetriegruppe wird konstruiert und es wird gezeigt, dass es die Vakuumstruktur natürlich realisiert. Modifikationen werden präsentiert, die die beobachtete Abweichung vom vorhergesagten Wert für den Mischungswinkel  $\theta_{13}$  erklären können. Dieser Mechanismus wird in einem Model an der elektroschwachen Skala angewandt, das einen Kandidaten für Dunkle Materie enthält, und dessen Phänomenologie wird studiert. Konsistenzbedingungen für CP Transformationen im Kontext diskreter Flavoursymmetrien werden entwickelt und es wird gezeigt, dass diese nicht-triviale Implikationen für existierende Modelle liefern. Abschließend geben wir einen Ausblick, und diskutieren wie das Standardmodell aus der Perspektive der Physik an der Planck-Skala verstanden werden kann.



# Contents

<b>1. Introduction and Overview</b>	<b>9</b>
<b>2. Discrete Symmetry Groups and Lepton Mixing</b>	<b>13</b>
2.1. Flavour in the Standard Model . . . . .	13
2.1.1. Theoretical Background . . . . .	13
2.1.2. Experimental Situation . . . . .	15
2.2. Leptonic Mixing from Remnant Symmetries . . . . .	17
2.3. Some Properties of Non-Abelian Discrete Symmetries . . . . .	20
2.3.1. Building the Flavour Group . . . . .	20
2.3.2. On the Origin of Discrete Flavour Symmetries . . . . .	24
2.4. Prototype Model for Tri-Bimaximal Mixing . . . . .	25
2.5. Model Building Pathways Beyond Vanishing $\theta_{13}$ . . . . .	27
2.5.1. New Starting Points . . . . .	28
2.5.2. Deviations from Tri-Bi-Maximal Mixing . . . . .	29
<b>3. The Vacuum Alignment Problem in Flavour Models</b>	<b>33</b>
3.1. The Vacuum Alignment Problem and Solutions in the Literature . . . . .	33
3.1.1. Supersymmetric Models with R-Symmetries . . . . .	37
3.1.2. Extra-Dimensional Models . . . . .	40
3.2. Group Extensions and Vacuum Alignment . . . . .	40
3.2.1. Generalities about the Vacuum Alignment Problem . . . . .	40
3.2.2. Semidirect Product Groups . . . . .	42
3.2.3. General Group Extensions . . . . .	44
3.3. Some Small Candidate Groups . . . . .	46
3.3.1. The Smallest Group $Q_8 \rtimes A_4$ . . . . .	46
3.3.2. Other Small Groups . . . . .	47
<b>4. A Concrete Model based on <math>Q_8 \rtimes A_4</math></b>	<b>49</b>
4.1. Introduction . . . . .	49
4.2. Lepton Masses . . . . .	50
4.3. Vacuum Alignment . . . . .	52
4.4. Deviations from TBM . . . . .	56
4.4.1. Higher Order Corrections . . . . .	56
4.4.2. Trimaximal Mixing . . . . .	60
4.4.3. Cosmological Implications of Accidental Symmetries . . . . .	61
4.5. Seesaw UV Completion . . . . .	62
4.6. Supersymmetrisation . . . . .	63
<b>5. Flavour Symmetry Breaking at the Electroweak Scale</b>	<b>65</b>
5.1. Model and Symmetry Breaking . . . . .	66

## Contents

5.2. Lepton Flavour Structure . . . . .	67
5.3. Lepton Flavour Violation . . . . .	74
5.4. Dark Matter . . . . .	79
5.4.1. Dark Matter Candidates and their Stability . . . . .	79
5.4.2. Dark Matter Phenomenology . . . . .	82
5.5. Extension to Quark Sector . . . . .	84
5.6. Collider Phenomenology . . . . .	87
5.7. Summary & Conclusions . . . . .	91
<b>6. CP and Discrete Flavour Symmetries</b>	<b>93</b>
6.1. Introduction . . . . .	93
6.2. Generalized CP Transformations . . . . .	95
6.2.1. CP and the Outer Automorphism Group . . . . .	95
6.2.2. Physical Implications of a Generalized CP Symmetry . . . . .	98
6.3. Applications to Questions in the Literature . . . . .	99
6.4. Summary & Conclusions . . . . .	109
<b>7. Outlook: Naturalness &amp; Big Desert Scenarios</b>	<b>111</b>
7.1. Naturalness and a Big Desert . . . . .	111
7.2. Planck Scale Boundary Conditions and the Higgs Mass . . . . .	113
7.3. Radiative Symmetry Breaking in the Minimal Left-Right Symmetric Model . . . . .	117
7.3.1. Gildener Weinberg Method in the Minimal LR Symmetric Potential . . . . .	117
7.3.2. Spontaneous Breaking of Parity . . . . .	119
<b>8. Summary and Conclusions</b>	<b>123</b>
<b>A. Group Theoretical Details</b>	<b>127</b>
A.1. Important Series of Subgroups of $SU(3)$ . . . . .	127
A.2. Clebsch-Gordon Coefficients . . . . .	127
A.2.1. $A_4$ . . . . .	127
A.2.2. $Q_8 \rtimes A_4$ . . . . .	128
A.3. CP Definition for Small Groups . . . . .	129
A.4. Vacuum Alignment and Scalar Spectrum of EW Model . . . . .	131
A.4.1. Vacuum alignment . . . . .	131
A.4.2. Scalar Spectrum . . . . .	131
A.5. Discrete — Mathematica Package . . . . .	134
<b>Acknowledgements</b>	<b>135</b>
<b>Bibliography</b>	<b>136</b>



# Chapter 1.

## Introduction and Overview

The Standard Model (SM) of particle physics provides a very successful description of nature down to length scales of  $10^{-18}$  m, which are currently being tested at the Large Hadron Collider (LHC). It is based on the gauge group  $SU(3)_C \times SU(2)_L \times U(1)_Y$ , of which the electroweak part is spontaneously broken by the Higgs mechanism. The recent observation by ATLAS [1] and CMS [2] of a resonance at 126 GeV, which has all the properties one would expect from a SM Higgs particle marks a striking success of the model. However, a number of basic questions are left unanswered by the SM Higgs mechanism.

First, there is the *flavour puzzle*: in the SM, particle masses and mixings are generated through the interaction of the particles with a background Higgs field that permeates all of space. The numerical values of the masses are determined from the coupling strength of this interaction, which may be different for every particle and their measured values are very different indeed: varying from the top quark with Yukawa coupling close to one to the electron, whose coupling is six orders of magnitude smaller. The flavour puzzle will be the topic of the main part of the thesis. The second puzzle will be touched upon only in the last chapter and goes by the name *hierarchy* or *naturalness problem*. Here the question is to understand the SM in the context of a more complete theory in which the SM is thought to be embedded. For example the SM cannot account for the existence of gravity and it is therefore expected that the SM will at the very latest be superseded by a more complete theory at the energy scale where gravitational interactions become strong. The large ratio of this Planck scale of  $M_{Pl} = 1.2 \cdot 10^{19}$  GeV to the electroweak scale of the order of 100 GeV is unnatural from an effective field theory perspective. In Chapter 7 we provide a separate introduction to this issue and we will therefore focus on the flavour problem here, which is the main objective of this work.

Of the twenty-eight parameters in the SM (with Majorana neutrinos), twenty-two are flavour parameters, which parametrize the interactions of fermions with the Higgs field. In this work we will try to address this issue using symmetries. To appreciate why this might be a fruitful approach it is suggestive to entertain the following *gedankenexperiment*. Imagine the SM without its gauge symmetries: this would be a theory of vector bosons, fermions and scalars that interact with each other in all possible ways<sup>1</sup>. Since there is no gauge principle, for example each of the gluons would interact with each of the quarks with a different coupling strength and the model thus has a gargantuan number of free parameters. Imposing gauge symmetry, all of these effective couplings are still there, but they can all be expressed through the three gauge couplings of the SM.

Flavour symmetries may thus be a useful tool to reduce the number of free parameters in the flavour sector and a step towards solving the flavour puzzle. Before discussing how such a symmetry can be concretely implemented, let us also briefly mention another motivation

---

<sup>1</sup>For the sake of argument, we here ignore the fact that such a theory cannot be consistently quantised.

for flavour symmetries that is tied to the naturalness problem of the SM Higgs. To solve this problem within effective field theory, it is generally necessary to introduce new physics at the TeV scale such as supersymmetry, for example. However, bounds from flavour observables such as flavour changing neutral currents (FCNCs) and lepton flavour violating (LFV) decays put severe restrictions on the flavour structure of the new physics model. One possibility to solve this flavour problem is the so-called Minimal Flavour Violation (MFV) paradigm [3, 4] that postulates the SM Yukawa couplings to be the only source of flavour violation.

Now, how can such a flavour symmetry look like? The first difference to the *gedankenexperiment* outlined above is that there is no symmetry apparent in the experimental data. There, if one measured the couplings strength of the various gluons to fermions, it would be hard to miss the symmetry structure. In flavour symmetry models, the fact that we do not see the symmetry directly in the data is accounted for by breaking the symmetry spontaneously. Since all parameters we have measured in the flavour sector are really mass terms, one would not expect to see the symmetry there, in the same way as the  $SU(2)_L$  symmetry is not apparent in the spectrum of quarks and leptons. However, there are some regularities in the flavour parameters that may be indicative of a symmetry: for example the quark and charged lepton mass matrices show a hierarchical structure and mass matrices of the type [5]

$$M_u \sim \begin{pmatrix} \epsilon^8 & \epsilon^6 & \epsilon^4 \\ \epsilon^6 & \epsilon^4 & \epsilon^2 \\ \epsilon^4 & \epsilon^2 & 1 \end{pmatrix}, \quad M_d \sim M_e^T \sim \epsilon^3 \begin{pmatrix} \epsilon^5 & \epsilon^4 & \epsilon^4 \\ \epsilon^3 & \epsilon^2 & \epsilon^2 \\ \epsilon & 1 & 1 \end{pmatrix}, \quad (1.1)$$

where  $\epsilon \approx 0.2 \sim \theta_C$  is of the order of the Cabibbo angle, and each entry should be understood to be multiplied by an order one coupling, capture the essential features of (i) hierarchical mass spectra and (ii) mixing angles that scale with mass ratios. For example the Cabibbo angle may be approximated by

$$\theta_C \approx \sqrt{\frac{m_d}{m_s}},$$

where  $m_d$  and  $m_s$  are the masses of down and strange quarks, respectively. In the neutrino sector the pattern is quite different: the neutrino masses show a much smaller hierarchy,  $(m_1 : m_2 : m_3) \sim (\epsilon^2 : 1 : 1)$  and two of the leptonic mixing angles are large and do not seem to scale with mass hierarchies.

Flavour symmetries can come in many different forms. For example they can be global or local, continuous or discrete, abelian or non-abelian. As an example, consider one of the first flavour symmetries [6] presented by Froggatt and Nielsen in 1979, which can account for the hierarchical mass matrices of Eq. (1.1). They introduced a global  $U(1)$  symmetry under which the various fermion generations transform with different charges. The charge assignments are chosen such that the effective operator that leads to an element of the mass matrix of size  $\epsilon^n$  in Eq. (1.1) has a charge  $-n$  and therefore has to be multiplied by  $(S/\Lambda)^n$ . After symmetry breaking the scalar  $S$  obtains a vacuum expectation value (VEV)  $\langle S \rangle / \Lambda = \epsilon \approx 0.2$ , and the structure (1.1) is realized.

Many different options have been explored in the literature but no overall consensus of a unique symmetry group has emerged. In the quark sector, continuous flavour symmetries such as  $U(2)$  have gained popularity again [7, 8], as an outgrowth of studies of minimal flavour violation.

Here we follow an approach [9–13] that explains the lepton flavour structure – which is quite different from the quark sector – as the result of mismatched remnant symmetries of the

charged lepton and neutrino mass matrices, as will be reviewed in Chapter 2. Such symmetries may arise from the spontaneous breakdown of discrete non-abelian flavour symmetries and have proven to be successful in describing the large mixing angles observed in the lepton sector. To realize this idea in concrete particle physics models, it is necessary to break the discrete flavour symmetry into different subgroups using (at least) two different scalar fields - also known as flavons - that transform under this symmetry. This, however, leads to a non-trivial technical problem known as the *vacuum alignment problem*. The most general scalar potential formed out of two such scalar fields does not admit the required vacuum configuration without fine-tuning couplings in the scalar potential. Such fine-tuning is not acceptable as it generally destroys all predictive power of a model.

In Chapter 3 we first review the solutions that have been put forward in the literature. These solutions usually require the introduction of extra dimensions or continuous R-symmetries within supersymmetry and therefore the flavour symmetry breaking scale has to be unobservably high. This is hardly appealing as the only observable consequences of such models are the predicted lepton mixing angles, many of which have now been ruled out by the recent measurement of  $\theta_{13}$ . The reason why these models solve the vacuum alignment problem can be traced back to the fact that particle content and symmetries of the models have been adjusted such, that there emerges an accidental symmetry in the scalar potential under which both flavons transform independently under the flavour group, which in itself has nothing to do with the scale of symmetry breaking. Using this insight, we present a solution to vacuum alignment problem that realizes this accidental symmetry by a minimal extension of the flavour group. We give general conditions that are necessary for a model to solve the vacuum alignment problem and present the results of a scan over all discrete groups of order smaller than 1000.

In Chapter 4 a concrete model based on the symmetry group  $Q_8 \times A_4$  is presented, which is one of the smallest such extensions of the popular flavour group  $A_4$ . The predictions for lepton masses and mixings are discussed and it is shown that the required vacuum configuration can be naturally obtained, without the need for extra dimensions or supersymmetry. Furthermore, strategies are discussed to bring the model back into agreement with the recently measured and quite large value of  $\theta_{13}$ .

The fact that this mechanism of vacuum alignment does not require a particularly high flavour breaking scale is used in Chapter 5 where we present a model in which the flavour breaking scale is identified with the electroweak scale. Here the SM Higgs is part of a multiplet of scalar fields that also break the flavour symmetry. The role of the flavour symmetry is twofold: first, it restricts the lepton flavour structure such that there are only 5 free real parameters in the neutrino sector, thereby giving a predictive scheme for leptonic mixing that is in good agreement with experiment, and secondly it protects the model from large flavour violating amplitudes that usually plague multi-Higgs models. We discuss the bounds from lepton flavour and collider experiments. As a bonus, there is a dark matter candidate in the model, whose stability and phenomenology we study.

In Chapter 6 we discuss generalized CP transformations in the context of models with discrete flavour symmetries, which has interesting implications in light of the beginning of the era of leptonic CP violation. We show that a naive CP transformation given by complex conjugation is often not consistent with the symmetries of the model. The requirement that a CP transformation should not lead out of the orbit of group transformations leads to non-trivial consistency conditions that have so-far not been fully appreciated in the literature. Using this formalism we can clear up issues surrounding the so-called geometrical CP violation in models based on the flavour groups  $T'$  and  $\Delta(27)$ .

## *Chapter 1. Introduction and Overview*

In Chapter 7 we take a step back and discuss the naturalness problem in light of the recent Higgs discovery. We discuss two scenarios where the particle physics action is directly embedded into gravity without any intermediate scale and discuss their viability. Finally, we conclude in Chapter 8.

Parts of this thesis have been published before, are in print or preparation. Sections 2.5.1 and 7.2 are based on collaboration with Kher Sham Lim and Manfred Lindner [14, 15], Chapters 3 and 4 are based on collaboration with Michael A. Schmidt [16, 17] and Chapters 5 and 6 and Section 7.3 are based on collaboration with Manfred Lindner and Michael A. Schmidt [18–22].

## Chapter 2.

# Discrete Symmetry Groups and Lepton Mixing

In this chapter we start by giving a short review about flavour in the Standard Model and the experimental status of lepton flavour observables. We then review how the large mixing angles in the lepton sector may be understood as a result of mismatched remnant symmetries of the mass matrices. This leads us to a brief discussion of non-abelian discrete flavour symmetries, which may be viewed as being built up out of the remnant symmetries. After this, we show how such an idea may be realized in a prototypical particle physics model. Finally, we attempt to give an overview of the vast literature that has emerged since the discovery of a non-vanishing value for the mixing angle  $\theta_{13}$ .

## 2.1. Flavour in the Standard Model

### 2.1.1. Theoretical Background

After all the media coverage, even my grandfather knows that it is the Higgs field  $H = (H^+, H^0)^T$  that gives masses to all fermions in the Standard Model. Denoting the quark and lepton fields by  $Q = (u, d)^T$ ,  $u^c, d^c$  and  $L = (\nu, e)^T$ ,  $e^c$ , respectively<sup>1</sup>, we have the interactions

$$\mathcal{L}_Y = Q^T Y_u u^c H - Q^T Y_d d^c \tilde{H} - L^T Y_e e^c \tilde{H} + \text{h.c.} \quad (2.1)$$

The conjugate of the Higgs field is given by  $\tilde{H} = i\sigma_2 H^*$  and the transformation properties of all the fields under the Standard Model gauge group  $SU(3)_C \times SU(2)_L \times U(1)$  can be found in Table 2.1. All fermions are written as left-handed Weyl spinors and Lorentz, color, isospin and generational indices are suppressed. After electroweak symmetry breaking and in the unitary gauge  $H_0 = \frac{1}{\sqrt{2}}(v + h)$  with  $v = (\sqrt{2}G_F)^{-1/2} = 246 \text{ GeV}$ , these Yukawa couplings generate

$$\mathcal{L}_Y = [u^T M_u u^c + d^T M_d d^c + e^T M_e e^c] \left(1 + \frac{h}{v}\right) + \text{h.c.} \quad (2.2)$$

where the mass matrices are given by

$$M_A = \frac{v}{\sqrt{2}} Y_A \quad \text{for} \quad A = u, d, e. \quad (2.3)$$

This equation already shows that the Higgs-mediated interaction is flavour-diagonal in the basis where the mass matrices are diagonal, a feature that is lost in many extensions of the Standard Model. Defining the mass eigenstates  $(u^0, u^{c0}, d^0, d^{c0})$  by

$$u = V_u u^0, \quad u^c = V_{u^c} u^{c0}, \quad d = V_d d^0, \quad \text{and} \quad d^c = V_{d^c} d^{c0}, \quad (2.4)$$

<sup>1</sup>We use a standard notation [5] and for an introduction we recommend [23].

gauge group	$Q$	$u^c$	$d^c$	$L$	$e^c$	$H$
$SU(3)_C$	$\underline{\mathbf{3}}$	$\overline{\mathbf{3}}$	$\overline{\mathbf{3}}$	$\underline{\mathbf{1}}$	$\underline{\mathbf{1}}$	$\underline{\mathbf{1}}$
$SU(2)_L$	$\underline{\mathbf{2}}$	$\underline{\mathbf{1}}$	$\underline{\mathbf{1}}$	$\underline{\mathbf{2}}$	$\underline{\mathbf{1}}$	$\underline{\mathbf{2}}$
$U(1)_Y$	1/6	-2/3	-1/3	-1/2	1	1/2

**Table 2.1:** Quantum Numbers of Standard Model particles.

with unitary matrices chosen such that

$$V_u^T M_u V_{u^c} = \text{diag}(m_u, m_c, m_t) \quad \text{and} \quad V_d^T M_d V_{d^c} = \text{diag}(m_d, m_s, m_b), \quad (2.5)$$

then the only flavour violating interaction in the SM is the charged current interaction

$$\mathcal{L}_{cc} = \frac{g}{\sqrt{2}} \left[ u^\dagger \sigma^\mu d \right] W_\mu^+ + \text{h.c.} = \frac{g}{\sqrt{2}} \left[ u^{0\dagger} \sigma^\mu V d^0 \right] W_\mu^+ + \text{h.c.}, \quad (2.6)$$

with the famous Cabibbo–Kobayashi–Maskawa (CKM) matrix

$$V = V_u^\dagger V_d, \quad (2.7)$$

that seems to describe all flavour effects in the quark sector to high accuracy. In the lepton sector, we can repeat this analysis by defining

$$e = V_e e^0, \quad e^c = V_{e^c} e^{c0} \quad (2.8)$$

where the unitary matrices satisfy

$$V_e^T M_e V_{e^c} = \text{diag}(m_e, m_\mu, m_\tau). \quad (2.9)$$

Note that as it stands, there is no mass term for neutrinos and we are thus free to redefine  $\nu = V_\nu \nu^0$  such that the charged-current interaction is flavour diagonal. However, as will be reviewed in the next section, it is known that neutrinos have a finite mass, which we accommodate by adding the unique dimension-five term[24]

$$\mathcal{L}_W = \frac{(Y_\nu)_{ij}}{\Lambda} (L_i H)(L_j H) + \text{h.c.}, \quad (2.10)$$

which after electroweak symmetry breaking generates a Majorana mass term for neutrinos

$$\mathcal{L}_{\nu\text{-mass}} = \frac{1}{2} \nu^T M_\nu \nu + \text{h.c.} \quad \text{with} \quad M_\nu = Y_\nu \frac{v^2}{\Lambda}. \quad (2.11)$$

This mass term is the unique<sup>2</sup> possibility to give neutrinos mass without introducing new light states into the standard model. It can be viewed as being generated by the exchange of heavy particles, as in the famous seesaw mechanism [26–30]. If one introduces additional light neutral fermionic states, it is possible to generate Dirac masses for neutrinos. We will not

<sup>2</sup>In the SM, forbidding this operator is equivalent to forbidding Majorana mass terms for neutrinos. However the operator may also be only generated radiatively from other other higher-dimensional operators with  $\Delta L = 2$  [25].

discuss this possibility further as it is somewhat less appealing than the higher dimensional operator option, which explains the smallness of neutrino masses through the existence of a heavy mass scale  $\Lambda$ . The neutrino mass term fixes  $V_\nu$  to satisfy

$$V_\nu^T M_\nu V_\nu = \text{diag}(m_1, m_2, m_3), \quad (2.12)$$

where  $m_i$  are the masses of the light neutrinos. As was the case for quarks, the only flavour violating interaction is the leptonic charged current, which reads

$$\mathcal{L}_{cc} = \frac{g}{\sqrt{2}} \left[ e^\dagger \sigma^\mu \nu \right] W_\mu^+ + \text{h.c.} = \frac{g}{\sqrt{2}} \left[ e^{0\dagger} \sigma^\mu U \nu^0 \right] W_\mu^+ + \text{h.c.}, \quad (2.13)$$

with the leptonic mixing matrix

$$U = V_e^\dagger V_\nu, \quad (2.14)$$

also known as the Pontecorvo–Maki–Nakagawa–Sakata (PMNS) matrix. This matrix may be parametrized as  $U = \tilde{U} P$  with

$$\tilde{U} = \begin{pmatrix} 1 & 0 & 0 \\ 0 & c_{23} & s_{23} \\ 0 & s_{13} & c_{23} \end{pmatrix} \times \begin{pmatrix} c_{13} & 0 & s_{13} e^{-i\delta_{CP}} \\ 0 & 1 & 0 \\ -s_{13} e^{i\delta_{CP}} & 0 & c_{13} \end{pmatrix} \times \begin{pmatrix} c_{12} & s_{12} & 0 \\ -s_{12} & c_{12} & 0 \\ 0 & 0 & 1 \end{pmatrix}, \quad (2.15)$$

where  $s_{ij} = \sin \theta_{ij}$ ,  $c_{ij} = \cos \theta_{ij}$  and  $P = \text{diag}(e^{i\varphi_1}, e^{i\varphi_2}, 1)$  a diagonal phase matrix containing the so-called Majorana phases.

### 2.1.2. Experimental Situation

Over the span of the last decade, the experimental knowledge of lepton flavour parameters has greatly expanded, with major advances on the last missing mixing angle  $\theta_{13}$  made in the last twelve months. The mixing angles  $\theta_{ij}$  and the CP violating phase  $\delta_{CP}$  may be accessed in neutrino oscillation experiments, while the Majorana phases can only be measured in lepton number violating processes such as neutrinoless double beta decay. We first discuss the experimental determination of oscillation parameters and come back to the other types of experiments later.

Neutrino oscillation experiments are greatly simplified by the fact that nature has chosen the mixing parameters such, that it is usually sufficient to only consider a two-flavour sub-sector of the full three-flavour framework. The parameter set  $\{\Delta m_{31}^2 \equiv m_3^2 - m_1^2, \theta_{23}\}$  can be measured using atmospheric neutrinos and will thus be often referred to as atmospheric parameters. After the initial discovery of atmospheric neutrino oscillations by the SuperKamiokande experiment [31] in 1998, these parameters have also been measured in long baseline experiments, which look for the disappearance of a muon neutrino beam coming from an accelerator. The solar parameters  $\{\Delta m_{21}^2 \equiv m_2^2 - m_1^2, \theta_{12}\}$  were originally determined in oscillation experiments using neutrinos produced in fusion processes in the sun, but today the best measurement comes from long baseline reactor experiments such as KamLAND [32]. The third mixing angle  $\theta_{13}$  can be measured in reactor experiments with very short baselines compared to the solar reactor experiments, and in experiments using neutrino beams. The first indication for a non-vanishing value for this reactor angle came from the long baseline experiment T2K [33] and MINOS [34] and the reactor experiment DoubleCHOOZ [35] in 2011 and was established by the reactor experiments DayaBay [36] and RENO [37] in early 2012.

	$\Delta m_{21}^2$ [ $10^{-5}$ eV $^2$ ]	$ \Delta m_{31}^2 $ [ $10^{-3}$ eV $^2$ ]	$\sin^2 \theta_{12}$ [ $10^{-1}$ ]	$\sin^2 \theta_{23}$ [ $10^{-1}$ ]	$\sin^2 \theta_{13}$ [ $10^{-2}$ ]	$\delta$ [ $\pi$ ]
best fit	$7.62_{-0.19}^{+0.19}$	$2.55_{-0.09}^{+0.06}$	$3.20_{-0.17}^{+0.16}$	$6.13_{-0.40}^{+0.22}$	$2.46_{-0.28}^{+0.29}$	$0.8_{-0.8}^{+1.2}$
$3\sigma$	7.12 – 8.20	2.31 – 2.74	2.7 – 3.7	3.6 – 6.8	1.7 – 3.3	0 – 2

**Table 2.2:** Global Fit of neutrino oscillation parameters adapted from [39]. The errors of the best fit values indicate the one sigma ranges. In the global fit there is a nearly degenerate minima at  $\sin^2 \theta_{23} = 0.430_{-0.030}^{+0.031}$ , see Fig. 2.1. We only report the values corresponding to normal hierarchy of neutrinos.

While the two flavour description of the neutrino oscillation experiments holds at leading order, more information on the oscillation parameters can be obtained if one performs a global fit over all available experiments. By now, there are (at least) three competing groups [38–40] performing these global fits and we here report the values obtained by the Valencia group [39] in Table 2.2. Note that  $\theta_{13}$  is now among the most precisely measured leptonic mixing angles. So far there is very little information about the Dirac CP phase  $\delta_{CP}$  and whether the neutrino spectrum shows a normal ( $\Delta m_{31}^2 > 0$ ) or inverted ( $\Delta m_{31}^2 < 0$ ) hierarchy. These questions can be answered by oscillation experiments and will be a major goal of experimental efforts in the coming years<sup>3</sup>.

Let us also briefly summarize the experimental information on lepton flavour coming from experiments that are complementary to oscillation experiments. The absolute mass scale of neutrinos can be obtained by precisely measuring the endpoint of the tritium beta decay spectrum. The best limit on the effective electron neutrino mass  $m(\nu_e)$  is given by

$$\sqrt{\sum_i |U_{ei}|^2 m_i^2} \leq 2.3 \text{ eV} \quad (2.16)$$

at 95% confidence level by the MAINZ experiment [41]. The KATRIN experiment [42] will aim to improve this bound by an order of magnitude and will therefore be competitive with bounds coming from cosmology. The seven-year measurement of the cosmic microwave background by WMAP [43] places an upper limit of  $\sum m_i \leq 0.58$  eV on the sum of neutrino masses, which can be further improved to  $\sum m_i \leq 0.36$  eV if one includes information from supernovae, large scale structure surveys and the Hubble constant measurement [44]. While these bounds are supposed to be robust with regards to reasonable deformations of the standard  $\Lambda$ CDM model of cosmology, they depend on some cosmological assumptions and the direct kinematical determination of the absolute neutrino mass scale by KATRIN is therefore complementary.

Let us also briefly mention two other types of experiments that test symmetries in the lepton sector: neutrinoless double beta decay experiments such as GERDA [45] and EXO [46] among others, search for processes that violate lepton number by two units.<sup>4</sup> If light neutrino exchange is the dominant mechanism for neutrino-less double beta decay, the current upper limit [46] can be expressed as  $|m_{ee}| = |\sum_i U_{ei}^2 m_i| \leq (140 - 380)$  meV, where the uncertainty is due to the calculation of nuclear matrix elements.

Another type of experiment that tests symmetries of the lepton sector and so far has only produced upper bounds are experiments that look for violations of lepton flavour involving

<sup>3</sup>Note that the large value of  $\theta_{13}$  makes experiments looking for leptonic CP violation feasible (see Eq. (2.15)).

<sup>4</sup>Any signal would imply that (unless there are fine-tuned cancellations) neutrinos are Majorana particles [47, 48].



## 2.2. Leptonic Mixing from Remnant Symmetries

charged leptons. For example the experiment MEG searches for the process  $\mu \rightarrow e\gamma$  and has recently reported a limit of  $\text{Br}(\mu \rightarrow e\gamma) < 2.4 \cdot 10^{-12}$  [49]. Lepton flavour violation involving neutral leptons, a.k.a. neutrino oscillations, is well established and should therefore also exist in its charged lepton variant. However, in the Standard Model any lepton flavour violating amplitude has to involve a (tiny) neutrino mass term so that, for example, the SM prediction for  $\mu \rightarrow e\gamma$  is  $\text{Br}(\mu \rightarrow e\gamma) \sim (m_\nu/m_W)^4 \sim 10^{-52}$ , i.e. unobservably small. However in extensions of the Standard Model this link is broken and these experiments can give important constraints on such models, as we will see in Section 5.3.

## 2.2. Leptonic Mixing from Remnant Symmetries

In Section 2.1.1 we have seen that the leptonic mixing matrix

$$U = V_e^\dagger V_\nu. \quad (2.17)$$

can be determined from the unitary matrices  $V_e$  and  $V_\nu$  satisfying

$$V_e^T M_e M_e^\dagger V_e^* = \text{diag}(m_e^2, m_\mu^2, m_\tau^2) \quad \text{and} \quad V_\nu^T M_\nu V_\nu = \text{diag}(m_1, m_2, m_3). \quad (2.18)$$

where the mass matrices are defined by  $\mathcal{L} = e^T M_e e^c + \frac{1}{2} \nu^T M_\nu \nu$ . We will now show how certain mixing patterns can be understood as a consequence of mismatched horizontal symmetries acting on the charged lepton and neutrino sectors [9–13, 50]. For this purpose let us assume that there is a (discrete) symmetry group  $G$  under which the left-handed lepton doublets transform under a unitary 3-dimensional representation  $\rho : G \rightarrow \text{GL}(3, \mathbb{C})$ :

$$L \rightarrow \rho(g)L, \quad g \in G. \quad (2.19)$$

The experimental data clearly shows (i) that all lepton masses are unequal and (ii) there is mixing amongst all three mass eigenstates. Therefore this symmetry cannot be a symmetry of the entire Lagrangian but has to be broken to different subgroups  $G_e$  and  $G_\nu$  in the charged lepton and neutrino sectors, respectively. If the fermions transform as

$$e \rightarrow \rho(g_e)e, \quad \nu \rightarrow \rho(g_\nu)\nu \quad g_e \in G_e, g_\nu \in G_\nu, \quad (2.20)$$

for the symmetry to hold, the mass matrices have to fulfil

$$\rho(g_e)^T M_e M_e^\dagger \rho(g_e)^* = M_e M_e^\dagger \quad \text{and} \quad \rho(g_\nu)^T M_\nu \rho(g_\nu) = M_\nu. \quad (2.21)$$

It can easily be seen that if one chooses  $G_e$  or  $G_\nu$  to be a non-abelian group, this would lead to a degenerate spectrum, which is not compatible with the data – we therefore restrict ourselves to the abelian case. We further demand neutrinos to be Majorana particles, which implies that there cannot be a complex eigenvalue of the matrices  $\rho(g_\nu)$  and they therefore satisfy  $\rho(g_\nu)^2 = 1$ , and we can further choose  $\det \rho(g) = 1$ . This forces the group  $G_\nu$  to be a subgroup of the Klein group  $Z_2 \times Z_2$ . To be able to uniquely determine the mixing from the group structure it is necessary to have all neutrinos transform as inequivalent singlets of  $G_\nu$ . The same is true for the charged leptons, which shows that  $G_e$  cannot be smaller than  $Z_3$ . We can now determine the mixing via the unitary matrices  $\Omega_e$  and  $\Omega_\nu$ , which satisfy

$$\Omega_e^\dagger \rho(g_e) \Omega_e = \rho(g_e)_{diag}, \quad \Omega_\nu^\dagger \rho(g_\nu) \Omega_\nu = \rho(g_\nu)_{diag}, \quad (2.22)$$

Chapter 2. Discrete Symmetry Groups and Lepton Mixing

where  $\rho(g)_{diag}$  are diagonal unitary matrices. These conditions determine  $\Omega_e, \Omega_\nu$  up to a diagonal phase matrix  $K_{e,\nu}$  and permutation matrices  $P_{e,\nu}$

$$\Omega_{e,\nu} \rightarrow \Omega_{e,\nu} K_{e,\nu} P_{e,\nu}. \quad (2.23)$$

It follows from Eq. (2.21) that one can choose  $\Omega_{e,\nu}$  such that they coincide with  $V_{e,\nu}$ . This can be seen as

$$\Omega_e^T M_e M_e^\dagger \Omega_e^* = \Omega_e^T \rho^T M_e M_e^\dagger \rho^* \Omega_e^* = \rho_{diag}^T \Omega_e^T M_e M_e^\dagger \Omega_e^* \rho_{diag}^*$$

has to be diagonal (only a diagonal matrix is invariant when conjugated by an arbitrary phase matrix) and the phasing and permutation freedom can be used to bring it into the form  $\text{diag}(m_e^2, m_\mu^2, m_\tau^2)$ , and analogously for  $\Omega_\nu$ . From these group theoretical considerations we can thus determine the PMNS matrix

$$U = \Omega_e^\dagger \Omega_\nu, \quad (2.24)$$

up to a permutation of rows and columns. It should not be surprising that it is not possible to uniquely pin down the mixing matrix, as it is not possible to predict lepton masses in this approach.

Let us now try to apply this machinery to some interesting cases. We have seen that the smallest residual symmetry in the charged lepton sector is given by the group  $G_e = \langle T | T^3 = E \rangle \cong Z_3$ . We use a basis where the generator is given by

$$\rho(T) = T_3 \equiv \begin{pmatrix} 0 & 1 & 0 \\ 0 & 0 & 1 \\ 1 & 0 & 0 \end{pmatrix}. \quad (2.25)$$

This matrix will be our standard three-dimensional representation of  $Z_3$  and the notation  $T_3$  will be used throughout this work. It is diagonalized by

$$\Omega_e^\dagger \rho(T) \Omega_e = \text{diag}(1, \omega^2, \omega) \quad \text{and} \quad \Omega_e = \Omega_T \equiv \frac{1}{\sqrt{3}} \begin{pmatrix} 1 & 1 & 1 \\ 1 & \omega^2 & \omega \\ 1 & \omega & \omega^2 \end{pmatrix}, \quad (2.26)$$

with  $\omega = e^{i2\pi/3}$ . Obviously it is enough to consider the generators of  $G_e$ , as e.g.  $\rho(T^2)$  is diagonalized by the same matrix,

$$\Omega_T^\dagger \rho(T^2) \Omega_T = \Omega_T^\dagger \rho(T) \Omega_T \Omega_T^\dagger \rho(T) \Omega_T = \text{diag}(1, \omega, \omega^2).$$

Having fixed the basis by choosing the  $Z_3$  generator the way we just did, it is now essentially a question of choosing generators and studying the predicted mixing matrix. Let us first look at the case where there is only one generator  $S$  of  $G_\nu$ , satisfying  $\rho(S)^2 = 1$  and  $\det \rho(S) = 1$ :

$$\rho(S) = S_3 \equiv \begin{pmatrix} 1 & 0 & 0 \\ 0 & -1 & 0 \\ 0 & 0 & -1 \end{pmatrix}. \quad (2.27)$$

Due to the degenerate eigenvalues there is a two-parameter freedom in the matrix  $\Omega_\nu$  and it will turn out to be useful to write it as

$$\Omega_\nu^\dagger \rho(S) \Omega_\nu = \text{diag}(-1, 1, -1) \quad \text{with} \quad \Omega_\nu = \Omega_U U_{13}(\theta, \delta), \quad (2.28)$$

## 2.2. Leptonic Mixing from Remnant Symmetries

and

$$\Omega_U = \begin{pmatrix} 0 & 1 & 0 \\ \frac{1}{\sqrt{2}} & 0 & -\frac{i}{\sqrt{2}} \\ \frac{1}{\sqrt{2}} & 0 & \frac{i}{\sqrt{2}} \end{pmatrix} \quad \text{and} \quad U_{13}(\theta, \delta) = \begin{pmatrix} \cos \theta & 0 & e^{i\delta} \sin \theta \\ 0 & 1 & 0 \\ -e^{-i\delta} \sin \theta & 0 & \cos \theta \end{pmatrix}. \quad (2.29)$$

Obviously this does not completely fix the leptonic mixing matrix yet, as the first and third eigenvalue are the same and the corresponding eigenstates can be rotated into each other without breaking the symmetry. To completely fix the mixing matrix we have to enlarge  $G_\nu$  by another generator. Let us look at the effect of adding the symmetry generator  $U$  with<sup>5</sup>

$$\rho(U) = U_3 \equiv - \begin{pmatrix} 1 & 0 & 0 \\ 0 & 0 & 1 \\ 0 & 1 & 0 \end{pmatrix}. \quad (2.30)$$

This fixes the value of  $\theta$  to zero,  $\Omega_U^\dagger \rho(U) \Omega_U = \text{diag}(-1, -1, 1)$ , and thus the mixing matrix to the famous tri-bimaximal mixing (TBM) form

$$U = \Omega_U^\dagger \Omega_U = U_{HPS} \equiv \begin{pmatrix} \sqrt{\frac{2}{3}} & \frac{1}{\sqrt{3}} & 0 \\ -\frac{1}{\sqrt{6}} & \frac{1}{\sqrt{3}} & \frac{1}{\sqrt{2}} \\ -\frac{1}{\sqrt{6}} & \frac{1}{\sqrt{3}} & -\frac{1}{\sqrt{2}} \end{pmatrix}, \quad (2.31)$$

attributed to Harrison, Perkins and Scott [51–53], corresponding to the mixing angles  $\sin^2 \theta_{12} = \frac{1}{3}$ ,  $\sin^2 \theta_{23} = \frac{1}{2}$ , and  $\sin^2 \theta_{13} = 0$ . Until very recently, this pattern gave a good description of the mixing matrix and the fact that this mixing pattern can be obtained from simple symmetry considerations has prompted a lot of model building activity. In light of the recent measurement of a non-vanishing  $\theta_{13}$  there has been interest in the physical situation where the (broken) flavour symmetry does not fully determine the mixing angles [54, 55]. For example if the residual symmetry in the neutrino sector  $G_\nu$  is taken to be  $G_\nu = \langle S \rangle \cong Z_2$ , we have seen that the leptonic mixing matrix is given by  $U = U_{HPS} U_{13}(\theta, \delta)$ . This is called trimaximal mixing (TMM) [56–63] and the result of a deviation from  $\theta = 0$  in terms of mixing angles is shown in Fig. 2.1 where one can read off that a 13-rotation about an angle of  $\theta \simeq 0.2$  is required to accommodate the relative large value of  $\theta_{13}$ . In Section 2.5.1, we will show that interesting new mixing patterns that can be obtained from flavour groups of reasonable size all lie on the parabola  $U = U_{HPS} U_{13}(\theta, \delta = 0)$ . It should be clear from the discussion above that, a different choice of generators of the residual symmetry groups leads to a different mixing pattern. For example, if we do not take  $G_\nu$  to be the Klein group  $G_\nu = \langle S, U | S^2 = U^2 = E; SU = US \rangle \cong Z_2 \times Z_2$  that leads to tri-bimaximal mixing, but rather the isomorphic group  $G_\nu = \langle S, X | S^2 = X^2 = E; SX = XS \rangle \cong Z_2 \times Z_2$  with  $X = T^2 S T$  and

$$\rho(X) = \begin{pmatrix} -1 & 0 & 0 \\ 0 & 1 & 0 \\ 0 & 0 & -1 \end{pmatrix}, \quad (2.32)$$

the physical results will be different. This fixes

$$\Omega_X^\dagger \rho(X) \Omega_X = \text{diag}(-1, -1, 1) \quad \text{with} \quad \Omega_X = \Omega_U U_{13}(\theta = -\frac{\pi}{4}, \delta = \frac{\pi}{2}) \quad (2.33)$$

<sup>5</sup>The minus sign is needed to have  $\det \rho(U) = 1$ .

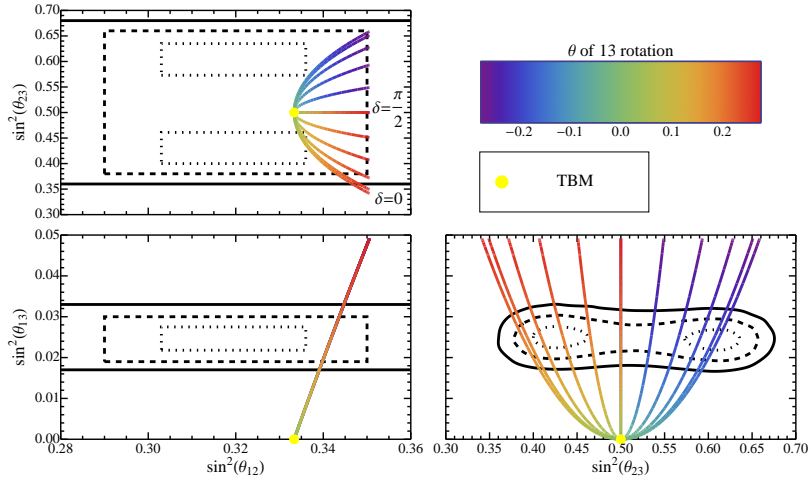


**Figure 2.1:** Deviations from tri-bimaximal mixing of the form  $U = U_{HPS}U_{13}(\theta, \delta)$  (2.29). The yellow point represents TBM, the continuous lines give the deviations with the angle  $\theta$  given by the colour code in the top right corner for  $\delta = \frac{n}{5} \frac{\pi}{2}$  for  $n = 0, \dots, 5$ , where  $n = 0$  is the outermost parabola etc. The one, two and three sigma regions of a recent global fit [39] are indicated by dotted, dashed and continuous contours, respectively. This pattern of perturbations can shift the mixing angles in the direction of the experimental data for  $\theta \sim .1 - .2$ . Note that the corrections to the solar angle are smaller than the corrections to the other angles.

which gives

$$\|U\| = \|\Omega_e^\dagger \Omega_X\| = \frac{1}{\sqrt{3}} \begin{pmatrix} 1 & 1 & 1 \\ 1 & 1 & 1 \\ 1 & 1 & 1 \end{pmatrix}, \quad (2.34)$$

corresponding to the mixing angles  $\sin^2 \theta_{12} = \frac{1}{2}$ ,  $\sin^2 \theta_{13} = \frac{1}{3}$  and  $\sin^2 \theta_{23} = \frac{1}{2}$ . Here we used the notation  $\|U\|$ , which gives the matrix of absolute values of matrix entries. We will refer to this mixing pattern as bimaximal mixing(BM).

## 2.3. Some Properties of Non-Abelian Discrete Symmetries

### 2.3.1. Building the Flavour Group

In the last section we have seen how interesting neutrino mixing patterns can arise from mismatched remnant symmetries of the neutrino and charged lepton mass matrices. Here we want to discuss how one could try to reconstruct the complete flavour symmetry out of these remnant symmetries. Clearly if one part of the Lagrangian exhibits a certain enhanced symmetry, it does not mean that this symmetry has to be a symmetry of the entire Lagrangian. For example the Higgs potential in the Standard Model only depends on the invariant  $H^\dagger H = \sum_i^4 h_i^2$  and is thus invariant under a larger symmetry  $SO(4) \cong SU(2)_L \times SU(2)_R$ , where  $h_i$  are the four real components of the doublet. The accidental symmetry  $SU(2)_R$  (which is also called the custodial symmetry of the SM Higgs sector<sup>6</sup>) is broken in other parts of the Lagrangian, e.g. by Yukawa couplings and gauge interactions.

<sup>6</sup>Strictly speaking, the diagonal subgroup  $SU(2)_V$  left-over after EWSB is the custodial symmetry.

### 2.3. Some Properties of Non-Abelian Discrete Symmetries

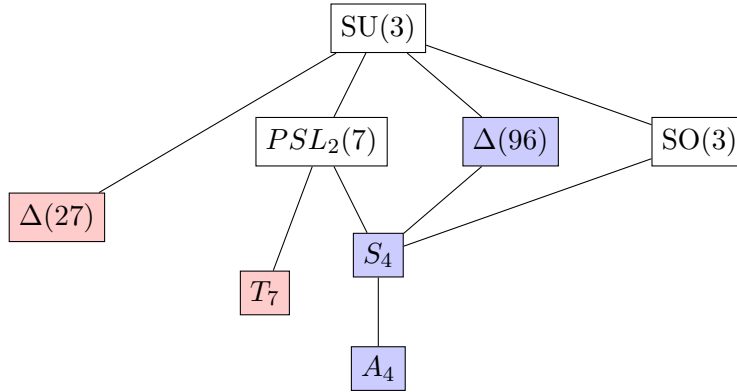


**Figure 2.2:** Tree of (selected) discrete subgroups of  $SU(3)$  that contain three-dimensional representations. The blue groups are used in so-called direct models, the red ones are used in indirect models (see text). The location of the colored groups indicates the size of group with the smallest group  $A_4$ , that contains 12 elements, at the bottom.

If one accepts that there are the remnant symmetries  $G_e = \langle T \rangle \cong Z_3$  and  $G_\nu = \langle S, U \rangle \cong Z_2 \times Z_2$  we discussed in the last section, there are three logical ways to construct the flavour group:

- all remnant symmetries are accidental, i.e. there is no flavour symmetry and the remnant symmetries only emerge because of the chosen particle content etc. No model without some flavour symmetry is known where this can be the case. However, so called indirect models [64] are of this type as the symmetries of the mass matrices arise accidentally and are different from the symmetries of the original models.
- some remnant symmetries are accidental, some are part of the flavour group. Some of the most prominent models fall into this category, e.g. the flavour group  $A_4$  is generated by the generators  $S$  and  $T$ . In  $A_4$  models [9, 10, 65–69] that predict TBM the symmetry  $U$  is an accidental symmetry as we will discuss in detail in Section 2.4. This is why we have also discussed the case  $G_\nu = \langle S \rangle \cong Z_2$ , which leads to trimaximal mixing, as this is the most natural deformation of  $A_4$  models.
- all remnant symmetries are part of  $G_f$ . The group generated by  $S$ ,  $T$  and  $U$  is the group  $S_4$  [12, 70–86], which has also been widely used for model building. It has been claimed [12, 13] that this is the unique symmetry that leads to TBM but this claim is obviously incorrect [84, 87] and results from the flawed notion that symmetries of the mass matrices have to be symmetries of the Lagrangian. Models that realize the last two cases are also known as direct models [64].

A tree of (selected) discrete subgroups of  $SU(3)$  that contain three-dimensional representations is shown in Fig. 2.2. All of the groups represented in this graph will at some point be used in this thesis and we therefore briefly describe them here.

All of these groups may be written as *semidirect products* of two smaller groups. As the concept of a semidirect product plays a prominent part in the later parts of the thesis we define it here: given two groups  $N$  and  $H$  and a group homomorphism <sup>7</sup>  $\varphi : H \rightarrow \text{Aut}(N)$ , one

<sup>7</sup>A (group) homomorphism  $\rho : G \rightarrow H$  is a mapping preserving the group structure, i.e.  $\rho(g_1 g_2) = \rho(g_1) \rho(g_2) \forall g_{1,2} \in G$ . A *surjective* homomorphism  $\rho : G \rightarrow H$  has the additional property  $\text{im}(\rho) = H$ .

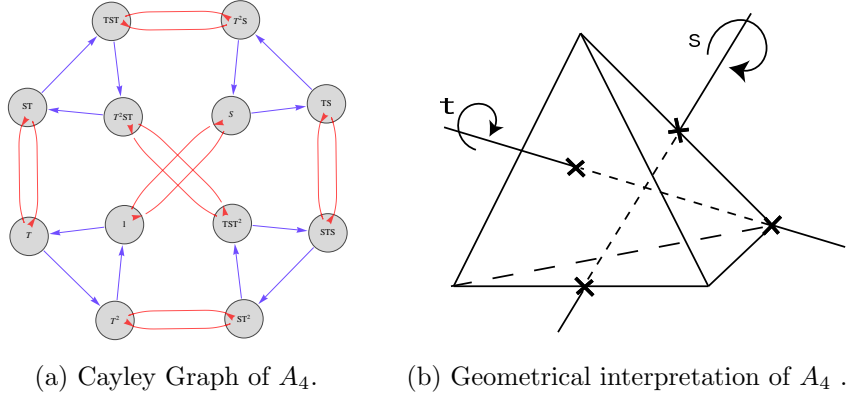


**Figure 2.3:** The symmetry group  $A_4$ . The twelve group elements are connected by the generators  $S$  (red) and  $T$  (blue). The picture 2.3b is taken from [88].

can define the semidirect product group  $N \rtimes_{\varphi} H$  via the multiplication rule

$$(n_1, h_1) * (n_2, h_2) = (n_1 \varphi_{h_1}(n_2), h_1 h_2) \quad \text{for } n_{1,2} \in N \text{ and } h_{1,2} \in H. \quad (2.35)$$

Note that there can be more than one semidirect product between two groups, but in the following we will often drop the index  $\varphi$ , as long as it is clear which group we are referring to. (Another equivalent definition we will use is that a group  $G$  is a *semidirect product* of a subgroup  $H$  and normal<sup>8</sup> subgroup  $N$  if there exists a homomorphism  $G \rightarrow H$  which is the identity on  $H$  and whose kernel<sup>9</sup> is  $N$ .)

Let us present in some detail the case of the smallest group in Fig. 2.2, namely the tetrahedral group  $A_4$ . We will give the details for the other groups in the appendix. The group  $A_4$  may be written as  $A_4 \cong (Z_2 \times Z_2) \rtimes Z_3$  where the Klein group  $N \cong Z_2 \times Z_2$  is defined by  $\langle S, X | X^2 = S^2 = E, XS = SX \rangle$ , the group  $H \cong Z_3$  is defined by  $\langle T | T^3 = E \rangle$  and the semidirect product is given by

$$\varphi_T(S) = TST^{-1} = XS, \quad \varphi_T(X) = TXT^{-1} = S. \quad (2.36)$$

Note that the last relation allows one to replace one generator of  $N$ , e.g.  $X = T^2ST$ , and we arrive at the standard presentation of  $A_4$ :

$$\langle S, T | S^2 = T^3 = E, (ST)^3 = E \rangle, \quad (2.37)$$

that is represented graphically in Fig. 2.3a.

The other small groups in the tree shown in Fig. 2.2 can be represented in a similar way<sup>10</sup>:

$$\Delta(3n^2) \cong (Z_n \times Z_n) \rtimes Z_3, \quad \Delta(6n^2) \cong (Z_n \times Z_n) \rtimes S_3, \quad T_n \cong Z_n \times Z_3 \quad (2.38)$$

where  $S_4 \cong \Delta(24)$  and the defining homomorphisms are given in App. A.1.  $S_3$  denotes the group of permutations of three elements. It is in itself a semi-direct product  $S_3 \cong Z_3 \rtimes Z_2 = \langle r, a; r^3 = a^2 = E, ara^{-1} = r^2 \rangle$  and is not to be confused with the matrix defined in Eq. (2.27).

<sup>8</sup>A *normal* subgroup  $N$  of a group  $G$ , denoted by  $N \triangleleft G$ , is a subgroup, which is invariant under conjugation by an arbitrary group element of  $G$ , i.e.  $gNg^{-1} = N$ .

<sup>9</sup>The *kernel* of a representation  $\rho$  is defined by  $\ker \rho = \{g \in G | \rho(g) = \mathbb{1}\}$ .

<sup>10</sup>With respect to particle physics,  $\Delta(3n^2)$  has been studied in [89–92],  $T_7$  has been studied in [93–95] and  $\Delta(6n^2)$  has been studied in [88, 96].

### 2.3. Some Properties of Non-Abelian Discrete Symmetries

Another important class of groups can be constructed out of the known ones by so-called non-split extensions of groups. As we will also encounter this concept later on, we here give a definition and use the group  $T'$  as an example, as this is the most well-known group that can be seen as a non-split extension of  $A_4$  and that has been used for model-building [97–104]. A group  $G$  is an extension of  $H$  by  $N$  if there is a *short exact sequence*

$$1 \rightarrow N \xrightarrow{f} G \xrightarrow{g} H \rightarrow 1 \quad (2.39)$$

defined by the homomorphisms  $f$  and  $g$ , which have to be injective and onto, respectively. Therefore  $N \cong \ker g$  is a normal subgroup of  $G$  and  $G/N \cong H$ . An extension is called split iff it may be written as a semidirect product  $G = N \rtimes H$ .

$T'$  is now a non-split extension of  $A_4 = \langle S, T \rangle$  by  $Z_2 = \langle R, R^2 = E \rangle$ , which we denote by  $T' = Z_2.A_4$ . Let  $T'$  be generated by  $r, s, t$ ,

$$\langle s, t, r | s^2 = r, t^3 = (st)^3 = r^2 = E \rangle; \quad (2.40)$$

the short exact sequence is then defined by the images of the generators of the homomorphisms in the short exact sequence

$$f(R) = r, \quad g(s) = S, \quad g(t) = T, \quad g(r) = E. \quad (2.41)$$

These type of extensions are of importance when one constructs representations of larger groups out of the representations of smaller groups. To give an example, we consider the case of the group  $A_4$ . The presentation given in Eq. (2.37) may be represented by the three one-dimensional representations

$$\underline{\mathbf{1}}_i : \quad \rho_{\underline{\mathbf{1}}_i}(S) = 1, \quad \rho_{\underline{\mathbf{1}}_i}(T) = \omega^{i-1} \quad i = 1, 2, 3. \quad (2.42a)$$

These representations are really just representations of  $\langle T \rangle \cong Z_3$  and for a good reason: we have seen that  $A_4$  can be understood as the split extension (a.k.a. the semidirect product) of  $Z_3$  by the Klein group  $Z_2 \times Z_2$ . For any group  $G$  that is an extension of  $H$  one can construct representations of  $G$   $\rho_G : G \rightarrow \text{GL}(n, \mathbb{C})$  that are inherited from the representations of  $H$   $\rho_H : H \rightarrow \text{GL}(n, \mathbb{C})$  by  $\rho_G = \rho_H \circ g$  with the onto homomorphism  $g : G \rightarrow H$  given in Eq. (2.39). Additionally, there is the three-dimensional representation  $\rho_{\underline{\mathbf{3}}_1}$  that is known to us from the last chapter

$$\underline{\mathbf{3}}_1 : \quad \rho_{\underline{\mathbf{3}}_1}(S) = S_3, \quad \rho_{\underline{\mathbf{3}}_1}(T) = T_3. \quad (2.42b)$$

These representations<sup>11</sup> can be multiplied according to the rules given in Table 2.4; also the character table can be found there.

Using the construction from above we can now take it one step further and realize that all group extensions of  $A_4$  have representations that correspond to representations of  $A_4$ . As group representations play an important role in model building this insight will be helpful to solve the vacuum alignment problem in Section 3.2.

<sup>11</sup>It will turn out to be useful to use the notation  $\underline{\mathbf{3}}_1$  instead of  $\underline{\mathbf{3}}$ , as will become clear later.

	1	$T$	$T^2$	$S$
$\underline{\mathbf{1}}_1$	1	1	1	1
$\underline{\mathbf{1}}_2$	1	$\omega$	$\omega^2$	1
$\underline{\mathbf{1}}_3$	1	$\omega^2$	$\omega$	1
$\underline{\mathbf{3}}$	3	0	0	-1

(a) Character Table.

$$\begin{aligned}
 \underline{\mathbf{1}}_i \times \underline{\mathbf{1}}_2 &= \underline{\mathbf{1}}_{i+1} \pmod{3} \\
 \underline{\mathbf{1}}_i \times \underline{\mathbf{1}}_3 &= \underline{\mathbf{1}}_{i+2} \pmod{3} \\
 \underline{\mathbf{1}}_i \times \underline{\mathbf{3}}_1 &= \underline{\mathbf{3}}_1 \\
 \underline{\mathbf{3}}_1 \times \underline{\mathbf{3}}_1 &= \underline{\mathbf{1}}_1 + \underline{\mathbf{1}}_2 + \underline{\mathbf{1}}_3 + \underline{\mathbf{3}}_{1S} + \underline{\mathbf{3}}_{1A}
 \end{aligned}$$

(b) Kronecker products.

**Figure 2.4:** Character table of  $A_4$  and its Kronecker products. A character  $\chi_\rho(g)$  is defined by  $\text{tr}\rho(g)$ . Characters are functions on conjugacy classes, which are shown in the top row. The conjugacy classes are specified according to a representative of the conjugacy class. The values for the Clebsch-Gordon coefficients are given in App. A.2.

### 2.3.2. On the Origin of Discrete Flavour Symmetries

We have seen that global non-abelian discrete symmetries may be used to construct models that realize certain mixing patterns in the leptonic flavour sector. These models can be motivated by a bottom-up approach from approximate remnant symmetries of the charged and neutral lepton mass matrices. From a top-down approach, however, it is important to know about the origin of discrete flavour symmetries. In this section we attempt to summarize two approaches to tackle this question, namely the case of spontaneous breaking of a continuous flavour symmetry down to a discrete subgroup and the possibility that the flavour symmetry may arise from discrete symmetries of additional compactified space-time dimensions.

The smallest continuous symmetry group that has a three dimensional representation is the group  $\text{SO}(3)$ . The spontaneous breakdown of gauged  $\text{SO}(3)$  theories to discrete subgroups has been discussed long ago [105–109], where it was shown that the spontaneous symmetry breaking  $\text{SO}(3) \rightarrow A_4$  can be realized utilizing the seven dimensional representation  $\underline{\mathbf{7}}$  that can be described by  $T^{abc}$ , a symmetric traceless tensor in three dimensions. Amazingly, the most general potential formed out of this scalar field is rather compact [105]

$$V = -\frac{\mu^2}{2} T^{abc} T^{abc} + \frac{\lambda}{4} (T^{abc} T^{abc})^2 + c T^{abc} T^{bcd} T^{def} T^{efa} \quad (2.43)$$

and it can be shown that in the parameter range  $\mu^2 > 0$  and  $-\lambda/2 < c < 0$ , the global minimum of the potential conserves an  $A_4$  subgroup. If one assigns the SM fermions to representations smaller or equal to three, one sees that since

$$\underline{\mathbf{3}} \times \underline{\mathbf{3}} = \underline{\mathbf{1}} + \underline{\mathbf{3}} + \underline{\mathbf{5}}$$

the fermions cannot couple to the  $\underline{\mathbf{7}}$  at leading order. If one insists on such a leading order coupling no breaking to a discrete subgroup can be realized [110]. However, unless the flavour symmetry breaking field transforms as a Higgs field (and the flavour symmetry breaking scale is therefore the electroweak scale), fermion masses always arise from higher-dimensional operators and there is no conceptual problem to couple e.g.  $\underline{\mathbf{7}} \times \underline{\mathbf{7}}$  to fermions.

As the global symmetry of the SM with Yukawa couplings switched off is  $\text{U}(3)^5$  [3], it is natural to ask the question whether discrete family symmetries can be obtained from spontaneous symmetry breaking to subgroups of  $\text{U}(3)$ . While the  $\text{U}(3)$  case seems to be too difficult [111], recently the spontaneous breaking of  $\text{SU}(3)$  has been discussed [112] and it was



## 2.4. Prototype Model for Tri-Bimaximal Mixing

shown that the potential for a single 15 dimensional representation has global minima that break to  $A_4$  or  $T_7$ , depending on the potential parameters. In the case of a single  $\mathbf{10}$  scalar field the group  $\Delta(27)$  can be obtained. For more exotic subgroups of  $SU(3)$  a translation was given in [113] between the invariant subgroup and the representation and VEV of  $SU(3)$  needed to break to it. However, no dynamical mechanism was presented to realize these VEVs.

In summary, the spontaneous breakdown of larger continuous groups to discrete subgroups always requires large representations and the communication of the remnant symmetry to the Yukawa sector either requires larger fermion representations or higher dimensional operators. Furthermore, in any flavour model there needs to be an additional breaking step where the non-abelian discrete symmetry is broken into different subgroups in the charged lepton and neutrino sectors. To construct a model that realizes both is a formidable task, and it might very well be impossible<sup>12</sup>.

For these reasons, another origin of family symmetries is quite popular: one can explain the emergence of flavour symmetries by the introduction of additional compactified extra-dimensions where fields are localised at different fixed points of orbifolds. A  $d$ -dimensional orbifold is just the quotient of  $\mathbb{R}^d$  divided by a discrete group  $S$ , so there is little surprise that discrete flavour symmetries may emerge from such a setup. Indeed it has been shown that  $A_4$  may emerge from the orbifold  $T_2/Z_2$  [114] and that pretty much every other discrete group can be realized in such a bottom-up approach [115, 116] where one does not dynamically explain the existence of the orbifold. In top-down models there are additional constraints from string selection rules [117, 118] and anomaly cancellation conditions [119].

## 2.4. Prototype Model for Tri-Bimaximal Mixing

Let us now briefly describe a model [9, 10] that in a prototypical way realizes the ideas outlined above, namely the breaking of a discrete flavour group to mismatched subgroups in the charged lepton and neutrino sectors. We will take the group  $A_4$ , which is the smallest group that has a three dimensional irreducible representation.

As discussed in Section 2.2, the lepton doublets have to be assigned to the three-dimensional representation and it turns out to be preferential to assign the  $SU(2)$  singlets  $e^c$ ,  $\mu^c$  and  $\tau^c$  to the one dimensional representations  $\mathbf{1}_1$ ,  $\mathbf{1}_2$  and  $\mathbf{1}_3$ <sup>13</sup>. We have also already seen that, to get a phenomenologically interesting mixing matrix, we need to break the flavour symmetry to the subgroups  $G_e = \langle T \rangle \cong Z_2$  and  $G_\nu = \langle S, U \rangle \cong Z_2 \times Z_2$  in the charged lepton and neutrino mass matrices, respectively. The simplest realization of this idea is to introduce two (real) scalar fields  $\chi, \phi \sim \mathbf{3}_1$ , which to leading order (LO) only couple to the charged lepton mass operator

$$-\mathcal{L}_e^{(5)} = y_e(L\chi)_{\mathbf{1}_1} e^c \tilde{H}/\Lambda + y_\mu(L\chi)_{\mathbf{1}_3} \mu^c \tilde{H}/\Lambda + y_\tau(L\chi)_{\mathbf{1}_2} \tau^c \tilde{H}/\Lambda + \text{h.c.} , \quad (2.44)$$

and the neutrino mass operator

$$\mathcal{L}_\nu^{(6)} = x_a(LHLH)_{\mathbf{1}_1} \xi/\Lambda^2 + x_d(LHLH)_{\mathbf{3}_1} \cdot \phi/\Lambda^2 + \text{h.c.} . \quad (2.45)$$

<sup>12</sup>For some of the issues involved, see [109].

<sup>13</sup>This assignment enables one to explain the hierarchies in the charged lepton masses by different Frogatt-Nielsen charges of  $e^c$ ,  $\mu^c$  and  $\tau^c$ , which would not be possible if one had the assignment  $(e^c, \mu^c, \tau^c) \sim \mathbf{3}_1$ .

	$L$	$e^c$	$\mu^c$	$\tau^c$	$\chi$	$\phi$	$\xi$
$A_4$	$\mathbf{3}_1$	$\mathbf{1}_1$	$\mathbf{1}_2$	$\mathbf{1}_3$	$\mathbf{3}_1$	$\mathbf{3}_1$	$\mathbf{1}_1$
$Z_4$	$i$	$-i$	$-i$	$-i$	$1$	$-1$	$-1$

**Table 2.3:** Particle content of the prototype model. The flavons  $\chi$ ,  $\phi$  and  $\xi$  do not transform under the SM. The leptons transform in the usual way given in Table 2.1.

We have further introduced another scalar  $\xi \sim \mathbf{1}_1$  to generate the flavour group invariant part of the mass matrix. For easy referencing, the particle content of this minimal model is summarized in Table 2.3.

The leading-order separation can be explained by an auxiliary  $Z_4$  symmetry, under which the fields transform as  $\phi \rightarrow -\phi$ ,  $L \rightarrow iL$  and  $\ell^c \rightarrow -i\ell^c$  with all the other fields invariant, where  $\ell^c = e^c + \mu^c + \tau^c$  is a shorthand notation. This is a discrete subgroup of the continuous lepton number symmetry. For complex flavons one can also use a  $Z_3$  subgroup of lepton number.

We thus need the vacuum configuration

$$\langle \phi \rangle \sim (u, 0, 0), \quad \langle \chi \rangle \sim (v', v', v'), \quad \langle \xi \rangle \sim w \quad (2.46)$$

which realizes

$$\rho_{\mathbf{3}_1}(T) \langle \chi \rangle = \langle \chi \rangle \quad \text{and} \quad \rho_{\mathbf{3}_1}(S) \langle \phi \rangle = \langle \phi \rangle, \quad (2.47)$$

i.e. the  $A_4$  symmetry is broken to  $\langle T \rangle \cong Z_3$  by the VEV of  $\chi$  and to  $\langle S \rangle \cong Z_2$  by the VEV of  $\phi$ . Overall there is no symmetry conserved by this vacuum configuration and it is a highly non-trivial problem to dynamically realize this VEV configuration, as will be discussed in great detail in Chapter 3. Anyhow, assuming this VEV configuration we get the mass matrices

$$M_E = \frac{vv'}{\Lambda\sqrt{2}} \Omega_T^* \text{diag}(y_e, y_\mu, y_\tau) \quad \text{and} \quad M_\nu = \frac{v^2}{2\sqrt{3}\Lambda^2} \begin{pmatrix} \tilde{a} & 0 & 0 \\ 0 & \tilde{a} & \tilde{d} \\ 0 & \tilde{d} & \tilde{a} \end{pmatrix}, \quad (2.48)$$

with  $\tilde{a} = x_a w$  and  $\tilde{d} = \frac{1}{2} x_d u$ . It can be easily checked that not only are  $M_E$  and  $M_\nu$  invariant under the remnant symmetries  $T$  and  $S$

$$\rho(T)^T M_E M_E^\dagger \rho(T)^* = M_E M_E^\dagger \quad \rho(S)^T M_\nu \rho(S) = M_\nu \quad (2.49)$$

that are part of the  $A_4$ , but there is also the accidental symmetry

$$M_\nu = \rho(U)^T M_\nu \rho(U), \quad (2.50)$$

which we have encountered before in Eq. (2.30). Thus the mixing matrix is of the tri-bimaximal form. The mass spectrum is given by

$$\Omega_T^T M_E = \frac{vv'}{\sqrt{2}} \text{diag}(y_e, y_\mu, y_\tau), \quad \Omega_U^T M_\nu \Omega_U = \text{diag}(\tilde{a} + \tilde{d}, \tilde{a}, \tilde{d} - \tilde{a}). \quad (2.51)$$

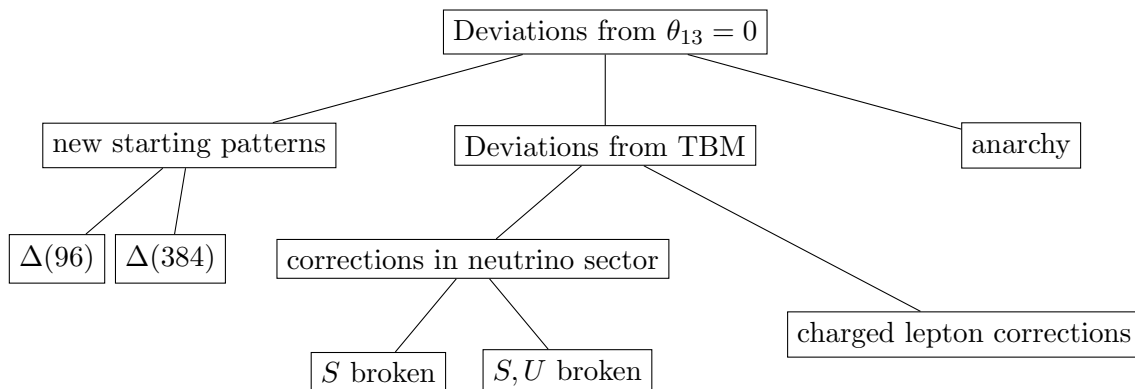


**Figure 2.5:** Various possibilities to go beyond  $\theta_{13} = 0$ .

There are thus only two parameters determining the three neutrino masses, which is a special feature of this particular model and not a consequence of the remnant symmetries  $S$  and  $U$ , as the most general neutrino mass matrix invariant under this Klein group is given by [120]

$$M_\nu \sim \begin{pmatrix} \tilde{a} + 2\tilde{b} & 0 & 0 \\ 0 & \tilde{a} - \tilde{b} & \tilde{d} \\ 0 & \tilde{d} & \tilde{a} - \tilde{b} \end{pmatrix} \quad (2.52)$$

and thus has three independent masses. It has been pointed out [121] that this can lead to testable predictions in neutrinoless double beta decay. To get the right values for the atmospheric and solar mass splitting one needs to have a certain cancellation [122], i.e. for the (overly simplistic) case of real  $\tilde{a}, \tilde{d}$ , one needs  $\tilde{d} \approx -1.88\tilde{a}$ .

## 2.5. Model Building Pathways Beyond Vanishing $\theta_{13}$

In Section 2.2 we have seen how special structures such as the tri-bimaximal neutrino mixing pattern can be explained in terms of a mismatched breaking of a flavour symmetry into different subgroups in the charged lepton and neutrino sectors. The recent results of the reactor experiments Double Chooz, Daya Bay and RENO have, however, laid to rest this simple picture of lepton mixing. In this section we attempt to give an overview of the vast literature that has emerged since word of these results reached model builders.

One logical possibility that looks much more favoured now, is that there might not be any special structure in lepton mixings that needs to be explained. It could rather be that mixing angles are determined at a high scale from some (quasi-) random process. Indeed if one randomly draws unitary  $3 \times 3$  matrices with a probability measure given by the Haar measure of  $U(3)$ , i.e. the unique measure that is invariant under a change of basis for the three generations, one finds a probability of 44% for nature to have taken a more ‘unusual’ choice [123]. This cannot be interpreted, however, as an indication in favour of anarchy [124, 125], as the sample (3 mixing angles and one mass ratio) is clearly too small to reconstruct the probability measure to any degree of certainty [126]. The only statement one can make is that the (very limited) data cannot rule out the anarchy hypothesis. For any values of the mixing angles one can always find a flavour model which is in better agreement with the data<sup>14</sup>.

<sup>14</sup>It has been argued [127] that this can be done without increasing the degree of complexity of the model.

$n$	$G$	$n$	$G$	$n$	$G$	$n$	$G$
4	$\Delta(6 \cdot 4^2)$	9	$(Z_{18} \times Z_6) \rtimes S_3$	13	$\Delta(6 \cdot 26^2)$	18	$(Z_{18} \times Z_6) \rtimes S_3$
5	$\Delta(6 \cdot 10^2)$	10	$\Delta(6 \cdot 10^2)$	14	$\Delta(6 \cdot 14^2)$	24	$Z_3 \times \Delta(6 \cdot 8^2)$
7	$\Delta(6 \cdot 14^2)$	11	$\Delta(6 \cdot 22^2)$	15	$Z_3 \times \Delta(6 \cdot 10^2)$		
8	$\Delta(6 \cdot 8^2)$	12	$Z_3 \times \Delta(6 \cdot 4^2)$	16	$\Delta(6 \cdot 16^2)$		

**Table 2.4:** Groups generated by  $T_3$ ,  $S_3$  and  $U(n)$ , that lead to new starting points. The series  $\Delta(6n^2)$  is defined in Eq. (A.2) and the group  $(Z_{18} \times Z_6) \rtimes S_3$ , apart from being defined by  $\langle T_3, S_3, U(9) \rangle$ , is the group number 259 of order 648 in the `SmallGroups` catalogue of GAP [128].

Considerations of anarchy might however be useful when thinking about constructing flavour models in the sense that any model should be a lot better than anarchy. Two general avenues seem to be promising:

- build models that give sharp predictions for the leptonic mixing angles in the experimentally allowed regions. These models might then be falsified in the same way that models that give tri-bimaximal mixing have been ruled out, i.e. by a further refinement of the experimental determination of these angles. This seems to be the only fruitful direction for models that explain flavour at high energy scales such as the seesaw or GUT scale, because mixing angles are generically the only experimentally testable predictions of such models.
- build models that can be tested in another sector by additional observables. Such observables typically include rare lepton flavour violating (LFV) decays of leptons and mesons and – ideally – a direct experimental access to the very fields that mediate the flavour symmetry breaking. Typically such models will feature extended Higgs sectors, but they will not uniquely determine the mixing angles, rather only giving relations among the deviations from patterns such as tri-bimaximal mixing.

The various possibilities are summarized in Fig. 2.5 and we will now discuss them in turn.

### 2.5.1. New Starting Points

As reviewed in Section 2.2, to uniquely (up to discrete permutations) determine the mixing angles from group theoretic considerations, it is essential (i) to have unbroken remnant symmetries in the charged lepton and neutrino sectors and (ii) to have enough symmetries in each sector that there are three inequivalent one-dimensional representations in each sector. For the charged lepton sector this implies the existence of at least a  $Z_3$  symmetry and for the neutrino sector one needs at least a Klein group  $Z_2 \times Z_2$  (there cannot be a cyclic group of order larger than 2 in the neutrino sector as complex representations would forbid neutrino mass terms.) The way to generate new mixing structures apart from TBM is now to embed these abelian symmetries in different ways into some larger group. Once the group and the embedding is specified, the Clebsch-Gordan coefficients of the specified group uniquely (up to permutation of rows and columns) specifies the mixing pattern. We have performed such an analysis [14]<sup>15</sup>, considering all discrete groups of order smaller than 1536 using the

<sup>15</sup>Recently a similar scan appeared [55], however, there the symmetry group of neutrinos was always taken to be  $Z_2$ , which does not allow one to predict sharp mixing patterns, but rather determines the mixing angles up to a two-parameter freedom.

computer algebra program GAP [129]. Our results can easily be presented in a systematic way: in Section 2.2, we saw that if the  $Z_3$  symmetry in the charged lepton sector is generated by the matrix  $T_3$  given in (2.25) and the Klein group is generated by the matrices  $S_3$  and  $U_3$  of Eqns. (2.27) and (2.30), the resulting mixing matrix is of the TBM form (2.31). Now, all new mixing patterns<sup>16</sup> found in the scan can be written as

$$U = U_{HPS}U_{13}(\theta = \frac{1}{2} \arg(z), \delta = 0), \quad (2.53)$$

which is the result of the remnant symmetry  $G_e = \langle T_3 \rangle \cong Z_3$  in the charged lepton sector and the choice of  $S_3$  and

$$U(n) = - \begin{pmatrix} 1 & 0 & 0 \\ 0 & 0 & z \\ 0 & z^* & 0 \end{pmatrix} \quad \text{with} \quad \langle z \rangle \cong Z_n, \quad n \in \mathbb{N} \quad (2.54)$$

as generators of a Klein group  $Z_2 \times Z_2$  in the neutrino sector. Note that for any  $z$  with modulus one, we have  $[S_3, U(n)] = 0$  and  $U(n)^2 = \mathbb{1}_3$  and therefore the group generated by  $S_3$  and  $U(n)$  is always a Klein group,  $\langle S, U \rangle \cong Z_2 \times Z_2$ . For the group generated by  $T_3$ ,  $S_3$  and  $U(n)$  to be finite,  $z$  has to be of the form given in (2.54), as may be seen by looking at the group element  $(U(n)T)^2 = \text{diag}(z, z, z^{*2})$ , which is of finite order  $n \in \mathbb{N}$  iff  $z^n = 1$ . The requirement  $\langle z \rangle \cong Z_n$  further fixes  $n$  to be the smallest  $n$  for which  $z^n = 1$ . The names of the groups generated for  $n = 4, \dots, 16$  can be found in Table 2.4 and the groups  $\Delta(96)$  ( $n = 4$ ) and  $\Delta(384)$  ( $n = 8$ ) have been obtained before in [50].

The predictions for mixing angles for all groups of order smaller than or equal to 1536 is presented in Fig. 2.6. It should be clear that if one allows for groups of arbitrary size, the parabola depicted in Fig. 2.6 will be densely covered. As one can see, the mixing patterns corresponding to  $n = 5$ ,  $n = 9$  and  $n = 16$  give a good descriptions of the leptonic mixing matrix.

If we broaden our scan and allow for arbitrary remnant abelian symmetries  $G_e$  in the charged lepton sector while keeping  $G_\nu$  fixed to being isomorphic to a Klein group, we find that up to size 511 there are no new mixing patterns apart from the known ones that can be generated by finite modular groups [50] and their subgroups. For completeness, we show these mixing patterns in Fig. 2.7. It should be appreciated that only a limited number of starting points can be realized using small groups.

### 2.5.2. Deviations from Tri-Bi-Maximal Mixing

The PMNS matrix is given by  $U = V_e^\dagger V_\nu$ , where  $V_e$  diagonalizes the charged lepton mass matrix  $M_e$  and  $V_\nu$  diagonalizes  $M_\nu$ . Therefore deviations from TBM can be categorized in two categories, namely if corrections dominantly stem from the charged lepton or the neutrino sectors. This distinction is of course meaningless within the SM as a rotation can change a charged-lepton correction into a neutrino sector correction. Within flavour models, there is however a distinction, and we will therefore focus on model building based on small groups of the form  $A_4$  etc. In particular, we will present a couple of minimal extensions of the prototype TBM model introduced in Section 2.4.

<sup>16</sup>By new mixing patterns, we mean ones that have not been found before, e.g. in a scan over finite modular groups [50].

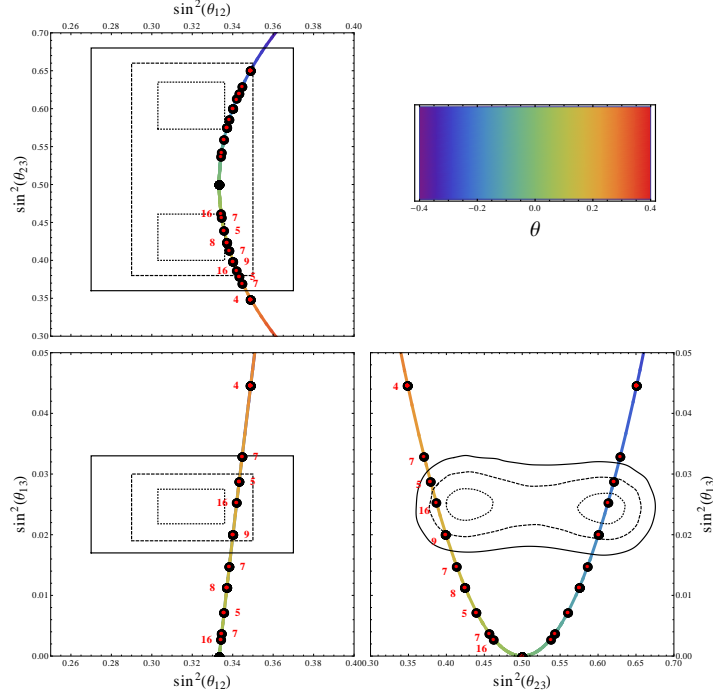


**Figure 2.6:** The new starting points that may be obtained from remnant symmetries  $G_e \cong Z_3$  and  $G_\nu \cong Z_2 \times Z_2$  originating from flavour groups of size smaller than 1536. The index  $n$  refers to the one of the generators of the Klein group (2.54). The group corresponding to  $n$  can be found in Table 2.4.

**Corrections to the neutrino mass matrix:** In Section 2.2, we discussed that a deviation from  $\theta_{13} = 0$  can be explained by a breaking of the accidental symmetry  $U$  of the neutrino mass matrix,  $M_\nu = \rho(U)^\dagger M_\nu \rho(U)$ . From Fig. 2.1, we can read off that an additional  $1 - 3$  rotation with a rotation angle of  $\theta \sim .1 - .2$  is needed.

This can easily be implemented in our prototype model of Section 2.4 by the introduction of yet another flavon field  $\tilde{\xi}$  [62, 63, 120, 130], which transforms as  $(\mathbf{1}_2, i)$  under  $A_4 \times Z_4$ , giving another leading order operator

$$\delta \mathcal{L}_\nu^{(6)} = x_c (LHLH)_{\mathbf{1}_3} \tilde{\xi} / \Lambda^2 + \text{h.c.} . \quad (2.55)$$

that contributes to the neutrino mass matrix as

$$\delta M_\nu = \frac{v^2}{2\sqrt{3}\Lambda^2} \tilde{c} \begin{pmatrix} 1 & 0 & 0 \\ 0 & \omega & 0 \\ 0 & 0 & \omega^2 \end{pmatrix}, \quad (2.56)$$

with  $\tilde{c} = x_c \tilde{w}$ . Clearly this mass matrix breaks the accidental symmetry  $U$  via the VEV  $\langle \tilde{\xi} \rangle = \tilde{w}$  of the additional singlet. In Section 4.4.2 a fully dynamical mechanism will be presented that realizes this VEV configuration. As discussed before, the mass matrix is diagonalized by the matrix  $\Omega_U U_{13}(\theta, \delta)$ . In the case where all mass entries are real, the mixing angle  $\theta$  is calculated to be

$$\tan 2\theta = \frac{\sqrt{3}\tilde{c}}{2\tilde{a} - \tilde{c}}. \quad (2.57)$$

## 2.5. Model Building Pathways Beyond Vanishing $\theta_{13}$

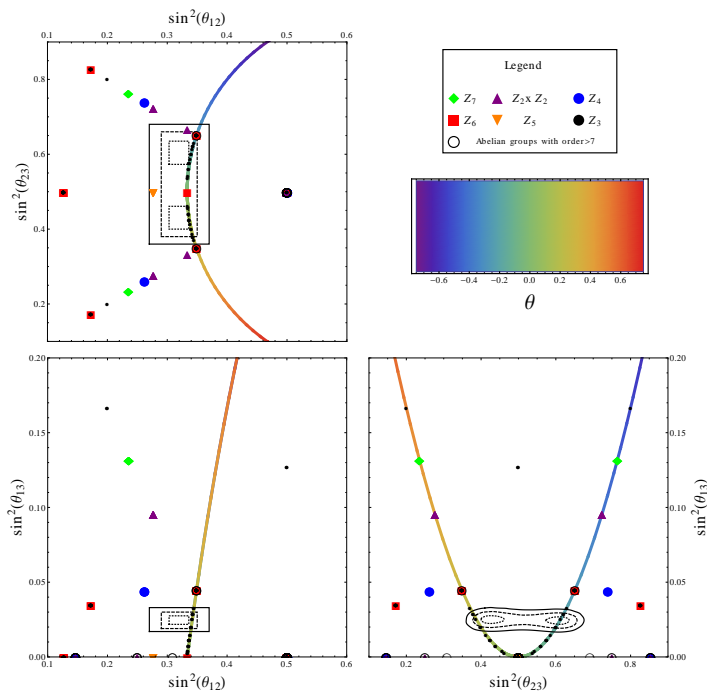


**Figure 2.7:** The starting points that may be obtained from remnant symmetries  $G_\nu \cong Z_2 \times Z_2$  and an arbitrary abelian symmetry  $G_e$ , originating from flavour groups of size smaller than 511. The structure of the group  $G_e$  is indicated by the label given in the insert. All of these groups are known from the literature and the groups interesting for phenomenology are shown in more detail in Fig. 2.6.

Note that this type of leading order correction is not as easily possible in  $S_4$  models as here the symmetry  $U$  does not emerge as an accidental symmetry of the mass matrix. If one parametrizes the deviations of the leptonic mixing matrix from tri-bimaximal mixing as [131]

$$\sin \theta_{13} = \frac{r}{\sqrt{2}} \quad \sin \theta_{12} = \frac{1}{\sqrt{3}}(1 + s) \quad \sin \theta_{23} = \frac{1}{\sqrt{2}}(1 + a) . \quad (2.58)$$

where  $r$  is the deviation of the reactor angle,  $s$  is the deviation of the solar angle and  $a$  is the deviation of the atmospheric angle, we find to first order in  $c$  the sum rule

$$a \approx -\frac{1}{2}r \cos \delta_{CP}, \quad s \approx 0, \quad (2.59)$$

where  $\delta_{CP}$  is the Dirac CP phase. Note that this information is also contained in Fig. 2.1.

One can go one step further and also break the remnant symmetry  $S$  in the neutrino mass matrix. This is what generally happens if one includes higher-dimensional operators in the neutrino sector and it has been done also at leading order in a variety of models e.g. by the introduction of additional triplets that break the symmetry and couple to neutrinos at LO. Such models generally cease to be predictive as even sum rules such as the one just presented are broken.

**Corrections to the charged lepton mass matrix:** Another possibility is to break the generator  $T$  that generates the remnant  $Z_3$  symmetry in the charged lepton sector [132–139] while keeping the generators  $S$  and  $U$  in the neutrino sector intact. If one wants to generate a correction at leading order, one can introduce another flavon field that couples to the

charged lepton  $(Le^c)\mathbf{3}_1\tilde{H}/\Lambda$  operator and therefore has to transform as a  $\mathbf{3}_1$  of  $A_4$ . To break the generator  $T$  the field has to have a different vacuum configuration from  $\chi$  but it has to transform in exactly the same way as  $\chi$  under all symmetries. It will be shown in the next section that this vacuum mismatch cannot be dynamically realized by any known mechanism for vacuum alignment, as all mechanisms depend on different transformation properties for fields that break the symmetry in different directions.

The next possibility is to appeal to higher dimensional operators that are always meant to be present and will generically always break all remnant symmetries unless one introduces further shaping symmetries. The problem with this approach is, however, that if one introduces all higher dimensional operators consistent with the symmetries of the model, one generically ends up with a large number of operators and loses much if not all of the predictive power of the models [120]. A concrete analysis can only be performed in a complete model, as for consistency one should include higher dimensional operators not only in the charged lepton, but also in the neutrino sector and in the scalar potential of the flavon fields. This will be presented for a complete dynamical model in Section 4.4.1.

A related possibility that has garnered much attention [138–140] recently is to try to connect the rather large value of  $\theta_{13}$  to the Cabibbo angle of the quark sector, which might be connected by the numerological relation

$$\theta_{13} \approx \frac{1}{\sqrt{2}}\theta_C \approx 9.2^\circ. \quad (2.60)$$

A relation between  $\theta_{13}$  and  $\theta_C$  can be rather naturally realized in models based on Grand Unified Theories (GUT) as there quark and leptons are unified into one multiplet and their mass matrices are necessarily related, albeit in a model-dependent way. However, the most famous GUT mass relation due to Georgi and Jarlskog [141], which is the result of most models based on  $SU(5)$  or  $SO(10)$ , gives

$$\theta_{13} \approx \frac{1}{3\sqrt{2}}\theta_C \approx 3.1^\circ,$$

if one assumes TBM in the neutrino sector, and is therefore too small. If one assumes the Georgi-Jarlskog operator is not there and the mass relation is due to one specific higher-dimensional operator [142], other GUT relations can be found and a more favourable value for  $\theta_{13}$  can be ‘predicted’.



## Chapter 3.

# The Vacuum Alignment Problem in Flavour Models

In Section 3.1 the vacuum alignment problem of flavour models is discussed and the two main solutions that exist in the literature are presented. In Section 3.2 a solution based on group theoretical considerations is presented and the results of a scan over a catalogue of small groups is discussed. In Section 3.3 some of the small groups found in the preceding section are introduced to set the stage for the model building efforts of the next chapter.

### 3.1. The Vacuum Alignment Problem and Solutions in the Literature

In the last chapter we have seen (in Section 2.2) how mismatched remnant symmetries of the charged lepton and neutrino mass matrices may account for structures in the leptonic mixing matrix, and in Section 2.4 how such an idea may be realized in a model based on  $A_4$ . There we had introduced two triplet flavons  $\chi, \phi \sim \mathbf{3}_1$ , where an additional symmetry makes sure that at leading order  $\chi$  only couples to charged leptons and  $\phi$  only couples to neutrinos. The vacuum configuration  $\langle \chi \rangle = (v', v', v')$  and  $\langle \phi \rangle = (u, 0, 0)$  of Eq. (2.46) realizes the breaking to two different subgroups. We will now show that the complete potential

$$V = V_\phi(\phi) + V_\chi(\chi) + V_{\text{mix}}(\chi, \phi) \quad (3.1)$$

does not admit solutions of this type, without fine-tuning the parameters in the part of the scalar potential that connects  $\phi$  and  $\chi$

$$V_{\text{mix}}(\chi, \phi) = \kappa \mathbf{3}_1(\phi\phi)_{\mathbf{3}_1}(\chi\chi)_{\mathbf{3}_1} + \left( \kappa \mathbf{1}_2(\phi\phi)_{\mathbf{1}_2}(\chi\chi)_{\mathbf{1}_3} + \text{h.c.} \right) + \rho \mathbf{3}_1 \chi(\phi\phi)_{\mathbf{3}_1},$$

via non-singlet contractions. Before discussing the full potential, it is useful to look at the potential for one of the triplets separately<sup>1</sup>

$$V_\phi = \mu_\phi^2 (\phi\phi)_{\mathbf{1}_1} + \lambda'_1 (\phi\phi)_{\mathbf{1}_1} (\phi\phi)_{\mathbf{1}_1} + \lambda'_2 (\phi\phi)_{\mathbf{1}_2} (\phi\phi)_{\mathbf{1}_3}, \quad (3.2)$$

where the cubic term is forbidden by the auxiliary  $Z_4$  symmetry (see Table 2.3). All solutions of the extremal conditions

$$0 = \frac{\partial V_\phi}{\partial \phi_i} = \frac{2}{3} \phi_i \left( \sqrt{3} \mu_\phi^2 + (2\lambda'_1 - \lambda'_2) (\phi_1^2 + \phi_2^2 + \phi_3^2) + 3\lambda'_2 \phi_i^2 \right) \quad (3.3)$$

<sup>1</sup>The operator  $(\phi\phi)_{\mathbf{3}_1} \cdot (\phi\phi)_{\mathbf{3}_1}$ , which one would naively expect, can be expressed as a linear combination of the other operators.

can be written in the form

$$\langle \phi \rangle = (u, u, u), \quad \langle \phi \rangle = (u, 0, 0) \quad \text{or} \quad \langle \phi \rangle = (u, u, 0). \quad (3.4)$$

Each of these solutions is degenerate with field configurations  $\langle \tilde{\phi} \rangle = g \langle \phi \rangle$  that are connected to these via a group transformation  $g \in A_4$ , i.e. the solutions given above are representatives of orbits of physically identical vacua. One can characterize the orbits by the conjugacy class(es)  $G \cdot Q_i = \{gQ_i g^{-1} | g \in A_4\}$  of the operators that leave the representative vacuum configuration  $\langle \phi \rangle$  invariant, i.e.  $Q_i \langle \phi \rangle = \langle \phi \rangle$ . The first vacuum configuration in (3.4) leaves  $T$  and  $T^2$  invariant, which both generate the same  $Z_3$  subgroup. The second vacuum configuration leaves invariant the  $Z_2$  subgroup generated by  $S$  and the last vacuum configuration breaks the  $A_4$  group completely. One can easily see that the Hessian  $\frac{\partial^2 V_\phi}{\partial \phi_i \partial \phi_j}$  of the third vacuum configuration  $\langle \phi \rangle = (u, u, 0)$  has two eigenvalues,

$$m_1^2 = -\frac{1}{2}m_2^2 = \frac{2\sqrt{3}\lambda'_2\mu_\phi^2}{4\lambda'_1 + \lambda'_2}, \quad m_3^2 = -\frac{4\mu_\phi^2}{\sqrt{3}},$$

that are necessarily of opposite sign, regardless of the choice of potential parameters. This field configuration therefore represents a saddle point and has no physical relevance. The first field configuration  $\langle \phi \rangle = (u, u, u)$  has the eigenvalues of the Hessian

$$m_1^2 = m_2^2 = -\frac{2\lambda'_2\mu_\phi^2}{\sqrt{3}\lambda'_1}, \quad m_3^2 = -\frac{4\mu_\phi^2}{\sqrt{3}}.$$

Combining this with the vacuum stability conditions  $\lambda'_1 > 0$ ,  $\lambda'_1 + \lambda'_2 > 0$  and  $\mu_\phi^2 < 0$ , we see that this is a (local) minimum for  $\lambda'_2 > 0$ . For the second field configuration  $\langle \phi \rangle = (u, 0, 0)$  the Hessian has the eigenvalues

$$m_1^2 = m_2^2 = \frac{\sqrt{3}\lambda'_2\mu_\phi^2}{\lambda'_1 + \lambda'_2}, \quad m_3^2 = -\frac{4\mu_\phi^2}{\sqrt{3}}.$$

and it is therefore a (local) minimum for  $\lambda'_2 < 0$ . As for the respective cases there is only one minimum, the local minima are global ones and it is therefore clear that for  $\lambda'_2 > 0$  the global minimum is of the form  $\langle \phi \rangle = (u, u, u)$  and for  $-\lambda'_1 < \lambda'_2 < 0$  it is of the form  $\langle \phi \rangle = (u, 0, 0)$ , as is shown in Fig. 3.1. In isolation, the two triplets can therefore realize the vacuum configuration required to describe lepton mixing.

To show that non-trivial cross-couplings between the two flavons forbid the mismatched VEV configuration  $\langle \chi \rangle \sim (1, 1, 1)$  and  $\langle \phi \rangle \sim (1, 0, 0)$ , it is useful to consider a slightly more general situation by looking at the potential for  $\phi$  augmented by the soft breaking terms<sup>2</sup>

$$V_{soft, Z_3} = m_s^2 (\phi_2 \phi_3 + \phi_1 \phi_2 + \phi_3 \phi_1), \quad (3.5)$$

<sup>2</sup>A symmetry is said to be softly broken if the symmetry breaking terms only have a mass-dimension smaller or equal to three. This does not change UV properties of the theory and can be considered to be a parametrization of spontaneous breaking in another sector.

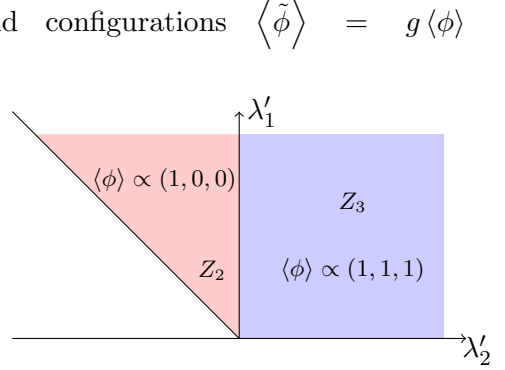


**Figure 3.1:** Phase diagram of the minimal potential of one scalar triplet of  $A_4$ .

### 3.1. The Vacuum Alignment Problem and Solutions in the Literature

which parametrizes the symmetry breaking of  $A_4$  to  $\langle T \rangle \cong Z_3$ , regardless of the details of how  $A_4$  is broken to  $\langle S \rangle \cong Z_3$ , and under which  $\phi$  transforms as  $\phi_1 \rightarrow \phi_2 \rightarrow \phi_3 \rightarrow \phi_1$ . The resulting minimization conditions

$$0 = \left\langle \left[ \frac{\partial V_\phi + V_{soft,Z_3}}{\partial \phi_i} \right] \right\rangle = m_s^2 u, \quad i = 2, 3 \quad (3.6)$$

thus require  $m_s^2 = 0$ , which requires a fine-tuning of potential parameters. On the contrary, the soft-breaking terms that respect the same  $Z_2$  symmetry  $\langle S \rangle$  as the VEV  $\langle \phi \rangle$  do not disturb the structure of the minimization conditions. However, if one looks at the minimization conditions for the flavon  $\chi$  with potential

$$V_\chi = \mu_0^2 (\chi\chi)_{\mathbf{1}_1} + \rho (\chi\chi\chi)_{\mathbf{1}_1} + \lambda_1 (\chi\chi)_{\mathbf{1}_1} (\chi\chi)_{\mathbf{1}_1} + \lambda_2 (\chi\chi)_{\mathbf{1}_2} (\chi\chi)_{\mathbf{1}_3}, \quad (3.7)$$

with the soft-breaking terms

$$V_{soft,Z_2} = m_A^2 \chi_1^2 + m_B^2 \chi_2^2 + m_C^2 \chi_2 \chi_3 \quad (3.8)$$

which parametrize the symmetry breaking of  $A_4$  to  $\langle S \rangle \cong Z_2$ , regardless of the details of how  $A_4$  is broken to  $\langle S \rangle \cong Z_2$ , one finds

$$0 = \left[ \frac{\partial V}{\partial \chi_1} \right]_{\chi_i=v'} = \frac{2}{\sqrt{3}} \left( m_0^2 + \sqrt{3} m_A^2 \right) v' + 4\lambda_1 v'^3, \quad (3.9a)$$

$$0 = \left[ \frac{\partial}{\partial \chi_2} V - \frac{\partial}{\partial \chi_3} V \right]_{\chi_i=v'} = 2 m_B^2 v', \quad (3.9b)$$

$$0 = \left[ \frac{\partial}{\partial \chi_1} V - \frac{\partial}{\partial \chi_3} V \right]_{\chi_i=v'} = (2 m_A^2 - m_C^2) v'. \quad (3.9c)$$

The vacuum alignment thus requires  $m_B^2 = 0$  and  $m_C^2 = 2m_A^2$  and therefore two completely different  $A_4$  contractions need to have the same coupling in the scalar potential, an option we exclude as fine-tuning. Again in this case soft breaking terms that respect the same symmetry  $\langle T \rangle \cong Z_3$  as  $\langle \chi \rangle$  do not change the structure of the minimization conditions. Even if one sets the terms  $m_{s,A,B,C}^2$  to zero, they will still be generated at loop-level and disturb the VEV alignment. The breaking of  $A_4$  to two different subgroups thus requires a systematic mechanism to forbid  $m_{s,A,B,C}^2$ .

In the specific example given above, where the communication between the two sectors proceeds via non-trivial couplings in the scalar potential, the soft breaking terms may be expressed in terms of those couplings as

$$m_A^2 = \frac{u^2}{2} \left( \text{Re} \kappa_{\mathbf{1}_2} + \frac{\text{Im} \kappa_{\mathbf{1}_2}}{\sqrt{3}} \right), \quad m_B^2 = \frac{2u^2 \text{Im} \kappa_{\mathbf{1}_2}}{\sqrt{3}}, \quad m_s^2 = \frac{v'}{\sqrt{3}} \left( v' \kappa_{\mathbf{3}_1} + \rho_{\mathbf{3}_1} \right),$$

while  $m_C^2$  is only created at higher order. Hence, the minima with two different subgroups cannot be realized as global minima of the most general scalar potential, without fine-tuning the parameters that connect the two sectors. This can be also seen from Fig. 3.2, where the distribution of the opening angle between the VEVs of the two triplet fields  $\phi$  and  $\chi$  is plotted for a random scan over order one parameters of the most general scalar potential. In agreement with our analytical study, one can identify three different phases of the theory: (i) one phase

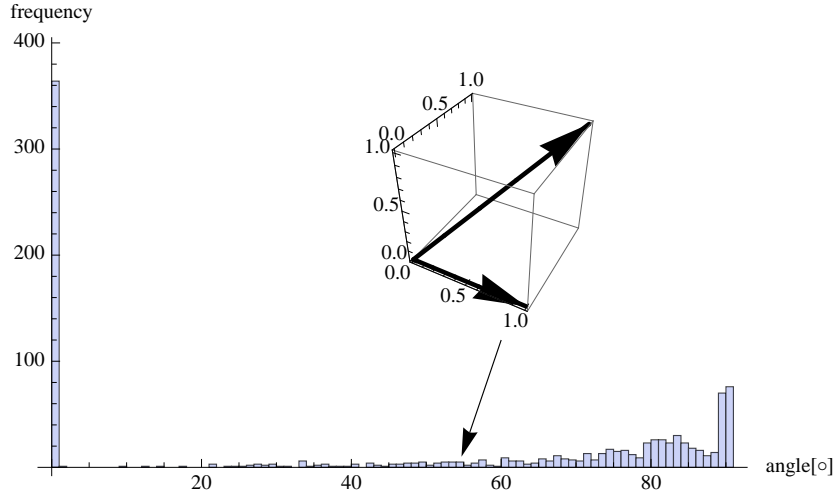


**Figure 3.2:** Distribution of the opening angle spanned by the two flavon fields for random values of potential parameters for the most general scalar potential given in Eq. (3.1). The tri-bimaximal vacuum configuration depicted in the inlay corresponds to an opening angle of  $54.7^\circ$ . As discussed in the text, the figure shows that there is no phase where this vacuum configuration is realized, but rather two phases can be identified: one phase where both flavons conserve the same subgroup and point in the same direction (angle=0) and one phase where the symmetry is broken completely. The TBM vacuum is part of the later phase but it is not special.

where both VEVs are aligned in the  $(1, 0, 0)$  direction and conserve a  $Z_2$  subgroup, (ii) another phase where both VEVs are aligned, but this time in the  $Z_3$ -conserving  $(1, 1, 1)$  direction and (iii) a third phase where the symmetry is broken completely. The VEV configuration Eq. (2.46) is part of this phase but it is only realized on a smaller dimensional sub-manifold of couplings, indicating fine-tuning<sup>3</sup>. The discussion using soft-breaking terms makes it clear that this problem cannot be solved by the introduction of additional singlets and the like, but rather requires additional ingredients, which – this being particle physics after all – means additional symmetries. The symmetry should forbid all couplings between the flavon sectors that break  $A_4$  to  $Z_2$  and  $Z_3$ , respectively, except for the quartic coupling where both couple in pairs to singlets. This is equivalent to demanding that there are two independent  $A_4$  symmetries  $A_4^v \times A_4^f$  in the flavon potential, under which  $\phi$  transforms only under the first group factor,  $\phi \sim (\mathbf{3}_1, \mathbf{1}_1)$  and  $\chi \sim (\mathbf{1}_1, \mathbf{3}_1)$ . This cannot be a symmetry of the entire Lagrangian, however, as it must be broken by couplings to the leptons (e.g. the ones given in Eqs. (2.44) and (2.45)).

Note, that the Kronecker product  $\mathbf{3} \times \mathbf{3} = \mathbf{1}_1 + \mathbf{1}_2 + \mathbf{1}_3 + \mathbf{3}_S + \mathbf{3}_A$  allows couplings of the form  $(\chi\chi)\mathbf{1}_2(\phi\phi)\mathbf{1}_3$ ,  $(\chi\chi)\mathbf{1}_3(\phi\phi)\mathbf{1}_2$  and  $(\chi\chi)\mathbf{3}(\phi\phi)\mathbf{3}$  in the minimal  $A_4$  model discussed above and the desired vacuum alignment is thus not possible, without some additional mechanism. This kind of coupling cannot be forbidden by assigning  $\chi$  or  $\phi$  to a unitary representation of an additional internal symmetry group commuting with the flavour group, because non-trivial contractions such as  $(\chi^\dagger\chi)\mathbf{3}$  and  $(\phi^\dagger\phi)\mathbf{3}$  will always be invariant under the commuting group. In particular, it is not possible to forbid the coupling by introducing an additional commuting group factor, which is a discrete group or a compact Lie group.

Setting these couplings to zero cannot be considered a viable option as loop effects such as

<sup>3</sup>For a recent attempt to characterize the fine-tuning of a new physics model by the Hausdorff dimension of the phenomenologically allowed sub-manifold of couplings, see [143]. Here we follow [87] and demand that for a natural model the alignment is realized ‘in a whole region of the parameter space’. We will come back to this in detail later.

### 3.1. The Vacuum Alignment Problem and Solutions in the Literature

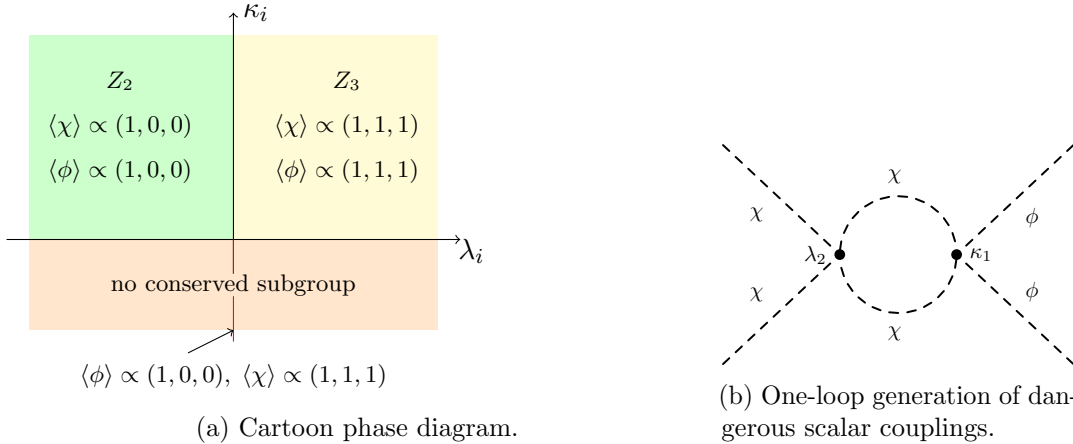


**Figure 3.3:** The left hand side shows the schematic phase diagram that emerges from the discussion of the potential given in Eq. (3.1). There are parts of parameter space where the symmetry is broken to the subgroups  $Z_3$  and  $Z_2$  respectively and a part of parameter space where the symmetry is broken totally. The TBM vacuum configuration Eq. (2.46) is part of this phase but it is only realized on a smaller dimensional sub-manifold. This requires a tuning of parameters as quantum corrections will push away from this manifold, even if one somehow starts on it. This is illustrated in the figure on the right-hand side.

the one depicted in Fig. 3.3b and renormalization group running will generate these couplings, as they are not protected by symmetries. Also it would severely limit the predictive power of these theories as one would have to fine-tune scalar couplings instead of Yukawa couplings. For this reason, the vacuum alignment problem has been mainly studied within the context of supersymmetric models as well as in extra-dimensional models using brane constructions. In the following two sections we will briefly review these approaches and we will then show how the required vacuum alignment can be achieved with an internal symmetry group by extending the flavour group in a non-trivial way.

#### 3.1.1. Supersymmetric Models with R-Symmetries

In supersymmetric models there is another possibility to arrange for the correct vacuum alignment if one introduces a continuous R-symmetry [69]. While we do not give a review of supersymmetry, we briefly recall the notion of R symmetries. Under an R-symmetry different components of the same superfields transform differently. We use a superfield notation<sup>4</sup> under which a chiral superfield

$$\Phi(\theta) = \phi + \theta\psi + \theta^2 F \quad (3.10)$$

can be written as an expansion in the superspace coordinate  $\theta^\alpha$ , which is a Weyl spinor of the Lorentz group. The expansion parameters are the components of the chiral superfield, namely the scalar  $\phi$ , the Weyl fermion  $\psi$  and the auxiliary field  $F$ . A continuous  $U(1)_R$  symmetry then acts as

$$\Phi(\theta) \rightarrow e^{iR_\Phi\alpha}\Phi(\theta e^{-i\alpha}), \quad V(\theta) \rightarrow V(\theta e^{-i\alpha}), \quad (3.11)$$

where  $R_\Phi$  denotes the R-charge of the chiral superfield  $\Phi$  and  $V$  is a vector superfield. While the gaugino always has R-charge 1, the R-charges of the component fields of  $\Phi$  are given by

$$R(\phi) = R_\Phi, \quad R(\psi) = R_\Phi - 1. \quad (3.12)$$

<sup>4</sup>For an introduction to these concepts, see e.g. [144].

A supersymmetric Lagrangian

$$\mathcal{L} = \int d^4\theta K + \left( \int d^2\theta W + \text{h.c.} \right) \quad (3.13)$$

is invariant under this symmetry if  $R(K) = 0$  and  $R(W) = 2$ . In the MSSM, if one assigns an R-charge of  $1/3$  to all chiral superfields, of the SUSY conserving terms only the  $\mu$ -term  $\mu H_u H_d$  is forbidden. As this term is needed for electroweak symmetry breaking, one usually introduces the discrete R-symmetry

$$\Phi(\theta) \rightarrow \pm \Phi(-\theta) \quad (3.14)$$

which is called *R-parity*. Under this symmetry, the MSSM fields  $Q$ ,  $U^c$ ,  $D^c$ ,  $L$ , and  $E^c$  are odd, and  $H_u$  and  $H_d$  are even. Since the gauginos are also odd, all supersymmetric partners of SM fields are odd and the lightest of these fields is therefore stable and a dark matter candidate. R-parity also forbids all renormalizable operators that break baryon or lepton numbers and stabilizes the lightest superpartner.

So how can a continuous R-symmetry be helpful to solve the vacuum alignment problem in flavour models? The first thing to notice is that if one introduces a chiral superfield with  $U(1)_R$  charge 2, terms in the superpotential  $W$  are at most linear in this field. If we demand that the R symmetry should contain the MSSM R-Parity, the chiral superfields  $Q$ ,  $U^c$ ,  $D^c$ ,  $L$ , and  $E^c$  should have R-charge 1 and  $H_u$  and  $H_d$  should have R-charge zero. This of course also fixes the R-charges of the flavons to be zero, as to allow the interactions

$$\begin{aligned} W \supset & y_e(L\chi)_{\mathbf{1}_1} e^c H_d / \Lambda + y_\mu(L\chi)_{\mathbf{1}_3} \mu^c H_d / \Lambda + y_\tau(L\chi)_{\mathbf{1}_2} \tau^c H_d / \Lambda + \\ & + (LH_u LH_u)_{\mathbf{1}_1} (x_a \xi + \tilde{x}_a \tilde{\xi}) / \Lambda^2 + x_d (LH_u LH_u)_{\mathbf{3}_1} \cdot \phi / \Lambda^2 \end{aligned} \quad (3.15)$$

that correspond to the interactions given in Eq.(2.45), which lead, in conjunction with the symmetry breaking pattern

$$\langle \chi \rangle = (v', v', v'), \quad \langle \phi \rangle = (u, 0, 0), \quad \langle \xi \rangle = w, \quad (3.16)$$

to the tri-bimaximal mixing pattern, as discussed in Section 2.4. Note that an abelian symmetry  $Z_3$  is again employed to separate the charged lepton and neutrino sectors. To get the correct vacuum alignment, it is necessary to introduce for every flavon  $\varphi$  an additional chiral superfield  $\varphi_0$  with R-charge 2 that transforms in the same way as the original field under  $A_4$  and  $Z_3$ . These fields are commonly referred to as *driving fields*. Furthermore, it is necessary to introduce an additional singlet flavon  $\tilde{\xi}$ , which transforms in the same way as  $\xi$ . The complete particle content is summarized in Table 3.1.

The superpotential containing the driving fields and flavon fields is given by

$$\begin{aligned} W_D = & M(\chi_0 \chi) + g(\chi_0 \chi \chi) \\ & + g_1(\phi_0 \phi \phi) + g_2 \tilde{\xi}(\phi_0 \phi) + g_3 \xi_0(\phi \phi) + g_4 \xi_0 \xi^2 + g_5 \xi_0 \xi \tilde{\xi} + g_6 \xi_0 \tilde{\xi}^2. \end{aligned} \quad (3.17)$$

Each contraction is uniquely determined, as not more than 3 triplets are contracted here. The two a priori identical fields  $\xi$  and  $\tilde{\xi}$  have been rotated such that only  $\tilde{\xi}$  couples to  $(\phi_0 \phi)$ . To determine the vacuum alignment, one has to minimize the scalar potential

$$V = V_{\text{SUSY}} + V_{\text{soft}}, \quad (3.18)$$

### 3.1. The Vacuum Alignment Problem and Solutions in the Literature

	$L$	$e^c$	$\mu^c$	$\tau^c$	$H_{u,d}$	$\chi$	$\phi$	$\xi$	$\tilde{\xi}$	$\chi_0$	$\phi_0$	$\xi_0$
$A_4$	$\mathbf{\underline{3}}_1$	$\mathbf{\underline{1}}_1$	$\mathbf{\underline{1}}_2$	$\mathbf{\underline{1}}_3$	$\mathbf{\underline{1}}_1$	$\mathbf{\underline{3}}_1$	$\mathbf{\underline{3}}_1$	$\mathbf{\underline{1}}_1$	$\mathbf{\underline{1}}_1$	$\mathbf{\underline{3}}_1$	$\mathbf{\underline{3}}_1$	$\mathbf{\underline{1}}_1$
$Z_3$	$\omega$	$\omega^2$	$\omega^2$	$\omega^2$	1	1	$\omega$	$\omega$	$\omega$	1	$\omega$	$\omega$
$U(1)_R$	1	1	1	1	0	0	0	0	0	2	2	2

**Table 3.1:** Particle content of the SUSY  $A_4$  model. The driving fields with R-charge 2 are needed to realize the correct vacuum alignment.

where  $V_{\text{SUSY}}$  is the SUSY conserving part of the scalar potential,

$$V_{\text{SUSY}} = \sum_i \left| \frac{\partial W}{\partial \varphi_i} \right|^2, \quad (3.19)$$

and  $V_{\text{soft}}$  denotes the soft-breaking terms. If we assume the scale of flavour breaking to be much larger than the soft-terms, we can solve the equations in the supersymmetric limit:

$$0 = \frac{\partial W_D}{\partial \chi_{0,i}} = \frac{1}{\sqrt{3}} (M\chi_i + g\chi_{\{i+1\}}\chi_{\{i+2\}}), \quad (3.20)$$

$$0 = \frac{\partial W_D}{\partial \phi_{0,i}} = \frac{1}{\sqrt{3}} (g_2\tilde{\xi}\phi_i + g_1\phi_{\{i+1\}}\phi_{\{i+2\}}), \quad (3.21)$$

$$0 = \frac{\partial W_D}{\partial \xi_{0,i}} = g_4\xi^2 + g_5\xi\tilde{\xi} + g_6\tilde{\xi}^2 + \frac{g_3}{\sqrt{3}}(\phi_1^2 + \phi_2^2 + \phi_3^2), \quad (3.22)$$

where we have used the notation  $\{i\} = i \bmod 3$ . These equations have as a solution the desired vacuum configuration given in Eq. (3.16), with

$$\langle \tilde{\xi} \rangle = 0, \quad v' = -\frac{M}{g}, \quad u^2 = -\frac{\sqrt{3}g_4}{g_3}w^2, \quad (3.23)$$

where  $w$  remains undetermined. This is indicative of a flat direction in the potential that has to be stabilized in some way [145]. Recently the cosmological implications of these flat directions have been studied and they were found to be in conflict with the standard thermal history of the universe [146].

The effect of adding soft supersymmetry breaking terms has been studied in [147] where it was shown that these can give rise to non-vanishing VEVs of the scalar components of the driving fields and the auxiliary components of the flavon fields. This may have unwanted phenomenological consequences in the form of large lepton flavour violating interactions and thus probably requires another solution to the SUSY flavour problem in terms of gauge mediation [148] or via a separate mechanism (see e.g. [149]). The vacuum alignment problem is only solved in the limit where the flavour breaking scale is much larger than the supersymmetry breaking scale, and all the driving fields etc. therefore have to be unobservably heavy.

Let us take a step back and ask ourselves why this non-trivial setup is able to solve the vacuum alignment problem. This can be readily understood once one realizes that at the renormalizable level  $W_D$  exhibits an ‘accidental’ symmetry  $A_4^v \times A_4^f$ , under which  $\phi$  and  $\phi_0$  transform only under the first group factor,  $\phi, \phi_0 \sim (\mathbf{\underline{3}}_1, \mathbf{\underline{1}}_1)$  and  $\chi, \chi_0 \sim (\mathbf{\underline{1}}_1, \mathbf{\underline{3}}_1)$ .

### 3.1.2. Extra-Dimensional Models

One almost obvious possibility to solve the vacuum alignment problem is to physically separate the two flavon fields by localizing them on different branes in an extra-dimensional space-time [9]. In the easiest case, the spacetime is assumed to be the product of a Minkowski space-time and an interval stretching from  $y = 0$  to  $y = R$ . If one localizes the field  $\chi$  on a brane at  $y = 0$  with potential

$$V_\chi = \mu_0^2 (\chi\chi)_{\mathbf{1}_1} + \rho (\chi\chi\chi)_{\mathbf{1}_1} + \lambda_1 (\chi\chi)_{\mathbf{1}_1} (\chi\chi)_{\mathbf{1}_1} + \lambda_2 (\chi\chi)_{\mathbf{1}_2} (\chi\chi)_{\mathbf{1}_3} \quad (3.24)$$

and the field  $\phi$  on a brane at  $y = R$  with

$$V_\phi = \mu_0'^2 (\phi\phi)_{\mathbf{1}_1} + \lambda_1' (\phi\phi)_{\mathbf{1}_1} (\phi\phi)_{\mathbf{1}_1} + \lambda_2' (\phi\phi)_{\mathbf{1}_2} (\phi\phi)_{\mathbf{1}_3} \quad (3.25)$$

from the discussion in the last section it is clear that there is finite range of parameters for which the total potential energy  $\int d^4x [V_\chi + V_\phi]$  has the global minimum  $\langle \chi \rangle = (v', v', v')$  and  $\langle \phi \rangle = (u, 0, 0)$ . Obviously the vacuum alignment problem is again solved by engineering an ‘accidental’ symmetry  $A_4^v \times A_4^f$ .

To generate the effective lepton operators one has to localise  $e^c$ ,  $\mu^c$  and  $\tau^c$  at the brane at  $y = 0$  and  $L$  at the brane at  $y = R$ . The neutrino mass operator  $(LHLH)\phi$  can then be written down as a local interaction at the brane at  $y = R$  while the charged lepton mass operator  $(L\tilde{H}\ell^c)\chi$  connects fields that are localised at different branes. One therefore has to introduce an additional fermionic field  $F(x, y) = (F_1, \overline{F_2})$  that lives in the bulk, transforms as a triplet under  $A_4$  and has the same SM quantum numbers  $(1, 1, -1)$  as a right-handed lepton. Via the brane localized interactions

$$S \supset \int d^4x dy Y_e e^c (\chi F_1) \delta(y) + Y_L (F_2 L) H \delta(y - R),$$

one can generate the charged lepton Yukawa couplings. One loop interactions involving  $F$  also generate the dangerous couplings that connect  $\phi$  and  $\chi$  via non-trivial singlets. These interactions lead to a shift in the vacuum expectation values, but they are naturally small, being suppressed by  $1/(R\Lambda)^4$ . The setup of this model can be transferred to the case of warped extra dimensions [150, 151], where the flavour symmetry might help to ameliorate bounds from flavour observables [150, 152]. However, also in this case the flavour symmetry breaking scale is usually high.

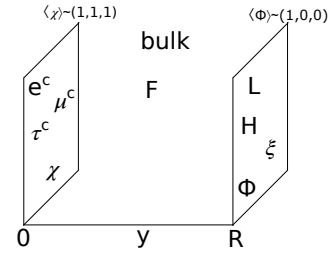


**Figure 3.4:** Sketch of an extra-dimensional model that solves the vacuum alignment problem. The fields  $e^c$ ,  $\mu^c$  and  $\tau^c$  are localized at the brane at  $y = 0$  and  $L$  is localized at  $y = R$ .

## 3.2. Group Extensions and Vacuum Alignment

### 3.2.1. Generalities about the Vacuum Alignment Problem

The distilled wisdom of the solutions of the vacuum alignment problem we have studied so far is that one needs to engineer the particle content and symmetries of the model such that there emerges an accidental symmetry  $A_4^v \times A_4^f$  in the scalar potential that separates the flavons of the neutrino and charged lepton sectors. While the approaches outlined above make use



### 3.2. Group Extensions and Vacuum Alignment

of well-known ingredients in a model builder's toolbox, the concrete implementations in the literature (which are mostly based on SUSY models with continuous R-symmetries) require a plethora of unobservable new fields that live in a cascade of hidden sectors, each solving the technical problem the last model building trick has brought up. For example, to realize the flavour structure one has to introduce flavons, to realize their VEV structure one introduces driving fields and to lift their flat directions and to break the  $U(1)_R$  symmetry one introduces yet additional fields. One is left with models that have only lepton mixing angles as their (usually wrong) experimental predictions.

It is therefore of paramount importance to find new solutions to the vacuum alignment problem that realize the accidental symmetry in a more economical way, preferably such that the symmetry breaking may be realized at an energy scale at which it can be experimentally tested. A first step in this direction was made by Babu and Gabriel [153], who have suggested a group-theoretical mechanism to forbid the dangerous cross-couplings and thus a way to realise the VEV alignment without using R-symmetries in supersymmetry or brane constructions.

They proposed an extension of the flavour group  $A_4$  in such a way that the Standard Model leptons only transform under the  $A_4$  subgroup of the full flavour group. In the scalar sector, the flavon  $\chi$  of the charged lepton sector also transforms only under the  $A_4$  subgroup, while the flavon  $\phi$  of the neutrino sector transforms under the full flavour group  $G$ . For a suitably chosen group  $G$ , it is then possible that the additional group transformations forbid the contractions  $(\phi\phi)_{\mathbf{1}_{2,3}}$  and  $(\phi\phi)_{\mathbf{3}_1}$ , which lead to the dangerous couplings in the scalar potential and make the correct vacuum alignment impossible. In other words, the additional discrete symmetry leads to an accidental symmetry at the renormalizable level in the flavon potential,  $G \times A_4$ , allowing for a different breaking of the two  $A_4$  subgroups of the accidental symmetry. The coupling to leptons only respects the diagonal  $A_4$  subgroup, which is thus broken to different subgroups in the charged lepton and neutrino sectors, as desired.

Note that this construction requires that the additional group generators cannot all commute with the generators of  $A_4$ , i.e. the flavour group  $G$  cannot be a direct product of  $A_4$  with some other group. It thus has to be a non-trivial extension of  $A_4$ . Such extensions can come in the form of semidirect products or non-split extensions and have been introduced in Section 2.3.1.

In their work, Babu and Gabriel used a special type of semidirect product, a so-called *wreath product* of  $A_4$  with  $S_3$ , i.e. the product of four factors of  $S_3$  which are evenly permuted by the group  $A_4$ . It is thus a very complicated flavour group of order  $12 \cdot 6^4 = 15552$  and requires the use of very large representations up to dimension 48. This model further suffers from a fine-tuning problem, as the diagonal and off-diagonal elements of the neutrino mass matrix are generated by operators with very different mass dimension, 5 and 10, even though both entries should be of comparable size.

In the remainder of this and in the following chapter, we address these issues and are present the result of a search for simpler and more attractive semidirect product groups  $G = N \rtimes H$  as well as general group extensions  $G$  satisfying  $G/N \cong H$  with  $H$  being  $A_4$ ,  $T_7$ ,  $S_4$ ,  $T'$  or  $\Delta(27)$ <sup>5</sup>, which lead to an accidental symmetry  $G \times H$  in the flavon potential at the renormalizable level. We include all discrete groups up to order 1000 in our search and find several candidate groups. The smallest candidate groups are of order 96, in particular the semidirect product group of the quaternion group with  $A_4$ ,  $Q_8 \rtimes A_4$ , which we discuss in more detail in Section 3.3. This group does not have representations of size larger than four and, in the model we present in

<sup>5</sup>This mechanism is of course not limited to these five groups, but is also relevant for other flavour groups, such as the ones generating new starting points with  $\theta_{13} \neq 0$  discussed in Section 2.5.1.

Chapter 4, on-and-off-diagonal entries in the neutrino mass matrix are generated at the same order.

In the following, we explain the type of groups we are searching for and why we are searching for them. We always use the group  $A_4$  as an example, but the arguments hold for any group. In a first step, we directly extend the group by adding new generators which do not commute with the generators of the flavour group. In the second subsection, we generalize our approach and look for general (non-split) group extensions. The group theoretical notions we use are defined in the footnotes of this section.

### 3.2.2. Semidirect Product Groups

To reproduce the success of  $A_4$  models, we search for an extended flavour group

$$G = \langle S, T, X_1, \dots, X_n | S^2 = T^3 = (ST)^3 = r_\alpha^X(X_1, \dots, X_n) = r_\beta^{\text{mix}}(S, T, X_1, \dots, X_n) = 1 \rangle$$

that contains  $H = \langle S, T | S^2 = T^3 = (ST)^3 = 1 \rangle \simeq A_4$  as a subgroup. Here  $X_i$  denote the additional generators of the extended group and  $r_\alpha^X, r_\beta^{\text{mix}}$  with  $\alpha = 1, \dots, s_\alpha$  and  $\beta = 1, \dots, s_\beta$  denote additional relations between the generators, which we do not specify here. Note that there are no additional relations involving only  $S$  and  $T$ . As we discussed in the last section, not all of the additional generators can commute with  $H$  as then it would always be possible to contract the indices such that  $(\phi\phi)$  does not transform under the additional generators but transforms under  $S$  and/or  $T$ . Therefore there have to be non-trivial relations  $r_\beta^{\text{mix}}$  to forbid the dangerous couplings discussed in scalar potential. Any discrete group that contains  $H$  as subgroup can be written in this way.

We further demand that there should be representations  $\rho_{\mathbf{i}} : G \rightarrow GL(V)$  with

$$\rho_{\mathbf{i}}(X_j) = \mathbb{1} \quad \forall j = 1, \dots, n \quad (3.26)$$

where  $\rho_{\mathbf{i}}(S)$  and  $\rho_{\mathbf{i}}(T)$  corresponding to the usual  $A_4$  representations  $\mathbf{i} = \underline{\mathbf{1}}_1, \underline{\mathbf{1}}_2, \underline{\mathbf{1}}_3$  and  $\underline{\mathbf{3}}$ , e.g.

$$\rho_{\underline{\mathbf{3}}}(S) = \begin{pmatrix} 1 & 0 & 0 \\ 0 & -1 & 0 \\ 0 & 0 & -1 \end{pmatrix}, \quad \rho_{\underline{\mathbf{3}}}(T) = \begin{pmatrix} 0 & 1 & 0 \\ 0 & 0 & 1 \\ 1 & 0 & 0 \end{pmatrix}. \quad (3.27)$$

If the SM fermions are assigned to these representations, the  $A_4$  predictions for the mixing angles remain unchanged. The existence of the representation  $\rho \equiv \rho_{\underline{\mathbf{3}}}$  gives a first constraint on the flavour group  $G$ : the image of the representation  $\rho$  is isomorphic to  $H$ , i.e.  $\text{im}(\rho) \cong H$ , and its kernel is a normal subgroup of  $G$  with the quotient group <sup>6</sup>  $G/N \cong \text{im}(\rho) \cong H$  (by the first isomorphism theorem). The representation  $\rho$  thus essentially defines a surjective homomorphism from  $G$  onto  $H$ , which is the identity on  $H$  and whose kernel is  $N$ . Groups of this type are known as semidirect product groups  $G = N \rtimes H$ , which is a generalisation of the direct product  $N \times H$  and has been introduced in Eq. (2.35). Again, as  $N$  and  $H$  cannot commute,  $G$  can not be trivial, i.e.  $G \neq N \times H$ .

Once we have found such a group we can assign the lepton doublets, charged leptons and the flavon  $\chi$  that couples to the charged lepton sector in the usual way to representations  $\underline{\mathbf{3}}$  and  $\underline{\mathbf{1}}_i$ ,  $i = 1, 2, 3$ , while assigning the flavon  $\phi$  of the neutrino sector to an irreducible representation

<sup>6</sup>The *quotient group*  $G/N$  is defined by the set of the left cosets  $gN$  with  $g \in G$ .

### 3.2. Group Extensions and Vacuum Alignment

Subgroup $H$	Order of $G$	GAP	Structure Description	$Z(G)$
$A_4$	96	204	$Q_8 \rtimes A_4$	$Z_2$
	288	860	$T' \rtimes A_4$	
	384	617, 20123	$((Z_2 \times Q_8) \times Z_2) \times A_4$	
	576	8273	$(Z_2.S_4) \times A_4$	
	768	1083945	$(Z_4.Z_4^2) \times A_4$	$Z_4$
		1085279	$((Z_2 \times Q_{16}) \times Z_2) \times A_4$	$Z_2$
$S_4$	192	1494	$Q_8 \rtimes S_4$	$Z_2$
	384	18133, 20092	$(Z_2 \times Q_8) \times S_4$	$Z_2$
		20096	$((Z_4 \times Z_2) \times Z_2) \times S_4$	$Z_4$
	576	8282	$T' \rtimes S_4$	$Z_2$
		8480	$(Z_3 \times Q_8) \times S_4$	$Z_6$
	768	1086052, 1086053	$((Z_2 \times Q_8) \times Z_2) \times S_4$	$Z_2$
	960	11114	$(Z_5 \times Q_8) \times S_4$	$Z_{10}$
$T'$	192	1022	$Q_8 \rtimes T'$	$Z_2^2$
	648	533	$\Delta(27) \times T'$	$Z_3$
	768	1083573, 1085187	$((Z_2 \times Q_8) \times Z_2) \times T'$	$Z_2^2$

**Table 3.2:** Candidate groups  $G$  up to order 1000 that may be written as non-trivial semidirect products  $G = N \rtimes H$  for the groups  $H = A_4, T_7, S_4, T', \Delta(27)$  and that lead to an enhanced symmetry in the scalar potential making the correct vacuum alignment possible. No such groups were found for  $H = T_7, \Delta(27)$ . Details of the groups may be accessed using the computer algebra system GAP by using the command `SmallGroup(Order, GAP)`.  $Q_8$  denotes the quaternion group, which is defined in Section 3.3 and the generalized quaternion group of order 16,  $Q_{16}$ , is defined by  $Q_{16} = \langle x, y | x^8 = 1, x^2 = y^4, y^{-1}xy = y^{-1} \rangle$ . The expression of the form  $N.H$  is the GAP notation of a central extension, i.e.  $N$  is a normal subgroup of  $G$ , which is contained in the centre of  $G$ , and  $H$  is the quotient group  $G/N \cong H$ . Note that there can be more than one semidirect product of  $N$  by  $H$ .

of  $G$ , which is faithful<sup>7</sup> on  $N$ , and contains  $\mathbf{3}$  in the Kronecker product  $\phi^n$  at some order  $n$ . The problematic cross-couplings  $(\chi\chi)\mathbf{1}_2(\phi\phi)\mathbf{1}_3$ ,  $(\chi\chi)\mathbf{1}_3(\phi\phi)\mathbf{1}_2$  and  $(\chi\chi)\mathbf{3}(\phi\phi)\mathbf{3}$  can now be forbidden, provided that the Kronecker product  $\phi \times \phi$  does not contain the representations  $\mathbf{3}$  as well as  $\mathbf{1}_2, \mathbf{3}$ . Thus, the flavon potential of  $\phi$  and  $\chi$  exhibits an ‘accidental’ symmetry  $G \times H$  at the renormalizable level. This accidental symmetry is broken to  $G$  at higher order in the flavon potential. We thus systematically search for flavour groups  $G$  containing a subgroup  $H$  and a normal subgroup  $N$  satisfying  $G/N \cong H (\cong A_4)$ , which lead to an ‘accidental’ symmetry  $G \times H$  in the renormalizable part of the flavon potential. Using the computer algebra system GAP [129] and its `SmallGroups` catalogue [128], we perform a scan over all discrete groups  $G$  up to order 1000. As the vacuum alignment problem is not specific to the group  $A_4$ , we search for semidirect product groups  $N \rtimes H$  with the desired properties for the groups  $H = A_4, T_7,$

<sup>7</sup>A representation  $\phi$  is *faithful*, if the homomorphism  $\phi : G \rightarrow \text{GL}(V)$  is injective. It is *faithful on a subgroup*  $N$ , if  $\phi|_N$  is faithful. If this representation  $\phi$  was not faithful on  $N$ , it would be possible to restrict to the smaller group  $G/\ker \phi|_N$  (by the third isomorphism theorem), which leads to the same flavour structure, and study its predictions.

$S_4$ ,  $T'$  and  $\Delta(27)$ , which are known to be interesting for flavour model building and have been introduced in Section 2.3.1. We apply the following conditions:

1.  $G = N \rtimes H \neq N \times H$  with  $H$  being one of the groups  $A_4$ ,  $T_7$ ,  $S_4$ ,  $T'$  or  $\Delta(27)$ ;
2. there is an irreducible representation  $\phi$ , which is faithful on  $N$ ;
3.  $\phi^n$  contains  $\underline{\mathbf{3}}$  for some  $n$ ;
4. there is an ‘accidental’ symmetry  $G \times H$  in the renormalizable part of the flavon potential, i.e. there are only couplings via the trivial singlet between  $\chi$  and  $\phi$  at the renormalizable level, e.g. only  $(\chi^2)_{\underline{\mathbf{1}}_1}(\phi^2)_{\underline{\mathbf{1}}_1}$  exists for real representations  $\chi$ ,  $\phi$ ;

It turns out that there are only candidates for  $A_4$ ,  $T'$  or  $S_4$  up to order 1000, which are presented in Tab. 3.2. Although there are semidirect product groups which fulfil the first three criteria for  $H = T_7$ , or  $H = \Delta(27)$ , none of them leads to the desired accidental symmetry in the scalar potential. This might be related to the fact that these groups have complex three-dimensional representations, and there are more couplings that would have to be forbidden by the additional symmetries than in the case of  $H = A_4$ ,  $T'$  and  $S_4$ , which have real three dimensional representations. Additionally, there are simply less groups up to order 1000 that can be considered as an extension of  $T_7$  or  $\Delta(27)$  compared to the other groups.

Looking at the list of candidate groups, we further note that the normal subgroup  $N$  is non-abelian for all of our candidate groups. In addition, the defining homomorphism of Eq. (2.35) of each semidirect product is injective for  $H = A_4$ ,  $S_4$ <sup>8</sup> and in case of  $H = T'$ , each group  $N \rtimes T'$  allows for a defining homomorphism with image  $A_4$  or  $T'$ . The quaternion group  $Q_8$ , which frequently appears in Tab. 3.2, is the smallest non-abelian group allowing for a defining homomorphism with these properties. Furthermore we observe that all candidate groups have a non-trivial centre<sup>9</sup>  $Z(G) \triangleleft N$ . Representations can be classified according to their way of representing the elements in the centre, i.e. whether (a subgroup of) the centre is represented trivially (mapped to the identity) or not. In particular, the unfaithful representations  $\chi$  of  $G$ , which are directly related to irreducible representations  $\chi^H$  of  $H$  with  $\chi|_H \equiv \chi^H$  map the centre to the identity. They are single valued (in analogy to the representations of  $SU(2)$  with integer spin). However, groups that fulfil these conditions do not necessarily have to have a non-trivial centre. For example the wreath product  $S_3^4 \rtimes A_4$ , introduced by Babu and Gabriel [153], has a trivial centre.

### 3.2.3. General Group Extensions

Let us have a closer look at the construction in the last section. In order to obtain the same flavour structure within  $G$  as within  $H$ , we demanded the existence of representations  $\rho_i$ , which are directly related to the representations  $\rho_i^H$  of  $H$ . The representations  $\rho_i$  can be explicitly constructed using the surjective homomorphism from  $G$  to  $H$ , which we will denote by  $\xi : G \rightarrow H$ :

$$\rho_i \equiv \rho_i^H \circ \xi .$$

Hence, as soon as there is a surjective homomorphism  $\xi : G \rightarrow H$ , there are representations  $\rho_i$  with the desired property. Therefore, it is enough to look for groups  $G$  and a surjective

<sup>8</sup>The same applies for the wreath product  $S_3^4 \rtimes A_4$  introduced by Babu and Gabriel [153].

<sup>9</sup>The *centre* of a group,  $Z(G)$ , is the set of elements that commute with all elements of the group  $G$ , i.e.  $Z(G) \equiv \{x \in G \mid gx = xg \quad \forall g \in G\}$ . It forms a normal subgroup of  $G$ , i.e.  $Z(G) \triangleleft G$ .

### 3.2. Group Extensions and Vacuum Alignment

Quotient Group $H$	Order of $G$	GAP	Structure Description
$A_4$	96	201	$Z_2.(Z_2^2 \times A_4)$
	144	127	$Z_2.(A_4 \times S_3)$
	192	1017	$Z_2.(D_8 \times A_4)$
$S_4$	96	67, 192	$Z_4.S_4$
	144	121, 122	$Z_6.S_4$
	192	187, 963	$Z_8.S_4$
		987, 988	$Z_2.((Z_2^2 \times A_4) \times Z_2)$
		1483, 1484	$Z_2.(Z_2^2 \times S_4)$
		1492	$Z_2.((Z_2^4 \times Z_3) \times Z_2)$
$T'$	192	1007	$Z_2^2.(Z_2^2 \times A_4)$

**Table 3.3:** Candidate groups  $G$  up to order 200 that cannot be written as semidirect product. The expression of the form  $N.H$  in the last column is the GAP notation of a central extension, i.e.  $N$  is a normal subgroup of  $G$ , which is contained in the centre of  $G$ , and  $H$  is the quotient group  $G/N \cong H$ . Here, we explicitly choose  $N = Z(G)$  and therefore  $N.H = Z(G).G/Z(G)$ . The candidate groups of order 200-500 can be found in Table A.1.

homomorphism  $\xi : G \rightarrow H$ . This automatically implies the existence of a normal subgroup  $N = \ker \xi$  and a quotient group  $G/N \cong H$ . Thus, we are only dropping the condition that  $H$  is a subgroup of  $G$ . Actually, this type of extension is a general problem in group theory, which aims to find all possible groups  $G$  given two groups  $N$  and  $H$ , such that  $G/N \cong H$ . In the mathematical literature, this is denoted by *short exact sequence*. One example of such an extension is  $T'$ .  $A_4$  is not a subgroup of  $T'$ , but  $A_4 \cong T'/Z_2$ . In  $T'$  models [97–104], the flavour structure of the lepton sector is essentially described by the quotient group  $T'/Z_2 \cong A_4$  and the additional group structure, i.e. the two dimensional representations  $\mathbf{2}_i$ , are used to describe the quark sector. Hence, group extensions of the kind we described are not limited to the VEV alignment, but can be used more generally to lift properties of one group  $H$  to a larger group  $G$ , which addresses additional questions in flavour physics. Therefore, we propose to use these kind of constructions more systematically.

However, in our case we are mainly interested in a solution to the vacuum alignment problem, and therefore do not consider these other possibilities further. We perform another scan looking for groups solving the vacuum alignment problem with the first condition of the previous scan relaxed to

1.  $G/N \cong H$  with  $H$  being one of the groups  $A_4, T_7, T'^{10}, S_4, \Delta(27)$ ,

while keeping the other conditions. It turns out that there are only candidates for  $A_4, T'$  and  $S_4$  up to order 1000. We collect all candidates up to order 200, which are not contained in the previous search for semidirect product groups, in Tab. 3.3 and present the candidates of order 200 – 500 in Tab. A.1.

<sup>10</sup>We included  $T'$  in this scan, although  $T'$  is an extension of  $A_4$  via  $T'/Z_2 \cong A_4$ . However, the second condition excludes several candidates for  $T'$ , because the  $Z_2$  in  $T'/Z_2 \cong A_4$  is a subgroup of the  $N$  in the second condition.

### 3.3. Some Small Candidate Groups

In this section, we discuss the smallest group extensions of  $A_4$ ,  $S_4$  and  $T'$  we found in our scan. We go into more detail for the semidirect product group  $Q_8 \rtimes A_4$ , since we will use this group in the next chapter.

#### 3.3.1. The Smallest Group $Q_8 \rtimes A_4$

While the  $A_4$  subgroup is presented by

$$\langle S, T | S^2 = T^3 = (ST)^3 = 1 \rangle, \quad (3.28)$$

the quaternionic subgroup  $Q_8$  (also known as  $D'_4$ , the double group of the dihedral group of order 4) is defined by

$$\langle X, Y | X^4 = 1, X^2 = Y^2, Y^{-1}XY = X^{-1} \rangle, \quad (3.29)$$

and its Cayley graph is depicted in Fig. 3.5. The semidirect product  $Q_8 \rtimes A_4$  we are considering here is defined by the additional relations between the generators of  $Q_8$  ( $X, Y$ ) and  $A_4$  ( $S, T$ )

$$SXS^{-1} = X, \quad SYS^{-1} = Y^{-1}, \quad TXT^{-1} = YX, \quad TYT^{-1} = X, \quad (3.30)$$

and its Cayley graph is shown in Fig. 3.6. Note that the last relation allows one to replace the generator  $Y = T^2XT$ , leading to the presentation

$$\langle S, T, X | S^2 = T^3 = X^4 = SXSX^3 = (ST)^3 = T^2XT^2X^3T^2X^3 = STX^3T^2STX^3T^2 = E \rangle.$$

One can further see that the group element  $X^2$  commutes with all other elements. This generates the centre  $Z(Q_8 \rtimes A_4) = \{E, X^2\}$  and representations can be classified according to  $\rho(X^2) = \pm \mathbb{1}$ .

The defining representation matrices for the representations are given in Table 3.4. Notice that there is a 3-dimensional representation

$$\rho_{\mathbf{3}_1}(S) = S_3 \equiv \begin{pmatrix} 1 & 0 & 0 \\ 0 & -1 & 0 \\ 0 & 0 & -1 \end{pmatrix}, \quad \rho_{\mathbf{3}_1}(T) = T_3 \equiv \begin{pmatrix} 0 & 1 & 0 \\ 0 & 0 & 1 \\ 1 & 0 & 0 \end{pmatrix}, \quad \rho_{\mathbf{3}_1}(X) = \mathbb{1}_3,$$

which is exactly the representation we were looking for in Eq. (3.26) to solve the vacuum alignment problem. Obviously, this representation only knows about the  $A_4$  subgroup generated by  $S$  and  $T$  and it is therefore not faithful. The other crucial ingredient we needed was a faithful representation of  $G$  that did not contain any  $A_4$  representation in its symmetric product. This representation can be easily identified to be  $\mathbf{4}_1$ :

$$\rho_{\mathbf{4}_1}(S) = S_4 \equiv \sigma_3 \otimes \sigma_1, \quad \rho_{\mathbf{4}_1}(T) = T_4 \equiv \begin{pmatrix} 0 & 1 & 0 & 0 \\ 0 & 0 & 1 & 0 \\ 1 & 0 & 0 & 0 \\ 0 & 0 & 0 & 1 \end{pmatrix}, \quad \rho_{\mathbf{4}_1}(X) = X_4 \equiv -i\sigma_2 \otimes \sigma_3.$$

	$\underline{\mathbf{1}}_1$	$\underline{\mathbf{1}}_2$	$\underline{\mathbf{1}}_3$	$\underline{\mathbf{3}}_1$	$\underline{\mathbf{3}}_2$	$\underline{\mathbf{3}}_3$	$\underline{\mathbf{3}}_4$	$\underline{\mathbf{3}}_5$	$\underline{\mathbf{4}}_1$	$\underline{\mathbf{4}}_2$	$\underline{\mathbf{4}}_3$
$S$	1	1	1	$S_3$	$T_3 S_3 T_3^2$	$T_3 S_3 T_3^2$	$\mathbb{1}_3$	$T_3^2 S_3 T_3$	$S_4$	$S_4$	$S_4$
$T$	1	$\omega$	$\omega^2$	$T_3$	$T_3$	$T_3$	$T_3$	$T_3$	$T_4$	$\omega^2 T_4$	$\omega T_4$
$X$	1	1	1	$\mathbb{1}_3$	$S_3$	$T_3^2 S_3 T_3$	$T_3 S_3 T_3^2$	$T_3^2 S_3 T_3$	$X_4$	$X_4$	$X_4$

**Table 3.4:** Representations of  $Q_8 \times A_4$  in the chosen basis. The first 4 representations are the unfaithful  $A_4 = \langle S, T \rangle$  representations to which the leptons are assigned (with  $\rho(X) = \mathbb{1}$ ). Note that the representations  $\underline{\mathbf{4}}_i$  are double valued, i.e.  $\rho(Z(G) = X^2) = -\mathbb{1}$ , whereas the other representations are single valued ( $\rho(X^2) = \mathbb{1}$ ).  $\underline{\mathbf{1}}_{2,3}$  and  $\underline{\mathbf{4}}_{2,3}$  are complex, the other representations are real.

An explicit matrix representation of these generators for the remaining representations is given in Table 3.4 and the character table is presented in Table 6.3, and will be discussed there in more detail in Section 6.3.5. The Kronecker products

$$\underline{\mathbf{3}}_i \times \underline{\mathbf{3}}_i = \underline{\mathbf{1}}_1 + \underline{\mathbf{1}}_2 + \underline{\mathbf{1}}_3 + \underline{\mathbf{3}}_{iS} + \underline{\mathbf{3}}_{iA} \quad (3.31a)$$

$$\underline{\mathbf{3}}_i \times \underline{\mathbf{3}}_j = \sum_{\substack{k=1 \\ k \neq i,j}}^5 \underline{\mathbf{3}}_k \quad (i \neq j) \quad (3.31b)$$

$$\underline{\mathbf{3}}_i \times \underline{\mathbf{4}}_j = \underline{\mathbf{4}}_1 + \underline{\mathbf{4}}_2 + \underline{\mathbf{4}}_3 \quad (3.31c)$$

$$\underline{\mathbf{4}}_1 \times \underline{\mathbf{4}}_1 = \underline{\mathbf{1}}_{1S} + \underline{\mathbf{3}}_{1A} + \underline{\mathbf{3}}_{2S} + \underline{\mathbf{3}}_{3S} + \underline{\mathbf{3}}_{4S} + \underline{\mathbf{3}}_{5A} \quad (3.31d)$$

$$\underline{\mathbf{4}}_1 \times \underline{\mathbf{4}}_2 = \underline{\mathbf{1}}_{2S} + \underline{\mathbf{3}}_{1A} + \underline{\mathbf{3}}_{2S} + \underline{\mathbf{3}}_{3S} + \underline{\mathbf{3}}_{4S} + \underline{\mathbf{3}}_{5A} \quad (3.31e)$$

show that if one uses the unfaithful triplet  $\chi \sim \underline{\mathbf{3}}_1$  to break  $A_4$  in the charged lepton sector and the four dimensional faithful representation  $\phi \sim \underline{\mathbf{4}}_1$  in the neutrino sector, there are no dangerous cross-coupling terms of the form  $(\phi\phi)\underline{\mathbf{3}}_1(\chi\chi)\underline{\mathbf{3}}_1$  etc. allowed by the symmetry that would forbid the required VEV alignment. This will be the crucial property used to solve the vacuum alignment problem in the model of the next chapter.

### 3.3.2. Other Small Groups

For concreteness, we also briefly describe the groups that form the smallest extensions of  $S_4$  and  $T'$ .

**$\mathbf{Z}_4 \cdot \mathbf{S}_4 \cong \mathbf{SG}(96, 67)$ :** This group (in the GAP notation  $\mathbf{SG}(96, 67)$ <sup>11</sup>) is the smallest extension of  $S_4$  that allows for a solution of the vacuum alignment problem. It is generated by 2 generators  $A$  and  $B$  that fulfil the relations:

$$A^4 = B^4 = AB^{-1}A^{-1}BA^{-1}B^{-1} = E, \quad (3.32)$$

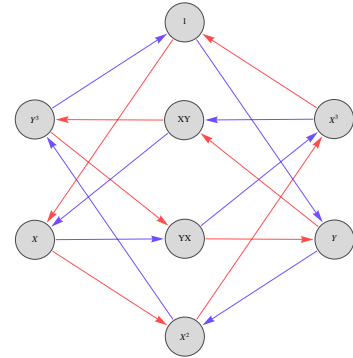


**Figure 3.5:** Cayley graph of  $Q_8$ . The generator  $X$  is depicted by red arrows and the generator  $Y$  is depicted by blue arrows.

<sup>11</sup>In order to uniquely specify each group, we denote it by  $\mathbf{SG}(O, N)$  where  $O$  is its order and  $N$  is the number in the GAP4 [129] SmallGroups catalogue [128].

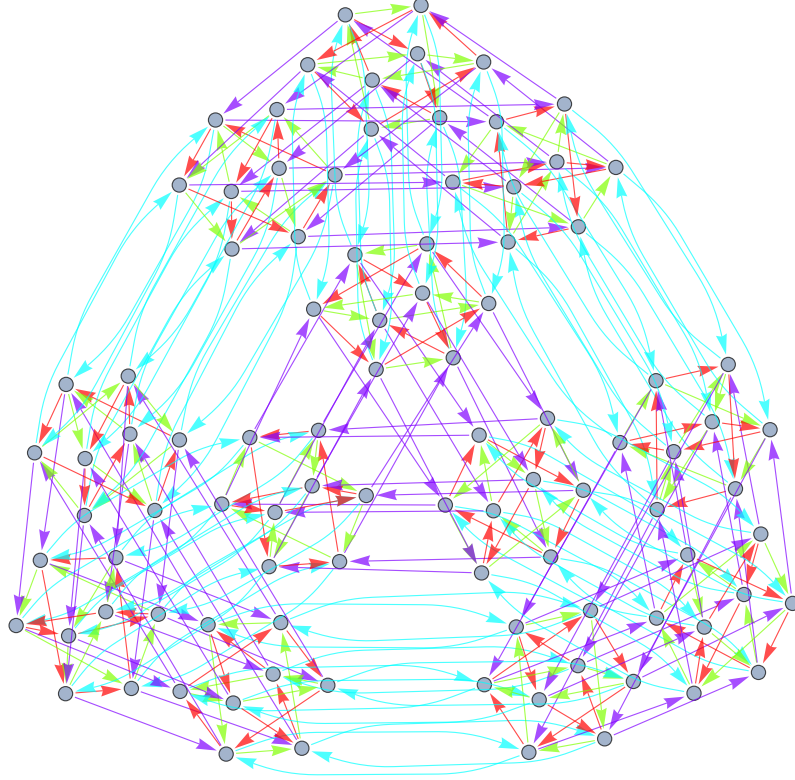


**Figure 3.6:** Cayley graph of  $Q_8 \times A_4$ . One can clearly distinguish the 12 normal  $Q_8$  subgroups generated by  $X$ (red) and  $Y$ (green) that are conjugated by the generators  $S$ (turquoise) and  $T$ (violet) of  $A_4$ .

and the faithful representation that solves the VEV alignment problem is given by

$$A = \frac{1}{\sqrt{2}} \begin{pmatrix} 0 & 0 & z^{13} & z^{19} \\ 0 & 0 & z^{13} & z^7 \\ z^{11} & z^{23} & 0 & 0 \\ z^5 & z^5 & 0 & 0 \end{pmatrix} \quad \text{and} \quad B = \frac{1}{\sqrt{2}} \begin{pmatrix} 0 & 0 & z^5 & z^5 \\ 0 & 0 & z^{23} & z^{11} \\ z^{19} & z & 0 & 0 \\ z^7 & z & 0 & 0 \end{pmatrix}, \quad (3.33)$$

with  $z = e^{i\pi/12}$ .

**$Q_8 \times T' \cong \text{SG}(192, 1022)$ :** The group  $T' = \langle s, t, r | s^2 = r, t^3 = (st)^3 = r^2 = E \rangle$  may be extended by a semi-direct product in the same way as  $A_4$ . For the generators  $s$  and  $t$  the defining homomorphism is the same as for  $Q_8 \times A_4$  given in Eq. (3.30) and for  $r$  we have:

$$rXr^{-1} = X \quad rYr^{-1} = Y.$$

The generator  $r$  therefore commutes with all group elements and the centre is therefore enlarged to  $Z(Q_8 \times T') = \{E, r, rX^2, X^2\} \cong Z_2 \times Z_2$ . The relevant representations can be constructed from the homomorphism  $g : Q_8 \times T' \rightarrow Q_8 \times A_4$  defined by  $g : \{r, s, t\} \rightarrow \{E, S, T\}$ . To solve the vacuum alignment problem, the leptons should be assigned to  $L \sim \rho_{\mathbf{3}_1} \circ g$  and the neutrino sector flavon  $\phi \sim \rho_{\mathbf{4}_1} \circ g$ . The additional representations may be used to describe the quark sector [103].



# Chapter 4.

## A Concrete Model based on $Q_8 \rtimes A_4$

In this chapter, we present a model based on the discrete flavour symmetry group  $Q_8 \rtimes A_4$ , which is the smallest symmetry group that allows for a natural vacuum alignment. We start by an introduction, which motivates the choice of representations and the model building setup and then in Section 4.2 present the model and its predictions in the lepton sector. In Section 4.3 it is shown that the model naturally leads to the correct vacuum alignment, without fine-tuning couplings in the scalar potential. In Section 4.4 we go on to show how the recent large value of  $\theta_{13}$  may be accommodated within the model. We close the chapter by discussing a seesaw UV completion of the model and a possibility to supersymmetrise it.

### 4.1. Introduction

Having developed the machinery to solve the vacuum alignment problem in the last chapter, we are now in a position to put the mechanism to use in a concrete model. The strategy is clear and has been outlined in Section 3.2:

- we want to reproduce the ‘success’ of  $A_4$  models, therefore the leptons should transform only under the representation  $\mathbf{1}_1$ ,  $\mathbf{1}_2$ ,  $\mathbf{1}_3$  and  $\mathbf{3}_1$  and thus transform trivially under the additional group generator  $X$ . Clearly, the lepton doublets have to transform as a three-dimensional representation (see Section 2.2),  $L \sim \mathbf{3}_1$ , and we assign the leptonic singlets  $e^c$ ,  $\mu^c$  and  $\tau^c$  to the one dimensional representations  $\mathbf{1}_1$ ,  $\mathbf{1}_2$  and  $\mathbf{1}_3$ , the same way as in the prototype model of Section 2.4.
- to couple the lepton doublets and singlets in a Yukawa-type operator,  $L\ell^c\tilde{H} \sim \mathbf{3}_1$ , we need to introduce an (effective) flavon that transforms as  $\mathbf{3}_1$ . As we want to create this operator at dimension five (otherwise the  $\tau$  Yukawa coupling would become too large) we thus have to introduce a scalar field  $\chi \sim \mathbf{3}_1$  that couples to leptons as  $L\chi\ell^c\tilde{H}$ .
- to generate neutrino masses we need another (effective) flavon that can couple to the Weinberg operator  $LHLH \sim \mathbf{3}_1$ . Two obvious points are in order: as the symmetry has to be broken to a different subgroup in the neutrino sector than in the charged lepton sector the flavon cannot be identified with  $\chi$ , but it has to be a different (effective) field. Furthermore it is clear that some symmetry should be present that makes sure that only  $\chi$  couples to the charged lepton operator at leading order.
- the most minimal option would now be to assign a real scalar singlet  $\phi \sim \mathbf{4}_1$  and since  $\phi^4$  contains a representation  $\mathbf{3}_1$  a coupling  $LHLH\phi^4$  exists.

However, a model of this type cannot be made to work for a couple of reasons. Analysing the scalar potential, we see that the most general VEV configurations  $\phi \sim (a, a, b, -b)$  that

break the group to the  $Z_2$  subgroup generated by  $S$  cannot be realised in the flavon potential<sup>1</sup>

$$V_\phi(\phi) = \mu_1^2(\phi\phi)_{\underline{\mathbf{1}}_1} + \alpha_1(\phi\phi)_{\underline{\mathbf{1}}_1}^2 + \sum_{i=2,3} \alpha_i(\phi\phi)_{\underline{\mathbf{3}}_i} \cdot (\phi\phi)_{\underline{\mathbf{3}}_i}, \quad (4.1)$$

due to the relation

$$0 = b \left. \frac{\partial V_\phi}{\partial \phi_1} \right|_{\langle \phi \rangle} - a \left. \frac{\partial V_\phi}{\partial \phi_3} \right|_{\langle \phi \rangle} = \frac{4}{\sqrt{3}} ab(a^2 - b^2)(\alpha_2 + \alpha_3). \quad (4.2)$$

The achievable VEV configurations with  $a^2 = b^2$  or  $ab = 0$  lead to a restoration of symmetry in the operator  $(LL)_{\underline{\mathbf{3}}_1} (\phi^4)_{\underline{\mathbf{3}}_1}$  that generates the  $(LL)_{\underline{\mathbf{3}}_1}$  entry in the mass matrix and consequently it vanishes in the vacuum,  $\langle (\phi^4)_{\underline{\mathbf{3}}_1} \rangle \sim ab(a^2 - b^2)$ <sup>2</sup>.

This type of model is also not so interesting from a general point of view, as it shares a couple of unpleasant features with the model of Babu and Gabriel [153] when viewed as an effective field theory:

- the off-diagonal entries in the neutrino mass matrix, generated by  $(LHLH\phi^4)$ , would be of very different order than the diagonal ones generated by the operator  $(LHLH)$ . To satisfy neutrino data, however, the two entries have to be of almost the same size.
- as  $(LHLH\chi^2)$  is allowed and of smaller dimension than  $(LHLH\phi^4)$ , tri-bimaximal mixing is not a leading-order prediction of the model.

All of these issues can of course be cured by introducing a UV completion that does not confirm the effective field theory prejudices.

Here we restrict ourselves to natural solutions within effective field theory. To solve all of these problems, we will discuss a model with two flavons in the neutrino sector,  $\phi_1 \sim \underline{\mathbf{4}}_1$  and  $\phi_2 \sim \underline{\mathbf{4}}_1$ , where an additional symmetry forbids the allowed term  $\chi \cdot (\phi_1\phi_2)_{\underline{\mathbf{3}}_1}$  that could disturb the VEV alignment between the two sectors. We identify this symmetry with the one that separates the charged lepton from the neutral lepton sector, i.e. we postulate the additional  $Z_4$  symmetry  $L \rightarrow iL$ ,  $\ell^c \rightarrow -i\ell^c$  and  $\phi_2 \rightarrow -\phi_2$ . This is the same symmetry we have encountered in Section 2.4 and one can think of this  $Z_4$  symmetry as a discrete version of lepton number with  $\phi_2$  being doubly charged under this (discrete) lepton number.

## 4.2. Lepton Masses

After all the preparative considerations of the last chapters, we are now finally in the position to present a model based on the symmetry group  $Q_8 \times A_4$  augmented by the auxiliary symmetry  $Z_4$  introduced at the end of the last section. The leptonic and scalar particle content is given in Tab. 4.1. As advertised, for the standard model leptons we use the unfaithful representations  $\underline{\mathbf{1}}_{1,2,3}$  and  $\underline{\mathbf{3}}_1$  that transform as irreducible representations under the subgroup  $A_4$ . In the charged lepton sector we use the unfaithful representation  $\chi \sim \underline{\mathbf{3}}_1$  and the charged lepton

<sup>1</sup>The operator  $(\phi\phi)_{\underline{\mathbf{3}}_4} \cdot (\phi\phi)_{\underline{\mathbf{3}}_4}$ , which one would naively expect, can be expressed as a linear combination of the other operators.

<sup>2</sup>If one introduces a soft-breaking term that conserves the  $Z_2$  subgroup generated by  $S$ ,  $V_S = \alpha(\phi_1\phi_2 + \phi_3\phi_4)$  in the potential, the minimum with  $a \neq b$  can then be realised. We do not pursue this option further here, as we are interested in genuine spontaneous symmetry breaking.

sector is thus analogous to the usual construction in an  $A_4$  model. In the neutrino sector, we introduce the real flavons  $\phi_{1,2} \sim \underline{\mathbf{4}}_1$ .

To keep the discussion simple, we use an effective field theory description. To lowest order, the charged lepton masses arise from the operators

$$- \mathcal{L}_e^{(5)} = y_e(L\chi)_{\underline{\mathbf{1}}_1} e^c \tilde{H}/\Lambda + y_\mu(L\chi)_{\underline{\mathbf{3}}_3} \mu^c \tilde{H}/\Lambda + y_\tau(L\chi)_{\underline{\mathbf{1}}_2} \tau^c \tilde{H}/\Lambda + \text{h.c.}, \quad (4.3)$$

with  $\tilde{H} = i\sigma_2 H^*$ , and the neutrino masses are generated from the effective interactions

$$\mathcal{L}_\nu^{(7)} = x_a(LHLL)_{\underline{\mathbf{1}}_1} (\phi_1\phi_2)_{\underline{\mathbf{1}}_1} / \Lambda^3 + x_d(LHLL)_{\underline{\mathbf{3}}_1} \cdot (\phi_1\phi_2)_{\underline{\mathbf{3}}_1} / \Lambda^3 + \text{h.c.} \quad (4.4)$$

The notation should be self-explanatory and the relevant Kronecker products are given in App. A.2. We will show in the next section that the vacuum configuration

$$\langle \chi \rangle = (v', v', v')^T, \quad \langle \phi_1 \rangle = \frac{1}{\sqrt{2}}(a, a, b, -b)^T, \quad \langle \phi_2 \rangle = \frac{1}{\sqrt{2}}(c, c, d, -d)^T, \quad (4.5)$$

with  $v', a, b, c, d \in \mathbb{R}$ , can be obtained as the global minimum of the most general scalar potential. This configuration gives

$$\langle (\phi_1\phi_2)_{\underline{\mathbf{3}}_1} \rangle = \frac{1}{2}(bc - ad, 0, 0)^T \quad \text{and} \quad \langle (\phi_1\phi_2)_{\underline{\mathbf{1}}_1} \rangle = \frac{1}{2}(ac + bd)$$

and it breaks the flavour symmetry to the  $Z_2$  subgroup generated by  $S$ . There are also physically inequivalent minima of the potential that break to the  $Z_2$  subgroups generated by  $SY$  and  $SYX$  which lead to the same structure  $\langle (\phi_1\phi_2)_{\underline{\mathbf{3}}_1} \rangle \propto (1, 0, 0)^T$ . We will discuss these issues in more detail the next section.

As the leptons only transform under the subgroup  $\langle S, T \rangle \cong A_4$ , the structure of the mass matrices exactly mirrors the discussion of the prototype model in Section 2.4. The leading order mass matrices are given by

$$M_E = \frac{vv'}{\Lambda\sqrt{2}} \Omega_T^* \text{diag}(y_e, y_\mu, y_\tau), \quad M_\nu = \frac{v^2}{2\sqrt{3}\Lambda^2} \begin{pmatrix} \tilde{a} & 0 & 0 \\ 0 & \tilde{a} & \tilde{d} \\ 0 & \tilde{d} & \tilde{a} \end{pmatrix} \quad (4.6)$$

with  $\tilde{a} = x_a \frac{1}{2}(ac + bd)$  and  $\tilde{d} = x_d \frac{1}{2}(bc - ad)$ . Again, the matrix  $M_\nu$  is invariant under the accidental symmetry  $U$  and thus the mixing matrix is of the tri-bimaximal form and the mass spectrum is thus given by<sup>3</sup>

$$\Omega_T^T M_E = \frac{vv'}{\sqrt{2}} \text{diag}(y_e, y_\mu, y_\tau), \quad \Omega_U^T M_\nu \Omega_U = \text{diag}(\tilde{a} + \tilde{d}, \tilde{a}, \tilde{d} - \tilde{a}). \quad (4.7)$$

Note that in this model both  $\tilde{a}$  and  $\tilde{d}$  are generated by the the same VEVs of the same flavons. This is quite different from the usual  $A_4$  models reviewed in Section 2.4 where an additional flavon  $\xi$  has to be introduced to generate  $\tilde{a}$ . The two entries  $\tilde{a}$  and  $\tilde{d}$  in the mass matrix have to be quite close to each other in magnitude [122, 154] to account for the small ratio of solar to atmospheric mass squared difference. Here, both contributions stem from VEVs of the same fields, and a similar order of magnitude might therefore be considered more natural.

<sup>3</sup>The charged lepton mass hierarchy can be explained by a Froggatt-Nielsen  $U(1)$  symmetry in the usual way.

	$L$	$e^c$	$\mu^c$	$\tau^c$	$\chi$	$\phi_1$	$\phi_2$
$Q_8 \times A_4$	$\mathbf{3}_1$	$\mathbf{1}_1$	$\mathbf{1}_2$	$\mathbf{1}_3$	$\mathbf{3}_1$	$\mathbf{4}_1$	$\mathbf{4}_1$
$Z_4$		i	-i	-i	1	1	-1

**Table 4.1:** Particle content of the minimal model with the correct spontaneous symmetry breaking. The flavons  $\chi$ ,  $\phi_1$  and  $\phi_2$  do not transform under the SM. The leptons transform in the usual way given in Table 2.1.

Indeed, in the numerical minimisation of the potential, we found a tendency for a similar size of the two  $\phi$  contractions.

Since in this model there is no need for a singlet flavon  $\xi$ , the number of degrees of freedom exactly matches the numbers of degrees of freedom of one complex  $A_4$  triplet and one complex singlet, which is commonly used [9, 69]. The difference here is that we do not have to introduce additional degrees of freedom to obtain the correct vacuum alignment and we thus think it is an attractive and economical model.

The mass matrices we have presented here are the leading order mass matrices and they will undergo small changes due to higher dimensional operators that contribute at next-to-leading order. These will be studied in Section 4.4.1.

### 4.3. Vacuum Alignment

In this section we demonstrate that the pattern of vacuum expectation values we used in the last section can be obtained as the global minimum of the scalar potential. The most general scalar potential invariant under the flavour symmetry is given by

$$V(\chi, \phi_1, \phi_2) = V_\chi(\chi) + V_\phi(\phi_1, \phi_2) + V_{\text{mix}}(\chi, \phi_1, \phi_2), \quad (4.8)$$

with

$$\begin{aligned} V_\phi(\phi_1, \phi_2) &= \mu_1^2(\phi_1\phi_1)_{\mathbf{1}_1} + \alpha_1(\phi_1\phi_1)_{\mathbf{1}_1}^2 + \sum_{i=2,3} \alpha_i(\phi_1\phi_1)_{\mathbf{3}_i} \cdot (\phi_1\phi_1)_{\mathbf{3}_i} \\ &\quad + \mu_2^2(\phi_2\phi_2)_{\mathbf{1}_1} + \beta_1(\phi_2\phi_2)_{\mathbf{1}_1}^2 + \sum_{i=2,3} \beta_i(\phi_2\phi_2)_{\mathbf{3}_i} \cdot (\phi_2\phi_2)_{\mathbf{3}_i} \\ &\quad + \gamma_1(\phi_1\phi_1)_{\mathbf{1}_1}(\phi_2\phi_2)_{\mathbf{1}_1} + \sum_{i=2,3,4} \gamma_i(\phi_1\phi_1)_{\mathbf{3}_i} \cdot (\phi_2\phi_2)_{\mathbf{3}_i}, \\ V_\chi(\chi) &= \mu_3^2(\chi\chi)_{\mathbf{1}_1} + \rho_1(\chi\chi\chi)_{\mathbf{1}_1} + \lambda_1(\chi\chi)_{\mathbf{1}_1}^2 + \lambda_2(\chi\chi)_{\mathbf{1}_2}(\chi\chi)_{\mathbf{1}_3}, \\ V_{\text{mix}}(\chi, \phi_1, \phi_2) &= \zeta_{13}(\phi_1\phi_1)_{\mathbf{1}_1}(\chi\chi)_{\mathbf{1}_1} + \zeta_{23}(\phi_2\phi_2)_{\mathbf{1}_1}(\chi\chi)_{\mathbf{1}_1}. \end{aligned} \quad (4.9)$$

Note that, by construction, there are no non-trivial couplings between the  $\chi$  and  $\phi$  breaking sectors that would disturb the vacuum alignment. The potential thus has an ‘accidental’  $(Q_8 \times A_4) \times A_4 \times Z_4$  symmetry under which the flavons transform as  $\chi \sim (\mathbf{1}_1, \mathbf{3}_1, 1)$ ,  $\phi_1 \sim (\mathbf{4}_1, \mathbf{1}_1, 1)$  and  $\phi_2 \sim (\mathbf{4}_1, \mathbf{1}_1, -1)$ . This symmetry is explicitly broken to  $(Q_8 \times A_4) \times Z_4$  by the couplings to leptons and by higher dimensional operators in the potential. As the accidental symmetry is discrete, there is no pseudo-Goldstone boson, as can easily happen in constructions of this type [153].

Let us now demonstrate that this model does not suffer from a vacuum alignment problem. At first, we discuss the possible minima of the potential focusing on the little group in the neutrino sector, i.e. the subgroup that leaves the VEV invariant. If there is a minimum in which the symmetry generator  $Q \in G$  is left unbroken, i.e.  $Q \langle \phi_{1,2} \rangle = \langle \phi_{1,2} \rangle$ , there obviously are degenerate minima  $\langle \tilde{\phi}_{1,2} \rangle = g \langle \phi_{1,2} \rangle$  that leave  $gQg^{-1}$  unbroken, with  $g \in G$ <sup>4</sup>. The physically distinct minima are therefore characterised by the conjugacy class(es)  $G \cdot Q_i = \{gQ_i g^{-1} | g \in G\}$  of the group element(s)  $Q_i$ . Obviously, only conjugacy classes with an eigenvalue +1 can lead to a non-trivial little group. For the four dimensional representation  $\underline{\mathbf{4}}_1$ , there are five such classes which are represented by 1,  $S$ ,  $SY$ ,  $SYX$ ,  $T$  as well as  $T^2$ , where the groups generated by  $T$  and  $T^2$  are identical. For the three dimensional representation  $\underline{\mathbf{3}}_1$ , where  $X$  and  $Y$  are represented trivially, all conjugacy classes have an eigenvalue +1 and can lead to a non-trivial little group. The relevant little group in the neutrino sector is the one of  $\langle (\phi_1 \phi_2) \underline{\mathbf{3}}_1 \rangle$ .

In the following, we will firstly discuss the possible little groups of  $\langle \phi_i \rangle$  and then its implications for the little group of  $\langle (\phi_1 \phi_2) \underline{\mathbf{3}}_1 \rangle$ . There are three physically distinct minima of  $\phi_1$  that preserve a  $Z_2$  subgroup:

- $\langle \phi_1 \rangle = \frac{1}{\sqrt{2}}(a, a, b, -b)^T$  results in the little group  $\langle S \rangle$ ,
- $\langle \phi_1 \rangle = (0, a, b, 0)^T$  in  $\langle SY \rangle$  and
- $\langle \phi_1 \rangle = \frac{1}{\sqrt{2}}(-a, b, -a, b)^T$  in  $\langle SYX \rangle$ .

In addition, there is one preserving a  $Z_3$  subgroup:

- $\langle \phi_1 \rangle = \frac{1}{\sqrt{2}}(a, a, a, b)^T$  preserves  $\langle T \rangle = \langle T^2 \rangle$ .

Obviously, there are also minima leading to little groups, which are generated by more than one generator. For example  $\langle \phi_1 \rangle \propto (1, 1, 1, -1)^T$  preserves  $\langle S, T \rangle \cong A_4$ . The same discussion applies to  $\phi_2$ . The little group of  $\langle (\phi_1 \phi_2) \underline{\mathbf{3}}_1 \rangle$  contains the intersection of the little groups of  $\langle \phi_1 \rangle$  and  $\langle \phi_2 \rangle$ .

In the following, we will concentrate on the three little groups  $\langle S \rangle$ ,  $\langle SY \rangle$  and  $\langle SYX \rangle$ , which we listed above. If both  $\langle \phi_1 \rangle$  and  $\langle \phi_2 \rangle$  preserve the same  $Z_2$  subgroup, we obtain  $\langle (\phi_1 \phi_2) \underline{\mathbf{3}}_1 \rangle = \frac{1}{2}(bc - ad, 0, 0)^T$  and  $\langle (\phi_1 \phi_2) \underline{\mathbf{1}}_1 \rangle = \frac{1}{2}(ac + bd)$  due to the fact that  $X = Y = \mathbb{1}$  for the SM representations ( $\underline{\mathbf{1}}_1$  and  $\underline{\mathbf{3}}_1$ ) with  $a, b$  being the VEVs of  $\phi_1$  and  $c, d$ , the corresponding ones of  $\phi_2$ . Thus, it is impossible to distinguish these minima from low-energy neutrino phenomenology at the leading order. They are, however, physically distinct, since  $\langle \phi_1 \phi_1 \rangle$  as well as  $\langle \phi_2 \phi_2 \rangle$  are different and they lead to different mass spectra in the scalar sector, which we discuss to in Chapter 5.

First let us discuss the minimization of the potential. There are 11 real scalar fields and thus eleven minimization conditions. Due to the symmetry, these eleven conditions reduce to

<sup>4</sup>Strictly speaking  $g$  should be in  $\rho(G)$ , where  $\rho$  is the representation in question. For faithful representations  $\rho(G) \cong G$ .

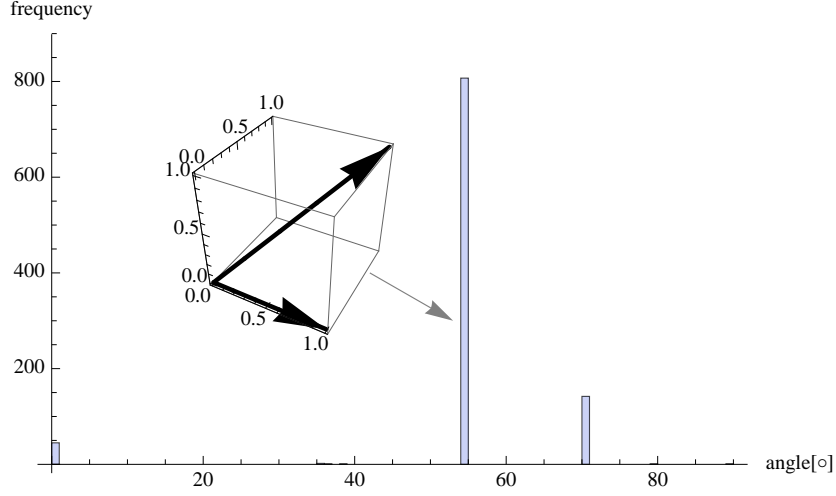


**Figure 4.1:** Distribution of the opening angle spanned by the flavon field  $\chi$  and the effective operator  $(\phi_1\phi_2)_{\mathbf{3}_1}$  for random values of potential parameters for the most general scalar potential given in Eq. (4.8). The tri-bimaximal vacuum configuration depicted in the inlay corresponds to an opening angle of  $54.7^\circ$ . We see that this vacuum configuration is obtained for a finite portion of parameter space, i.e. there is a phase with the TBM vacuum. This is to be contrasted with the potential without the alignment mechanism in Fig. 3.2.

only five independent ones:

$$a(\alpha_+(a^2 + b^2) + \alpha_-(a^2 - b^2) + \gamma_+(c^2 + d^2) + \gamma_-(c^2 - d^2) + U_1) + \Gamma bcd = 0 \quad (4.10a)$$

$$b(\alpha_+(a^2 + b^2) - \alpha_-(a^2 - b^2) + \gamma_+(c^2 + d^2) - \gamma_-(c^2 - d^2) + U_1) + \Gamma acd = 0 \quad (4.10b)$$

$$c(\beta_+(c^2 + d^2) + \beta_-(c^2 - d^2) + \gamma_+(a^2 + b^2) + \gamma_-(a^2 - b^2) + U_2) + \Gamma abd = 0 \quad (4.10c)$$

$$d(\beta_+(c^2 + d^2) - \beta_-(c^2 - d^2) + \gamma_+(a^2 + b^2) - \gamma_-(a^2 - b^2) + U_2) + \Gamma abc = 0 \quad (4.10d)$$

$$v'(4\sqrt{3}\lambda_1 v'^2 + 3\rho_1 v' + U_3) = 0, \quad (4.10e)$$

where the equations have been rescaled to eliminate overall constant factors and with the shorthand notations

$$U_i = \frac{1}{2}(\mu_i^2 + \sqrt{3}\zeta_{i3}v'^2) \quad \text{for } i = 1, 2, \quad U_3 = 2\mu_3^2 + \zeta_{13}(a^2 + b^2) + \zeta_{23}(c^2 + d^2)$$

and

$$\left\{ \begin{array}{l} \xi_+ = \frac{\xi_1}{2}, \quad \xi_- = \frac{\xi_2 + \xi_3}{2\sqrt{3}} \quad \text{for } \xi = \alpha, \beta \\ \gamma_+ = \frac{\sqrt{3}\gamma_1 + \gamma_4}{4\sqrt{3}}, \quad \gamma_- = \frac{\gamma_2 + \gamma_3}{4\sqrt{3}} \quad \text{and } \Gamma = \frac{\gamma_4}{\sqrt{3}} \end{array} \right\} \text{for } \langle S \rangle$$

$$\left\{ \begin{array}{l} \xi_+ = \frac{\sqrt{3}\xi_1 + \xi_2 + \xi_3}{2\sqrt{3}}, \quad \xi_- = \frac{2\xi_3 - \xi_2}{2\sqrt{3}} \quad \text{for } \xi = \alpha, \beta, \\ \gamma_+ = \frac{\sqrt{3}\gamma_1 + \gamma_3}{4\sqrt{3}}, \quad \gamma_- = \frac{\gamma_3}{2\sqrt{3}} \quad \text{and } \Gamma = \frac{\gamma_2 + \gamma_4}{2\sqrt{3}} \end{array} \right\} \text{for } \langle SY \rangle$$

$$\left\{ \begin{array}{l} \xi_+ = \frac{\xi_1 + \sqrt{3}\xi_2}{2}, \quad \xi_- = \frac{\xi_3 - 2\xi_2}{2\sqrt{3}} \quad \text{for } \xi = \alpha, \beta, \\ \gamma_+ = \frac{\sqrt{3}\gamma_1 + \gamma_2}{4\sqrt{3}}, \quad \gamma_- = \frac{\gamma_3 + \gamma_4}{4\sqrt{3}} \quad \text{and } \Gamma = \frac{\gamma_2}{\sqrt{3}} \end{array} \right\} \text{for } \langle SYX \rangle .$$

The first four equations result from the derivatives taken with respect to the components of  $\phi_1$  and  $\phi_2$  and the last one comes from the three-components of  $\chi$ . Note that the equations

### 4.3. Vacuum Alignment

for  $v'$  and  $a, b, c, d$  essentially decouple and their contributions to the other sector can be reabsorbed in the respective mass terms. Note further that they are invariant under symmetries  $(a, c) \leftrightarrow (b, d)$ ,  $(a, b) \rightarrow -(a, b)$ ,  $(c, d) \rightarrow -(c, d)$  as well as  $(a, b, \alpha_i, U_1) \leftrightarrow (c, d, \beta_i, U_2)$ , which are inherited from the symmetries of the potential.

The number of free VEVs thus exactly matches the number of algebraically independent minimization conditions, which shows that there generally is a range of parameter values of the scalar couplings, for which this solution is a local minima. To be able to determine the global minimum a numerical study is needed. We have varied all parameters in the range  $[-4, 4]$  and only found minima corresponding to the ones given above, and minima where all symmetries are broken; i.e. we have found global minima where the VEVs of  $\phi_1$  and  $\phi_2$  both conserve the subgroups  $\langle S \rangle$ ,  $\langle SY \rangle$ ,  $\langle SYX \rangle$  or  $\langle T \rangle$  or no subgroup. In particular, we have not found any minima that leave a larger symmetry group intact (except for the minimum with vanishing VEVs, which does not break the group). Each of these minima can be realised as global minimum of the potential, which we checked in the random number scan we performed. However, it was impractical to determine the parameter regions where each solution is realized as a global minimum.

It is, however, instructive to re-perform the analysis we reported on in Section 3.1. There we had performed a random scan over order one parameters of the most general renormalizable scalar potential of  $A_4$  and had found the distribution shown in Fig. 3.2 for the opening angle between the two flavons  $\phi$  and  $\chi$ . It was found that there are two phases: one where both flavons break to the same subgroup and the opening angle is zero and another one where there is no conserved subgroup. The vacuum configuration  $\langle \chi \rangle \sim (1, 1, 1)$  and  $\langle \phi \rangle \sim (1, 0, 0)$  corresponds to an opening angle of  $54.7^\circ$  and the distribution of opening angles presented in Fig. 3.2 clearly shows that this VEV configuration corresponds to a fine-tuned situation within the phase of complete symmetry breakdown. The corresponding scan for global minima of the potential given in Eq. (4.8) is shown in Fig. 4.1. Here we plot the opening angle between  $\chi$  and  $(\phi_1 \phi_2)_{\mathbf{3}_1}$ ,

as this is the effective operator that couples to neutrinos in Eq. (4.4) and plays the role of  $\phi$ . Clearly the distribution of opening angles is very different in this case and we can identify one phase with opening angle equal to zero where both fields break to the same subgroup and another phase where the opening angle corresponds to the desired mismatched VEV configuration<sup>5</sup>. A cartoon of the resulting phase diagram is shown in Fig. 4.2. In conclusion, we have unambiguously shown that there is a finite portion of parameter space where the desired VEV configuration can be realized and that there is no fine-tuning associated with this configuration. Furthermore it should be stressed that there are no loose ends here: there are no flat directions that have to be lifted and no Goldstone modes that have to be made heavy. In the next section we will show that this finding is stable under the inclusion of

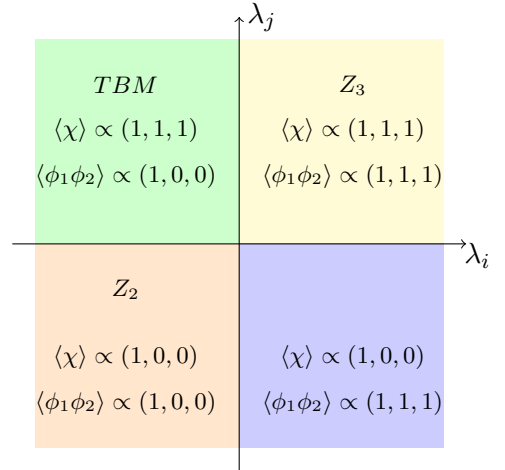


Figure 4.2: Cartoon phase diagram.

<sup>5</sup>The third bump at  $70.53^\circ$  in Fig. 4.1 corresponds to situations where  $\chi \sim (1, 1, -1)$  and  $\phi \sim (1, 1, 1)$  and equivalent configurations. The VEV  $\chi \sim (1, 1, -1)$  is degenerate with  $\chi \sim -(1, 1, 1)$ , which on the level of neutrino masses is equivalent to  $\chi \sim (1, 1, 1)$ , and we therefore do not count these solutions as a separate phase.

higher-dimensional operators and in Section 4.6 we will present a supersymmetrisation of the model that addresses the hierarchy problem that is always present in models with scalar fields in 4 dimensions.

## 4.4. Deviations from TBM

In light of the recent measurement of  $\theta_{13}$ , we discuss various possibilities to obtain non-vanishing  $\theta_{13}$  in our setup. First we will see what can be obtained when one includes next-to-leading order corrections to the model and then we will discuss a minimal extension of the model that realizes the trimaximal mixing configuration introduced in Section 2.5.2 and which can be considered the natural deformation of  $A_4$  models.

### 4.4.1. Higher Order Corrections

The results presented above are corrected by higher order operators. Here we discuss the next-to-leading order corrections. Let us briefly comment on the magnitude of the scale  $\Lambda$  under the assumption that all operators are suppressed by the same scale.<sup>6</sup> If we require a perturbative value for the  $\tau$  Yukawa coupling,  $y_\tau < 4\pi$ , this translates into [9]

$$\frac{v'}{\Lambda} > 0.002.$$

Furthermore taking  $m_\nu \sim 0.05$  eV and assuming couplings of order one,  $x_{a,d} \sim \mathcal{O}(1)$ , we find

$$\Lambda \approx 6 \cdot 10^{14} \left(\frac{u}{\Lambda}\right)^2 \text{ GeV} \quad \text{with} \quad u = a, b, c, d$$

so that the natural cutoff values are  $2 \cdot 10^9 \text{ GeV} < \Lambda < 6 \cdot 10^{14} \text{ GeV}$  assuming all VEVs to be of a similar size  $v' \sim a \sim b \sim \dots$ . However  $\Lambda$  can easily be in the TeV region for moderately small couplings in the UV completion, as will be shown in Section 5. Note that the ratio of  $\frac{v'}{\Lambda} > 0.002$  does not pose a severe hierarchy problem and thus does not necessarily require a solution e.g. in the form of supersymmetry.

**Corrections to the charged lepton mass matrix:** The next-to-leading order correction to the charged lepton mass matrix takes the form:

$$-\mathcal{L}_e^{(6)} = y'_e (L(\chi\chi)_{\mathbf{3}_1})_{\mathbf{1}_1} e^c \tilde{H}/\Lambda^2 + y'_\mu (L(\chi\chi)_{\mathbf{3}_1})_{\mathbf{1}_3} \mu^c \tilde{H}/\Lambda^2 + y'_\tau (L(\chi\chi)_{\mathbf{3}_1})_{\mathbf{1}_2} \tau^c \tilde{H}/\Lambda^2 + \text{h.c.} .$$

As these operators can be obtained by replacing  $\chi$  by  $(\chi\chi)_{\mathbf{3}_1}$  in Eq. (4.3) and

$$\langle (\chi\chi)_{\mathbf{3}_1} \rangle = v' \langle \chi \rangle,$$

they do not introduce a new structure in the charged lepton mass matrix [114], but merely renormalise the leading contribution. Note that there are no other contributions at this level, since  $\phi_i \phi_i$  does not contain  $\mathbf{3}_1$  by construction. Operators with new structures are suppressed by  $1/\Lambda^3$ .

<sup>6</sup>Of course, this assumption does not have to be true for e.g. a UV completion where the charged lepton mass operators are generated by vector-like fermions and the neutrino mass operators are generated by a seesaw .



**Corrections to the neutrino mass matrix:** The next-to-leading order operators contributing to the neutrino mass matrix are given by

$$\Lambda^4 \mathcal{L}_\nu^{(8)} = x_c (LHLH)_{\mathbf{1}_2} (\phi_1 \phi_2 \chi)_{\mathbf{1}_3} + x_b (LHLH)_{\mathbf{1}_3} (\phi_1 \phi_2 \chi)_{\mathbf{1}_2} + x_h (LHLH)_{\mathbf{1}_1} (\phi_1 \phi_2 \chi)_{\mathbf{1}_1} + (LHLH)_{\mathbf{3}_1} \cdot \left[ x_e \chi (\phi_1 \phi_2)_{\mathbf{1}_1} + x_f (\chi \cdot (\phi_1 \phi_2))_{\mathbf{3}_1} + x_g (\chi \cdot (\phi_1 \phi_2))_{\mathbf{3}_1} \right] + \text{h.c.}, \quad (4.11)$$

where  $(\dots)_S$  denotes the symmetric contraction and  $(\dots)_A$  the antisymmetric one. These operators perturb the mixing matrix and their effect will be discussed in Section 4.4.1.

**Corrections to the Scalar Potential:** Corrections to the potential arise at dimension five:

$$V^{(5)} = \sum_{L,M=1}^2 \sum_{i,j=2}^4 \frac{\delta_{ij}^{(LM)}}{\Lambda} \chi \cdot \left\{ (\phi_L \phi_L)_{\mathbf{3}_i} \cdot (\phi_M \phi_M)_{\mathbf{3}_j} \right\}_{\mathbf{3}_1} + \frac{\chi^3}{\Lambda} \left( \delta_1^{(3)} \chi^2 + \delta_2^{(3)} (\phi_1 \phi_1)_{\mathbf{1}_1} + \delta_3^{(3)} (\phi_2 \phi_2)_{\mathbf{1}_1} \right) \quad (4.12)$$

where all parameters are real and  $\delta_{ij}^{(LM)} = 0$  for  $i \geq j$ . Upon minimisation, these interactions lead to a shift in the vacuum expectation values of the form:

$$\langle \chi \rangle = (v' + \delta v'_1, v' + \delta v'_2, v' + \delta v'_2)^T, \quad (4.13a)$$

$$\langle \phi_1 \rangle = \frac{1}{\sqrt{2}} (a + \delta a_1, a + \delta a_2, b + \delta a_3, -b + \delta a_4)^T, \quad (4.13b)$$

$$\langle \phi_2 \rangle = \frac{1}{\sqrt{2}} (c + \delta b_1, c + \delta b_2, d + \delta b_3, -d + \delta b_4)^T \quad (4.13c)$$

Generically, the magnitude of these shifts will be suppressed by one power of  $\Lambda$ ,

$$\frac{\delta u}{u} \sim \frac{u}{\Lambda}, \quad (4.14)$$

where  $u$  denotes a generic vacuum expectation value. The VEVs of  $\chi_2$  and  $\chi_3$  stay equal at next-to-leading order, i.e.  $\langle \chi_2 \rangle - \langle \chi_3 \rangle = \mathcal{O}(1/\Lambda^2)$  and  $\langle \chi_3 \rangle \approx \langle \chi_2 \rangle = \delta v'_2$ . To calculate the correction to neutrino masses, the following shorthand notations for the shifts in the vacuum expectation values are useful:

$$\delta \langle (\phi_1 \phi_2)_{\mathbf{3}_1} \rangle = \frac{1}{4} \begin{pmatrix} a(\delta b_4 - \delta b_3) + c(\delta a_3 - \delta a_4) - d(\delta a_1 + \delta a_2) + b(\delta b_1 + \delta b_2) \\ a(\delta b_3 + \delta b_4) - c(\delta a_3 + \delta a_4) + d(\delta a_1 - \delta a_2) + b(\delta b_2 - \delta b_1) \\ a(\delta b_1 - \delta b_2) + c(\delta a_2 - \delta a_1) - d(\delta a_3 + \delta a_4) + b(\delta b_3 + \delta b_4) \end{pmatrix} \equiv \begin{pmatrix} \delta \Phi_1 \\ \delta \Phi_2 \\ \delta \Phi_3 \end{pmatrix}$$

and

$$\delta \langle (\phi_1 \phi_2)_{\mathbf{1}_1} \rangle = \frac{1}{4} (a(\delta b_1 + \delta b_2) + c(\delta a_1 + \delta a_2) + d(\delta a_3 - \delta a_4) + b(\delta b_3 - \delta b_4)) \equiv \delta \Phi_0.$$

To get a feeling for the size of the deviations from the leading order vacuum alignment, we have performed a numerical minimisation of the potential for a number of random values for the potential parameters. We found it instructive to plot  $\frac{\max_i \delta u_i}{\max_i u_i}$  against  $\frac{\max_i u_i}{\Lambda}$ , where  $u_i$  denotes any of the leading-order VEVs and  $\delta u_i$  any of the deviations. Fig. 4.3 shows

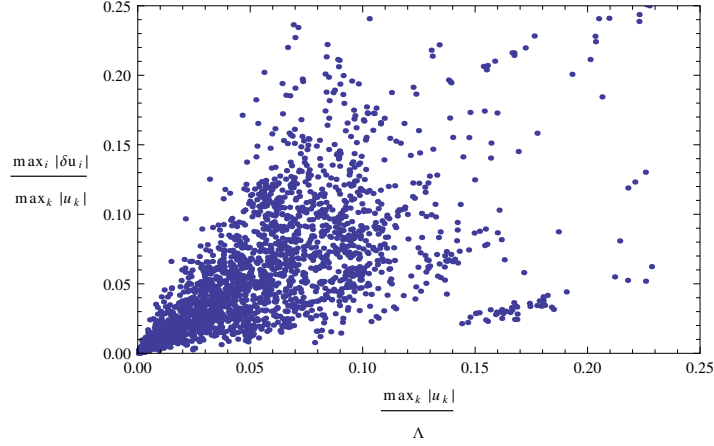


**Figure 4.3:** Vacuum shifts  $\frac{\max_i |\delta u_i|}{\max_k |u_k|}$  induced by higher dimensional operators as a function of  $\frac{\max_k |u_k|}{\Lambda}$  for randomly chosen potential parameters of order unity. All points correspond to phenomenologically viable data points.

the VEV deviation scales plotted against the ratio  $u/\Lambda$ . The corrections are small for small  $u/\Lambda$ .

**Corrections to Masses and Mixings:** To next-to-leading order, the charged lepton matrix  $M_E$  is modified from Eq. (4.6) by

$$\delta M_E = \frac{v}{\Lambda\sqrt{2}} \begin{pmatrix} \delta v'_1 & 0 & 0 \\ 0 & \delta v'_2 & 0 \\ 0 & 0 & \delta v'_2 \end{pmatrix} U_0 \begin{pmatrix} y_e & 0 & 0 \\ 0 & y_\mu & 0 \\ 0 & 0 & y_\tau \end{pmatrix} + \frac{vv'^2}{\Lambda^2\sqrt{2}} U_0 \begin{pmatrix} y'_e & 0 & 0 \\ 0 & y'_\mu & 0 \\ 0 & 0 & y'_\tau \end{pmatrix}. \quad (4.15)$$

In the neutrino sector there are also new structures. The corrections to the neutrino mass matrix can be parametrised as

$$\delta M_\nu = \begin{pmatrix} \delta\tilde{a} + \tilde{b} + \tilde{c} & \tilde{f} & \tilde{e} \\ \tilde{f} & \delta\tilde{a} + \omega\tilde{b} + \omega^2\tilde{c} & \delta\tilde{d} \\ \tilde{e} & \delta\tilde{d} & \delta\tilde{a} + \omega^2\tilde{b} + \omega\tilde{c} \end{pmatrix} \frac{v^2}{2} \quad (4.16)$$

with

$$\delta\tilde{a} = \frac{v'x_h(bc-ad)}{6\Lambda^4} + \frac{x_a\delta\Phi_0}{\sqrt{3}\Lambda^3}, \quad \delta\tilde{d} = \frac{-x_d\delta\Phi_1}{2\sqrt{3}\Lambda^3} + \frac{v'x_e(ac+bd)}{4\sqrt{3}\Lambda^4}, \quad (4.17a)$$

$$\tilde{b} = \frac{v'x_b(bc-ad)}{6\Lambda^4}, \quad \tilde{e} = \frac{-x_d\delta\Phi_2}{2\sqrt{3}\Lambda^3} + \frac{v'x_e(ac+bd)}{4\sqrt{3}\Lambda^4} + \frac{(x_f+x_g)v'(bc-ad)}{8\sqrt{3}\Lambda^4}, \quad (4.17b)$$

$$\tilde{c} = \frac{v'x_c(bc-ad)}{6\Lambda^4}, \quad \tilde{f} = \frac{-x_d\delta\Phi_3}{2\sqrt{3}\Lambda^3} + \frac{v'x_e(ac+bd)}{4\sqrt{3}\Lambda^4} + \frac{(x_f-x_g)v'(bc-ad)}{8\sqrt{3}\Lambda^4}. \quad (4.17c)$$

Since the leptons only transform under the  $A_4$  subgroup of the model, the neutrino phenomenology runs exactly parallel to the  $A_4$  case. The effects of the operators  $\tilde{a}, \dots, \tilde{f}$  have been studied in [120] where it has been shown that a sizeable deviation from  $\sin^2\theta_{13} = 0$  is

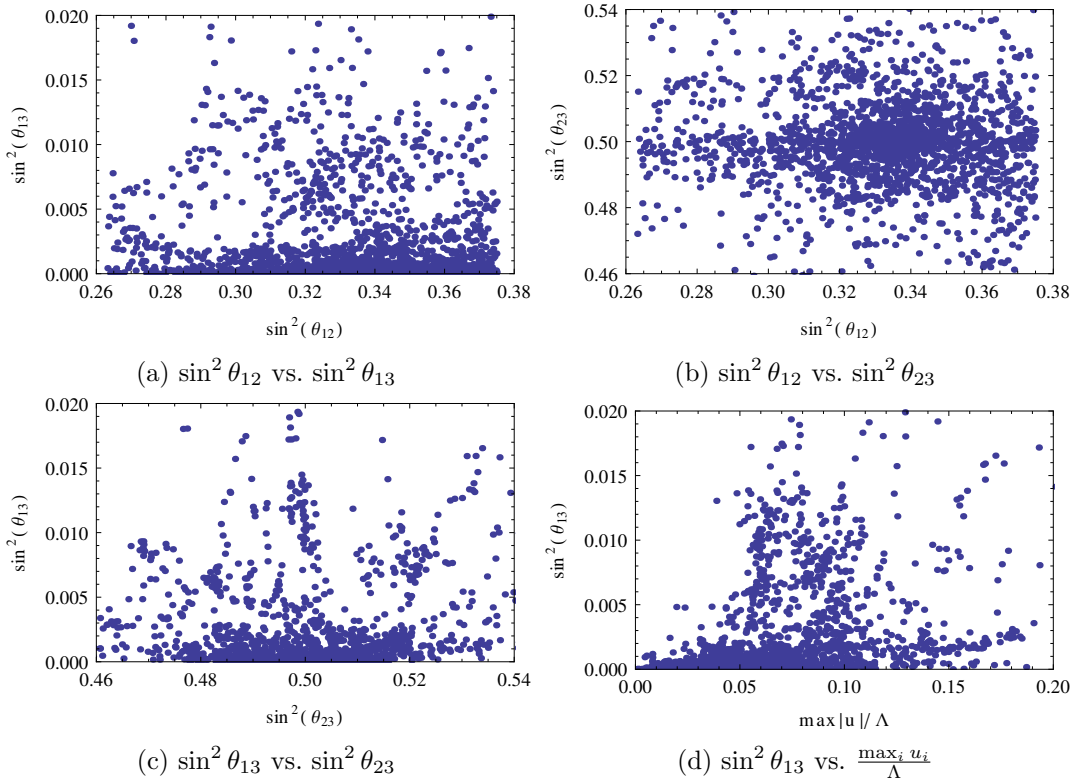


**Figure 4.4: Scatter Plot of Mixing Angles.** To illustrate the typical size of corrections to the mixing angles, we have performed a scatter plot. We took all dimensionless scalar potential couplings to be of order one and varied the ratio of the mass parameters in the potential such that the ratio of the VEVs and cutoff-scale is smaller than one. All dimensionless parameters that modify the neutrino and charged lepton mass matrices are taken to be of the same order as the leading order parameters. All points lie within the  $3\sigma$  range of the mass and mixing parameters (as of Nov. 2011). The mixing angle  $\sin^2 \theta_{12}$  is varied more than the other two mixing angles. We have used the `MixingParameterTools` [156] package to extract the mixing angles.

possible without introducing large corrections to the other mixing angles. Recently it has been shown that  $\sin^2 \theta_{13} \gtrsim 0.1$  is possible for  $\tilde{c}/\tilde{a} \gtrsim 0.25$  in the case of normal mass ordering [155].

We performed a random scan in order to get an idea of the size of the corrections from higher dimensional operators. For a collection of tree-level parameters of order unity, we have varied the higher dimensional parameters (4.12) of the potential in the range  $[0.5, 1.5]$  and the dimensionless parameters in the corrections to the lepton masses in Eq. (4.11) have been taken to be of the same order as the leading order contributions. The suppression scale  $\Lambda$  has been varied in a wide range.

In Fig. 4.4, the resulting scatter plots are shown, where all data points lie within the  $3\sigma$  limits of the global fits cited in the introduction. As can be seen from Fig. 4.4d, for  $u/\Lambda \gtrsim 0.05$  there are points that deviate from tri-bimaximal mixing in the right way to be compatible with the recent measurements of  $\theta_{13}$ .

Allowing for couplings considerably smaller than order one in  $V_\phi$ <sup>7</sup>, the VEV corrections  $\delta\Phi_i$  become dominant and  $\tilde{e}$  and  $\tilde{f}$  are the main corrections to the neutrino mass matrix. This is shown in Fig. 4.5 and is in agreement with the result [120]. Note that the values are roughly

<sup>7</sup>For details, please consult the Mathematica notebook published as a supplement together with the Mathematica package `Discrete` described in Section A.5

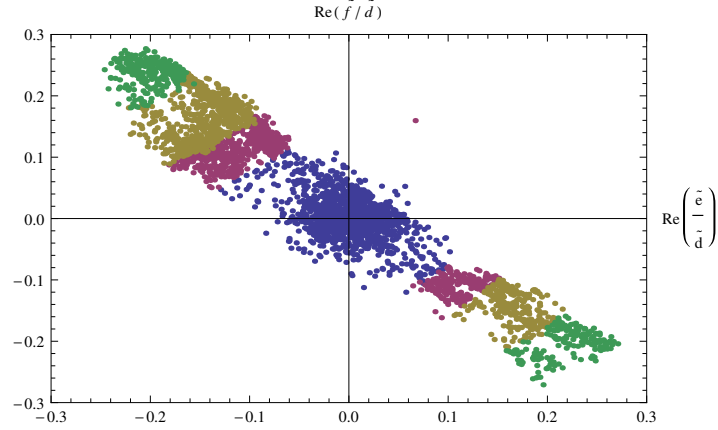


**Figure 4.5:** The matrix entries  $\tilde{e}$  and  $\tilde{f}$  are the dominant corrections to the neutrino mixing matrix in the case where the corrections from the VEVs of  $\phi_1$  and  $\phi_2$  dominate. Here we show the correlation between the two quantities. The blue, violet, yellow and green points correspond to values of  $\sin\theta_{13}^2$  in the ranges  $[0, 0.005]$ ,  $[0.005, 0.01]$ ,  $[0.01, 0.02]$ , and  $[0.02, 0.03]$ , respectively. The imaginary parts are much smaller  $|\text{im}(\tilde{e}/\tilde{d})|, |\text{im}(\tilde{f}/\tilde{d})| \lesssim 0.003$ .

along a diagonal line, i.e.  $\tilde{e}$  and  $\tilde{f}$  are similar in size, but have a different relative sign.

In conclusion one has to say that while NLO corrections can account for the measured deviation of TBM, the large number of parameters makes it impossible to make predictions regarding the other lepton mixing angles. There are, for example, no correlations between the deviations from TBM if one assumes the most general structure of NLO corrections.

#### 4.4.2. Trimaximal Mixing

Another possibility to generate deviations from TBM is the introduction of an additional flavon  $\tilde{\xi} \sim (\mathbf{1}_2, i)$  that breaks the accidental symmetry  $U$  in the neutrino sector by the VEV  $\langle \tilde{\xi} \rangle = \tilde{w}$ . This scalar can couple to neutrinos via the effective operator

$$\delta\mathcal{L}_\nu^{(7)} = x_c(LHLH)\mathbf{1}_2\tilde{\xi}^2/\Lambda^3 + \text{h.c.} . \quad (4.18)$$

that contributes to the neutrino mass matrix as

$$\delta M_\nu = \frac{v^2}{2\sqrt{3}\Lambda^3}\tilde{c} \begin{pmatrix} 1 & 0 & 0 \\ 0 & \omega & 0 \\ 0 & 0 & \omega^2 \end{pmatrix} \quad (4.19)$$

with  $\tilde{c} = x_c\tilde{w}^2$ . In Section 2.5.2 it has been shown that a correction of this type leads to the so-called trimaximal mixing pattern, which gives a good fit to the neutrino mixing data and predicts a testable correlation (2.59) between the deviation from TBM in the various mixing angles. The purpose of this section is to demonstrate that the TMM VEV configuration can also be naturally obtained in the  $Q_8 \times A_4$  model. At the renormalizable level the scalar potential for  $\tilde{\xi}$  is given by

$$V_{\tilde{\xi}}(\tilde{\xi}) = \mu_4^2\tilde{\xi}^*\tilde{\xi} + \lambda_{\tilde{\xi}}(\tilde{\xi}^*\tilde{\xi})^2 \quad (4.20)$$

and the cross-coupling terms

$$V_{\text{cross}} = \tilde{\xi}^* \tilde{\xi} \left( \zeta_{14} (\phi_1 \phi_1) \underline{\mathbf{1}}_{\mathbf{1}} + \zeta_{24} (\phi_2 \phi_2) \underline{\mathbf{1}}_{\mathbf{1}} + \zeta_{34} (\chi \chi) \underline{\mathbf{1}}_{\mathbf{1}} \right). \quad (4.21)$$

Note that there are no non-trivial contractions between  $\tilde{\xi}$  and the other flavons at the renormalizable level. Note further that this is a direct consequence of the model and that no additional symmetries have been required. The minimization conditions for the fields are now a trivial extension of (4.10). Indeed the first 5 conditions can be brought in the exact same form with the replacement  $U_i \rightarrow U_i + \frac{1}{2} \zeta_{i4} \tilde{w}^2$  for  $i = 1, 2, 3$ . The remaining equation is

$$0 = \left\langle \frac{\partial}{\partial \tilde{\xi}} V \right\rangle = \tilde{w}^* \left[ \left( \mu_{\tilde{\xi}}^2 + \frac{1}{2} \zeta_{14} (a^2 + b^2) + \frac{1}{2} \zeta_{24} (c^2 + d^2) + \zeta_{34} \frac{v^2}{\sqrt{3}} \right) + 2\lambda_{\tilde{\xi}} \tilde{w}^* \tilde{w} \right]. \quad (4.22)$$

Again we see that the minimization conditions reduce to the same number as the number of VEVs. There is therefore no problem to obtain the TMM VEV configuration. All of this is very trivial and almost embarrassing to write down. It should be noted that this a major feature of this approach to the vacuum alignment problem. If one wants to change the model based on R-symmetries presented in Section 3.1.1 by introducing a non-trivial singlet scalar one also has to change the driving field particle content, auxiliary symmetries and other details [63].

#### 4.4.3. Cosmological Implications of Accidental Symmetries

Let us briefly comment on possible cosmological implications of the unbroken remnant symmetries of the scalar potential. After symmetry breaking, there are 3 symmetries remaining. There are the obvious symmetries

$$Z_3 : \chi \rightarrow T_3 \chi, \quad \phi_i \rightarrow \phi_i \quad \text{and} \quad (4.23)$$

$$Z_2 : \phi_i \rightarrow S_4 \phi_i, \quad \chi \rightarrow \chi \quad (4.24)$$

but there is another accidental symmetry of the potential<sup>8</sup> $V_\phi$  not part of  $Q_8 \times A_4$ :

$$Z_2 : \phi_i \rightarrow O_4 \phi_i, \quad \chi \rightarrow \chi \quad \text{with} \quad O_4 = \text{diag}(\sigma_1, \mathbb{1}_2). \quad (4.25)$$

In the scalar potential, these symmetries are only broken through higher dimensional operators. All of these symmetries are explicitly broken by the interactions with leptons. Let us discuss the situation where  $J$  is the lightest scalar odd under the unbroken  $Z_2$  symmetry generated by  $S$ , e.g.  $J = \frac{1}{\sqrt{2}} ((\phi_1)_3 + (\phi_1)_4)$ . It can then decay into neutrinos through the effective interaction

$$\mathcal{L} = -\frac{1}{2} g_{J\nu_i\nu_j} J \nu_i \nu_j + \text{h.c.}, \quad (4.26)$$

with a lifetime roughly given by

$$\tau(J \rightarrow \nu\nu) \sim \frac{16\pi}{m_J} \frac{u^2}{m_\nu^2} \sim 4 \cdot 10^8 \text{ s} \left( \frac{u}{m_J} \right) \left( \frac{u}{10^{10} \text{ GeV}} \right), \quad (4.27)$$

<sup>8</sup>In Chapter 6 will encounter this symmetry as the outer automorphism  $h_4$  of Eq. (6.30).

for  $m_\nu = 0.05$  eV and  $u$  a generic flavon VEV. Depending on the model parameters, this decay time can be problematic. If the lifetime is larger than the age of the Universe,  $J$  becomes a dark matter candidate. A large lifetime naturally occurs, if  $J$  is a pseudo-Goldstone boson [157], which leads to  $m_J/u \ll 1$ . Pseudo-Goldstone bosons often appear in these constructions. For example, the tree-level scalar potential of the next-larger group in Tab. 3.2,  $T' \times A_4$ , has the large continuous accidental symmetry  $\text{Sp}(4)$ .

However, in general, there is also the decay channel via higher dimensional operators in the scalar potential, which couple  $J$  to the  $\langle S \rangle$ -breaking VEV of  $\chi$ , e.g. by operators of the type  $\phi_1^4 \cdot \chi H^\dagger H$ . It will generically be the dominant decay process in the model outlined above and result in much shorter lifetimes of

$$\tau \sim 16\pi \frac{m_J \Lambda^6}{u^8} \sim 3.3 \cdot 10^{-21} \left( \frac{m_J}{u} \right) \left( \frac{u/\Lambda}{0.01} \right)^{-7} \left( \frac{10^{12} \text{ GeV}}{\Lambda} \right) \text{ s},$$

ensuring that any potential abundance of  $J$  will decay before big bang nucleosynthesis. In the model by Babu and Gabriel [153], these higher dimensional operators are absent and therefore this decay through neutrinos is the only decay channel, which poses a potential problem for such models.

For any model with discrete symmetries there is the potential problem of the formation of domain walls. We do not go into details here but point out that the problem may be solved (i) through low-scale inflation or (ii) through explicit symmetry breaking contributions that can come either from quantum effects (anomalies) or from Planck-suppressed operators. These contributions break the degeneracies between the vacua and lead to a decay of domain walls [145].

## 4.5. Seesaw UV Completion

The neutrino sector of the effective theory outlined above may be UV completed by introducing the left-handed Weyl spinors  $N$ ,  $S_2$  and  $S_3$  that transform under  $(Q_8 \times A_4) \times Z_4$  as  $N \sim (\mathbf{3}_1, -i)$ ,  $S_2 \sim (\mathbf{4}_2, i)$  and  $S_3 \sim (\mathbf{4}_3, -i)$ , where  $S_2$  and  $S_3$  can be combined in a Dirac spinor.

This leads to the following new interactions in the Lagrangian

$$\mathcal{L} = x_{LN} L H N + x_{N2} N S_2 \phi_1 + x_{N3} N S_3 \phi_2 + m S_2 S_3 + x_{23} S_2 S_3 \chi + \text{h.c.}, \quad (4.28)$$

where the contraction of each operator is uniquely determined by the group theory of  $Q_8 \times A_4$ . The neutral fermion mass matrix is then schematically given by

$$\frac{1}{2} \begin{pmatrix} 0 & x_{LN} \langle H \rangle & 0 & 0 \\ \dots & 0 & x_{N2} \langle \phi_1 \rangle & x_{N3} \langle \phi_2 \rangle \\ \dots & \dots & 0 & m + x_{23} \langle \chi \rangle \\ \dots & \dots & \dots & 0 \end{pmatrix} \quad (4.29)$$

in the basis  $(\nu, N, S_2, S_3)$ . In the following, we assume that the direct mass term is larger than the mass terms generated by VEVs. Therefore, we are in the seesaw regime, which was first studied for gauge singlets in [26–30] and in more generality in [158, 159]. Hence, the masses of the singlets  $N$  are generated as

$$m_N = \frac{x_{N2} x_{N3}}{m} \begin{pmatrix} A & 0 & 0 \\ 0 & A & B \\ 0 & B & A \end{pmatrix} \quad \text{with} \quad A = -2(ac + bd) \quad \text{and} \quad B = i\sqrt{3}(bc - ad). \quad (4.30)$$

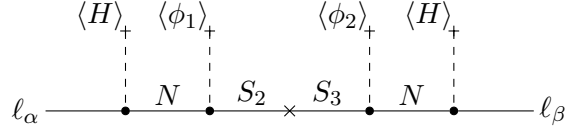


**Figure 4.6:** Neutrino masses in the UV completion.

This particular form has been denoted linear seesaw [160]. The light neutrino masses are generated via a standard seesaw [26–30]. Hence, the operator  $x_{23}S_2S_3\chi$  only enters at next-to leading order. Alternatively, it is possible to forbid it together with all next-to leading order corrections, which have been discussed in the previous section, by introducing an additional  $Z_2$  symmetry  $\chi \rightarrow -\chi$  and  $\ell^c \rightarrow -\ell^c$ . The neutrino mass matrix is then given by

$$M_\nu = x_{LN}^2 v^2 m_N^{-1} \quad (4.31)$$

This can also be seen from Fig. 4.6. This matrix is diagonalized by  $V_\nu = \Omega_U : \Omega_U^T M_\nu \Omega_U = \text{diag}(\frac{1}{B+A}, \frac{1}{A}, \frac{1}{B-A})$ . However, there are two degenerate eigenvalues as the relative phase of  $A$  and  $B$  is given by  $\pi/2$ . This can be solved by adding another copy of  $S_2$  or  $S_3$ , for example, lifting the degeneracy. Another possibility will be presented in Section 5, where the neutrino mass is generated radiatively.

The charged lepton mass operators can be generated in the same way as in [153] by introducing additional states that have masses allowed by EW symmetry and mix with the SM states after EW symmetry breaking.

## 4.6. Supersymmetrisation

Supersymmetrisation of the model is rather straightforward, indeed if one allows for non-renormalizable couplings in the scalar potential, the discussion of Section 4.3 can be adopted in a one-to-one fashion by replacing the fields of the non-SUSY model given in Table 4.1 by superfields. Here we briefly report the modifications needed if one sticks to the renormalizable level in the superpotential of the flavons. Since this implies that there should not be terms involving more than 3 fields in the superpotential and as there is no cubic invariant containing the  $\phi_{1,2}$  fields only, only the quadratic terms  $\phi_{1,2}^2 = \sum_i \phi_{1,2}^i{}^2$  can be written in the superpotential of the  $\phi$ s. These terms are invariant under a much larger symmetry  $\text{SO}(4)^2$  given by the individual rotations of  $\phi_1$  and  $\phi_2$ . To get rid of this unwanted continuous accidental symmetry, we have to add the singlet  $\xi \sim \mathbf{1}_1$  and the triplet  $\tilde{\chi} \sim \mathbf{3}_2$  which transform as singlets under the SM gauge group, given in Table 4.2.

The resulting schematic superpotential

$$W = S(\phi_1^2 + \phi_2^2 + \chi^2 + \tilde{\chi}^2)\mathbf{1}_1 + \xi^3 + \xi^2 + \xi + \phi_1^2 + \phi_2^2 + \chi^2 + \chi^3 + \tilde{\chi}(\phi_1^2 + \phi_2^2)\mathbf{3}_2 + \tilde{\chi}^2 + \tilde{\chi}^3.$$

leads to a scalar potential of the form

$$V = V_{\text{SUSY}} + V_{\text{soft}}$$

where

$$V_{\text{SUSY}} = \sum_i \left| \frac{\partial W}{\partial \varphi_i} \right|^2$$

	$L$	$e^c$	$\mu^c$	$\tau^c$	$\chi$	$\phi_1$	$\phi_2$	$\tilde{\chi}$	$\xi$
$Q_8 \times A_4$	$\mathbf{3}_1$	$\mathbf{1}_1$	$\mathbf{1}_2$	$\mathbf{1}_3$	$\mathbf{3}_1$	$\mathbf{4}_1$	$\mathbf{4}_1$	$\mathbf{3}_2$	$\mathbf{1}_1$
$Z_4$	i	-i	-i	-i	1	1	-1	1	1

**Table 4.2:** Chiral superfield particle content of SUSY  $Q_8 \times A_4$  model. All other fields of the MSSM are not charged under the flavour symmetry. The fields  $\tilde{\chi}$  and  $\xi$  are needed if one insists on the renormalizability of the flavon superpotential, otherwise they can be dispensed with.

and  $\varphi_i$  is any of the fields in the theory.  $V_{\text{soft}}$  contains all supersymmetry-breaking soft terms invariant under the flavour symmetry.

We have studied the potential resulting from this superpotential and the most general soft-breaking terms and we have found a portion of parameter space with the right vacuum alignment, with non-vanishing VEVs for both the singlet and triplet contractions of the product  $\phi_1\phi_2$ . The neutrino mass operators are again given by

$$W \supset x_a(LH_u LH_u)_{\mathbf{1}_1}(\phi_1\phi_2)_{\mathbf{1}_1}/\Lambda^3 + x_d(LH_u LH_u)_{\mathbf{3}_1}(\phi_1\phi_2)_{\mathbf{3}_1}/\Lambda^3. \quad (4.32)$$

As in the non-SUSY model before, the on-and off-diagonal terms of the neutrino mass matrix, which have to be quite close to each other in magnitude, are generated by VEVs of the same fields. The additional scalar field  $\tilde{\chi}$  couples to leptons only at next-to next-to leading order and it is thus not problematic.

Details can be found in the Mathematica notebook accompanying [16], which can be downloaded from the [webpage](#) of the Mathematica package `Discrete` introduced in Section A.5. We have checked that there exist a phase of parameter values for which the global minimum of the potential has the correct vacuum alignment for the most general softly broken supersymmetric potential. The symmetry breaking is also complete, i.e. there are no flat directions left as is the case in the type of models reviewed in Section 3.1.1 based on R-symmetries. Note that here the inclusion of soft-breaking terms does not pose a problem and the flavour symmetry breaking scale therefore does not have to be much smaller than the SUSY breaking scale.



## Chapter 5.

# Flavour Symmetry Breaking at the Electroweak Scale

In Section 2.5 we have seen that the recent observation of a rather larger value of  $\theta_{13}$  prompts one to consider two different directions in model building based on discrete flavour symmetry groups. One option is to have new starting points, but our comprehensive scan of flavour groups has shown that smallish groups of order smaller than 100 do not admit leading-order mixing patterns that fit the experimental data exceptionally well. If one goes to larger groups there are solutions that seem more favourable.

Here we pursue another strategy, namely we want to build models that deviate from tri-bimaximal mixing in a controlled way such that a certain predictivity in mixing angles is preserved, as reviewed in Section 2.5.2. Furthermore we want the symmetry breaking sector of the models to be testable, which is why we aim to implement the models at the electroweak scale. This is motivated by the fact that one should try to search for ways to test the paradigm of discrete flavour symmetries. All discrete symmetries need to be spontaneously broken and if the symmetry breaking scale is located e.g. at the GUT or seesaw scale there is scant hope of finding any remnants of this symmetry in low energy observables, as mentioned before in Section 2.5. Indeed the wisdom of effective field theories tells us that any such link will be highly dependent on assumptions about the detailed implementation of the symmetry and physics between the two scales. So far it has been very difficult to realize a complete model of flavour at the electroweak scale, because the only known mechanisms to achieve the correct vacuum alignment, which breaks the flavour symmetry into different non-commuting subgroups, rely on R-symmetries in supersymmetry or extra dimensions and need very high energy scales, as reviewed in Section 3.1.

With the vacuum alignment mechanism based on group theory developed in Chapter 3 and fleshed out into a concrete model in Chapter 4, it is now possible to build such a complete model. As we want to explain the lepton flavour structure at a low energy scale, it is desirable to find a rationale for the smallness of neutrino masses. The most well-travelled and easiest route to get small neutrino masses from TeV scale physics is to generate the effective neutrino mass operator either at higher dimensional level or at higher loop order. In Section 5.1, we will show that both ideas can be economically implemented in the electroweak version of the model given in Chapter 4, without introducing new symmetries apart from the ones introduced there. In Section 5.2 we discuss the predicted lepton structure and Section 5.3, we show how the model fares against lepton flavour violating observables, usually the most stringent test of such models. In Section 5.4.1, we show that the model naturally includes a dark matter candidate and discuss its phenomenology in Section 5.4.2. We then briefly discuss various possible extensions to the quark sector in Section 5.5 and in Section 5.6 we discuss direct constraints from colliders.

## 5.1. Model and Symmetry Breaking

We utilize the symmetry  $Q_8 \times A_4$  introduced in Chapter 3, which allows for natural vacuum alignment, and implement the model discussed in Chapter 4 at the electroweak scale. To this end, we promote the flavon field  $\chi \sim (\mathbf{3}_1, 1)$  of that model, which couples to the charged lepton sector, to EW Higgs doublets. The particle content of the lepton sector is given in Tab. 4.1. The vacuum configuration

$$\langle \chi_i \rangle = \begin{pmatrix} 0 \\ \frac{v}{\sqrt{6}} \end{pmatrix}, \quad \langle \phi_1 \rangle = \frac{1}{\sqrt{2}}(a, a, b, -b)^T, \quad \langle \phi_2 \rangle = \frac{1}{\sqrt{2}}(c, c, d, -d)^T \quad (5.1)$$

can be naturally obtained from the most general scalar potential following the discussion in Section 4.3. As the discussion is very similar to the one given there, we relegate it to App. A.4.1, where also the scalar mass spectrum is discussed. However, let us briefly recall the salient features of the VEV configuration (5.1): the scalar singlets  $\phi_1$  and  $\phi_2$  break the symmetry group to the subgroup  $\langle S | S^2 = E \rangle \cong Z_2$  and the EW doublets  $\chi$  break the discrete symmetry group down to the subgroup  $\langle T | T^3 = E \rangle \cong Z_3$ , while simultaneously breaking the electroweak gauge group  $SU(2)_L \times U(1)_Y$  down to the electromagnetic  $U(1)_{\text{em}}$ . The normalization is chosen such that  $\sum_i v_i^2 = v^2 = (\sqrt{2}G_F)^{-1} = (246 \text{ GeV})^2$ , in accordance with our earlier definition. Because of the unbroken  $Z_3$  symmetry in the charged lepton sector, it is useful to go to a basis [161–164]

$$(H, \varphi', \varphi'')^T = \Omega_T^\dagger \chi \sim (1, \omega^2, \omega), \quad (L_e, L_\mu, L_\tau)^T = \Omega_T^\dagger L \sim (1, \omega^2, \omega), \quad (5.2)$$

where this symmetry is represented diagonally. We have indicated the transformation properties under the unbroken subgroup  $\langle T \rangle \cong Z_3$  under which  $(e^c, \mu^c, \tau^c)$  transform as  $(1, \omega, \omega^2)$ . This has been denoted flavour triality in [162]. In this basis the vacuum configuration (5.1) implies that only the field  $H$  acquires a VEV  $\langle H \rangle = (0, v/\sqrt{2})^T$ , while  $\varphi'$  and  $\varphi''$  are inert doublets (and thus do not obtain a VEV). The potential for the electroweak doublets  $\chi$  is given by

$$V_\chi(\chi) = \mu_3^2 \chi^\dagger \chi + \sum_{r=\mathbf{1}, \mathbf{2}, \mathbf{3}_{1S}, \mathbf{1A}} \lambda_{\chi r} (\chi^\dagger \chi)_r (\chi^\dagger \chi)_{r^*} + \lambda_{\chi A} \text{Im} \left[ (\chi^\dagger \chi)_{\mathbf{3}_{1S}} (\chi^\dagger \chi)_{\mathbf{3}_{1A}} \right], \quad (5.3)$$

and after symmetry breaking the nine-physical scalars contained in  $\chi$  arrange themselves in the following multiplets under the remnant  $U(1) \times Z_3$  symmetry. There is one real scalar  $h = \sqrt{2} \text{Re} H^0$  with mass

$$m_h^2 = \frac{2}{9} \left( 3\lambda_{\chi \mathbf{1}_1} + \sqrt{3}\lambda_{\chi \mathbf{3}_{1,S}} \right) v^2 \quad (5.4)$$

that plays the role of the Standard Model Higgs. Note that since this scalar is a complete singlet under all remnant symmetries, it can in principle mix with components of  $\phi_1$  and  $\phi_2$  that transform in the same way. This is discussed in Eq. (A.23) in the appendix and in the following we will for the most part assume the mixing to be small enough to treat  $h$  as a mass eigenstate.

The next four degrees of freedom arrange themselves in the charged scalars  $\varphi'^+$  and  $\varphi''^+$  that transform as  $(1, \omega^2)$  and  $(1, \omega)$  under  $U(1) \times Z_3$ , respectively, and have the masses

$$m_{\varphi'^+}^2 = \frac{v^2}{12} \left( -2\sqrt{3}\lambda_{\chi \mathbf{3}_{1,S}} - \lambda_{\chi A} \right), \quad m_{\varphi''^+}^2 = \frac{v^2}{12} \left( -2\sqrt{3}\lambda_{\chi \mathbf{3}_{1,S}} + \lambda_{\chi A} \right). \quad (5.5)$$

	$L$	$e^c$	$\mu^c$	$\tau^c$	$\chi$	$\phi_1$	$\phi_2$	$S$	$\eta_1$	$\eta_2$	$\eta_3$
$Q_8 \times A_4$	$\mathbf{3}_1$	$\mathbf{1}_1$	$\mathbf{1}_2$	$\mathbf{1}_3$	$\mathbf{3}_1$	$\mathbf{4}_1$	$\mathbf{4}_1$	$\mathbf{3}_2$	$\mathbf{3}_5$	$\mathbf{3}_4$	$\mathbf{3}_5$
$Z_4$	$i$	$-i$	$-i$	$-i$	$1$	$1$	$-1$	$-1$	$i$	$i$	$-i$
$SU(2)_L$	$2$	$1$	$1$	$1$	$2$	$1$	$1$	$1$	$2$	$2$	$2$
$U(1)_Y$	$-1/2$	$1$	$1$	$1$	$1/2$	$0$	$0$	$0$	$1/2$	$1/2$	$1/2$

**Table 5.1:** Particle content of the minimal model that realizes flavour symmetry breaking at the electroweak scale. The flavon  $\chi$  contains the Higgs field and ties the electroweak to the flavour breaking scale. The scalars  $\eta_i$  and fermionic multiplet  $S$  are needed for one-loop generation of neutrino masses.

The final four real scalars sit in the two complex neutral scalars  $\varphi'^0$  and  $\varphi''0^*$ , that both transform as  $(0, \omega^2)$  and the mass eigenstates are given by the neutral scalars

$$\begin{pmatrix} \Phi_1 \\ \Phi_2 \end{pmatrix} = \begin{pmatrix} \cos \alpha & \sin \alpha \\ -\sin \alpha & \cos \alpha \end{pmatrix} \begin{pmatrix} \varphi'^0 \\ \varphi''0^* \end{pmatrix}, \quad \text{with} \quad \tan 2\alpha = \frac{6\lambda_{\chi 1_2} + \sqrt{3}(3\lambda_{\chi 3_{1,A}} + \lambda_{\chi 3_{1,S}})}{6\lambda_{\chi A};}$$

their masses may be succinctly written as

$$m_{\Phi_1}^2 + m_{\Phi_2}^2 = -2 \tan(2\alpha) \left( m_{\varphi''+}^2 - m_{\varphi'+}^2 \right) + m_{\varphi''+}^2 + m_{\varphi'+}^2 - \frac{v^2 \lambda_{\chi 3_{1,A}}}{\sqrt{3}}; \quad (5.6)$$

$$m_{\Phi_1}^2 - m_{\Phi_2}^2 = 2 |\sec(2\alpha)| \left| m_{\varphi''+}^2 - m_{\varphi'+}^2 \right|. \quad (5.7)$$

The mass spectra for the other scalars can be found in App. A.4.2. Two comments are in order here: (i) in the potential (5.3) there is only one mass term for the three doublets. Using the minimization conditions, the mass term can be swapped for the Higgs VEV  $v$  and therefore (ii) all of the squared scalar masses are given as a product of dimensionless scalar couplings times  $v^2$ . The additional scalar masses may therefore not be arbitrarily large. Note that in usual multi-Higgs doublet models each doublet has its own mass term and therefore there is always a decoupling limit where all non-SM particles are unobservably heavy. Such a setup is therefore directly testable at colliders, as we will study in Section 5.6. However, before discussing this, we show that the model accomplishes (i) the description of the (lepton) flavour structure in terms of a small number of parameters and (ii) the protection against bounds on new physics from flavour observables such as lepton flavour violating processes.

## 5.2. Lepton Flavour Structure

In this section we discuss the one-loop generation of neutrino masses and phenomenological implications of the predicted flavour structure.

### 5.2.1. Lepton Masses

The charged lepton sector is described by

$$- \mathcal{L}_e = y_e L \tilde{\chi} e^c + y_\mu L \tilde{\chi} \mu^c + y_\tau L \tilde{\chi} \tau^c + \text{h.c.}, \quad (5.8)$$

where  $\tilde{\chi} = i\sigma_2\chi$  and here and in the following we do not specifically indicate the contractions if there is only one invariant that can be formed out of the particle content of the operator. In the physical basis of Eq. (5.2) this term reads

$$-\mathcal{L}_e = \tilde{H} (y_e L_e e^c + y_\mu L_\mu \mu^c + y_\tau L_\tau \tau^c) + \tilde{\varphi}' (y_e L_\mu e^c + y_\mu L_\tau \mu^c + y_\tau L_e \tau^c) + \tilde{\varphi}'' (y_e L_\tau e^c + y_\mu L_e \mu^c + y_\tau L_\mu \tau^c) + \text{h.c.} \quad (5.9)$$

and we thus see that  $H$  couples diagonally to leptons while  $\varphi'$  and  $\varphi''$  do not. Note that here the mass terms are of dimension four and there is therefore no need for a complicated UV completion, in contrast to the mass terms in Eq. (4.3). The mass matrix is thus given by

$$M_E = \frac{v}{\sqrt{2}} \Omega_T^* \text{diag}(y_e, y_\mu, y_\tau), \quad (5.10)$$

with  $\Omega_T$  given in Eq. (2.26). Neutrino masses are generated at one loop level, through the interactions with the fermionic singlets  $S$  and the scalar doublets  $\eta$ , as shown in Fig. 5.1. The couplings of  $S$  are given by

$$\mathcal{L}_\nu = h_1 L \eta_1 S + h_2 L \eta_2 S + \sqrt{3} M_S S S + \text{h.c.} . \quad (5.11)$$

The factor of  $\sqrt{3}$  cancels a factor coming from the normalization of Clebsch-Gordon coefficients. In order to calculate the neutrino mass matrix, we have to determine the mass matrix of the neutral components of  $\eta_1$ ,  $\eta_2$  and  $\eta_3$ . To shorten the notation we define the doublet  $\hat{\eta}_J$  to be the  $J$ -th component of the 9 component vector  $\hat{\eta} = (\eta_1, \eta_2, \eta_3)$  and real scalar field  $\hat{\eta}_k^0$  to be the  $k$ -th component of  $(\sqrt{2}\text{Re}\hat{\eta}^0, \sqrt{2}\text{Im}\hat{\eta}^0)$ . Besides the direct mass terms

$$\left(M_{\eta^0}^2\right)_{ij} = \frac{\partial^2 V_{\eta_i}^{(2)}}{\partial \hat{\eta}_i^0 \partial \hat{\eta}_j^0} \quad \text{with} \quad V_{\eta_i}^{(2)} = \sum_{i=1,2,3} \sqrt{3} M_i^2 \eta_i^\dagger \eta_i, \quad (5.12)$$

there are couplings which give off-diagonal contributions

$$\left(\delta M_{\eta^0}^2\right)_{ij} = \left\langle \frac{\partial^2 \delta V_{\eta_i}^{(2)}}{\partial \hat{\eta}_i^0 \partial \hat{\eta}_j^0} \right\rangle \quad (5.13)$$

to the mass matrix. Such interactions are needed to generate neutrino masses and the relevant ones can be determined from symmetry considerations<sup>1</sup>. Any contribution to neutrino mass has to be proportional to

- $M_S$ , which breaks the generalized lepton number  $L \rightarrow e^{i\alpha} L, S \rightarrow e^{-i\alpha} S$
- either of the couplings  $\lambda_1$  or  $\lambda_2$ , defined by<sup>2</sup>

$$V_{\eta,\chi} = \lambda_1 (\chi^T \sigma_2 \vec{\sigma} \chi) \mathbf{1}_1 (\eta_1^T \sigma_2 \vec{\sigma} \eta_3)^* \mathbf{1}_1 + \lambda_2 e^{i\alpha\lambda} (\chi^T \sigma_2 \vec{\sigma} \chi) \mathbf{3}_1 (\eta_2^T \sigma_2 \vec{\sigma} \eta_3)^* \mathbf{3}_1 + \text{h.c.}, \quad (5.14)$$

which break the generalized lepton number  $L \rightarrow e^{i\alpha} L, \eta_i \rightarrow e^{-i\alpha} \eta_i$ ,

<sup>1</sup>The complete expression for  $\delta V_{\eta_i}^{(2)}$  can be found in the appendix in Eq. (A.24). Only the parts presented here are relevant for neutrino masses.

<sup>2</sup>We can set a number of complex parameters real by phase redefinitions. We set  $y_e, h_1, h_2, M_S, \lambda_1, \lambda_3, \lambda_4$  real by rotating  $\ell^c, L, \eta_2, S, \chi, \eta_1, \eta_3$ , respectively, and display the phase of  $\lambda_2$  explicitly.

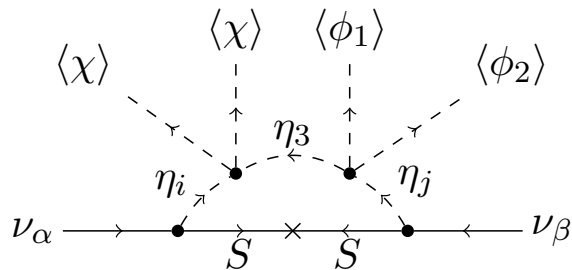


Figure 5.1: Neutrino mass generation at one loop.

- and  $\lambda_3$  or  $\lambda_4$  defined by<sup>3</sup>

$$V_{\eta,\phi} = \lambda_3(\phi_1\phi_2)\mathbf{1}_1(\eta_3^\dagger\eta_1)\mathbf{1}_1 + \lambda_4(\phi_1\phi_2)\mathbf{3}_1(\eta_3^\dagger\eta_2)\mathbf{3}_1 + \text{h.c.}, \quad (5.15)$$

which couples to the  $Z_4$ -breaking VEV of  $\phi_2$ .

The built-in multiple protection of the neutrino mass operator thus necessitates the large number of couplings involved in neutrino mass generation, and thus a large potential for suppression beyond the naive factor of  $1/(16\pi^2)$  from the loop integral. For simplicity, we assume that the direct mass terms  $M_i$  dominate over all other contributions; this is in fact a necessary condition to have a predictive theory of flavour, akin to the condition  $u/\Lambda \leq 1$  of Section 4.4.1. Hence, we can approximate the propagator as

$$\left[ k^2 - (M_{\eta_0}^2 + \delta M_{\eta_0}^2) \right]^{-1} = (k^2 - M_{\eta_0}^2)^{-1} + (k^2 - M_{\eta_0}^2)^{-1} \delta M_{\eta_0}^2 (k^2 - M_{\eta_0}^2)^{-1}, \quad (5.16)$$

where  $M_{\eta_0}^2$  is diagonal, and treat the mixing between the different components of  $\eta_i$  by mass insertions  $\delta M_{\eta_0}^2$ . The evaluation of the one loop diagram leads to

$$(M_\nu)_{\alpha\beta} = \frac{-i}{(2\pi)^4} \sum_{i=1}^3 \sum_{I,J,M=1}^{18} h_{\alpha i I} h_{\beta i J} I \left( (M_{\eta_0}^2)_{II}, (M_{\eta_0}^2)_{JJ}, (M_{\eta_0}^2)_{MM}, M_S \right) \quad (5.17)$$

where the Yukawa couplings  $h_{ikJ}$  depend on the two couplings  $h_{1,2}$  given in Eq. (5.11) via  $h_{\alpha k J} = \frac{\partial \mathcal{L}_\nu}{\partial L_\alpha \partial S_k \partial \hat{\eta}_J}$  and the dimensionless loop integral is given by<sup>4</sup>

$$I(m_1, m_2, m_3, m_4) = -\frac{1}{16\pi^2} \sum_i \frac{m_i^2 \log\left(\frac{m_i^2}{\mu^2}\right)}{\prod_{k \neq i} (m_i^2 - m_k^2)}. \quad (5.18)$$

<sup>3</sup>The contractions  $(\chi^T \sigma_2 \bar{\sigma} \chi)_{\mathbf{1}, \mathbf{2}, \mathbf{3}}$  vanish in the vacuum given in Eq. (5.1) and thus do not contribute to the masses here, because the  $Z_3$  symmetry generated by  $T$  is conserved by  $\langle \chi \rangle$ .

<sup>4</sup>Note that  $\mu$  drops out of the sum; it is displayed here to make the symmetric structure of the expression explicit, while keeping the argument of the logarithm dimensionless.

Evaluation of the sums leads to the following flavour structure of the neutrino mass matrix:

$$M_\nu = \begin{pmatrix} \hat{a} & \hat{e} e^{i\alpha_\lambda} & \hat{e} e^{i\alpha_\lambda} \\ \cdot & \hat{a} + \hat{b} e^{i\alpha_\lambda} & \hat{d} + \hat{e} e^{i\alpha_\lambda} \\ \cdot & \cdot & \hat{a} \end{pmatrix}, \quad (5.19)$$

where the four real coefficients are given by

$$\hat{a} = \frac{1}{36\sqrt{3}} h_1^2 \lambda_3 \lambda_1 v^2 (ac + bd) M_S I(M_1, M_1, M_3, M_S), \quad (5.20a)$$

$$\hat{d} = \frac{1}{72\sqrt{3}} h_1 h_2 \lambda_4 \lambda_1 v^2 (bc - ad) M_S I(M_1, M_2, M_3, M_S), \quad (5.20b)$$

$$\hat{b} = \frac{1}{108} h_2^2 \lambda_4 \lambda_2 v^2 (bc - ad) M_S I(M_2, M_2, M_3, M_S), \quad (5.20c)$$

$$\hat{e} = \frac{1}{216} h_1 h_2 \lambda_3 \lambda_2 v^2 (ac + bd) M_S I(M_1, M_2, M_3, M_S). \quad (5.20d)$$

Hence, neutrino masses are suppressed by one insertion of the EW breaking VEV  $\lambda_1 \langle \chi^2 \rangle / M_0^2$ , with  $M_0$  being the largest mass of the particles in the loop  $M_0 \sim \max_{i=1,2,3,S} M_i$ , and one mass insertion of the flavour breaking VEV  $\lambda_2 \langle \phi_1 \phi_2 \rangle / M_0^2$ . A phenomenologically viable neutrino mass scale is obtained for e.g.  $M_0 \sim \mathcal{O}(\text{TeV})$ ,  $\langle \chi \rangle, \langle \phi_i \rangle \sim \mathcal{O}(100 \text{ GeV})$  and  $h_i, \lambda_i \sim \mathcal{O}(0.01 - 0.1)$ . The next-to-leading order corrections are suppressed by  $\lambda_1 \langle \chi^2 \rangle / M_0^2$  or  $\lambda_2 \langle \phi_1 \phi_2 \rangle / M_0^2$ , which amounts to an  $\mathcal{O}(0.0001 - 0.001)$  correction for our typical values and can to a good approximation be neglected.

## 5.2.2. Phenomenological Implications

As the neutrino mass matrix is described by five physical real parameters, there are four predictions in the lepton sector at leading order. They can easily be read off from Eq. (5.19) in terms of matrix elements, but the expressions in terms of mixing parameters are non-trivial. In the flavour basis, where the charged lepton mass matrix is diagonal, the neutrino mass matrix is given by

$$M_\nu^{fl} = \begin{pmatrix} \hat{a} + \frac{2\hat{d}}{3} + \left(2\hat{e} + \frac{\hat{b}}{3}\right) e^{i\alpha_\lambda} & -\frac{\hat{d}}{3} + \frac{\hat{b}}{3} e^{i\alpha_\lambda \omega^2} & -\frac{\hat{d}}{3} + \frac{\hat{b}}{3} e^{i\alpha_\lambda \omega} \\ \cdot & \frac{2\hat{d}}{3} + \frac{\hat{b}}{3} e^{i\alpha_\lambda \omega} & \hat{a} - \frac{\hat{d}}{3} + \left(\frac{\hat{b}}{3} - \hat{e}\right) e^{i\alpha_\lambda} \\ \cdot & \cdot & \frac{2\hat{d}}{3} + \frac{\hat{b}}{3} e^{i\alpha_\lambda \omega^2} \end{pmatrix}. \quad (5.21)$$

and it is instructive to look at the neutrino mass matrix in the tri-bimaximal basis  $M_\nu^{tbm} = U_{HPS}^T M_\nu^{fl} U_{HPS}$ , i.e.,

$$M_\nu^{tbm} = \begin{pmatrix} \hat{a} + \hat{d} + \left(\frac{\hat{b}}{2} + \hat{e}\right) e^{i\alpha_\lambda} & -\sqrt{2} \hat{e} e^{i\alpha_\lambda} & -i \frac{\hat{b}}{2} e^{i\alpha_\lambda} \\ \cdot & \hat{a} & 0 \\ \cdot & \cdot & -\hat{a} + \hat{d} + \left(\hat{e} - \frac{\hat{b}}{2}\right) e^{i\alpha_\lambda} \end{pmatrix}. \quad (5.22)$$

We will first discuss limiting cases analytically and then perform a numerical analysis of the general neutrino mass matrix. In the limit of  $|\lambda_2|v^2 \rightarrow 0$ , both  $\hat{b}$  and  $\hat{e}$  vanish and the mass matrix is of the form given in Eq. (2.48) that we studied in our prototype model of

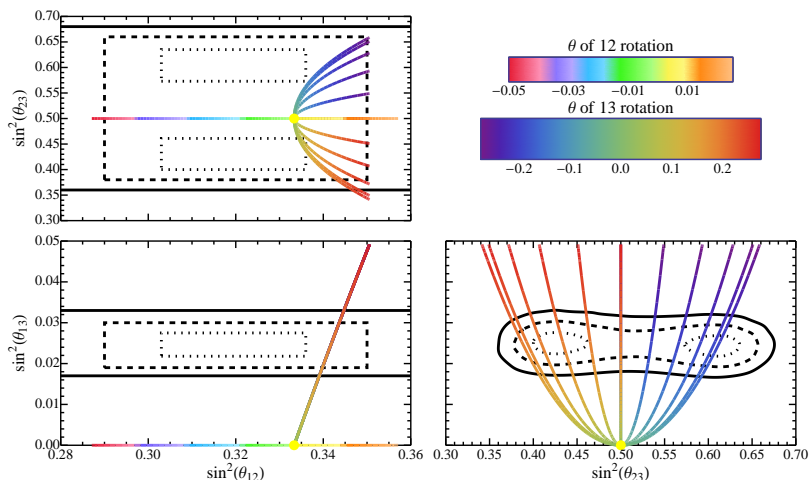


**Figure 5.2:** The deviations from tri-bimaximal mixing of the form  $U = U_{HPS}U_{12}$  and  $U = U_{HPS}U_{13}$  generated by the angle  $\theta$  defined in Eq. 5.23. The yellow point represents TBM, the continuous lines give the deviations from TBM with the angle  $\theta$  given by the colour codes in the top right corner for  $\delta = \frac{n\pi}{5}$  for  $n = 0, \dots, 5$ , where  $n = 0$  is the outermost parabola etc. The one, two and three sigma regions of a recent global fit [39] are indicated by dotted, dashed and continuous contours, respectively.

tri-bimaximal mixing in Section 2.4, so that the phenomenology is the same as discussed there. From Eq. (5.22) we can read off that switching on  $\hat{e} \neq 0$  while keeping  $\hat{b} = 0$  results in a correction to the PMNS matrix of the form  $U = U_{HPS}U_{12}(\tilde{\theta}_{12})P$  with  $U_{12}(\tilde{\theta}_{12})$  denoting the unitary matrix

$$U_{12}(\tilde{\theta}) = \begin{pmatrix} c_{12} & -s_{12}e^{-i\delta_{12}} & \\ s_{12}e^{i\delta_{12}} & c_{12} & \\ & & 1 \end{pmatrix}, \quad (5.23)$$

with  $c_{12} = \cos \tilde{\theta}_{12}$ ,  $s_{12} = \sin \tilde{\theta}_{12}$  and  $P$  being an arbitrary phase matrix. Due to the way the PMNS matrix is parametrized (2.15) with the 1-2 rotation to the right, this 1-2 correction only affects the solar angle, while maintaining the predictions of a maximal atmospheric and vanishing reactor angle. Since large corrections to this angle are not allowed, in the phenomenologically acceptable parameter space the relations  $\hat{e} \ll \hat{b}, \hat{a}, \hat{d}$  should hold.

On the other hand, if we take  $\hat{b} \neq 0$  while  $\hat{e} = 0$ , we see from Eq. (5.22) that this requires a 1-3 correction  $U = U_{HPS}U_{13}(\tilde{\theta}_{13})P$ , where  $U_{13}(\tilde{\theta}_{13})$ , analogous to  $U_{12}(\tilde{\theta}_{12})$ , denotes a complex rotation in the 1-3 plane. This correction is of the trimaximal mixing [56–63] form discussed in Section 2.5, which can perturb TBM back into agreement with experiment. The effect of the various deviations from TBM is illustrated in Fig. 5.2.

To gain an analytical understanding of how the additional parameters affect the mixing angles, we can perform a perturbative analysis in the limit of small  $\hat{e}$  and therefore small  $|\sin^2 \theta_{12} - \frac{1}{3}|$ . The PMNS matrix can be described by  $U_{HPS}U_{13}(\tilde{\theta}_{13})U_{12}(\tilde{\theta}_{12})P$ , where  $\tilde{\theta}_{12}$  and  $\tilde{\theta}_{13}$  are small in the phenomenologically interesting region and the Majorana phases are given by  $P = \text{diag}(e^{i\alpha_1/2}, 1, e^{i\alpha_3/2})$ . Hence, we can permute the matrices  $U_{12}$  and  $U_{13}$  and we define  $r_{1i} = \sin \tilde{\theta}_{1i} \cos \tilde{\delta}_{1i}$  and  $t_{1i} = \tan \tilde{\delta}_{1i}$ , which evaluate to

$$r_{13} = \frac{\hat{b} \sin \alpha_\lambda}{4\hat{a} + 2\hat{b} \cos \alpha_\lambda}, \quad t_{13} = \frac{2\hat{a} \cos \alpha_\lambda + \hat{b}}{2\hat{d} \sin \alpha_\lambda}, \quad (5.24a)$$

$$r_{12} = \frac{\sqrt{2}\hat{d}\hat{e}\sin\alpha_\lambda}{\Delta m_{21,0}^2}, \quad t_{12} = \frac{2(2\hat{a} + \hat{d})\cos\alpha_\lambda + \hat{b}}{2\hat{d}\sin\alpha_\lambda}, \quad (5.24b)$$

where  $\Delta m_{21,0}^2$  is the leading order solar mass squared difference, i.e. neglecting the small corrections of  $r_{13}$  and  $\hat{e}$ . The phases of the matrix  $P$  are given by

$$\tan\alpha_1 = \frac{2\hat{b}r_{13}\cos\alpha_\lambda - \sin\alpha_\lambda(2\hat{b}r_{13}t_{13} + \hat{b} + 2\hat{e})}{2(\hat{a} + \hat{b}r_{13}\sin\alpha_\lambda + \hat{d}) + \cos\alpha_\lambda(2\hat{b}r_{13}t_{13} + \hat{b} + 2\hat{e})}, \quad (5.25a)$$

$$\tan\alpha_2 = \frac{\sin\alpha_\lambda(\hat{b}(2r_{13}t_{13} - 1) + 2\hat{e}) + 2\hat{b}r_{13}\cos\alpha_\lambda}{2(\hat{a} + \hat{b}r_{13}\sin\alpha_\lambda - \hat{d}) + \cos\alpha_\lambda(-2\hat{b}r_{13}t_{13} + \hat{b} - 2\hat{e})}. \quad (5.25b)$$

Similar to [131], we can parameterize the leptonic mixing matrix in terms of deviations from the tri-bimaximal mixing angles

$$\sin\theta_{13} = \frac{r}{\sqrt{2}}, \quad \sin\theta_{12} = \frac{1}{\sqrt{3}}(1 + s), \quad \sin\theta_{23} = \frac{1}{\sqrt{2}}(1 + a). \quad (5.26)$$

The Dirac CP phase  $\delta_{CP}$  is undefined in the tri-bimaximal mixing limit and we leave it free and do not expand in it. Besides the contributions of  $\alpha_{1,3}$  to the Majorana phases  $\varphi_{1,2}$  of Eq. (2.15), there are also small corrections  $\delta\varphi_{1,2}$  from the matrices  $U_{12}(\tilde{\theta}_{12})$  and  $U_{13}(\theta_{13})$

$$\varphi_1 = \alpha_1 - \alpha_3 + \delta\varphi_1, \quad \text{and} \quad \varphi_2 = \pi - \alpha_3 + \delta\varphi_2. \quad (5.27)$$

This expansion leads to the following form of the leptonic mixing matrix

$$U_{PMNS} = \begin{pmatrix} \frac{s+i\delta\varphi_1-2}{\sqrt{6}} & \frac{2i(s+1)+\delta\varphi_2}{2\sqrt{3}} & -\frac{e^{-i\delta}r}{\sqrt{2}} \\ \frac{2(-a+e^{i\delta}r+s+1)-i\delta\varphi_1}{2\sqrt{6}} & \frac{\delta\varphi_2-i(2a+e^{i\delta}r+s-2)}{2\sqrt{3}} & -\frac{a+1}{\sqrt{2}} \\ \frac{2(a-e^{i\delta}r+s+1)-i\delta\varphi_1}{2\sqrt{6}} & \frac{i(2a+e^{i\delta}r-s+2)+\delta\varphi_2}{2\sqrt{3}} & -\frac{a-1}{\sqrt{2}} \end{pmatrix} P. \quad (5.28)$$

Equating the expanded form of  $U_{PMNS}$  to  $U_{HPS}U_{13}(\tilde{\theta}_{13})U_{12}(\tilde{\theta}_{12})P$  determines all free parameters  $s, r, a, \delta, \delta\varphi_1, \delta\varphi_2$  as well as some corrections to unphysical phases, which we suppressed for simplicity. The first order deviations from the mixing angles are

$$s = -\sqrt{2}r_{12}t_{12}, \quad r\cos\delta = -\frac{2r_{13}}{\sqrt{3}}, \quad a = \frac{r_{13}}{\sqrt{3}}. \quad (5.29)$$

and the CP phases are given by

$$\tan\delta_{CP} = \tan\tilde{\delta}_{13} \quad \varphi_1 = \alpha_1 - \alpha_3 - 2\sqrt{2}r_{12} \quad \varphi_2 = \pi - \alpha_3 - 2\sqrt{2}r_{12}. \quad (5.30)$$

Following [131], we can derive a sum rule, which relates the deviations of the atmospheric mixing angle with the ones of the reactor mixing angle

$$a = -\frac{1}{2}r\cos\delta_{CP}. \quad (5.31)$$

The masses are determined by

$$m_1^2 = \hat{a}^2 + \hat{b}(\hat{a} + \hat{d})\cos\alpha_\lambda + 2\hat{a}\hat{d} + \frac{\hat{b}^2}{4} + \hat{d}^2, \quad m_2^2 = \hat{a}^2, \quad (5.32)$$

$$m_3^2 = \hat{a}^2 + \hat{b}(\hat{a} - \hat{d})\cos\alpha_\lambda - 2\hat{a}\hat{d} + \frac{\hat{b}^2}{4} + \hat{d}^2,$$



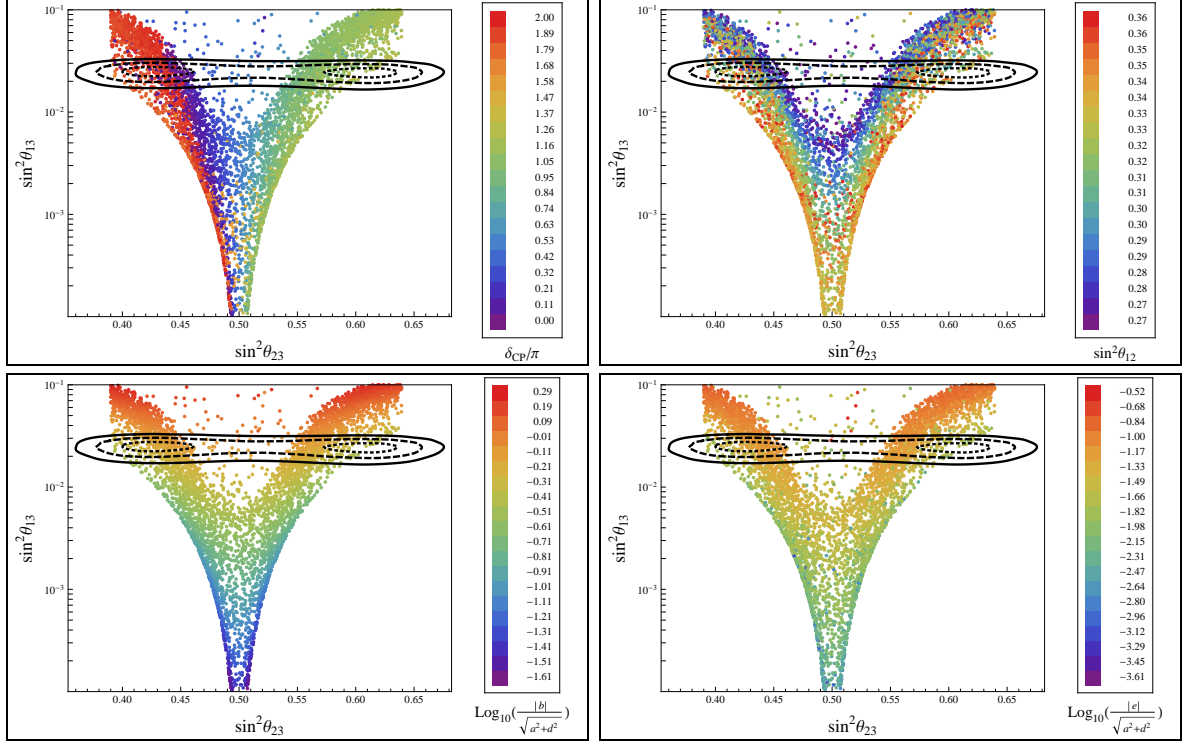


**Figure 5.3:** Dependence of the reactor angle  $\theta_{13}$  on the atmospheric mixing angle  $\theta_{23}$ . The various colour codings are given under each subfigure. Top left: For  $\sin^2 \theta_{23} < 1/2$  ( $\sin^2 \theta_{23} > 1/2$ ) the model predicts  $\delta_{CP} = 0, 2\pi$  ( $\delta_{CP} = \pi$ ). Top right: The scatterplot shows a band structure in  $\sin^2 \theta_{12}$ . Bottom left: For the points in the experimentally allowed region,  $\hat{b}$  has to be of similar size as  $\hat{a}, \hat{d}$ . Bottom right: For the points in the experimentally allowed region,  $\hat{e}$  has to be of approximately one order of magnitude smaller than  $\hat{a}, \hat{d}$ .

to leading order in the small mixings  $r_{13}, r_{12}$ , and the leading order ratio of mass squared differences is given by

$$\frac{\Delta m_{21}^2}{\Delta m_{32}^2} = \frac{4\hat{a}(2\hat{d} + \hat{b} \cos \alpha_\lambda) + 4\hat{d}(\hat{d} + \hat{b} \cos \alpha_\lambda) + \hat{b}^2}{4\hat{a}(2\hat{d} - \hat{b} \cos \alpha_\lambda) - 4\hat{d}(\hat{d} - \hat{b} \cos \alpha_\lambda) - \hat{b}^2}. \quad (5.33)$$

At next-to leading order,  $m_1$  and  $m_3$  receive corrections

$$\delta m_1^2 = \hat{b}(2r_{13}(\hat{a} + \hat{d}) \sin \alpha_\lambda + \hat{b} r_{13} t_{13} + \hat{e}) + 2(\hat{a} + \hat{d}) \cos \alpha_\lambda (\hat{b} r_{13} t_{13} + \hat{e}) \quad (5.34a)$$

$$\delta m_3^2 = -\hat{b}(-2r_{13}(\hat{a} - \hat{d}) \sin \alpha_\lambda + \hat{b} r_{13} t_{13} + \hat{e}) - 2(\hat{a} - \hat{d}) \cos \alpha_\lambda (\hat{b} r_{13} t_{13} + \hat{e}). \quad (5.34b)$$

To illustrate our findings numerically, we have performed a numerical scan over the model's parameter space. We have randomly drawn values for the model parameters of order unity, assuming a Gaussian distribution with an expectation value of one and a variance of 0.5. The plots in Fig. 5.3 show the relation between the atmospheric mixing angle  $\theta_{23}$  and the reactor angle  $\theta_{13}$ . From the bottom two plots one can read off that  $\hat{b}$  is of the same order as  $\hat{a}$  and  $\hat{d}$  for the experimentally measured  $\theta_{13}$  while  $\hat{e}$  has to be about one order of magnitude smaller. The colour codings of the two top panels show the mixing parameters  $\delta_{CP}$  and  $\sin^2 \theta_{12}$ . Clearly, the model is predictive: if  $\sin^2 \theta_{23}$  is found to be close to the best fit point in the octant with  $\sin^2 \theta_{23} < 1/2$ , the prediction for the CP phase is  $\delta_{CP} = 0, 2\pi$  while for  $\sin^2 \theta_{23} > 1/2$  it is predicted to be  $\delta_{CP} = \pi$ . To establish the correlation with  $\sin^2 \theta_{12}$  shown in the top

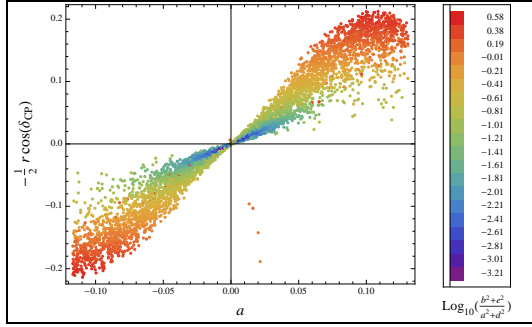


**Figure 5.4:** Numerical evaluation of the approximate atmospheric sum rule (5.31). The numerical evaluation shows that the sum rule holds to a good degree of approximation.

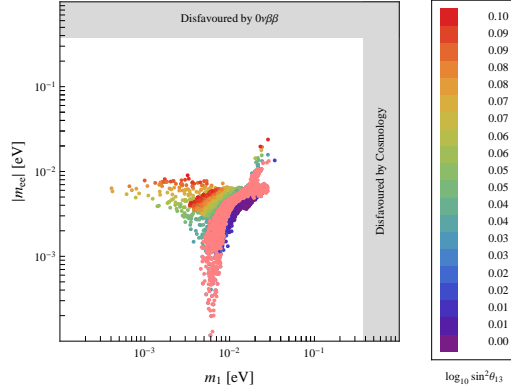


**Figure 5.5:** Expectation for the effective mass of neutrinoless double beta decay. The pink points lie within the 3 sigma region for all oscillation parameters. The points with colour coding lie within the 3 sigma range for all observables except  $\theta_{13}$ .

right panel, a precision determination of all the mixing angles is needed. In Fig. 5.4, as a consistency check of our analytical expressions, the atmospheric sum rule (5.31) is shown for the points obtained in the numerical scan. The colour coding gives an indication of the magnitude of deviations from TBM and for small values the approximate relation is fulfilled to good accuracy.

Finally, let us comment on the predictions for neutrinoless double beta decay. As can be read off from Eq. (5.21), the effective Majorana mass of the electron neutrino is given by

$$|m_{ee}| = \left| \hat{a} + \frac{2\hat{d}}{3} + \left( 2\hat{e} + \frac{\hat{b}}{3} \right) e^{i\alpha\lambda} \right|, \quad (5.35)$$

which can be expressed in terms of physical parameters as

$$|m_{ee}| = \left| \sum_i U_{ei}^2 m_i \right| \approx \frac{2m_1 - m_2}{3} \left| 1 - \frac{2m_1 + 2m_2}{2m_1 - m_2} s - i \frac{2\delta\varphi_1 m_1 - \delta\varphi_2 m_2}{2m_1 - m_2} \right|. \quad (5.36)$$

As the additional neutral fermions  $S$  do not mix with neutrinos, there is no additional contribution due to the heavy singlet, like in Ma's scotogenic model [165, 166]. In Fig. 5.5 we show the predicted range for the effective Majorana mass of the electron neutrino. As can be seen, the scan of parameters prefers moderately large values of the absolute mass scale, however, the effective Majorana mass of the electron neutrino can become small or even vanish.

### 5.3. Lepton Flavour Violation

In models with radiative neutrino mass generation, generally the particles in the loop can also mediate flavour changing processes, in particular lepton flavour violating rare decays. Before we enter into a detailed discussion of the various processes, we want to remind the reader

about the remnant  $Z_3$  symmetry in the charged lepton sector

$$(H, \varphi', \varphi'') \sim (1, \omega^2, \omega), \quad (L_e, L_\mu, L_\tau) \sim (1, \omega^2, \omega), \quad (e^c, \mu^c, \tau^c) \sim (1, \omega, \omega^2), \quad (5.37)$$

which suppresses several LFV rare decays. If the remnant  $Z_3$  would be a symmetry of the whole Lagrangian, only the following LFV rare decays

$$\tau^+ \rightarrow \mu^+ \mu^+ e^- \quad \text{and} \quad \tau^+ \rightarrow e^+ e^+ \mu^-$$

and their charged conjugates would be allowed. All other decays can only proceed through a coupling to the  $Z_3$  breaking VEVs of the neutrino sector. Those decays are naturally suppressed and the symmetry thus protects the model from large constraints. At first, we will discuss the radiative LFV rare decays  $l_i \rightarrow l_j \gamma$  in Section 5.3.1, focusing on the experimentally most well studied process, namely the process  $\mu \rightarrow e \gamma$ . In Section 5.3.2, we discuss the LFV rare decays with purely leptonic final states, which are allowed at tree level, but suppressed by a three-body final state. Finally, we calculate the anomalous magnetic moment of the muon and compare it to experiment in Section 5.3.3.

### 5.3.1. Radiative LFV Decays $l_i \rightarrow l_j \gamma$

Let us first discuss the process of type  $l_i \rightarrow l_j \gamma$  using an effective field theory approach. Such processes are described by effective operators of the form [167, 168]

$$L \sigma_{\mu\nu} F^{\mu\nu} \ell^c \tilde{H} / M^2 \sim (\underline{\mathbf{3}}_1, 1), \quad (5.38)$$

which transforms in the same way as the mass term under the flavour symmetry. It thus has to be multiplied by flavons to form an invariant. As we already mentioned, the remnant  $Z_3$  symmetry in the charged lepton sector forbids all radiative LFV rare decays. Hence, the effective operator in Eq. (5.38) has to involve VEVs of the neutrino sector in order to lead to non-vanishing decay rates. The lowest order operators that can multiply the mentioned LFV operator in the flavour basis read

$$\Omega_T^\dagger \langle (\phi_1^4)_{\underline{\mathbf{3}}_1} \rangle = \frac{1}{6} (ab(b^2 - a^2)) (1, 1, 1)^T, \quad (5.39a)$$

$$\Omega_T^\dagger \langle (\phi_2^4)_{\underline{\mathbf{3}}_1} \rangle = \frac{1}{6} (cd(d^2 - c^2)) (1, 1, 1)^T, \quad (5.39b)$$

$$\Omega_T^\dagger \langle (\phi_1^2 \phi_2^2)_{\underline{\mathbf{3}}_1} \rangle = \frac{1}{3} (ab(c^2 - d^2)) (1, 1, 1)^T, \quad (5.39c)$$

$$\Omega_T^\dagger \langle (\phi_1^2 \phi_2^2)_{\underline{\mathbf{3}}_1} \rangle = \frac{1}{3} (cd(a^2 - b^2)) (1, 1, 1)^T. \quad (5.39d)$$

There can be more than one contraction, but in the vacuum they all result in these expressions. The lowest order effective operators thus all give contributions that can be written as

$$\mathcal{L}_{eff} = i \frac{e}{M^2} \ell^{cT} H^\dagger \sigma_{\mu\nu} F^{\mu\nu} \mathcal{M} L + \text{h.c.} \quad \text{with} \quad \mathcal{M} = \begin{pmatrix} \alpha_1 & \alpha_1 & \alpha_1 \\ \alpha_2 & \alpha_2 & \alpha_2 \\ \alpha_3 & \alpha_3 & \alpha_3 \end{pmatrix} \frac{\langle \phi_1^4 \rangle}{M^4} \quad (5.40)$$

where  $\alpha_i$  are dimensionless couplings that should (naturally) be of order one and the mass scale  $M$  is the suppression scale of the higher dimensional operators. Note that the structure

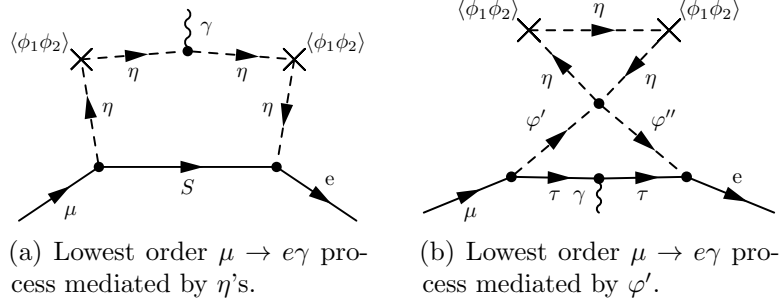


**Figure 5.6:** Lowest order  $\mu \rightarrow e\gamma$  processes mediated by  $\eta_i$  (left) and  $\varphi^{(\prime)}$  (right). There has to a coupling to the VEVs  $\langle\phi_1\phi_2\rangle$  of the neutrino sector, which suppresses the amplitudes.

of flavour symmetry breaking in the neutrino sector is encoded in  $\mathcal{M}$ . The symmetry thus automatically leads to a large suppression. From this matrix the LFV transition amplitudes can be determined as [167]

$$\frac{\text{Br}(l_i \rightarrow l_j \gamma)}{\text{Br}(l_i \rightarrow l_j \nu_i \bar{\nu}_j)} = \frac{12\sqrt{2}\pi^3\alpha}{G_F^3 m_i^2 M^4} \left( |\mathcal{M}_{ij}|^2 + |\mathcal{M}_{ji}|^2 \right)^2 \quad (5.41)$$

and the magnetic dipole moments  $a_i$  and electric dipole moments  $d_i$  of the charged leptons are given by [167]

$$a_i = 2m_i \frac{v}{\sqrt{2}M^2} \text{Re}\mathcal{M}_{ii}, \quad d_i = e \frac{v}{\sqrt{2}M^2} \text{Im}\mathcal{M}_{ii}. \quad (5.42)$$

Note that the matrix  $\mathcal{M}$  has additional dominant contributions to the diagonal entries stemming from operators that involve  $\chi$  instead of  $(\phi_i)^4$ . Using only the observables  $\mu \rightarrow e\gamma$ ,  $\tau \rightarrow \mu\gamma$  and  $\tau \rightarrow e\gamma$  as well as charged lepton electric and dipole moments, it is therefore very hard to test the underlying symmetry pattern, but it can give important indications distinguishing different models. For example in this model one would expect – barring the possibility of fine-tuned cancellations among the  $\alpha_i$  – similar branching ratios for the LFV decays  $\mu \rightarrow e\gamma$ ,  $\tau \rightarrow \mu\gamma$  and  $\tau \rightarrow e\gamma$ , as was also found in SUSY  $A_4$  models [167, 169].

In the following, we will focus on  $\mu \rightarrow e\gamma$ , which is the most tightly constrained LFV rare decay. The leading contribution to  $\mu \rightarrow e\gamma$  is given by the diagrams depicted in Fig. 5.6a. It is similar to the neutrino mass diagram Fig. 5.1 in the last section. LFV rare decays mediated by the flavour violating EW doublets  $\varphi^{(\prime)}$  are suppressed by one more loop order because of the necessity to couple to the neutrino sector VEVs. Hence, they only show up at two loop order, as shown in Fig. 5.6b. We will therefore not consider this diagram further.

Without any mass insertion along the  $\eta$  line, a one-loop diagram of this type evaluates to [166, 170, 171]

$$\text{Br}(\mu \rightarrow e\gamma) = \frac{3\alpha}{64\pi(G_F m_0^2)^2} C^4, \quad (5.43)$$

where  $m_0^2 = \frac{1}{3}(M_1^2 + M_2^2 + M_3^2)$  and, using  $x_J = (M_{\eta^+}^2)_{JJ}/m_0^2$  and  $h_{\alpha k J} = \frac{\partial \mathcal{L}_\nu}{\partial L_\alpha \partial S_k \partial \eta_J}$ ,

$$C^2 = \left| \sum_{i=1}^3 \sum_{J=1}^9 h_{\mu i J} h_{e i J}^* x_J^{-2} F_2(M_S^2/(M_{\eta^+}^2)_{JJ}) \right| \quad \text{and} \quad F_2(t) = \frac{1 - 6t + 3t^2 + 2t^3 - 6t^2 \ln t}{6(1-t)^4}.$$

In our model, we have  $C^2 = 0$  for the symmetry reasons given above and there have to be mass insertions to generate flavour violating interactions. Note that this is a welcome feature since LFV processes of this type severely constrain models that generate neutrino masses radiatively [166]. This can be seen as the experimental constraint  $\text{Br}(\mu \rightarrow e\gamma) < 2.4 \cdot 10^{-12}$  [49] requires  $C^4 \sim 1.5 \cdot 10^{-8}$  for  $M_S = m_0 = 100 \text{ GeV}$ . The flavour symmetry automatically reduces  $C^2$  by a factor  $\left(\frac{\delta M_{\eta^+}^2}{M_{\eta^+}^2}\right)^2$ . In the limit  $\left(\frac{\delta M_{\eta^+}^2}{M_{\eta^+}^2}\right)^2 \ll 1$ , the diagram 5.6a can be computed explicitly and we find

$$\text{Br}(\mu \rightarrow e\gamma) = \frac{\alpha}{16\pi(G_F m_0^2)^2} \tilde{C}^4 \quad (5.44)$$

where

$$\tilde{C}^2 = \frac{1}{m_0^4} \left| \sum_{i=1}^3 \sum_{J,K,L=1}^9 h_{\mu i J} \left(\delta M_{\eta^+}^2\right)_{JK} \left(\delta M_{\eta^+}^2\right)_{KL} h_{eiL}^* F_4(M_S, M_J, M_K, M_L) \right| \quad (5.45)$$

and  $F_4$  is a dimensionless loop integral, which we only give in the limit of degenerate  $\eta$  masses

$$\begin{aligned} G_2(t) &\equiv F_4(M_S = tm_0, M_J = m_0, M_K = m_0, M_L = m_0) \\ &= \frac{1}{48(t^2 - 1)^{12}} [1 - 12t^2 - 36t^4 + 44t^6 + 3t^8 - 24(2t^2 + 3)t^4 \ln t]. \end{aligned} \quad (5.46)$$

The dimensionless functions  $F_2$  and  $G_2$  are plotted in Fig. 5.7. The explicit form of the sum in the expression (5.45) for  $\tilde{C}^2$  is quite involved and will not be shown here, but it can be easily obtained using Eq. (A.24) from the appendix. Here, we only comment on the generic size of the branching ratio. In general, the processes  $\mu \rightarrow e\gamma$  and the radiative neutrino mass diagram break different approximate symmetries and it is therefore not necessarily the case that the smallness of neutrino masses implies a small branching ratio. This is also the case here. For example from Eq. (5.20), one can read off that the smallness of neutrino mass could be due to very small values for  $\lambda_1 \approx \lambda_2 \approx 10^{-9}$ , with all other couplings being order one. Then the dominant contributions to  $\tilde{C}^2$  would be of the type

$$\tilde{C}^2 \supset \frac{G_2(t)}{m_0^4} \frac{1}{432} h_2 \lambda_4 (bc - ad) [-h_1 \lambda_3 (ac + bd) + \omega^2 h_2 \lambda_4 (bc - ad)] , \quad (5.47)$$

where we have again used the limit of degenerate masses  $M_i = m_0$ , and could in principle be of order one. However, if we stick to the parts of parameter space where the smallness of neutrino mass is due to many moderately small couplings  $h_i, \lambda_i \sim \mathcal{O}(0.01 - 0.1)$  and  $m_0 \sim \mathcal{O}(\text{TeV})$ ,  $\langle \chi \rangle, \langle \phi_i \rangle \sim \mathcal{O}(100 \text{ GeV})$  (as discussed below (5.20)) instead of one very small coupling, the branching ratio is heavily suppressed by  $\tilde{C}^4 \sim (10^{-9} - 10^{-13})^2$ . These natural parameter values thus give an appealing explanation of both the smallness of neutrino masses and the suppression of LFV decays.

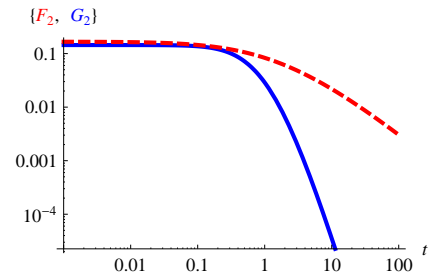


Figure 5.7: The functions  $F_2$ (red) and  $G_2$ (blue).

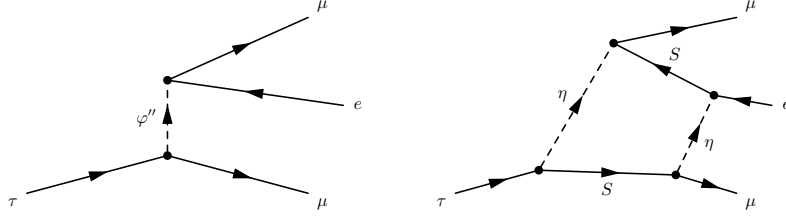


Figure 5.8: Lepton Flavour Violating rare decays.

### 5.3.2. LFV Decays $l_i \rightarrow ll$

Another class of processes that are of interest for our model are rare flavour violating decays of the type  $\mu \rightarrow eee$ . As in the case of the processes  $f_i \rightarrow f_j \gamma$  the allowed decay channels are restricted by the flavour symmetry. If we do not consider the heavily suppressed diagrams that couple to VEVs in the neutrino sector, it is clear that the process  $\mu \rightarrow eee$  is not allowed by the  $Z_3$  symmetry of the charged lepton sector and the most constraining process is given by  $\tau^- \rightarrow \mu^- \mu^- e^+$ .

This process can be mediated at tree-level by the neutral components of  $\varphi''$  as depicted in the first diagram of Fig. 5.8 and its branching ratio is given by [162, 164]

$$\text{Br}(\tau^- \rightarrow \mu^- \mu^- e^+) = \left( \frac{36m_\tau^2 m_\mu^2}{M_0^4} \right) \text{Br}(\tau \rightarrow \mu\nu\nu) = 2.3 \cdot 10^{-8} \left( \frac{55 \text{ GeV}}{M_0} \right)^4 \quad (5.48)$$

where we have used  $\text{Br}(\tau \rightarrow \mu\nu\nu) = .174$ . Compared to the experimental upper bound of  $2.3 \cdot 10^{-8}$  [172], the effective mass<sup>5</sup>

$$\frac{1}{M_0^4} = \left[ \frac{\sin^2 \alpha}{m_{\Phi_1}^2} + \frac{\cos^2 \alpha}{m_{\Phi_2}^2} \right]^2 \quad (5.49)$$

is thus only weakly constrained. All other processes mediated by  $\varphi^{(\prime)}$  are further suppressed by  $y_e y_\tau$  or  $y_\mu y_e$ . Rare LFV processes mediated by these fields are therefore naturally suppressed by smallish Yukawa couplings and do not put a serious constraint on the model.

Let us also estimate the magnitude of the second diagram in Fig. 5.8 mediating  $\tau \rightarrow \mu\mu e$ , as this diagram may in principle be larger because it is not suppressed by Yukawa couplings that are known to be small.

To get an estimate, we work in the limit of degenerate  $\eta$  masses  $M_1 = M_2 = M_3 = m_0$  and find

$$\Gamma(\tau^- \rightarrow \mu^- \mu^- e^+) = \left| \frac{1}{16\pi^2} \sum_{j,k=1}^9 \sum_{i,l=1}^3 h_{\tau ij} h_{\mu ik}^* h_{elk} h_{\mu lj}^* \frac{H(M_S/m_0)}{m_0^2} \right|^2,$$

where  $H(M_S/m_0)$  is a dimensionless loop integral and  $\text{Br}(\tau^- \rightarrow \mu^- \mu^- e^+) = \text{Br}(\tau \rightarrow \mu\nu\nu) \frac{\Gamma(\tau^- \rightarrow \mu^- \mu^- e^+)}{\Gamma(\tau^- \rightarrow \mu^- \bar{\nu}_\mu \nu_\tau)}$ . Evaluating the sum, we find  $\sum_{j,k=1}^9 \sum_{i,l=1}^3 h_{\tau ij} h_{\mu ik}^* h_{elk} h_{\mu lj}^* = \frac{1}{27} (h_1^4 - h_1^2 h_2^2 + h_2^4)$  and the experimental bound

$$\text{Br}(\tau^- \rightarrow \mu^- \mu^- e^+) = \left| \left( \frac{140 \text{ GeV}}{m_0} \right)^2 (h_1^4 + h_2^4 - h_1^2 h_2^2) H(M_S/m_0) \right|^2 \cdot 2.3 \cdot 10^{-8} \quad (5.50)$$

<sup>5</sup>In [162]  $\lambda_{\chi A} = 0$  was assumed, which implies  $\alpha = \pi/4$ .

can easily be evaded even for small values of  $m_0 \sim 178 \text{ GeV} \approx 308/\sqrt{3} \text{ GeV}$  (which would give the correct dark matter relic abundance of  $\eta$  in the degenerate limit we are considering here, as will be discussed in Section 5.4.2) and order one Yukawas (assuming  $H(t) \sim 1$ ). For the parameter ranges preferred by one-loop neutrino mass generation, i.e.  $h_i \sim 0.1$ , the expected branching ratio is too small to expect a signal in next-generation experiments. In summary, we can conclude that the flavour symmetry effectively protects against lepton flavour violating interactions.

### 5.3.3. Anomalous Magnetic Moment of Muon

Let us now briefly discuss EDMs. The contribution from the exchange of the neutral component  $\varphi''$  should give the largest contributions, as it is proportional to the tau Yukawa coupling squared. It has been calculated previously [161] and amounts to

$$\Delta a_\mu = \frac{G_F m_\tau^2}{2\sqrt{2}\pi^2} \left( \frac{m_\mu^2}{M_0^2} \right) = 1.5 \cdot 10^{-12} \left( \frac{100 \text{ GeV}}{M_0} \right)^2, \quad (5.51)$$

which is negligible and cannot account for the reported deviation of  $(290 \pm 90) \times 10^{-11}$  [173, 174], from the Standard Model. The charged components of  $\eta$  also contribute to the anomalous magnetic moment of the muon, with a strength given by [170, 174]

$$\begin{aligned} \Delta a_\mu &= -\frac{m_\mu^2}{3(4\pi^2)^2} \left[ \frac{h_1^2}{M_1^2} F_2 \left( \frac{M_S}{M_1} \right) + \frac{h_2^2}{M_2^2} F_2 \left( \frac{M_S}{M_2} \right) \right] \\ &= -1.8 \times 10^{-12} \sum_i \left( \frac{h_i}{.1} \right)^2 \left( \frac{100 \text{ GeV}}{M_i} \right)^2 \left( \frac{F_2(\frac{M_S}{M_i})}{F_2(1)} \right). \end{aligned} \quad (5.52)$$

This therefore gives a very mild constraint on the masses and Yukawa couplings of the  $\eta$ 's. In the preferred parameter space for neutrino mass generation, this contribution is negligible. Note that the contribution goes in the opposite direction of the reported excess and it can therefore not be used to explain it [175].

## 5.4. Dark Matter

In this section we discuss dark matter candidates of the model and their phenomenology.

### 5.4.1. Dark Matter Candidates and their Stability

To start off the discussion of possible dark matter candidates in our model, let us dwell on the remnant symmetries left over after symmetry breakdown. While the  $Q_8 \times A_4$  part of the symmetry group is completely broken, there is a  $Z_2$  symmetry given by

$$\mathcal{R}: \quad L \rightarrow -L \quad \ell^c \rightarrow -\ell^c \quad \eta_i \rightarrow -\eta_i, \quad (5.53)$$

which is the  $(-1)^{L'}$  remnant of the auxiliary  $Z_4$  symmetry  $i^{L'}$ , where  $L' = L + N_\eta$  is the generalized lepton number symmetry that is the sum of the usual SM lepton number with the  $\eta$  number  $N_\eta$ . At the renormalizable level after symmetry breaking, there is another  $Z_2$  symmetry of the model given by

$$\mathcal{A}: \quad S \rightarrow -S \quad \eta_i \rightarrow -\eta_i. \quad (5.54)$$

This is purely an accidental symmetry that emerges due to the particle content and the requirement of renormalizability and not a remnant of some symmetry we have imposed on the model. The reason why it emerges can be traced back to the fact that the SM fermions as well as  $\chi$  transform only under the generators  $S$  and  $T$  which form the subgroup  $A_4$  and thus there are no operators of the form  $\varphi \mathcal{O}_{A_4}$ , where  $\varphi$  is a field transforming non-trivially under  $X$  (e.g. fields transforming as  $\mathbf{3}_i$  with  $i \neq 1$  such as  $S$  and  $\eta$ ) and  $\mathcal{O}_{A_4}$  an arbitrary operator formed by fields transforming under  $A_4$ . These two symmetries in tandem make dark matter stable. Note that the remnant symmetry  $\mathcal{R}$  alone would not be sufficient, as e.g. the decay of the lightest particle contained in  $\eta_i$  to neutrinos and the neutral CP-even component of the Higgs would be possible. The symmetry  $\mathcal{A}$  makes the lightest component of  $S$  and  $\eta$  stable, which implies that the dark matter candidate is either fermionic or bosonic. This symmetry, however, is only an accidental symmetry and there is thus no reason for higher dimensional operators to respect this symmetry. Such a higher dimensional operator  $\mathcal{O}$  with  $\mathcal{A}[\mathcal{O}] \neq \mathcal{O}$  would lead to a decay of the dark matter candidate. On the contrary, all higher dimensional operators have to respect the symmetry  $\mathcal{R}[\mathcal{O}] = \mathcal{O}$ , as this symmetry is a remnant of an exact symmetry and is therefore also exact. We will now show that this requirement pushes up the dimensionality of the higher dimensional decay operators to a level where the dark matter candidate is stable for all practical purposes. Since the discussion depends on whether the dark matter candidate stems from  $\eta$  or from  $S$ , we discuss the two possibilities in turn.

**Scalar DM:** Any effective operator that would mediate a decay of the lightest component of  $\eta_i$  has to be of the form

$$\mathcal{O} = \eta_i \mathcal{O}_{SM}^{\Delta L=1} \langle \mathcal{O}_{\phi_k \phi_l} \rangle \quad (5.55)$$

where  $\langle \mathcal{O}_{\phi_k \phi_l} \rangle$  is built out of SM-singlet flavon fields and transforms even under  $\mathcal{R}$ . As  $\eta$  is odd under  $\mathcal{R}$ , the operator  $\mathcal{O}_{SM}^{\Delta L=1}$ , which is built up of SM fields, has to be also odd under  $\mathcal{R}$  to make the complete operator invariant. Obviously the complete operator  $\mathcal{O}$  is odd under the accidental symmetry  $\mathcal{A}$  and thus mediates DM decay.

Since  $\mathcal{R}$  acts upon SM particles as the discrete subgroup of lepton number  $(-1)^L$ , the operator  $\mathcal{O}_{SM}^{\Delta L=1}$  has to violate lepton number by an odd unit and has to transform as an electroweak doublet. The lowest dimensional operators in the SM arise at dimension six and violate  $L$  by one unit (See [176] for a recent review of gauge invariant dimension 6 operators.)

$$L u^c d^c d^c \quad \bar{L} \bar{d}^c \bar{d}^c \bar{d}^c \quad L \bar{Q} \bar{Q} d^c \quad \bar{e}^c \bar{Q} d^c d^c \quad (5.56a)$$

$$\chi^\dagger L Q Q Q \quad \chi^\dagger e^c u^c u^c d^c \quad \chi^\dagger \bar{L} \bar{Q} u^c d^c \quad \chi^\dagger \bar{e}^c Q Q \bar{u}^c \quad \chi^\dagger L Q \bar{u}^c \bar{d}^c. \quad (5.56b)$$

All dimension 6 operators in Eq. (5.56a) break baryon number by one unit,  $B - L$  by two units and preserve  $B + L$ . The dimension 7 operators in Eq. (5.56b) on the other hand break baryon number by one unit, preserve  $B - L$  and break  $B + L$  by two units. They are formed by adjoining a  $\chi$  to a dimension 6 proton decay operator. Since baryon number is an accidental symmetry in our model (in the same way as in the Standard Model), these operators are never generated<sup>6</sup> within the model and thus dark matter is stable within the model. They rather parametrize some baryon number violating physics, which from proton decay experiments is pushed to scales of the order of  $\Lambda_B \approx 10^{16}$  GeV.

To form a singlet under the flavour symmetry, the second operator  $\mathcal{O}_{\phi_k \phi_l}$  is needed to make the total operator  $\mathcal{O}$  a singlet under the flavour symmetry, as  $\eta_i$  transforms under  $X$  while

<sup>6</sup>Except through instantons and sphalerons, which do not play a role here, in the same way as in the SM.



$\mathcal{O}_{SM}^{\Delta L=1}$  does not. It has to be composed of an even number of flavons  $\phi_k$ , as under the  $Z_2$  subgroup generated by <sup>7</sup>  $X^2$  only  $\phi_k$  transforms non-trivially.

If we assume the presence of baryon number violating operators at scale  $\Lambda_B$ , the dark matter candidate  $\eta$  decays into quarks and one lepton. Under the assumption that the flavour part of the operator is related to the breaking of the flavour symmetry  $\Lambda_F$ , a DM decay operator formed by a dimension 6 SM operator  $\mathcal{O}_{SM}^{\Delta L=1}$  is suppressed by  $\Lambda_B^3$ :

$$\frac{\eta_i \mathcal{O}_{SM}^{\Delta L=1} \langle \phi_k \phi_l \rangle}{\Lambda_B^3 \Lambda_F^2}. \quad (5.57)$$

Hence, the lifetime of DM can be estimated to be

$$\Gamma^{-1} \sim \frac{8\pi\Lambda_B^6}{m_\eta^7} \left( \frac{\Lambda_F^2}{\langle \phi_k \phi_l \rangle} \right)^2 = 1.9 \cdot 10^{45} \text{Gyr} \left( \frac{\Lambda_B}{10^{16} \text{GeV}} \right)^6 \left( \frac{100 \text{GeV}}{m_\eta} \right)^7 \left( \frac{\Lambda_F^2}{\langle \phi_k \phi_l \rangle} \right)^2 \quad (5.58)$$

and the dark matter candidate is thus stable even on cosmological time-scales, if one assumes ‘traditional’ values of for the scale of baryon number violating physics. However the operators in Eq. (5.56a) are not those directly tested in proton decay experiments and the physics of baryon number violation might be such that the operators in Eq. (5.56a) are suppressed by a smaller energy scale than the one responsible for baryon decay. We will come back to the issue of induced proton decay at the end of the subsection, but now we want to turn the logic around and derive bounds on  $\Lambda_B$  and  $\Lambda_F$  from the fact that dark matter is still around.

Decaying DM models are constrained by WMAP to  $\Gamma^{-1} \geq 123 \text{Gyr}$  at 68% C.L. [177] and WMAP+SN Ia to  $\Gamma^{-1} \geq 700 \text{Gyr}$  at 95.5% C.L. [178]. Furthermore, decaying DM is constrained by possible neutrino final states [179], which serve as a conservative limit, since neutrinos are the least detectable SM particles. The exact bound depends on the DM mass ranging from  $10^{22} \text{s} = 10^8 \text{Gyr}$  at  $\mathcal{O}(1 \text{GeV})$  and increasing almost linearly on a log-log plot to  $10^{28} \text{s} \approx 10^{14} \text{Gyr}$  at  $\mathcal{O}(100 \text{TeV})$ . Diffuse gamma ray constraints from Fermi data yield a limit of  $\Gamma^{-1} \gtrsim 10^{26} \text{s} \approx 10^{12} \text{Gyr}$  [180] for the decay into a pair of charged leptons. Here, DM decays into one lepton and quarks, which might lead to further softer leptons in the final state. Hence, the bounds does not directly apply, but we will use it to obtain an order of magnitude estimate for the suppression scale of the lowest order DM decay operator in Eq. (5.55). Using the limit from diffuse gamma rays with  $\Gamma^{-1} \gtrsim 10^{26} \text{s}$  as a benchmark value, we obtain a limit on the suppression scale of

$$(\Lambda_B^3 \Lambda_F^2)^{1/5} \gtrsim 6 \cdot 10^7 \text{GeV} \left( \frac{m_\eta}{1 \text{TeV}} \right)^{7/10} \left( \frac{\langle \phi_k \phi_l \rangle}{(100 \text{GeV})^2} \right)^{1/5}. \quad (5.59)$$

Due to the high dimensionality of the operator, the bound on the suppression scale  $\Lambda_{L,F}$  does not depend strongly on the bound on the lifetime.

All of the operators in Eq. (5.56) lead to DM induced proton decay <sup>8</sup> into a final state lepton and final state mesons

$$\eta_i + N \rightarrow L + M. \quad (5.60)$$

As the proton as well as the DM are non-relativistic and they annihilate at rest, the induced proton decay leads to similar kinematics as in the ordinary proton decay, but the total rest

<sup>7</sup>This element generates the centre of the group and thus commutes with all group elements.

<sup>8</sup>Induced proton decay has been studied in the context of asymmetric DM [181]. However, their analysis does not apply in our case, because the induced proton decay is mediated via a different operator with different kinematics, since one of the final state particles has a non-negligible mass of the order of the proton mass.

energy  $E \sim m_\eta + m_N \approx m_\eta$  is much larger compared to the ordinary proton decay with  $E \sim m_N$ . Hence, the final state particles appear to originate from the decay of a much heavier particle and the experimental signatures change. Therefore, the existing limits on proton decay are not directly applicable. However, in generic GUT models, for example, the operators given in Eqs. (5.56a), (5.56b) and the proton decay operators are generated at the same energy scale.

**Fermionic DM:** Similarly to scalar DM consisting of the lightest component of  $\eta_i$ ,  $S$  can decay via higher-dimensional operators. They are generally of the form

$$S\mathcal{O}_{SM} \langle \mathcal{O}_{\phi_k\phi_l} \rangle, \quad (5.61)$$

where  $\mathcal{O}_{SM}$  transforms like a spin  $\frac{1}{2}$  fermion, which is a singlet under the SM group, but transform non-trivially under the flavour symmetry<sup>9</sup>. The lowest dimensional operators  $\mathcal{O}_{SM}$  emerge at dimension  $\frac{9}{2}$

$$u^c d^c d^c \quad \bar{Q}\bar{Q}d^c \quad \chi Q\bar{u}^c\bar{d}^c \quad \chi QQQ. \quad (5.62)$$

Note that these operators transform trivially under  $\mathcal{R}$ , as does  $S$ . All of these operators violate baryon number by one unit and therefore, they lead to induced proton decay. However, the kinematics is quite different compared to ordinary proton decay, because the lowest order operators do not contain a final state lepton.

Similarly to the scalar case, there are bounds from astrophysical observations. As DM decay only arises at dimension 8, the bound on the suppression scale does not depend strongly on the exact bound on the lifetime. Therefore, we again make a rough estimate of the bound on the suppression scale by using the same lifetime as in the scalar case and we obtain

$$(\Lambda_B^2 \Lambda_F^2)^{1/4} \gtrsim 9 \cdot 10^8 \text{ GeV} \left( \frac{m_\eta}{1 \text{ TeV}} \right)^{5/8} \left( \frac{\langle \phi_k\phi_l \rangle}{(100 \text{ GeV})^2} \right)^{1/4} \quad (5.63)$$

due to the lower dimensionality of the DM decay operator.

### 5.4.2. Dark Matter Phenomenology

We now give a brief overview of the phenomenology of the two different dark matter candidates. We will estimate the DM abundance and detection possibilities for the different scenarios and show that there is a region of parameter space where the correct abundance can be obtained. A detailed calculation is beyond the scope of the present work. Again, we discuss the different dark matter candidates separately.

#### Scalar DM:

The scalar dark matter candidate is a component of an inert EW doublet. Therefore, we are going to translate the analysis for scalar multiplet DM done in [182] to our setup. A detailed analysis would require the precise calculation of the  $\eta_i$  mass matrices. We assume that one of the triplets  $\eta_i$  is sufficiently lighter than the other two, such that we do not have to take them into account during freeze-out of DM, i.e. they have to be at least 20% heavier than the

<sup>9</sup>Note that  $S$  transforms under the symmetry generator  $X$ , while  $\mathcal{O}_{SM}$  does not. Therefore the operator  $\langle \mathcal{O}_{\phi_k\phi_l} \rangle$  is needed to form a singlet.

DM candidate [183]. In the following, we will denote the triplet containing the DM candidate by  $\eta_{DM}$  with direct mass term  $M_{\eta_{DM}}$ . We are going to assume, as we did previously in the section about the neutrino masses, that the direct mass term  $M_{\eta_{DM}}$  dominates over all mass terms induced by VEVs. Hence, the DM mass is approximately given by the direct mass term  $M_{\eta_{DM}}$ . In the limit that the mass splittings are below 1%, we can neglect the annihilations via other scalars and concentrate on the pure gauge (co)annihilation channels. Following [182], there is an upper bound on the DM mass of an inert doublet of  $m^* = 534 \pm 25 \text{ GeV} (3\sigma)$  from overclosing the universe in this limit. The correct DM abundance is obtained for  $m^*$ . As  $\eta_{DM}$  is in a triplet representations of  $Q_8 \times A_4$ , there are three almost degenerate doublets, which all contribute to the DM density equally. Therefore, the upper bound on the DM mass is lowered by approximately a factor of  $\sqrt{3}$  to  $m_\eta^* \approx 308 \text{ GeV}$ , which is consistent with direct searches for scalar particles, as discussed in Section 5.6.

Today, the mass splitting between DM and the next-to lightest particles forbids gauge interactions kinematically due to the small DM velocities, unless it is tuned to be very small ( $\lesssim \mathcal{O}(100) \text{ keV}$ ), and DM can only be detected via the couplings to scalars, specifically via the Higgs portal. The spin-independent cross section for scattering of DM off the neutron is given by [184]

$$\sigma_n \approx \frac{|\lambda_L|^2}{\pi} \frac{\mu^2}{M_{DM}^2} \frac{m_p^2}{m_H^4} f^2 \approx 2.7 \cdot 10^{-48} \left( \frac{\lambda_L}{0.01} \right)^2 \left( \frac{300 \text{ GeV}}{M_{DM}} \right)^2 \left( \frac{125 \text{ GeV}}{m_H} \right)^4 \left( \frac{f}{0.3} \right)^2 \text{ cm}^2 \quad (5.64)$$

with  $\lambda_L$  being the coupling of DM to the Higgs,  $\mu$  the reduced mass of the DM-neutron system,  $m_p$  the mass of the nucleon,  $m_H$  the mass of the Higgs and  $f$  parametrises the nuclear matrix element,  $0.14 < f < 0.66$  in [184]. The estimated cross section is well below the current experimental limits by XENON100 [185], which is the most sensitive DM direct detection experiment in that mass region.

Note, the discussed parameter point is only an example which proves the possibility to obtain the correct DM relic density. For larger mass splittings, the annihilation via scalar interactions cannot be neglected in the calculation of the DM relic abundance and the direct detection cross section is enhanced.

**Fermionic DM:** For the discussion of the fermionic DM candidate contained in  $S$ , we follow the discussion in [166] to show that it is possible to obtain the correct relic abundance. For completeness, we repeat the relevant steps with the necessary changes. At tree-level, there is only the mass term  $\sqrt{3}M_S S S = M_S(S_1^2 + S_2^2 + S_3^2)$  and thus all components of  $S$  are degenerate. At loop-level this degeneracy is lifted and for concreteness we here take  $M_{\tilde{S}_3} \gtrsim M_{\tilde{S}_2} \gtrsim M_{\tilde{S}_1}$ , where  $\tilde{S}_i$  are mass eigenstates. The states  $\tilde{S}_{2,3}$  can decay into  $\tilde{S}_1$  and leptons by the interchange of  $\eta$  and thus at the present time only  $\tilde{S}_1$  is around. However, due to the near degeneracy, the freeze-out of all three species runs in parallel. Coannihilation processes of the type  $S_i S_j \rightarrow \text{SM}$  with  $i \neq j$  are suppressed in comparison to annihilation processes  $S_i S_i \rightarrow \text{SM}$ , because they require an additional mass insertion along the  $\eta$  line. It is thus a very good approximation to consider the freeze-out of each component separately and the total relic abundance is thus just given by the sum of the abundances of  $S_1$ ,  $S_2$  and  $S_3$ .

The annihilation cross section for each  $S_k$  into leptons in the limit of vanishing lepton masses and scalar mass splittings [186] is given by

$$\langle \sigma v \rangle = b v^2 + \mathcal{O}(v^4), \quad b = \sum_{i=1,2} \frac{h_i^4 r_i^2 (1 - 2r_i + 2r_i^2)}{24\pi M_S^2}, \quad r_i = \frac{M_S^2}{M_i^2 + M_S^2}. \quad (5.65)$$

In the limit of  $M_S \ll M_i$ , the expression for the p-wave simplifies to

$$b = \frac{M_S^2}{24\pi} \sum_{i=1,2} \left( \frac{h_i}{m_i} \right)^4, \quad (5.66)$$

i.e. the cross section scales with  $(h_i/m_i)^4$ . The relic density of the SM singlets  $S$ , taking into account the mass degeneracy of the components of  $S$ , can then be obtained from [187]

$$\Omega_S h^2 = \frac{n_S^0 M_S}{\rho_c} h^2, \quad (5.67)$$

with  $n_S^0$  being the number density of  $S$  today, which is

$$(n_S^0)^{-1} = \left( \sum_k n_{S_k}^0 \right)^{-1} = (3n_{S_k}^0)^{-1} = \frac{0.088 g_*^{1/2} M_{Pl} M_S 3b}{x_f^2 s_0}, \quad (5.68)$$

where  $s_0 = 2970/\text{cm}^3$  is today's entropy density, the critical density is  $\rho_c = 3H^2/(8\pi G) = 1.05 \cdot 10^{-5} h^2 \text{GeV}/\text{cm}^3$ , the Planck mass  $M_{Pl} = 1.22 \cdot 10^{19} \text{GeV}$  and the dimensionless Hubble parameter  $h$ . At the freeze-out temperature, the ratio  $x_f = M_S/T$  is determined by

$$x_f = \ln \frac{0.0764 M_{Pl} (6b/x_f) c (2+c) M_S}{(g_* x_f)^{1/2}} \quad (5.69)$$

with the effective number of degrees of freedom  $g_*$  at freeze-out. After eliminating the cross section with Eq. (5.68) and Eq. (5.67), we obtain

$$x_f = \ln \frac{1.74 x_f^{1/2} s_0 h^2 c (2+c) M_S}{g_* (\Omega_S h^2) \rho_c}. \quad (5.70)$$

Following the discussion in [166, 187], we rewrite Eq. (5.67) and Eq. (5.70) as

$$\left[ \frac{M_S}{\text{GeV}} \right] = 1.95 \cdot 10^{-8} x_f^{-1/2} e^{x_f} \left[ \frac{\Omega_d h^2}{0.12} \right], \quad (5.71a)$$

$$\left[ \frac{b}{\text{GeV}^{-2}} \right] = 7.32 \cdot 10^{-11} x_f^2 \left[ \frac{\Omega_d h^2}{0.12} \right], \quad (5.71b)$$

using  $g_*^{1/2} = 10$  and  $c = 1/2$ . We solve these equations numerically for fixed values of  $h_1 = h_2$  and  $M_1 = M_2$  and show the resulting contour lines with the correct DM relic abundance in the plane  $M_1/h_1 = M_2/h_2$  vs.  $M_S$  in Fig. 5.9. Hence, it is possible to obtain the correct DM relic abundance for fermionic DM, although large Yukawa couplings  $h_i$  are required. Similarly to the scalar DM scenario, we expect the cross section to raise with non-vanishing mass splittings of the scalars  $\eta_i$ , which allows for smaller Yukawa couplings  $h_i$ .

## 5.5. Extension to Quark Sector

So far we restricted ourselves to the discussion of the flavour structure in the lepton sector. Given the different structures in the lepton and quark sector, one might wonder whether and how this model can be extended to the quark sector. In the following, we will discuss a few simple possibilities to incorporate the quark sector. It is necessary to specify how quarks transform under the flavour symmetry as this will to a certain extent determine the collider signatures of the model. A detailed discussion of quark flavour observables is postponed to future work.

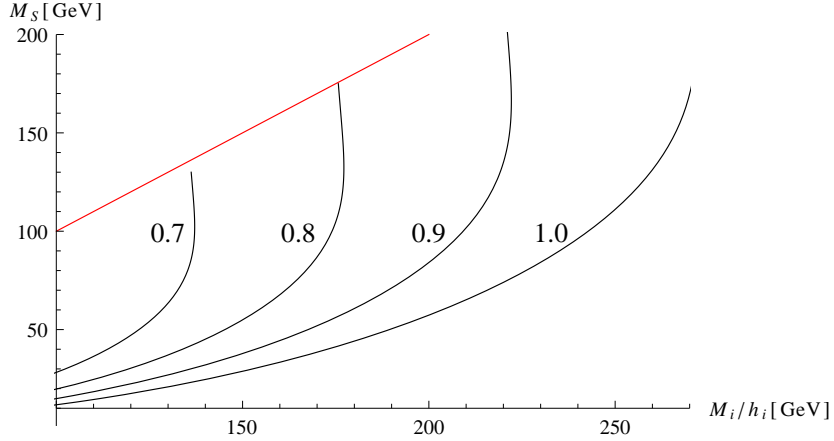


**Figure 5.9:** Contour lines for different values of  $h_1 = h_2$  with the correct DM abundance  $\Omega_S h^2 = 0.12$ .

### Quarks Sector Mirroring the Lepton Sector

We can use the same assignment for the quarks as for the leptons with respect to  $(Q_8 \times A_4) \times Z_4$ , i.e.

$$Q \sim (\mathbf{3}_1, 1), \quad u^c + c^c + t^c \sim (\mathbf{1}_1 + \mathbf{1}_2 + \mathbf{1}_3, 1), \quad d^c + s^c + b^c \sim (\mathbf{1}_1 + \mathbf{1}_2 + \mathbf{1}_3, 1). \quad (5.72)$$

This assignment leads to the following Yukawa couplings in the Lagrangian

$$-\mathcal{L}_q = y_u Q \chi u^c + y_c Q \chi c^c + y_t Q \chi t^c + y_d Q \tilde{\chi} d^c + y_s Q \tilde{\chi} s^c + y_b Q \tilde{\chi} b^c + \text{h.c.}, \quad (5.73)$$

which amount to the mass matrices of the quarks

$$M_U = \frac{v}{\sqrt{2}} \Omega_T^* \text{diag}(y_u, y_c, y_t) \quad \text{and} \quad M_D = \frac{v}{\sqrt{2}} \Omega_T^* \text{diag}(y_d, y_s, y_b). \quad (5.74)$$

Hence there is no mixing in the quark sector, i.e. the CKM mixing matrix  $V_{CKM} = V_d^\dagger V_u = \mathbb{1}$ , which is a good leading order approximation to the CKM mixing. The Cabbibo angle can be produced by a cross-talk of operators from the neutrino sector [10], e.g. the operator  $(Q \tilde{\chi} d^c) \mathbf{1}_2 (\phi_1 \phi_2)^2 / M^4$  leads to a non-vanishing Cabbibo mixing angle. It has to be of the order  $(\phi_1 \phi_2)^2 / (M^4) \sim 10^{-4} (m_s / 95 \text{ MeV})$ , in order to generate a large enough mixing in the down-type quark sector to explain the Cabbibo angle. Within the model, the operator can be generated at one loop with  $\varphi^{(\prime)}$  running in the loop. However, the contribution turns out to be too small and a different mechanism is required to generate this operator.

Flavor changing neutral currents (FCNC) are naturally suppressed at the leading order, since there is a selection rule  $\Delta D \Delta S \Delta B = \pm 2$  as well as  $\Delta U \Delta C \Delta T = \pm 2$  in the flavour basis for four Fermi operators similarly to the lepton sector.<sup>10</sup>

<sup>10</sup>It has been claimed in [162] that leptonic Kaon decays result in a relatively strong bound of  $M_0 > 510 \text{ GeV}$  on the effective mass  $M_0$  defined in Eq. (5.49). However, there seems to be an error in the calculation. The correct bound is significantly weaker, but we relegate the discussion to [18].

### Quarks Transforming under X

Another interesting possibility that is not possible in  $A_4$  models is to assign the quarks to representations that also transform under the group generator  $X$ . Since the top mass is large, we want it to be generated at the renormalizable level, while all the other quark masses might well be the result of higher order effects. Looking at the multiplication rule

$$\mathbf{3}_i \times \mathbf{3}_j = \sum_{\substack{k=1 \\ k \neq i,j}}^5 \mathbf{3}_k, \quad (i \neq j), \quad (5.75)$$

it is clear that if one assigns  $Q \sim (\mathbf{3}_2, 1)$  and  $U^c \sim (\mathbf{3}_3, 1)$  there is only one Yukawa coupling at the renormalizable level

$$- \mathcal{L}_t = y_t Q \chi U^c + \text{h.c.}, \quad (5.76)$$

which generates the top mass. The charm and up mass, as well as up sector mixing are generated by operators of the form

$$- \mathcal{L}_u = y_i^{(u,1)} [Q \chi U^c (\phi_1 \phi_1)]_i + y_i^{(u,2)} [Q \chi U^c (\phi_2 \phi_2)]_i \text{ h.c.}, \quad (5.77)$$

where the sum goes over all singlet contractions of the fields. There are certainly enough parameters to fit the quark masses and up-type mixing. Actually, there are no further predictions besides the large top mass, since there are too many free parameters.

In the down-type sector we can either utilize the same structure as in the up-type sector or, as the bottom quark mass is closer to the charm mass than to the top mass, we can use the assignment  $D^c \sim (\mathbf{3}_1, 1)$ . With this choice there is no tree-level operator of type (5.76) allowed and all down type quark masses and mixing arise from

$$- \mathcal{L}_d = y_i^{(d,1)} [Q \chi D^c (\phi_1 \phi_1)]_i + y_i^{(d,2)} [Q \chi D^c (\phi_2 \phi_2)]_i \text{ h.c.} \quad (5.78)$$

We will not discuss this possibility further here, as we are primarily focused on the lepton sector.

### Additional EW Higgs Doublet $H_q \sim \mathbf{1}_1$

Another possibility is that the flavour structure in the quark sector could be completely unrelated to the one in the lepton sector. In particular, the quarks might not transform under the flavour symmetry in the lepton sector. This can be simply achieved by assigning the quarks to the singlet representation of the flavour group. In order to generate the quark mass matrices, we have to introduce an additional EW Higgs Doublet  $H_q$ , which does not transform under the flavour group. Hence, the flavour structure in the quark sector is unchanged compared to the SM one. Therefore, we do not discuss this possibility further and we will only briefly comment on its collider phenomenology in Section 5.6.

The only effect<sup>11</sup> of the additional Higgs doublet on the discussion in the preceding sections is to rescale the VEV of  $H$  such that

$$\langle H^0 \rangle^2 + \langle H_q^0 \rangle^2 = \frac{1}{2} (\sqrt{2} G_F)^{-1} = \frac{1}{2} (246 \text{ GeV})^2$$

is maintained.

<sup>11</sup>Here we assume that  $H_q$  does not give leading order contribution to the Weinberg operator. Symmetries can always be adjusted in order for this to be the case. If  $H_q$  does give such a contribution there will be one more free physical phase in the neutrino mass matrix that cannot be rotated away.

## 5.6. Collider Phenomenology

Our model predicts several new particles with EW charges at the EW scale. In this section, we will concentrate on the simplest extension to the quark sector given in Section 5.5, where quark doublets are assigned to the triplet representation  $\mathbf{3}_1$  of the flavour group and obtain their masses from a coupling to the flavoured Higgs  $\chi$ , as discussed in the previous section. We will briefly comment on the possibility to have a separate Higgs for the quark sector in the last subsection. Besides the fermionic singlets  $S$ , there are several EW doublets, which can be grouped in three different categories, the Higgs  $h$ , which obtains a VEV, the two partners of the Higgs in the flavour triplet  $\chi$ , namely  $\varphi'$  and  $\varphi''$ , and the additional inert EW scalar doublets  $\eta_i$ . In the following, we sketch the different production and decay channels and discuss their implications for direct searches at colliders as well as the current bounds on the existence of new particles beyond the SM. However, a detailed study is beyond the scope of this presentation.

After a short summary of the main experimental results, we will discuss each class of new particles separately.

### 5.6.1. Summary of Relevant Experimental Results

Recently, ATLAS [1] as well as CMS [2] announced the discovery of a Higgs-like resonance at  $126.0 \pm 0.4(\text{stat.}) \pm 0.4(\text{sys.}) \text{ GeV}$  and  $125.3 \pm 0.4(\text{stat.}) \pm 0.5(\text{sys.}) \text{ GeV}$ , respectively. The discovery is based on an analysis of several channels. The two main channels are the decay into two photons and  $h \rightarrow ZZ^* \rightarrow 4l$ . While the  $h \rightarrow ZZ^* \rightarrow 4l$  rate seems to agree with the SM prediction, the  $h \rightarrow \gamma\gamma$  rate seems to be enhanced by a factor of 1.5 to 2. This deviation is somewhat intriguing, as in the SM this decay proceeds via a loop diagram and is thus sensitive to new physics contributions. However, so far, the deviation is at the  $2\sigma$  level or even at the  $1\sigma$  level [188–190], if the uncertainties are taken into account more conservatively. Besides the discovery of a Higgs-like resonance, the LHC has put strong constraints on any physics beyond the SM.

Charged Higgs particles are constrained by searches at LEP and LHC. At LEP, charged Higgs particles  $H^\pm$  are produced via a virtual  $Z^*$  in the s-channel, i.e.  $e^+e^- \rightarrow Z^* \rightarrow H^+H^-$ , and studied via their decays into  $\tau\nu_\tau$  as well as  $c\bar{s}$  assuming their branching ratios add up to 1, i.e.  $\text{Br}(H^+ \rightarrow \tau^+\nu_\tau) + \text{Br}(H^+ \rightarrow c\bar{s}) = 1$ . This results in a bound of  $m_{H^+} > 79.3 \text{ GeV}$  [172]. Independent of any assumptions on the branching ratio, the invisible Z decay leads to  $m_{H^+} \gtrsim 45 \text{ GeV}$  [172]. CMS searched for charged Higgs particles [191], which are produced in top decays,  $t \rightarrow H^+b$  and constrains their branching ratio  $\text{Br}(t \rightarrow H^+b)$  to less than 2%-4% for charged Higgs masses between 80 GeV and 160 GeV. Similarly, the search by the ATLAS experiment [192] yields bounds on the branching ratio  $\text{Br}(t \rightarrow H^+b)$  of the order of 1%-5% for charged Higgs masses in the range between 90 and 160 GeV, assuming  $\text{Br}(H^+ \rightarrow \tau^+\nu_\tau) = 1$ .

### 5.6.2. EW Higgs Doublet $H$

We will first consider the limit in which there is no mixing between the Higgs  $h$  and the flavons  $\phi_i$ . In the limit of no mixing, the tree-level couplings of the Higgs  $h$  contained in the EW Higgs doublet  $H$  to gauge bosons are identical to the SM couplings. In addition, the flavour conserving tree level couplings of the Higgs  $h$  to the fermions also agree with the SM ones. Note that there might be small corrections, since quark mixing vanishes at leading order and

the Higgs couplings conserve all flavour numbers separately. As there are no new coloured particles and the coupling of the Higgs to  $t\bar{t}$  is the same as in the SM, the loop-induced coupling of the Higgs  $h$  to gluons agrees with the SM one. In summary, the production of the Higgs  $h$  as well as all tree-level decay channels and the decay into gluons are exactly like in the SM. The only decay channel that has been measured so far and which is changed with respect to the SM, is the decay into two photons, because it is a one-loop effect. If any of the other new scalars were light enough, there would be additional tree level Higgs decays into pairs of these scalars and such scenarios are therefore constrained. The decay  $h \rightarrow S\bar{S}$ , if kinematically allowed, is loop suppressed.

Mixing of the Higgs  $h$  with the flavons  $\phi_i$  leads to a suppression of all tree-level couplings to gauge bosons and fermions. Hence, the production cross section is reduced according to the admixture of the flavon to the Higgs. As Higgs decays into  $ZZ^*$  are close to SM value, the admixture of the flavons to the Higgs  $h$  is limited.

Finally, let us discuss the diphoton decay channel. The SM contribution is dominated by the W boson contribution and the smaller top loop contribution, which interfere destructively. In our model, the decay into two photons receives additional contributions from charged scalars in the loop, which are contained in the EW doublets  $\varphi'$ ,  $\varphi''$  as well as  $\eta_i$ . Any enhancing contribution has to interfere constructively with the SM W boson loop or dominate over the W boson contribution. The contribution of additional charged scalars  $\rho_i$  with charge one, coupled to the Higgs via the Higgs portal

$$\mathcal{O}_{\rho_i} = c_{\rho_i} H^\dagger H |\rho_i|^2, \quad (5.79)$$

has recently been studied in [193]. The ratio of the effective coupling of the Higgs to two photons vs. the SM prediction is given by

$$R_{\gamma\gamma} = \left| 1 - \sum_i c_{\rho_i} h(m_{\rho_i}) \right|^2, \quad (5.80)$$

where the function  $h$  is depicted in Fig. 5.10. To obtain an enhancement of the factor of 2 (1.5), one thus needs a value of

$$\sum_i c_{\rho_i} h(m_{\rho_i}) = \left\{ \begin{array}{ll} -0.41 & (-0.22) \text{ for constructive interference} \\ 2.41 & (2.22) \text{ for destructive interference} \end{array} \right\}. \quad (5.81)$$

Hence, a large negative coupling  $c_\rho \sim -2$  is necessary to obtain an enhancement factor of 2 for a single singly charged scalar of mass 100 GeV. Such a large negative coupling destabilizes the vacuum and leads to charge breaking minima unless  $|c_\rho| < \sqrt{\lambda\lambda_\rho} \sim \sqrt{\lambda_\rho}/2$  is fulfilled, where  $\lambda_\rho$  denotes the quartic coupling  $\lambda_\rho |\rho|^4/2$ . Note that this requires very large values for  $\lambda_\rho$ .

Let us now use this formula to estimate the deviations from  $R_{\gamma\gamma} = 1$  that can be expected in this model. In total we have 11 charged scalars, 9 from the doublets  $\eta_{1,2,3}$  and two from the doublets  $\varphi', \varphi''$ . The interaction of the last two scalars with the Higgs field can be expressed as

$$c_{\varphi'} = \frac{m_h^2 + m_{\varphi'+}^2}{v^2}, \quad c_{\varphi''} = \frac{m_h^2 + m_{\varphi''+}^2}{v^2}, \quad (5.82)$$

with  $m_{\varphi'(i)+}^2$  defined in Eq. (5.5). In the limit of large  $m_{\varphi'(i)}^2$  these two fields contribute

$$c_{\varphi'} h(M_+^c) + c_{\varphi''} h(M_-^c) = 0.1 + \left( \frac{22 \text{ GeV}}{M_+^c} \right)^2 + \left( \frac{22 \text{ GeV}}{M_-^c} \right)^2. \quad (5.83)$$



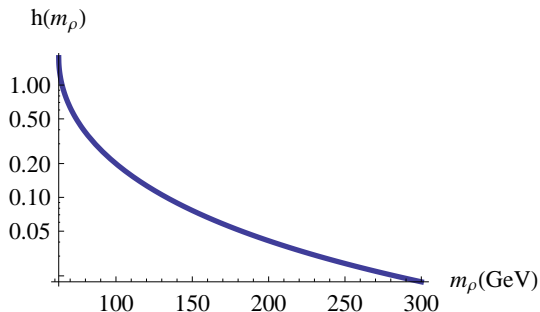


Figure 5.10: Plot of function  $h$  of Eq. (5.81).

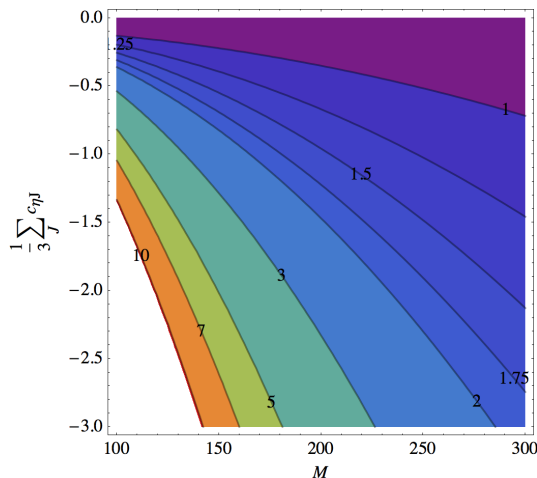


Figure 5.11:  $R_{\gamma\gamma}$  in the case where all charged scalars have the same common mass  $M$  as a function of  $\frac{1}{3} \sum_{J=1}^3 c_{\eta J}$ .

The couplings of the charged components of the  $\eta$  fields are given by

$$\mathcal{O}_\eta = \sum_{i,J=1}^3 c_{\eta J} H^\dagger H |\eta_J^{(i)}|^2, \quad (5.84)$$

as dictated by the symmetry. The coefficients  $c_{\eta J}$  are essentially unconstrained except for the fact that the combination that couples to the DM particle should not be too large, to avoid the bound from direct detection. In the limit where all charged scalars have a common mass  $M$ , we see from Fig. 5.11 that  $M = 200$  GeV requires  $\frac{1}{3} \sum_{J=1}^3 c_{\eta J} = -1.46$  ( $-0.95$ ) for  $R_{\gamma\gamma} = 2(1.5)$ .

In case the  $h \rightarrow \gamma\gamma$  anomaly persists, it would be interesting to measure  $h \rightarrow \gamma Z$ , since it originates from similar diagrams, where one photon is replaced by one  $Z$  boson. A cross-correlation of the two measurements would allow to determine the isospin of these particles. In our model all charged scalars are part of  $SU(2)$  doublets allowing to distinguish it from other models which have EW multiplets in the loop with different EW charges, like singlets or triplets.

### 5.6.3. Further Scalars

Besides the Higgs  $h$ , there are several additional scalars, the flavour-violating EW scalar doublets  $\varphi^{(\prime)}$  as well as  $\eta_i$ , which do not acquire a VEV, and the flavons  $\phi_i$ , which acquire a VEV. See App. A.4 for the scalar mass spectrum.

**Flavour-violating Higgs Doublets  $\varphi^{(\prime)}$ :** The neutral components of the flavour-violating Higgs doublets  $\varphi^{(\prime)}$  do not have tree-level couplings to  $t\bar{t}$ . Hence, they are not produced via gluon fusion, but only via vector boson fusion or associate production. Consequently, their production cross section is roughly one order of magnitude suppressed compared to the SM Higgs production cross section with the same mass, which is dominated by gluon fusion. The most sensitive Higgs searches for heavy Higgs bosons use the decay channels into EW vector bosons,  $h \rightarrow WW^{(*)}, ZZ^{(*)}$  and the strongest bounds reach roughly  $\sigma_{SM}/5$ . In addition, there

are additional decay channels for the heavy Higgs bosons into the lighter Higgs bosons, which will suppress the branching fraction into EW gauge bosons. Hence, the current searches only start constraining the neutral components of the flavour-violating Higgs doublets  $\varphi^{(\prime)}$ . The prospects for searches of flavour-violating decays into leptons have been studied in [194–197].

As the charged Higgs particles contained in  $\varphi^{(\prime)}$  do not couple to  $t\bar{b}$ , the LHC limits do not apply. Hence, the charged Higgs particles in our model are only constrained by the LEP limits discussed previously.

Although there are no tight constraints yet, upcoming searches will test the allowed range of masses, because the flavour-violating Higgs doublets  $\varphi^{(\prime)}$  stem from the same flavour triplet as the Higgs doublet  $H$ , and therefore their masses are determined to be given by scalar couplings times the EW VEV. Their masses may therefore not be raised arbitrarily high, as discussed below Eq. (5.5)<sup>12</sup>.

**EW Scalar Doublets  $\eta_i$ :** The neutral components of the EW scalar doublets  $\eta_i$  do not couple to quarks and particularly not to  $t\bar{t}$ . Hence, similarly to the flavour-violating Higgs doublets, they are not produced via gluon fusion and the current bounds from heavy Higgs searches do not constrain  $\eta_i$ . Also, the charged components of  $\eta_i$  are not constrained by the current LHC searches, because they do not couple to quarks directly. Therefore, they are only constrained by the LEP searches.

**Flavons  $\phi_i$ :** The flavons  $\phi_i$  do not have gauge interactions and they do not couple to fermions directly. However, they mix with the Higgs  $h$ , which is constrained by the Higgs searches to be small, since a large mixing suppresses the production cross section of  $h$  and therefore all rates relative to the SM expectation. In conclusion, the scalar mass eigenstates which are dominantly composed of the flavons  $\phi_i$  are only produced via mixing with the Higgs  $h$  and thus there are no limits from current searches.

**Variant with Additional EW Higgs Doublet  $H_q$ :** As we discussed in Section 5.5, another simple possibility to incorporate quarks in the model is by assigning all quarks to the trivial representation of the flavour group and introducing an additional EW Higgs doublet  $H_q$ , which transforms trivially under the flavour group. This leads to different collider signatures compared to the previously discussed scenario. Soon, these scenarios can be experimentally distinguished at the LHC. We will highlight the most important differences.

The discussion of the fermions  $S$  as well as the scalars  $\eta_i$  remains the same. The main changes are in the Higgs phenomenology. In contrast to the other scenario, the component in  $\chi$  which obtains a VEV does not couple to quarks and therefore it is not produced in gluon fusion, unless there is mixing between  $\chi$  and  $H_q$ . Instead, the newly introduced Higgs  $H_q$  will be produced in gluon fusion. In this setup, the observed resonance at 126 GeV would be associated with the mass eigenstate, which is dominantly composed of Higgs  $H_q$ . As  $H_q$  has exactly the same couplings to gauge bosons and quarks, but does not couple to leptons (especially  $\tau$ 's), the decays into leptons are suppressed by the mixing between  $H_q$  and  $H$  (contained in  $\chi$ ). This leads to a slight enhancement of the remaining branching ratios (O(10%)). The diphoton branching ratio can be enhanced in the same way as discussed in Section 5.6.2.

<sup>12</sup>Note that if one introduces soft-breaking terms that respect the  $Z_3$  symmetry, it is possible to adjust the mass terms arbitrarily [162]. Alternatively one may introduce an EW singlet scalar that transforms as  $\underline{\mathbf{3}}_1$  and breaks to the same subgroup as  $\chi$ . This can be realized without introducing a vacuum alignment problem.

#### 5.6.4. Fermionic Singlets $S$

The additional fermionic states  $S$  are SM singlets and only charged under the discrete flavour group. Furthermore, they only couple to lepton doublets and therefore their production cross section at the hadron colliders is suppressed compared to coloured particles and there are no relevant analyses at present. The production depends on the exact mass spectrum of  $\eta_i$  as well as  $S$ . The production via t-channel  $\eta_i$  exchange is always present in a lepton collider, e.g.  $e^+e^- \rightarrow S\bar{S}$ . If  $S$  is lighter than one of the components of  $\eta_i$ , it is possible to produce  $S$  via EW production of these heavier components of  $\eta_i$  and subsequent decay into  $S$  and one lepton. Unless  $S$  is the DM candidate, the fermionic singlet  $S$  will decay into a lepton and one of the lighter components of  $\eta_i$ , which will subsequently cascade down to DM via EW gauge interactions. The signal is missing transverse energy and leptons (and possibly EW gauge bosons) in the final state.

If  $S$  is lighter than all  $\eta_i$ 's and therefore a DM candidate, there are bounds from mono-photon searches at LEP [198]. As  $S$  only couples to leptons, the searches at hadron colliders are weaker due to the additional suppression from loops that couple leptons to quarks. The mono-photon searches at LEP probe the effective DM annihilation operator  $(\bar{e}S)(e\bar{S})/\Lambda_t^2$ , which are induced by the exchange of a scalar doublet  $\eta_{1,2}$ . The scale  $\Lambda_t$  of this operator is determined by  $\Lambda_t^{-2} = \sum_k |h_k|^2/M_k^2$  for  $M_k \gg M_S$ . The analysis in [198] quotes a limit of (200 – 340) GeV for  $M_S < 90$  GeV. Hence, this does not impose a strong constraint, since the smallness of neutrino masses points towards larger cutoff scales  $\Lambda_t$ .

## 5.7. Summary & Conclusions

We have presented a complete model of lepton flavour structure at the electroweak scale. We have shown how neutrino masses are generated at one-loop level and discussed phenomenological consequences of the flavour structure. We have shown how the non-trivial flavour structure suppresses phenomenologically problematic flavour violating processes in the lepton sector. The model naturally contains a dark matter candidate and we have studied its phenomenology. Finally we have presented possibilities to extend the model to the quark sector and discussed collider constraints.

In conclusion, this work shows that it is possible to explain the lepton flavour structure at accessible scales without running into immediate problems with flavour observables and other bounds. It would be interesting to perform a more in depth study of the model's parameter space. In particular a careful study of the possibilities to extend the model to the quark sector would be interesting.



# Chapter 6.

## CP and Discrete Flavour Symmetries

In this chapter, we give a consistent definition of CP transformations as outer automorphisms of the symmetry group. After an introduction, we give general consistency conditions of how to define CP in the context of discrete symmetry groups. We apply this formalism to define CP for a number of small groups that have been studied in this context and comment on recent claims in the literature that complex Clebsch-Gordon coefficients may give an explanation of CP violation in nature. We further demonstrate that whenever there exists a generalized CP transformation this implies vanishing CP phases.

### 6.1. Introduction

After the discovery of a sizeable value of  $\theta_{13}$  by the reactor experiments DoubleChooz [35], DayaBay [36] and RENO [37] the door has been pushed wide open to measure the last undetermined parameters of the Standard Model, namely the CP phases of the lepton sector. Of special interest is the Dirac CP-phase  $\delta_{CP}$  as it can be experimentally determined in neutrino oscillation experiments in the foreseeable future.<sup>1</sup>

In the lepton sector, there is the proud/infamous tradition to explain the structure of mixing angles through the introduction of non-abelian discrete symmetries. The relative lack of success with regard to the reactor angle  $\theta_{13}$  has not deterred the field from using the same set of ideas to try and predict the missing CP phase  $\delta_{CP}$  using discrete symmetries. For example, there have been attempts to explain CP violation as a result of complex Clebsch-Gordon coefficients of groups such as  $T'$  [199, 200] and  $\Delta(27)$  [201–205] and sometimes inconsistent definitions of CP have been used in the study of discrete groups. In order to relate CP violation to the complex Clebsch-Gordan coefficients, a CP symmetry has to be imposed on the Lagrangian to forbid any CP violating coupling. This CP symmetry is then broken spontaneously [206, 207].

To clarify these issues, we here give a consistent general definition of CP transformations in the context of non-abelian discrete flavour groups. We will show that in many cases it is not possible to define CP in the naive way,  $\phi \rightarrow \phi^*$ , but rather a non-trivial transformation in flavour space is needed. Indeed there is a one-to-one correspondence between generalised CP transformations [208–210] and the outer automorphism group of the flavour group. It should not be surprising that outer automorphisms play a role in the definition of CP as complex conjugation is an outer automorphism of the field of complex numbers and the definition of CP transformations as automorphisms in the context of gauge theories has been discussed long ago by Grimus and Rebelo [211]. Generalised CP transformations in the context of discrete symmetries have been used before for  $A_4$  [212–215].

---

<sup>1</sup> To discern Majorana phases from possible future signals of neutrinoless double beta decay experiments will always be model dependent and thus seems less promising.

While the outer automorphism groups of continuous groups is either trivial or a  $Z_2^2$ , the outer automorphism group of discrete groups can be very rich. For example the well-known flavour group  $\Delta(27)$  has an automorphism group of order 432.

As a result of our investigation of generalised CP transformations, we present consistent definitions of CP for all groups of order smaller than 30 that contain three dimensional representations. Highlights are the case of  $A_4$ , where we show that the one complex phase in the scalar potential of a single triplet does not break CP, which clears up some confusion about the recent observation that one can obtain CP conserving solutions from an apparently explicitly CP-breaking potential [163]. In the case of  $T'$  we show that the one consistent CP definition cannot be reconciled with the claimed geometrical origin of CP violation and therefore the results obtained there have to be considered as unphysical and basis dependent. For the group  $\Delta(27)$  we are able to explain the so-called calculable phases as a result of an accidental generalised CP symmetry that had so far been overlooked in the literature.

Another motivation for this work comes from a technical issue that has to do with an implementation of the  $Q_8 \times A_4$  model of Chapter 4 if one wants to promote all flavons to electroweak doublets. In this case we have

$$\phi_i = (\phi_i^{(1)}, \phi_i^{(2)}, \phi_i^{(3)}, \phi_i^{(4)})^T \sim \underline{\mathbf{4}}_1 \quad \text{with} \quad i = 1, 2 \quad \text{and} \quad \chi = (\chi^{(1)}, \chi^{(2)}, \chi^{(3)})^T \sim \underline{\mathbf{3}}_1,$$

where each component transforms in the same way as a Higgs doublet under electroweak symmetry. In Chapter 3, we have seen that to realize the vacuum structure (4.5) it is crucial that couplings such as

$$(\chi^\dagger \chi)_{\underline{\mathbf{3}}_3} (\phi^\dagger \phi)_{\underline{\mathbf{1}}_2}$$

that connect the symmetry transformations in the two sectors be forbidden at the renormalizable level, or in other words there should be an accidental symmetry in  $A_4 \times (Q_8 \times A_4)$  of the scalar potential under which  $\chi$  transforms as  $(\underline{\mathbf{3}}, \underline{\mathbf{1}}_1)$  and the  $\phi_i$  fields transform as  $(\underline{\mathbf{1}}, \underline{\mathbf{4}}_1)$ . Due to the relation  $\underline{\mathbf{4}}_1 \times \underline{\mathbf{4}}_1 = \underline{\mathbf{1}}_{1S} + \underline{\mathbf{3}}_{1A} + \underline{\mathbf{3}}_{2S} + \underline{\mathbf{3}}_{3S} + \underline{\mathbf{3}}_{4S} + \underline{\mathbf{3}}_{5A}$  the above coupling is not allowed but because of the doublet structure additional couplings are allowed that might be problematic. The most problematic coupling is<sup>3</sup>

$$\lambda (\chi^\dagger \chi)_{\underline{\mathbf{3}}_{1,S}} \cdot (\phi_i^\dagger \phi_i)_{\underline{\mathbf{3}}_1} + \text{h.c.}, \quad (6.1)$$

where

$$(a^\dagger b)_{\underline{\mathbf{3}}_1} = \frac{1}{2} \begin{pmatrix} -a_4^\dagger b_1 + a_3^\dagger b_2 - a_2^\dagger b_3 + a_1^\dagger b_4 \\ -a_3^\dagger b_1 - a_4^\dagger b_2 + a_1^\dagger b_3 + a_2^\dagger b_4 \\ a_2^\dagger b_1 - a_1^\dagger b_2 - a_4^\dagger b_3 + a_3^\dagger b_4 \end{pmatrix} \quad \text{for} \quad a, b \sim \underline{\mathbf{4}}_1.$$

Clearly  $(\phi_1^\dagger \phi_1)_{\underline{\mathbf{3}}_1}$  is purely imaginary, while  $(\chi^\dagger \chi)_{\underline{\mathbf{3}}_{1,S}}$  is real and  $\lambda$  therefore has to be purely imaginary. As all dangerous couplings are of this sort a natural idea is to get rid of these couplings by imposing a CP symmetry

$$\Phi(t, \vec{x}) \rightarrow CP[\Phi(t, \vec{x})] = \Phi^*(t, -\vec{x}),$$

where  $\Phi$  stands for any doublet field and the reference to the space-time coordinates  $(t, \vec{x})$  will be suppressed in the following. While this symmetry would clearly forbid the dangerous

<sup>2</sup>With the sole exception of  $SO(8)$ , whose outer automorphism group is  $S_3$ .

<sup>3</sup>The coupling  $(\chi^\dagger \chi)_{\underline{\mathbf{3}}_{1,A}} (\phi_i^\dagger \phi_i)_{\underline{\mathbf{3}}_1}$  would not destabilize the symmetry breaking pattern.

couplings it turns out that it is incompatible with the internal structure of the discrete symmetry group, as we will now demonstrate.

The outline of the chapter is as follows. In Section 6.2.1, we define a generalised CP transformation and discuss its connection with the outer automorphism group. The implications of a generalised CP transformation for the physical phases are discussed in Section 6.2.2. In Section 6.3, we apply our general considerations to specific examples. In particular, we will discuss all groups of order less than 30 with a 3-dimensional representation. Finally, we conclude in Section 6.4.

## 6.2. Generalized CP Transformations

### 6.2.1. CP and the Outer Automorphism Group

In order to simplify the discussion, we will focus on finite discrete groups only. We do not consider the Lorentz group or any continuous group and therefore restrict ourselves to scalar multiplets unless necessary. The definition of (generalized) CP transformations as outer automorphisms of continuous groups has been given in [211]. An extension to higher spin representations of the Lorentz group and continuous groups is straightforward. Let us consider a scalar multiplet

$$\phi = \left( \varphi_R, \varphi_P, \varphi_P^*, \varphi_C, \varphi_C^* \right)^T \quad (6.2)$$

that contains real (R), pseudo-real (P) and complex (C) representations of the discrete group  $G$ . The discrete group  $G$  acts on  $\phi$  as

$$\phi \xrightarrow{G} \rho(g)\phi, \quad g \in G, \quad (6.3)$$

where  $\rho$  is a representation  $\rho : G \rightarrow GL(N, \mathbb{C})$ , which is generally reducible. In fact  $\rho(G) \subset U(N)$ , since we are only considering unitary representations. A *generalized CP transformation* has to leave  $|\partial\phi|^2$  invariant and is thus of the form

$$\phi \xrightarrow{CP} U\phi^* \quad (6.4)$$

with  $U$  being a unitary matrix. If the representation is real, i.e.  $\phi = \phi^*$ , there is always the trivial CP transformation  $\phi \rightarrow \phi^*$ , which acts trivially on the group. In the following, we will take  $\rho$  to be complex and *faithful*, i.e.  $\rho$  is injective. If  $\rho$  were not faithful then the theory would only be invariant under the smaller symmetry group isomorphic to  $G/\ker\rho$  and the restricted representation would be faithful.

Comparing first performing a group transformation and then performing a CP transformation with the inverse order of operations, as shown in Fig. 6.1, one finds the requirement that

$$U\rho(g)^*U^{-1} \in \text{Im}\rho \equiv \rho(G), \quad (6.5)$$

i.e. the CP transformation maps group elements  $\rho(g)$  onto group elements  $\rho(g')$ . It preserves the group multiplication, i.e.  $U\rho(g_1g_2)^*U^{-1} = U\rho(g_1)^*U^{-1}U\rho(g_2)^*U^{-1}$ , and therefore is a homomorphism. Furthermore the CP transformation is bijective, since  $U$  is unitary and therefore invertible. Hence, CP is an automorphism<sup>4</sup> of the group, as is depicted in Fig. 6.2.

<sup>4</sup>An *automorphism*  $\mu$  of a group  $G$  is a bijective homomorphism  $\mu : G \rightarrow G$ .

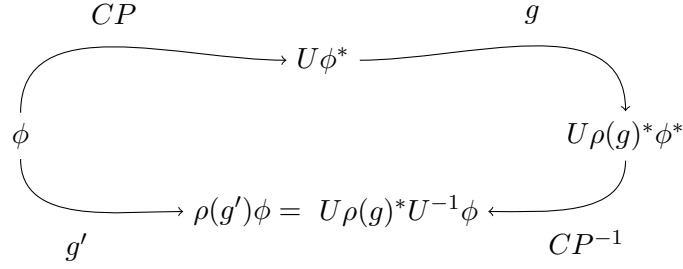


Figure 6.1: CP definition.

Indeed, the possible matrices  $U$  of Eq. (6.5) form a representation of the automorphism group<sup>5</sup>  $\text{Aut}(G)$  of  $G$ , which we are showing in the following.

$U$  represents the automorphism  $u : G \rightarrow G$  given by

$$u : g \in G \rightarrow \rho(g) \rightarrow U\rho(g)^*U^{-1} = \rho(g') \rightarrow g' = \rho^{-1}(U\rho(g)^*U^{-1}) \in G$$

or

$$U\rho(g)^*U^{-1} = \rho(u(g)) . \quad (6.6)$$

It is straightforward to show that this mapping  $u : G \rightarrow G$  is indeed an automorphism.

Vice versa, if  $u : G \rightarrow G$  is an automorphism, we can explicitly construct a matrix  $U$  in the following way. We first extend  $G$  to a group  $G'$  containing  $G$  as a normal subgroup and  $u(g) = g'gg'^{-1} \forall g \in G$  with  $g' \in G'$ . Taking the order of  $u$ <sup>6</sup> to be  $\text{ord}(u) = n$ , we define the homomorphism

$$\theta : Z_n = (\{0, \dots, n-1\}, +) \rightarrow \text{Aut}(G) : 1 \rightarrow \theta_1 \equiv u ,$$

which has a trivial kernel. This homomorphism thus defines the semidirect product group  $G' = G \rtimes_{\theta} Z_n$  with the group multiplication

$$(g_1, z_1) \star (g_2, z_2) = (g_1\theta_{z_1}(g_2), z_1 + z_2) .$$

Keeping track of the multiplication rules, we find

$$(E, 1) \star (g, z) \star (E, 1)^{-1} = (u(g), z) ,$$

where  $E$  is the identity element of  $G$ . The outer automorphism<sup>7</sup>  $u$  of  $G$  becomes an inner automorphism of  $G'$  and we can obtain a matrix representation of  $u$  by the standard techniques for finding matrix representations of groups, which are implemented in GAP [129] .

Hence, there is a unitary matrix  $U'$  with

$$U'\rho(g)U'^{-1} = \rho(u(g)) .$$

<sup>5</sup>The automorphism group  $\text{Aut}(G)$  is the set of all automorphisms of  $G$  with composition as group multiplication.

<sup>6</sup>The order of a group element  $u$  of  $G$  is given by the smallest  $n \in \mathbb{N}$  with  $u^n = \text{id}_G$ .

<sup>7</sup>An inner automorphism  $\mu_h$  of a group  $G$  is an automorphism, which is represented by conjugation with an element  $h$  of  $G$ , i.e.  $\mu_h \equiv \text{conj}(h) : g \rightarrow hgh^{-1}$ . If an automorphism can not be represented by conjugation with a group element, it is called an outer automorphism.



$$\begin{array}{ccc}
& \xrightarrow{\rho} \rho(g)^* & \xrightarrow{\quad} U\rho(g)^*U^{-1} = \rho(g') & \xleftarrow{\rho^{-1}} \\
& \curvearrowright & & \curvearrowleft \\
g \in G & \xrightarrow{\quad} & u : G \rightarrow G & \xrightarrow{\quad} u(g) = g' \in G
\end{array}$$

**Figure 6.2:** The matrix  $U$  that appears in the definition of CP defines an automorphism  $u : G \rightarrow G$  of the group  $G$ .

Note that Eq. (6.4) in combination with Eq. (6.2) implies the existence of a matrix  $W$  with  $W^2 = 1$  as well as  $\phi^* = W\phi$  and consequently  $\rho(g) = W\rho(g)^*W$ . This allows to write a CP transformation as

$$\phi \rightarrow U\phi^* = UW\phi$$

and therefore

$$U\rho(g)^*U^{-1} = \rho(u(g))$$

with  $U = U'W$ .

The automorphisms form a group with composition as group multiplication, i.e.  $u' = \tilde{u} \circ u$  is again an automorphism represented by

$$U'\rho(g)^*U'^{-1} = \rho(u'(g))$$

with

$$\rho(u'(g)) = \rho(\tilde{u}(u(g))) = \tilde{U}W\rho(u(g))W\tilde{U}^{-1} = \tilde{U}WU\rho(g)U^{-1}W\tilde{U}^{-1}$$

and thus

$$U' = \tilde{U}WU. \quad (6.7)$$

The trivial automorphism  $id(g) = g \forall g \in G$  is represented by  $U = W$  and the inverse automorphism  $u^{-1}$  is represented by  $WU^{-1}W$ . We thus have a homomorphism from the automorphism group to the group of matrices  $U$  defined in Eq. (6.4) with the conjunction  $\star: (A, B) \rightarrow A \star B \equiv AWB$ . With respect to this conjunction the matrices  $U$  form a representation of the automorphism group.

For any solution  $U$  of Eq. (6.5) the matrix  $\rho(g)U$  is also a solution for any  $g \in G$ , which corresponds to performing a CP transformation followed by a group transformation described by  $\rho(g)$ . The group transformation corresponds to an inner homomorphism<sup>8</sup>, which does not pose any new restrictions. It is therefore sufficient to consider automorphisms with inner automorphisms modded out. *Hence the group of generalized CP transformations is given by the outer automorphism group, which is defined by*

$$\text{Out}(G) \equiv \text{Aut}(G)/\text{Inn}(G). \quad (6.8)$$

<sup>8</sup>An *inner automorphism* is an automorphism which can be represented by conjugation, i.e.  $\text{conj}(h) : g \rightarrow hgh^{-1}$  with  $h \in G$ . The set of all inner automorphisms form the *inner automorphism group*  $\text{Inn}(G)$ . For every group  $G$  there is a natural group homomorphism  $G \rightarrow \text{Aut}(G)$  whose image is  $\text{Inn}(G)$  and whose kernel is the *centre of  $G$* ,  $Z(G)$ , i.e. the subset of  $G$  which commutes with all elements of  $G$ . In short

$$\text{Inn}(G) \cong G/Z(G).$$

Thus, if  $G$  has trivial centre it can be embedded into its own automorphism group.

As we will be using the character table in the discussion of the different groups, we will briefly comment on how automorphisms act on the character table. As automorphisms are mappings from the group into itself and there is a unique character table for each group up to reordering rows and columns, automorphisms are symmetries of the character table and can not change the character table besides exchanging rows and columns. Inner automorphisms act via conjugation on the group and hence they map group elements to group elements of the same conjugacy classes. Neither do they exchange representations and therefore they do not change the character table. Outer automorphisms on the other hand map elements from one conjugacy class to another as well as one representation to another.

We follow [211] and call a basis where  $U$  may be represented by the identity matrix times a phase,  $\phi \rightarrow e^{i\alpha} \phi^*$ , a *CP basis*. Note that under a change of basis  $\phi' = V\phi$  we have

$$\phi' \rightarrow (VUV^T)\phi' \quad (6.9)$$

and it is thus not always possible to perform a basis change to a CP basis where  $VUV^T$  is diagonal [216].

### 6.2.2. Physical Implications of a Generalized CP Symmetry

The existence of a generalized CP symmetry implies that there is no direct CP violation and CP violation can only be generated via spontaneous symmetry breaking. This has been studied in terms of weak basis invariants [217–219]. A necessary and sufficient set of weak basis invariants, which measure the CP violation in the lepton sector and vanish in the CP conserving case has been proposed in [219]. In the following, we will explicitly demonstrate that the weak basis invariant for Dirac CP violation vanishes for our generalized CP symmetry and refer the reader to [219] for the remaining weak basis invariants.

Let us consider a left-handed lepton doublet  $L = (\nu, e)^T$  with the following mass terms

$$\mathcal{L}_{mass} = -e^T M_e e^c - \frac{1}{2} \nu^T M_\nu \nu + \text{h.c.} .$$

It was shown in [217–219] that Dirac-type CP violation ( $\sin \delta_{CP} \neq 0$ ) is equivalent to

$$0 \neq \text{tr} [H_\nu, H_e]^3 \quad \text{with} \quad H_\nu = (M_\nu^\dagger M_\nu)^* \quad \text{and} \quad H_e = (M_e M_e^\dagger)^T, .$$

If  $L$  transforms under a generalised CP transformation as

$$L \xrightarrow{\text{CP}} UL^C \equiv U (i\sigma_2 L^*)$$

where  $L^C$  denotes charge conjugation with respect to the Lorentz group and  $U$  is unitary, the weak basis invariants  $H_{\nu,e}$  have to fulfil

$$H_\nu = U^T H_\nu^T U^* \quad H_e = U^T H_e^T U^*$$

and therefore (note  $[A, B]^T = -[A^T, B^T]$ )

$$\text{tr} [H_\nu, H_e]^3 = \text{tr} U^T [H_\nu^T, H_e^T]^3 U^* = -\text{tr} [H_\nu, H_e]^3 = 0 \quad (6.10)$$

and there is no Dirac-type CP violation.

### 6.3. Applications to Questions in the Literature

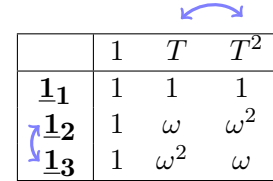
#### 6.3.1. $Z_3 \cong \text{SG}(3, 1)$

Let us start the discussion of examples by taking the cyclic group with three elements  $Z_3 \cong \langle T | T^3 = E \rangle$ , which is the smallest group with complex representations. There is one non-trivial automorphism  $u(T) = T^2$ , which is outer and since all group elements commute, the inner automorphisms are all trivial,  $\text{conj}(T) = \text{conj}(T^2) = id$ . The structure of the automorphism group is thus:

$$\text{Z}(Z_3) \cong Z_3 \qquad \text{Aut}(Z_3) \cong Z_2 \qquad (6.11)$$

$$\text{Inn}(Z_3) \cong Z_1 \qquad \text{Out}(Z_3) \cong Z_2. \qquad (6.12)$$

Looking at the character table of  $Z_3$  displayed in Table 6.1, we see that the outer automorphism  $u : T \rightarrow T^2$  indicated in blue acts on the character table by interchanging the conjugacy classes represented by  $T$  and  $u(T) = T^2$  and the representations  $\underline{\mathbf{1}}_2 \rightarrow \underline{\mathbf{1}}_2 \circ u = \underline{\mathbf{1}}_3$ , i.e. the rows and columns of the character table such that the table stays invariant, as an outer automorphism should do. Let us take a theory that contains the complex representation  $\varphi \sim \underline{\mathbf{1}}_2$ . The vector  $\phi = (\varphi, \varphi^*)^T$  is acted upon by the group generator  $T$  as



	1	$T$	$T^2$
$\underline{\mathbf{1}}_1$	1	1	1
$\underline{\mathbf{1}}_2$	1	$\omega$	$\omega^2$
$\underline{\mathbf{1}}_3$	1	$\omega^2$	$\omega$

**Table 6.1:** Character Table of  $Z_3$ . The automorphism  $u(T) = T^2$  (blue) interchanges rows and columns.

$$\rho(T) = \begin{pmatrix} \omega & 0 \\ 0 & \omega^2 \end{pmatrix}$$

and we have  $\rho(T)^* = \rho(T^2) \in \text{Im}\rho$  and therefore  $U = 1$  is a representation of the outer automorphism  $u(T) = T^2$ . The generalized CP transformation of Eq. (6.4) is therefore just the usual  $\varphi \rightarrow \varphi^*$ .

Another solution to Eq. (6.4) is the matrix

$$W = \begin{pmatrix} 0 & 1 \\ 1 & 0 \end{pmatrix}$$

that gives an inner automorphism (or a trivial map, actually) and also a trivial ‘CP transformation’  $\varphi \rightarrow \varphi$ . This is an example where the trivial automorphism is not represented by the identity, as discussed below Eq. (6.7). Note that the matrix  $W$  represents  $u^2 = id$ .

#### 6.3.2. $A_4 \cong (Z_2 \times Z_2) \rtimes Z_3 \cong \text{SG}(12, 3)$

The group  $A_4 = \langle S, T | S^2 = T^3 = (ST)^3 = E \rangle$  has been introduced in Section 2.3.1; it is very important for model building and serves as our first non-trivial example. Only the identity element commutes with all other elements and the natural homomorphism  $n : A_4 \rightarrow \text{Aut}(A_4)$  defined by  $n(g) = \text{conj}(g)$  is therefore injective. There is one non-trivial outer automorphism  $u(S, T) = (S, T^2)$  and the automorphism structure is thus given as:

$$\text{Z}(A_4) \cong Z_1 \qquad \text{Aut}(A_4) \cong S_4 \qquad (6.13)$$

$$\text{Inn}(A_4) \cong A_4 \qquad \text{Out}(A_4) \cong Z_2. \qquad (6.14)$$

The character table of  $A_4$  is given in Table 2.4 and it is easy to verify that the automorphism  $u$  represents a symmetry of the character table, again interchanging the representations  $\underline{\mathbf{1}}_2$  and  $\underline{\mathbf{1}}_3$ . Let us first discuss the case where we have only one real scalar field in the real representation  $\phi \sim \underline{\mathbf{3}}_1$  in the Ma-Rajasekaran [65] basis:

$$\rho_{\underline{\mathbf{3}}_1}(S) = S_3 \equiv \begin{pmatrix} 1 & 0 & 0 \\ 0 & -1 & 0 \\ 0 & 0 & -1 \end{pmatrix}, \quad \rho_{\underline{\mathbf{3}}_1}(T) = T_3 \equiv \begin{pmatrix} 0 & 1 & 0 \\ 0 & 0 & 1 \\ 1 & 0 & 0 \end{pmatrix}. \quad (6.15)$$

In this basis both group generators are real ( $\rho(g)^* = \rho(g) \in \text{Im}\rho$ ) and one might be tempted to take  $U = \mathbb{1}_3$  as this fulfils Eq. (6.5). However,  $A_4$  is a group with complex representations and therefore CP has to be an outer automorphism and the map derived from  $U = \mathbb{1}_3$  via Eq. (6.6) is the trivial automorphism  $u(g) = g$ , which is of course not outer. One also encounters this problem as soon as one considers contractions such as

$$(\phi\phi)_{\underline{\mathbf{1}}_2} = \frac{1}{\sqrt{3}} (\phi_1\phi_1 + \omega^2\phi_2\phi_2 + \omega\phi_3\phi_3)$$

which transform under this ‘CP’  $\phi \rightarrow U\phi^* = \phi$  as

$$(\phi\phi)_{\underline{\mathbf{1}}_2} \rightarrow (\phi\phi)_{\underline{\mathbf{1}}_2} \sim \underline{\mathbf{1}}_2,$$

which is in conflict with the expectation that CP should involve complex conjugation such that

$$(\phi\phi)_{\underline{\mathbf{1}}_2} \rightarrow [(\phi\phi)_{\underline{\mathbf{1}}_2}]^* \sim \underline{\mathbf{1}}_3.$$

Just imagine that the theory contains a real scalar triplet  $\chi$  and  $\xi \sim \underline{\mathbf{1}}_3$ . If one defines CP as  $\chi \rightarrow \chi$  and  $\xi \rightarrow \xi^*$  then the invariant  $(\chi\chi)_{\underline{\mathbf{1}}_2} \xi$  under CP is mapped to  $(\chi\chi)_{\underline{\mathbf{1}}_2} \xi^*$ , which is not invariant under the group. Clearly this shows that this definition of CP is not consistent if particles transforming under these representations are present, it has however been (implicitly) used in a number of works [163, 220, 221].

If we instead use the non-trivial solution of Eq. (6.5)

$$U = U_3 \equiv \begin{pmatrix} 1 & 0 & 0 \\ 0 & 0 & 1 \\ 0 & 1 & 0 \end{pmatrix}$$

that corresponds to the outer automorphism  $u(S, T) = u(S, T^2)$  we immediately see that

$$(\phi\phi)_{\underline{\mathbf{1}}_2} \rightarrow [(\phi\phi)_{\underline{\mathbf{1}}_2}]^* \sim \underline{\mathbf{1}}_3.$$

Note that this is the only consistent definition of CP (up to inner automorphisms) in any theory that involves the complex representations somewhere as the outer automorphism group is  $Z_2$ . We have encountered the matrix  $U_3$  before in Eq. (2.30), where we have seen that it extends  $A_4$  to  $S_4$ .

Using Eq. (6.4), we can immediately see that in this case the trivial solution  $U = \mathbb{1}_3$  does not exist. Let us consider the vector  $\phi = (\xi, \xi^*, \chi)^T$  with  $\xi \sim \underline{\mathbf{1}}_3$  and  $\chi \sim \underline{\mathbf{3}}_1$ , which transforms as

$$\rho(S) = \text{diag}(1, 1, S_3) \quad \rho(T) = \text{diag}(\omega, \omega^2, T_3), \quad (6.16)$$

### 6.3. Applications to Questions in the Literature

clearly fulfilling  $\rho(S)^* = \rho(S) \in \text{Im}\rho$  and  $\rho(T)^* \notin \text{Im}\rho$ . We are therefore forced to use  $U = \text{diag}(1, 1, U_3)$ , which gives  $U\rho(T)^*U^{-1} = \rho(T^2) \in \text{Im}\rho$  and  $U\rho(S)^*U^{-1} = \rho(S) \in \text{Im}\rho$  and therefore represents the outer automorphism  $u : (S, T) \rightarrow (S, T^2)$ . The only consistent CP transformation in this theory is therefore  $\xi \rightarrow \xi^*$  and  $\chi \rightarrow U_3\chi^* = U_3\chi$ . Since this case is of some relevance to model building, let us dwell on it a bit more and repeat the discussion for the basis

$$S = \frac{1}{3} \begin{pmatrix} -1 & 2 & 2 \\ 2 & -1 & 2 \\ 2 & 2 & -1 \end{pmatrix}, \quad T = \begin{pmatrix} 1 & 0 & 0 \\ 0 & \omega^2 & 0 \\ 0 & 0 & \omega \end{pmatrix},$$

first used by Altarelli and Feruglio [69]. Here the group elements are complex but the Clebsch-Gordon coefficients are real. The unique result of Eq. (6.4) is  $U = \mathbb{1}_3$  up to inner automorphisms. This basis is therefore a CP basis, as defined in Eq. (6.9). Note that in this basis

$$(\phi\phi)_{\underline{\mathbf{1}}_2} = (\phi_2\phi_2 + \phi_1\phi_3 + \phi_3\phi_1), \quad (\phi\phi)_{\underline{\mathbf{1}}_3} = (\phi_3\phi_3 + \phi_1\phi_2 + \phi_2\phi_1)$$

and thus

$$(\phi\phi)_{\underline{\mathbf{1}}_2} \rightarrow [(\phi\phi)_{\underline{\mathbf{1}}_2}]^* \sim \underline{\mathbf{1}}_3,$$

as it should be.

Let us look at a physical situation where a certain confusion about the definition of CP can be alleviated by our definition. If one considers the potential for one triplet Higgs doublet  $\chi = (\chi_1, \chi_2, \chi_3)^T$  in the basis of Eq. (6.15) there is one potentially complex coupling in the potential [65, 163, 221]

$$\lambda_5 (\chi^\dagger\chi)_{\underline{\mathbf{3}}_1} (\chi^\dagger\chi)_{\underline{\mathbf{3}}_1} + \text{h.c.} = \lambda_5 \left[ (\chi_1^\dagger\chi_2)^2 + (\chi_2^\dagger\chi_3)^2 + (\chi_3^\dagger\chi_1)^2 \right] + \text{h.c.} \quad (6.17)$$

It can easily be checked that the generalized CP transformation  $\chi \rightarrow U_3\chi^*$  acts as

$$I \equiv \left[ (\chi_1^\dagger\chi_2)^2 + (\chi_2^\dagger\chi_3)^2 + (\chi_3^\dagger\chi_1)^2 \right] \rightarrow \left[ (\chi_1^\dagger\chi_2)^2 + (\chi_2^\dagger\chi_3)^2 + (\chi_3^\dagger\chi_1)^2 \right] = I$$

and thus does not give a restriction on the phase of  $\lambda_5$ . Note that the naive CP transformation  $\chi \rightarrow \chi^*$  transforms the group invariant  $I$  into  $I^*$  and therefore restricts  $\lambda_5$  to be real as was e.g. done in [220]. However, we have seen that this naive CP transformation cannot be consistently implemented on the Lagrangian level if there are complex representations. Therefore it is inconsistent to call the phase of  $\lambda_5$  a CP phase. This also explains an observation made in [163], where it was shown that even for  $\arg \lambda_5 \neq 0$  the VEV configuration

$$\langle \chi \rangle = V(1, 1, 1), \quad \langle \chi \rangle = V'(1, 0, 0) \quad V, V' \in \mathbb{R}, \quad (6.18)$$

which of course respects both CP transformations, can be obtained without fine-tuning. This would have been somewhat surprising, as usually symmetry conserving solutions cannot be obtained from explicitly symmetry breaking potentials. However, the phase of  $\lambda_5$  does not break the consistent CP, as does the VEV configuration (6.18), therefore everything is consistent.

### 6.3.3. $T' \cong \text{SG}(24, 3)$

The group  $T' = \langle S, T | S^4 = T^3 = (ST)^3 = E \rangle$  is also an important group in the context of CP violation [199, 200]. It has two elements  $Z(T') = \{E, S^2\} \cong Z_2$  that commute with all group elements and therefore  $\text{Inn}(T') \cong G/Z(T') \cong A_4$ . There is one non-trivial outer automorphism (up to inner automorphisms)  $u(S, T) = (S^3, T^2)$ . Therefore the automorphism structure can be summarized as:

$$\begin{aligned} Z(T') &\cong Z_2 & \text{Aut}(T') &\cong S_4 \\ \text{Inn}(T') &\cong A_4 & \text{Out}(T') &\cong Z_2. \end{aligned} \quad (6.19)$$

A non-trivial CP transformation therefore has to be a representation of  $u$  in the sense of Eq. (6.4). Let us now see how it is represented for the various representations of  $T'$ .

There is a faithful pseudo-real representation

$$\underline{\mathbf{2}}_1 : S = A_1, \quad T = \omega A_2$$

with  $\sigma_2^\dagger S \sigma_2 = S^*$  and  $\sigma_2^\dagger T \sigma_2 = T^*$  and the two faithful complex representations

$$\underline{\mathbf{2}}_2 : S = A_1 \quad T = \omega^2 A_2; \quad \underline{\mathbf{2}}_3 : S = A_1, \quad T = A_2$$

with  $\sigma_2^\dagger S_2' \sigma_2 = S_2^{*'}$  and  $\sigma_2^\dagger T_2' \sigma_2 = T_2^{*'}$ , where

$$A_1 = \frac{-1}{\sqrt{3}} \begin{pmatrix} i & \psi\sqrt{2} \\ -\psi^{-1}\sqrt{2} & -i \end{pmatrix}, \quad A_2 = \begin{pmatrix} \omega & 0 \\ 0 & 1 \end{pmatrix}$$

with  $\psi = e^{2\pi i/24}$ . For all of the two-dimensional representations, we find the matrix

$$U = U_2 \equiv \text{diag}(\psi^{-5}, \psi^5),$$

which represents the automorphism  $u$  via  $U\rho(g)^*U^{-1} = \rho(u(g))$ . For the three-dimensional representation

$$\rho(S) = \frac{1}{3} \begin{pmatrix} -1 & 2\omega & 2\omega^2 \\ 2\omega^2 & -1 & 2\omega \\ 2\omega & 2\omega^2 & -1 \end{pmatrix}, \quad \rho(T) = \begin{pmatrix} 1 & 0 & 0 \\ 0 & \omega & 0 \\ 0 & 0 & \omega^2 \end{pmatrix}$$

the matrix  $U$  of Eq. (6.4) is given by  $U = \rho(T)$  with again  $U\rho(T)^*U^{-1} = \rho(T^2)$ ,  $U\rho(S)^*U = \rho(S^3)$ ; for the one dimensional representations we take  $U = \rho(T)$  as for the three-dimensional representations.

In summary, we have thus found the one unique non-trivial outer automorphism (up to inner automorphisms) of  $T'$  and thus the unique CP transformation

$$\underline{\mathbf{1}}_i \rightarrow \omega^{i-1} \underline{\mathbf{1}}_i^* \quad \underline{\mathbf{2}}_i \rightarrow \text{diag}(\psi^{-5}, \psi^5) \underline{\mathbf{2}}_i^* \quad \underline{\mathbf{3}}_1 \rightarrow \text{diag}(1, \omega, \omega^2) \underline{\mathbf{3}}_1^*. \quad (6.20)$$

Let us now use this insight to investigate a claim that there is geometrical CP violation in grand unified models based on  $T'$  [199, 200]. We follow [199] and introduce  $(T_1, T_2) \sim 2$ , which transforms as  $\underline{\mathbf{10}}$  of  $\text{SU}(5)$  and includes the first two generations of up-type quarks and

### 6.3. Applications to Questions in the Literature

the flavons  $\phi \sim \mathbf{3}$  and  $\phi' \sim \mathbf{3}$ . Auxiliary  $Z_{12} \times Z_{12}$  symmetries are introduced such that the one-two sector of the mass matrix is described by

$$\begin{aligned}
-\mathcal{L}_{TT} &= y_c TT\phi^2 + y_u TT\phi'^3 + \text{h.c.} & (6.21) \\
&= y_c \left[ \left( \frac{1}{8} + \frac{i}{4} \right) (T_1^2 (2\phi_2^2 - \phi_1\phi_3) + (2 + 2i)T_1T_2\phi_2\phi_3 + iT_2^2 (\phi_1\phi_2 - 2\phi_3^2)) \right] + \\
&+ y_u \left[ \frac{1}{6} (2\phi'_1\phi'_3 + \phi'_2{}^2) (iT_1^2\phi'_1 + (1 - i)T_1T_2\phi'_2 + T_2^2\phi'_3) \right] + \text{h.c.},
\end{aligned}$$

where we have omitted (Higgs-) fields that do not transform under the flavour symmetry and a suppression by some high-energy scale of a sufficient power to make  $y_i$  dimensionless is understood.

It is assumed that the VEVs

$$\langle \phi' \rangle = (1, 1, 1)V', \quad \langle \phi \rangle = (0, 0, 1)V, \quad V, V' \in \mathbb{R} \quad (6.22)$$

are real, which may be justified by a CP transformation. There is only one CP transformation<sup>9</sup> left invariant, namely the one corresponding to the outer automorphism  $u' = u \circ \text{conj}(T^2)$  represented on the 3 dimensional representation by the identity matrix:  $\phi' \rightarrow \phi'^*$  and  $\phi \rightarrow \phi^*$ .

The 1-2 elements of the up type quark mass matrix are given as follows as follows:

$$M_u \sim y_u \begin{pmatrix} i & \frac{i-1}{2} \\ \frac{i-1}{2} & 1 \end{pmatrix} V'^3 + y_c \begin{pmatrix} 0 & 0 \\ 0 & 1 - \frac{i}{2} \end{pmatrix} V^2.$$

At this point the parameters  $y_{u,s}$  and VEVs are chosen real and it is claimed that the phases that emerge from the complex Clebsch-Gordon coefficients explain CP violation. The question that naturally arises here is if this choice of parameters can be justified by a symmetry. The only candidate symmetry is a generalized CP symmetry of the type (6.5) we are considering here. As we have shown how the various fields have to transform under the generalized CP symmetry we can now easily determine how the invariants of Eq. (6.21) transform<sup>10</sup>:

$$CP[TT\phi^2] = \frac{1}{5}(4 - 3i)(TT\phi^2)^* \quad CP[TT\phi'^3] = -i(TT\phi'^3)^*. \quad (6.23)$$

Therefore invariance under CP requires  $\arg(y_c) = -\frac{1}{2}\arg(4 - 3i) = \frac{1}{2}\arctan\frac{3}{4}$  and  $\arg y_u = \frac{\pi}{4}$ , which is in conflict with the claims made in [199, 200]. Note that also the relative phase between the two couplings does not agree with ‘geometrical’ CP violation. This also shows that the results obtained there are completely basis dependent and therefore unphysical.

Note that the VEVs of Eq. (6.22) are invariant under the generalised CP trafo  $U_{new} = U\rho(T)^2 = \text{diag}(1, 1, 1)$ , but in the full model [199] there are additional scalar fields e.g.  $\psi \sim \mathbf{2}'$  with  $\langle \psi' \rangle \sim (1, 1)$  that are not invariant under the consistent CP transformation  $U_{new} = U\rho(T)^2$ , which in this basis reads  $\text{diag}(e^{i\pi 11/2}, e^{i\pi 5/2})$ . Thus such a VEV configuration would imply a spontaneous breaking of CP, if one would change the phases of the couplings to be in accordance with the consistent CP transformation.

<sup>9</sup>This also determines the phase of  $U$ .

<sup>10</sup>Note that inner automorphisms correspond to group transformations and therefore only outer automorphisms can give non-trivial constraints when acting on group invariants. Here there is only one non-trivial outer automorphism (up to inner automorphisms).

	$E$	$BABA$	$ABA$	$A$	$BAB$	$AB$	$A^2$	$B^2$	$B$	$BA^2BAB$	$AB^2ABA$
$\underline{\mathbf{1}}_1$	1	1	1	1	1	1	1	1	1	1	1
$\underline{\mathbf{1}}_2$	1	$\omega$	$\omega^2$	1	$\omega$	$\omega^2$	1	$\omega$	$\omega^2$	1	1
$\underline{\mathbf{1}}_3$	1	$\omega^2$	$\omega$	1	$\omega^2$	$\omega$	1	$\omega^2$	$\omega$	1	1
$\underline{\mathbf{1}}_4$	1	$\omega$	$\omega$	$\omega^2$	$\omega^2$	$\omega^2$	$\omega$	1	1	1	1
$\underline{\mathbf{1}}_5$	1	$\omega^2$	1	$\omega^2$	1	$\omega$	$\omega$	$\omega$	$\omega^2$	1	1
$\underline{\mathbf{1}}_6$	1	1	$\omega^2$	$\omega^2$	$\omega$	1	$\omega$	$\omega^2$	$\omega$	1	1
$\underline{\mathbf{1}}_7$	1	$\omega^2$	$\omega^2$	$\omega$	$\omega$	$\omega$	$\omega^2$	1	1	1	1
$\underline{\mathbf{1}}_8$	1	1	$\omega$	$\omega$	$\omega^2$	1	$\omega^2$	$\omega$	$\omega^2$	1	1
$\underline{\mathbf{1}}_9$	1	$\omega$	1	$\omega$	1	$\omega^2$	$\omega^2$	$\omega^2$	$\omega$	1	1
$\underline{\mathbf{3}}$	3	.	.	.	.	.	.	.	.	$3\omega$	$3\omega^2$
$\underline{\mathbf{3}}^*$	3	.	.	.	.	.	.	.	.	$3\omega^2$	$3\omega$

**Table 6.2:** Character table of  $\Delta(27)$ . The first line are representatives of the different conjugacy classes. Zeros in the character table are denoted by a dot . and  $\omega$  is the third root of unity  $\omega = e^{2\pi i/3}$ . The arrows illustrate the generators of the outer automorphism group  $u_1$  (blue) and  $u_2$  (red).

In [199], no dynamical mechanism to generate the VEV configuration was given but in [200] it was claimed that it can be done using 23 driving fields, a  $U_R(1)$  symmetry and shaping symmetries  $Z_{12} \times Z_8^3 \times Z_6^2 \times Z_4$  of the impressive order of 884736. However, they just assumed that all couplings should be real, which certainly does not coincide with the correct CP transformation we have given here.

### 6.3.4. $\Delta(27) \cong (Z_3 \times Z_3) \rtimes Z_3 \cong \text{SG}(27, 3)$

The group  $\Delta(27) = \langle A, B | A^3 = B^3 = (AB)^3 = E \rangle$  is another interesting group from the standpoint of CP violation. Its automorphism structure is quite involved. The centre of the group is isomorphic to  $Z_3$  and generated by the group element  $X = A^2BAB^2$  with  $\text{conj}(X) = id$  and the inner automorphism group has the structure  $Z_3 \times Z_3$ . The outer automorphism group is generated by

$$u_1 : (A, B) \rightarrow (ABA^2, B^2AB), \quad u_2 : (A, B) \rightarrow (ABAB, B^2). \quad (6.24)$$

It is isomorphic to  $\text{GL}(2, 3)$ , i.e. the general linear group of  $2 \times 2$  matrices over the field  $Z_3$ . The multitude of outer automorphisms can be traced back to the various symmetries of the character table shown in Tab. 6.2 that are due to the fact that there are so many one-dimensional representations. Together with the inner automorphisms these generators generate the full automorphism group, which is of order 432. In summary the automorphism structure presents itself as:

$$\begin{aligned} \text{Z}(\Delta(27)) &\cong Z_3 & \text{Aut}(\Delta(27)) &\cong (((Z_3 \times Z_3) \rtimes Q_8) \rtimes Z_3) \rtimes Z_2 \\ \text{Inn}(\Delta(27)) &\cong Z_3 \times Z_3 & \text{Out}(\Delta(27)) &\cong \text{GL}(2, 3). \end{aligned} \quad (6.25)$$

The outer automorphism  $u_1$  acts on the representations as

$$\underline{\mathbf{1}}_2 \leftrightarrow \underline{\mathbf{1}}_4, \quad \underline{\mathbf{1}}_3 \leftrightarrow \underline{\mathbf{1}}_7, \quad \underline{\mathbf{1}}_6 \leftrightarrow \underline{\mathbf{1}}_8, \quad \underline{\mathbf{3}} \leftrightarrow \underline{\mathbf{3}}^*,$$

where e.g.  $\underline{\mathbf{1}}_2 \rightarrow \underline{\mathbf{1}}_4$  is to be read as  $\rho_{\underline{\mathbf{1}}_4} = \rho_{\underline{\mathbf{1}}_2} \circ u_1$  etc., and the outer automorphism  $u_2$  acts as

$$\underline{\mathbf{1}}_2 \rightarrow \underline{\mathbf{1}}_9 \rightarrow \underline{\mathbf{1}}_8 \rightarrow \underline{\mathbf{1}}_3 \rightarrow \underline{\mathbf{1}}_5 \rightarrow \underline{\mathbf{1}}_6 \rightarrow \underline{\mathbf{1}}_2.$$



### 6.3. Applications to Questions in the Literature

From this it is trivial to determine the representations of the automorphisms for the one-dimensional representations. Let us therefore focus on the three dimensional representation  $\underline{\mathbf{3}}$  generated by

$$\rho(A) = T_3, \quad \rho(B) = \text{diag}(1, \omega, \omega^2).$$

The two generators of the outer automorphism group act on  $\phi \sim (\underline{\mathbf{3}}, \underline{\mathbf{3}}^*)$  as

$$U(u_1) = \begin{pmatrix} \tilde{U} & 0 \\ 0 & \tilde{U}^* \end{pmatrix} \quad \text{with} \quad \tilde{U} = \frac{1}{\sqrt{3}} \begin{pmatrix} \omega^2 & \omega & 1 \\ \omega & \omega^2 & 1 \\ 1 & 1 & 1 \end{pmatrix} \quad (6.26)$$

and

$$U(u_2) = \begin{pmatrix} 0 & \tilde{U} \\ \tilde{U}^* & 0 \end{pmatrix} \quad \text{with} \quad \tilde{U} = \begin{pmatrix} \omega^2 & 0 & 0 \\ 0 & 0 & \omega \\ 0 & \omega^2 & 0 \end{pmatrix}. \quad (6.27)$$

All automorphisms can be generated from the generators  $u_i$  by composition and the representation matrices  $U(\text{aut})$  may be obtained with the help of Eq. (6.7). We have therefore found a complete classification of possible CP transformations that may be implemented in a model based on  $\Delta(27)$ . There are 48 outer automorphisms generated by  $u_1$  and  $u_2$ , that may in principle give physically distinct CP transformations, with distinct physical implications. However, since a model that is invariant under CP will also be invariant under the subgroup generated by  $CP^n$ , it is sufficient to consider subgroups of the automorphism group.

It is instructive to look at some of these subgroups in detail. Let us for example consider the CP transformation  $\phi \rightarrow \phi^*$  or  $U(h_1) = \mathbb{1}_3$  that corresponds to the outer automorphism  $h_1 : (A, B) \rightarrow (A, B^2)$ , which can be expressed in terms of the generators as  $h_1 = u_1 \circ u_2^2 \circ u_1^{-1} \circ u_2 \circ u_1^{-1} \circ u_2^{-1} \circ u_1^{-1} \circ \text{conj}(A)^{-1} \circ u_1^{-1}$ . This outer automorphism squares to one and therefore generates a  $Z_2$  subgroup of the automorphism group. Contrary to the situation we have encountered before, where the outer automorphism group was a  $Z_2$ , this is not the only solution. As a further example we may consider the  $Z_2$  subgroup generated by  $u_1 \circ u_2^2 \circ u_1^{-1} \circ u_2 \circ u_1^{-1} \circ u_2^{-2}$  with  $h_2 : (A, B) \rightarrow (ABA, B)$  which according to (6.7) is represented by

$$U(h_2) = \begin{pmatrix} \omega & 0 & 0 \\ 0 & 0 & 1 \\ 0 & 1 & 0 \end{pmatrix}. \quad (6.28)$$

We will use this matrix later on. Let us now use this machinery to tackle a physical question, namely the so-called geometrical CP violation. ‘Geometrical’ CP-violation [201–204] denotes the following: If one considers a triplet of Higgs doublets  $H = (H_1, H_2, H_3) \sim \underline{\mathbf{3}}$  the only phase dependent term in the scalar potential is given by

$$I \equiv \sum_{i \neq j \neq k} (H_i^\dagger H_j)(H_i^\dagger H_k).$$

Let us now investigate how the term transforms under the two generators  $u_1$  and  $u_2$  of the outer automorphism group. We find

$$CP_{u_1}[I] = -\frac{1}{3}I^* + \frac{2}{3}I + \sum_i \frac{1}{3}(H_i^\dagger H_i)^2 + \sum_{i \neq j} (H_i^\dagger H_i)(H_j^\dagger H_j), \quad CP_{u_2}[I] = \omega^2 I$$

and we thus find the invariant combinations

$$CP_{u_1}[I - I^*] = I - I^* \quad CP_{u_2^3}[I] = I.$$

Clearly invariance under  $u_1$  requires further non-trivial relations among the other couplings in the scalar potential which do not depend on phases and thus do not concern us here.

Let us investigate the case where the theory is invariant under  $h_1$  which corresponds to the ‘usual’ CP transformation  $\phi \rightarrow \phi^*$  and forces the coupling  $\lambda_4$  multiplying  $I$  to be real. For  $\lambda_4 < 0$  one finds the global minimum

$$\langle H \rangle = \frac{v}{\sqrt{3}}(1, \omega, \omega^2)$$

and for  $\lambda_4 > 0$  one finds

$$\langle H \rangle = \frac{v}{\sqrt{3}}(\omega^2, 1, 1).$$

Both VEV configurations correspond to generalised CP transformations  $H \rightarrow UH^*$ . For  $\lambda_4 < 0$  it is for example given by  $U = \rho(B^2)$ , which is clearly part of  $\Delta(27)$  and therefore up to an inner automorphism corresponds to  $h_1$ . The phases of the VEVs thus do not imply spontaneous CP violation. For  $\lambda_4 > 0$  the VEV configuration leaves the CP transformation corresponding to the outer automorphism  $h_2$  given in Eq. (6.28) invariant. However, there is something that is much harder to understand about this VEV configuration: the generalised CP symmetry corresponding to this configuration is not a symmetry of the Lagrangian. It would be a symmetry if the phase of  $\lambda_4$  would be the same as  $\omega$ , as  $CP_{h_2}[I] = \omega I^*$ . So here we are confronted with the puzzling situation in which a VEV configuration is more symmetric than the original Lagrangian. This is also denoted as calculable phases.

This conundrum can be solved if there is a generalised CP trafo that is left invariant by the VEV and is compatible with  $\lambda_4$  being real. Since we have a complete classification of all generalised CP transformations we can answer this question and indeed we find the CP transformation

$$\begin{pmatrix} H \\ H^* \end{pmatrix} = U \begin{pmatrix} H^* \\ H \end{pmatrix} \quad \text{with} \quad U = \begin{pmatrix} 0 & \tilde{U} \\ \tilde{U}^* & 0 \end{pmatrix}, \quad \tilde{U} = \begin{pmatrix} 0 & 0 & \omega^2 \\ 0 & 1 & 0 \\ \omega & 0 & 0 \end{pmatrix}, \quad (6.29)$$

which represents the outer automorphism  $u : (A, B) \rightarrow (AB^2AB, AB^2A^2)$  via Eq. (6.6), where  $u = u_2^3 \circ \text{conj}(A)$  and that gives

$$CP_u[\langle H \rangle] = \langle H \rangle \quad \text{for} \quad \langle H \rangle = \frac{v}{\sqrt{3}}(\omega^2, 1, 1), \quad CP_u[I] = I.$$

Note that this CP transformation acts as  $H \rightarrow \tilde{U}H$ , which is not something you would naively expect, but it is an outer automorphism and therefore it is justified to call it a CP transformation. Furthermore, this becomes apparent when one looks at how the outer automorphism  $u$  acts on representations. It interchanges the one-dimensional representations

$$\mathbf{1}_2 \leftrightarrow \mathbf{1}_3, \quad \mathbf{1}_5 \leftrightarrow \mathbf{1}_9, \quad \mathbf{1}_6 \rightarrow \mathbf{1}_8,$$

and thus truly is a CP transformation.

**6.3.5.  $Q_8 \times A_4 \cong \text{SG}(96, 204)$** 

Let us also consider our favourite group,  $Q_8 \times A_4$ , the smallest group that may realize the VEV alignment, and which has been extensively introduced in Section 3.3. Its centre is given by  $Z(Q_8 \times A_4) = \{E, X^2\} \cong Z_2$  and its outer automorphism group is generated by

$$\begin{aligned} h_4 : (S, T, X) &\rightarrow (S, T^2, SX), & h_5 : (S, T, X) &\rightarrow (S, T^2, X^3), \\ h_6 : (S, T, X) &\rightarrow (ST^2STX^3, T, T^2XT). \end{aligned} \quad (6.30)$$

These generators act on the character table and representations in the way indicated in Tab. 6.3. Together with the inner automorphisms, the automorphism group is of order 576 and its structure may be summarised as:

$$\begin{aligned} Z(Q_8 \times A_4) &\cong Z_2 & \text{Aut}(Q_8 \times A_4) &\cong ((A_4 \times A_4) \times Z_2) \times Z_2 & (6.31) \\ \text{Inn}(Q_8 \times A_4) &\cong Z_2^4 \times Z_3 & \text{Out}(Q_8 \times A_4) &\cong D_{12}. \end{aligned}$$

Let us discuss how the generators of the automorphism act on the vector

$$\phi = \begin{pmatrix} \varphi_C \\ \varphi_C^* \end{pmatrix}$$

with  $\varphi_C \sim \underline{\mathbf{4}}_2$  upon which the group generators act as

$$\rho(S) = \begin{pmatrix} S_4 & 0 \\ 0 & S_4 \end{pmatrix}, \quad \rho(T) = \begin{pmatrix} \omega^2 T_4 & 0 \\ 0 & \omega T_4 \end{pmatrix}, \quad \text{and} \quad \rho(X) = \begin{pmatrix} X_4 & 0 \\ 0 & X_4 \end{pmatrix},$$

where  $S_4, T_4$  and  $X_4$  have been given in Section 3.3.1 and  $\rho(S, X)^* = \rho(S, X)$  but  $\rho(T)^* \notin \text{Im}\rho$ . One solution to Eq. (6.5) is the analogue of the  $A_4$  case,  $U = \text{diag}(U_4, U_4)$  with  $U_4 = \text{diag}(\tilde{U}_3 \equiv T_3 U_3 T_3^{-1}, 1)$ . This generator acts on the generators of the group as

$$U\rho(S)^*U^{-1} = \rho(S), \quad U\rho(T)^*U^{-1} = \rho(T^2), \quad U\rho(X)^*U^{-1} = \rho(SX) \quad (6.32)$$

and therefore represents the automorphism  $h_4$ . Before discussing other solutions of Eq. (6.5), let us demonstrate how this outer automorphism can be represented for the other representations. For the representation  $\underline{\mathbf{4}}_1$  we find  $U = U_4$ . For the one-dimensional representations we have  $U = 1$ .

Clearly the relation (6.32) cannot be fulfilled by  $\underline{\mathbf{3}}_1$  as  $\rho(X) = \mathbb{1}_3$ , so that

$$1 = U\rho(X)U^{-1} = \rho(SX) = S_3$$

for any  $U$ . The representation  $\underline{\mathbf{3}}_1$  is rather part of a larger representation that also includes  $\underline{\mathbf{3}}_5^{11}$ :

$$S = \text{diag}(S_3, T_3^2 S_3 T_3), \quad T = \text{diag}(T_3, T_3^2), \quad X = \text{diag}(\mathbb{1}_3, T_3^2 S_3 T_3), \quad U = \begin{pmatrix} 0 & T_3 \\ T_3^2 & 0 \end{pmatrix}.$$

The real representations  $\underline{\mathbf{3}}_{2,3,4}$  can be extended to representations of the CP-extended group by  $U = \tilde{U}_3$ . We have therefore seen that a CP transformation as defined in (6.5) can only be realised if both  $\underline{\mathbf{3}}_1$  and  $\underline{\mathbf{3}}_5$  are present in the Lagrangian, i.e. the condition of CP conservation

	$E$	$T$	$SYX$	$SY$	$X^2$	$T^2$	$XT$	$S$	$SX$	$X$	$SXT^2$
$\underline{1}_1$	1	1	1	1	1	1	1	1	1	1	1
$\underline{1}_2$	1	$\omega$	1	1	1	$\omega^2$	$\omega$	1	1	1	$\omega^2$
$\underline{1}_3$	1	$\omega^2$	1	1	1	$\omega$	$\omega^2$	1	1	1	$\omega$
$\underline{3}_1$	3	.	-1	-1	3	.	.	-1	-1	3	.
$\underline{3}_2$	3	.	3	-1	3	.	.	-1	-1	-1	.
$\underline{3}_3$	3	.	-1	3	3	.	.	-1	-1	-1	.
$\underline{3}_4$	3	.	-1	-1	3	.	.	3	-1	-1	.
$\underline{3}_5$	3	.	-1	-1	3	.	.	-1	3	-1	.
$\underline{4}_1$	4	1	.	.	-4	1	-1	.	.	.	-1
$\underline{4}_2$	4	$\omega^2$	.	.	-4	$\omega$	$-\omega^2$	.	.	.	$-\omega$
$\underline{4}_3$	4	$\omega$	.	.	-4	$\omega^2$	$-\omega$	.	.	.	$-\omega^2$

**Table 6.3:** Character table of  $Q_8 \times A_4$ . The first line are representatives of the different conjugacy classes. Zeros in the character table are denoted by a dot . and  $\omega$  is the third root of unity  $\omega = e^{2\pi i/3}$  and  $Y = T^2XT$ . The arrows illustrate the generators of the outer automorphism group  $h_4$ (blue),  $h_5$ (red),  $h_6$ (green).

requires non-trivial relations among real representations of the group, something one would not immediately suspect. To summarise: a consistent definition of CP acts as

$$\underline{4}_i \rightarrow U_4 \underline{4}_i^* \quad \underline{3}_i \rightarrow \tilde{U}_3 \underline{3}_{f(i)}^* \quad \underline{1}_i \rightarrow \underline{1}_i^*$$

with  $f : \{1, 2, 3, 4, 5\} \rightarrow \{5, 2, 3, 4, 1\}$ .

The natural question is now whether it is possible to have outer automorphisms of the group that act as CP in the sense that they interchange the complex representations  $\underline{1}_2, \underline{3}$  and  $\underline{4}_2, \underline{3}$  but transform the real representations only within themselves. This question can be answered using the explicit form of the generators of Eq. (6.30).

An outer automorphism swaps conjugacy classes and representations in such a way as to leave the character table 6.3 invariant. For illustration look at the automorphism  $h_4$  (6.32). It acts on the conjugacy classes as

$$G \cdot T \leftrightarrow G \cdot T^2, \quad G \cdot XT \leftrightarrow G \cdot SXT^2, \quad G \cdot X \leftrightarrow G \cdot SX,$$

where  $G \cdot T \equiv \{gTg^{-1} : g \in G\}$ , leaving all other conjugacy classes invariant. To obtain a symmetry of the character table one therefore needs to interchange the representations

$$\underline{1}_2 \leftrightarrow \underline{1}_3, \quad \underline{4}_2 \leftrightarrow \underline{4}_3, \quad \underline{3}_1 \leftrightarrow \underline{3}_5.$$

If we want to have a symmetry of the character table without interchanging any real representations that still acts as CP, we therefore have to have an automorphism that realises

$$G \cdot T \leftrightarrow G \cdot T^2, \quad G \cdot XT \leftrightarrow G \cdot SXT^2$$

while keeping all other conjugacy classes invariant. No such automorphism exists, as can be inferred from Eq. (6.30).<sup>12</sup>

<sup>11</sup>For  $\underline{3}_5$  we have  $\rho(S) = \rho(X)$  and therefore (6.32) would imply  $\rho(S) = \rho(X) = \mathbb{1}_3$ .

<sup>12</sup>It is convenient to use the computer algebra system GAP [129].

However, if we relax the condition to the point where we only demand that the representation  $\mathbf{3}_1$  transforms into itself we have to search for outer automorphisms that realise

$$G \cdot T \leftrightarrow G \cdot T^2, \quad G \cdot XT \leftrightarrow G \cdot SXT^2 \quad G \cdot X \leftrightarrow G \cdot X.$$

Indeed there is an automorphism that realises this:  $h_5 : (S, T, X) \rightarrow (S, T^2, X^3)$ . An explicit matrix representation for representation  $\mathbf{4}_1$  is given by

$$U_4(h_5) = \frac{1}{2} \begin{pmatrix} 1 & -1 & 1 & -1 \\ -1 & 1 & 1 & -1 \\ 1 & 1 & -1 & -1 \\ -1 & -1 & -1 & -1 \end{pmatrix} \quad (6.33)$$

and for the representation  $\mathbf{3}_1$  we find  $U = U_3$ .

Having found a consistent CP transformation for a theory that contains only the representations  $\mathbf{3}_1$ ,  $\mathbf{4}_1$  and  $\mathbf{1}_i$  we can now ask ourselves the question that led us to this study of generalized CP transformations, namely can all dangerous coupling terms such as the purely imaginary one given in Eq. (6.1) be forbidden by a CP transformation. Under CP, the doublets  $\phi_{1,2}$  and  $\chi$  transform as

$$\phi_i \rightarrow U_4 \phi^*, \quad \chi \rightarrow U_3 \chi^* \quad (6.34)$$

and thus the coupling (6.1) is invariant under the unique consistent CP transformation, even though it is purely imaginary. For this reason, and for minimality, actually, in the next chapter we have taken the fields  $\phi_i \sim \mathbf{4}_1$  to transform as EW singlets, not doublets.

For completeness we also give a representation of  $h_6$

$$U(h_6) = \frac{1}{2} \begin{pmatrix} 1 & -1 & -1 & -1 \\ -1 & 1 & -1 & -1 \\ -1 & -1 & 1 & -1 \\ 1 & 1 & 1 & -1 \end{pmatrix}, \quad (6.35)$$

from which all the other representation matrices can be derived using the Clebsch-Gordon coefficients.

## 6.4. Summary & Conclusions

We have given consistency conditions for the definition of CP in theories with discrete flavour symmetries that have sometimes been overlooked in the literature. We have shown that every generalised CP transformation furnishes a representation of an outer automorphism and that generalised CP invariance implies vanishing CP phases<sup>13</sup>. We have applied these ideas to popular flavour groups with three-dimensional representations. In particular, we have shown that there is one unique non-trivial CP transformation (up to group transformations) for the group  $T'$  and the geometric CP-violation that has been claimed in this group can only be viewed as an arbitrary basis-dependent explicit breaking of CP. In the case of  $\Delta(27)$  we have shown that the so-called geometric phases may be viewed as the result of an accidental generalised CP transformation of the scalar potential.

<sup>13</sup>A complete study of all groups with three-dimensional representations and group order smaller than 31 will be given in [19].

## Chapter 6. *CP and Discrete Flavour Symmetries*

The (outer) automorphism structure of small groups is very rich and it stands to wonder if not more physics might be hidden in there. This leads us to the following speculation:  $S_4$  is the smallest group that can really give TBM (with all the caveats involved) and it is isomorphic to the automorphism group of  $A_4$ . Maybe the accidental symmetry that makes  $A_4$  look like  $S_4$  on the level of mass matrices is connected to this fact. That would then open an interesting avenue for model building: interesting mixing patterns can be obtained from  $\Delta(6n^2)$  but since it is quite unappealing to start from such large groups, it might be nicer to start from smaller groups and obtain the accidental symmetry from the larger automorphism group in the same way as in  $A_4$  models. As an example how complicated structures can arise from simpler ones, look at the automorphism group of  $\Delta(27)$ , which is of order 432. The smallest group whose automorphism group contains  $\Delta(96)$  is given by  $(Z_4 \times Z_4) \rtimes Z_2 \cong \text{SG}(32, 34)$ . A systematic study of this playground is left for future work.

# Chapter 7.

## Outlook: Naturalness & Big Desert Scenarios

In this chapter, we take a step back from the (sometimes technical) issues of flavour model building and discuss physics beyond the Standard Model more broadly. Firstly, we discuss the naturalness dogma in light of the dearth of any signs of new physics from collider experiments, then present speculative signs that the Higgs mass might be understood as an imprint of Planck scale physics on the electroweak scale, with a big desert between the two scales. Thirdly, we present another big desert scenario where the hierarchy between the two scales is taken to be stabilized by classical conformal invariance.

### 7.1. Naturalness and a Big Desert

Much of research in beyond the standard model physics over the last decades has been motivated by the so-called ‘naturalness’ or ‘hierarchy problem’ of the SM Higgs sector. The origin of the problem lies in the fact that the SM Higgs mass term  $\mu^2 H^\dagger H$ , when viewed from an effective field theory perspective [144], is the only relevant coupling in the Standard Model and orders of magnitude smaller than its natural value.

In a nutshell, effective field theory is a way to describe physical processes with a characteristic energy scale  $E$  much smaller than some large energy scale  $\Lambda$ , where the theory is replaced by a more complete description. The modern view of the world is that nature is described by a series of effective (field) theories, each a UV completion of the next, much like a russian matryoshka doll. Starting from theories that describe physics over cosmological distances but have to be replaced at the length scales of superclusters, the succession of effective field theories features theories with degrees of freedom as varied as sound waves, molecules and atoms. The experimental discovery of the Higgs particle at 126 GeV, which we accept as fact throughout this chapter, without the discovery of any other new particles makes the Standard Model the latest member in the succession of effective field theories that actually describe reality with a range of validity from  $E \approx m_h$  up to at least several hundred GeV. In fact there are reasons to believe that the Standard Model might be valid up to a much higher energy scale. Before we discuss these reasons in detail, let us justify the reasoning based on the higher-dimensional operator analysis that we will use. In effective field theory, an effective operator  $\mathcal{O}$  that enters the Lagrangian as  $\lambda\mathcal{O}/\Lambda^d$  of scaling dimension  $4 + d$  grows with energy as  $(E/\Lambda)^d$  and thus –barring fine-tuning– will become strongly coupled for  $E \gtrsim \Lambda$  so that the suppression scale of the higher dimensional operator gives an indication of the scale of new physics. Note that this reasoning has been successful in the case of weak interactions, where the suppression scale of Fermi’s four-fermion operator has indicated the mass of the electroweak gauge bosons. In the Standard Model no such indication of new physics exists:

- the SM (on the classical level) conserves baryon number as an accidental symmetry. This

is a most welcome feature as baryon number violating operators such as  $QQQL/M^2$  are severely constrained by searches for proton decay, which give a bound of  $M \gtrsim 10^{22}$  GeV.

- another indication of new physics might come from lepton number violating operators. The lowest dimensional operator is given by the Weinberg operator  $(LH)^2/M$  and the observation of neutrino masses might be translated into  $M \approx 10^{14}$  GeV. Again this points to a high energy scale.
- another class of higher dimensional operators is given by operators that break flavour symmetries and e.g. lead to flavour-changing neutral currents in the quark sector. The non-observation of such processes allows one to constrain e.g. operators of the type  $(s^\dagger \sigma_\mu d)^2/M^2$ , which have to be suppressed by  $\Lambda \sim 10^3$  TeV [222] (or more in the case of CP violation).
- another bound comes from the precision study of the properties of electroweak gauge bosons. The operators  $H^\dagger \sigma^i H A_{\mu\nu}^i B^{\mu\nu}$  and  $|H^\dagger D_\mu H|^2$  [223] give a contribution to the electroweak precision observables  $S$  and  $T$ , respectively, and therefore have to be suppressed by a mass scale larger than at least 5 TeV [224].
- and – of course – no new physics has shown up at the LHC, sth. that would have rendered the entire discussion moot.

None of the arguments given above is air-tight. For example the first three points can be addressed by the introduction of a flavour symmetry, as was e.g. done in the electroweak model of Section 5. In the electroweak precision observables there can always be a cancellation of two large new physics contributions. However, it is notable and more than a bit depressing that the SM with a high cut-off scale seems to be a perfect match to the data with a natural suppression of baryon number violation, lepton number violation, flavour changing neutral currents and electroweak precision observables. On the other hand, any new physics model at the TeV scale has to be quite non-generic for it not to have shown up somewhere.

As the SM works so nicely, why not declare victory and go home? The problem is that the Standard Model with a super-high cut-off doesn't seem to make much sense when viewed as an effective field theory. Effective field theory may be viewed as an expansion of physical quantities such as cross-sections in terms of the ratio of the characteristic energy scale of the problem  $E$  over the scale of new physics  $\Lambda$ . This implies that the coupling  $\lambda$  that multiplies the operator  $\frac{1}{\Lambda^d} \mathcal{O}$  should not be smaller than the expansion parameter, as otherwise the expansion would not make much sense. The problem with the Standard Model is now that there is one coupling for which this is manifestly not the case. The Higgs mass term  $\mu^2 H^\dagger H$  phenomenologically has to be of the order of 100 GeV and thus if we take the cutoff scale of the Standard Model to be the Planck scale,  $\Lambda \sim M_{Pl} \sim 10^{19}$  GeV, the dimensionless coupling has to be of the order  $10^{-38}$ , which is also called the naturalness or hierarchy problem [225–229]. There have been two main approaches to this question:

- Supersymmetry makes the smallness of the Higgs mass technically natural by tying it to the Higgsino mass term, which—being a fermion—is protected by a chiral symmetry.
- Composite Higgs models in all its variants (Technicolor, Warped Extra Dimension,...) banish all fundamental scalars from the theory and thus get rid of the problem.



## 7.2. Planck Scale Boundary Conditions and the Higgs Mass

- models with large extra dimensions lower the fundamental Planck scale to the TeV scale and thus get rid of the hierarchy.

The discovery of the Higgs at 126 GeV without indications for new physics can be described as borderline. The MSSM would have preferred lower Higgs masses and composite models would have favoured a higher Higgs mass. Another approach is to assume that there are  $10^{500}$  string vacua and our values for parameters are anthropically selected.

In the following we want to present two scenarios that are not natural from the point of view of effective field theories. The essential idea is the following: if we view the Standard Model (or minimal extensions) not as just another effective field theory that is to be replaced by another more fundamental theory at energy scale  $\Lambda$ , but in itself as a fundamental theory of nature, then the naturalness problem disappears. Now one might wonder how such a view may be held in light of the fact that gravity certainly exists and is connected to the very high energy scale  $M_{Pl} \approx 1.2 \cdot 10^{19}$  GeV. The justification for this view boils down to the fact that gravity is special as it may not be quantised in the same way as the other interactions and it therefore stands to question if the traditional view that the large hierarchy between the Planck and electroweak scales really poses a hierarchy problem. Indeed this point has been argued in a number of publications [230–236], but there always remains a degree of uncertainty since here the ‘solution’ of the hierarchy problem always depends on properties of the quantum gravitational embedding at the Planck scale, which we will remain agnostic about in the following. In our discussion, we will be guided by the works of Meissner and Nicolai [231–233], who have argued for an approximate conformal symmetry of the particle physics action as a consequence of such an embedding.

In the remainder of the chapter we will present a possible scenario of how the Higgs mass may be interpreted by Planck scale boundary conditions and then discuss a scenario using classical conformal invariance.

## 7.2. Planck Scale Boundary Conditions and the Higgs Mass

Let us consider a minimal scenario, where classical conformal symmetry is only softly broken by an explicit mass term  $\mu^2 H^\dagger H$ , the only coupling with positive mass dimension in the Standard Model, and there is no new physics between the electroweak and Planck scales. This information alone is sufficient to pin down the SM Higgs boson mass  $m_h^2 = 2\lambda v^2$  in a range between the stability bound of approximately 127 GeV and the triviality bound of circa 170 GeV. Let us briefly recall where this bound comes from: for small Higgs masses the dominant coupling to the Higgs particle is given by the top quark, which drives the Higgs self-coupling to negative values, which would lead to an unstable potential. Therefore the condition that the Higgs self coupling  $\lambda$  should be positive all the way to the Planck scale translates into a lower bound of  $\lambda$  at the electroweak scale and therefore  $m_h$  [237, 238]. For large Higgs masses on the other hand, the Higgs self-coupling dominates and drives itself to ever larger values of  $\lambda$ . The requirement that  $\lambda$  should stay perturbative up to the Planck scale thus translates into an upper bound of the Higgs mass [239]. It should be noted that this mass range is somewhat complementary to the mass range preferred by theories that solve the hierarchy problem at the weak scale: in the MSSM at tree level the Higgs mass is bounded to be smaller than the  $Z$ -mass and including loop corrections it is more comfortable with Higgs masses smaller than 125 GeV, while composite Higgs scenarios would naturally favour

relatively heavy Higgs masses of more than a few hundred GeV. We will comment later on the precise value of the stability bound and its experimental and theoretical errors.

Having seen that the requirement of a direct Planck scale embedding alone brings us into the right ballpark of Higgs masses, we now want to go a step further and ask if more can be learned about the Planck scale embedding of the Standard Model by imposing boundary conditions on the Standard Model couplings at the Planck scale. We discuss the following conditions<sup>1</sup>:

- the vacuum stability condition  $\lambda(M_{pl}) = 0$  [241–247].
- the condition that the Higgs self-coupling should stop to evolve, i.e. a vanishing beta function of  $\lambda$ :  $\beta_\lambda(M_{pl}) = 0$  [241, 242].
- the Veltman condition  $\text{Str}\mathcal{M}^2 = 0$  [248–250], which states that the quadratic divergent part of the one-loop radiative correction to the Higgs bare mass parameter  $\mu^2$  should vanish:

$$\delta\mu^2 = \frac{\Lambda^2}{32\pi^2 v^2} \text{Str}\mathcal{M}^2 = \frac{1}{32\pi^2} \left( \frac{9}{4}g_2^2 + \frac{3}{4}g_1^2 + 6\lambda - 6\lambda_t^2 \right) \Lambda^2. \quad (7.1)$$

Note that even if this condition would be fulfilled one would still expect to have UV contributions to the Higgs mass parameter, which are not accounted for in the Veltman condition.

- vanishing anomalous dimension of the Higgs mass parameter  $\gamma_m(M_{pl}) = 0$ ,  $m(M_{pl}) \neq 0$ .

The various boundary conditions are imposed at the Planck scale on the SM couplings defined in the  $\overline{\text{MS}}$  scheme and are then evolved down to the electroweak scale using two-loop renormalization group equations (RGEs). At the electroweak scale (or the top mass scale, to be precise), the  $\overline{\text{MS}}$  couplings are expressed in physical parameters using one-loop matching conditions of the form

$$\lambda_t(M_t) = \frac{\sqrt{2}M_t}{v} (1 + \delta_t(M_t)), \quad \lambda(M_t) = \frac{M_H^2}{2v^2} (1 + \delta_H(M_t)), \quad (7.2)$$

where  $\delta_i$  parametrizes the loop contribution. To obtain a more precise result, we have followed the recent literature and included the higher loop pure QCD corrections to  $\delta_t$ . To determine the stability bound, we have further used the one-loop improved effective potential. We do not go into much detail here but refer the reader to our publication [15]. The boundary conditions we are considering here define one-parameter curves in the space of SM parameters at the Planck scale, which through the RGE are mapped onto one-parameter curves in the space of SM parameters at the weak scale, which through the matching conditions are expressed as curves in a space of measurable quantities such as masses etc. As we cannot plot such a higher-dimensional space we plot the curves projected on a subspace spanned by  $m_t$  and  $m_h$ , as these are the largest Higgs couplings at the weak scale. This plot is displayed in Fig. 7.1, where the various boundary conditions are represented as bands in the  $m_t - m_h$ - plane. The width of the bands are an estimate of the theoretical uncertainty, which we estimated as the difference between using one and two-loop beta functions for all the relevant SM couplings in

<sup>1</sup>Boundary conditions of this type have also been discussed in the context of anthropic considerations in the multiverse [240].

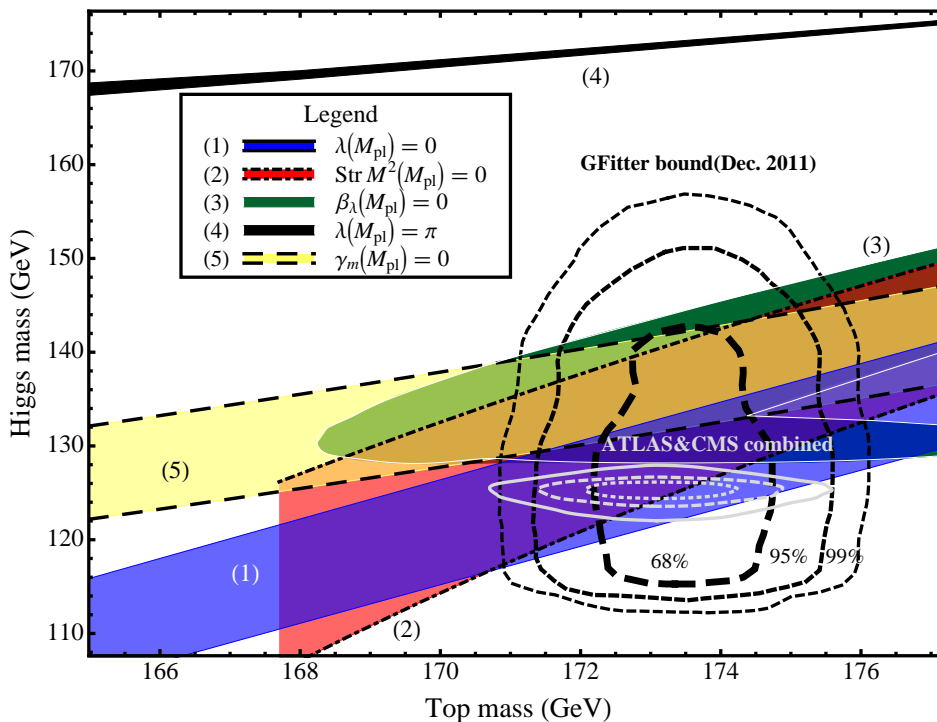


**Figure 7.1:** Higgs and top (pole) mass determinations for different boundary conditions at the Planck scale. The coloured bands correspond to the conditions discussed in the text and which are also labelled in the insert, with the width of the bands giving an indication of the combined theoretical and experimental error. Note that the Veltman condition is truncated at the point where its Higgs mass prediction violates the vacuum stability bound (both at two-loops). The black dashed lines show the electroweak precision fit from GFitter [251], which summarizes the experimental information before the Higgs seminar in Dec. 2011. The present best fit values are indicated in grey.

the determination of the Higgs pole mass. To be more precise, we define a “RGE error band” as the difference in determining the Higgs mass for a boundary condition of  $\lambda(M_{pl})$  with one and two-loop beta functions while the matching conditions remain the same for both cases. We will come back to this critical issue later, but before we do that let us take a look at the results of the analysis.

We see that all boundary conditions result in Higgs masses closer to the stability bound than to the triviality bound, which is opposite to the result of a scatter plot of order one values for  $\lambda$  at the Planck scale [15] and might be taken to be an indication of some structure. However, this is probably due to the fact that the boundary conditions we took are mostly one loop-expressions that connect the Higgs coupling to other smaller couplings and therefore give small starting values for  $\lambda$ . While at the time of publication, there were a couple of interesting boundary conditions in the experimentally allowed range<sup>2</sup>, today this is no longer the case. The observation of a Higgs-like particle by ATLAS [1] at  $126.0 \pm 0.4(\text{stat.}) \pm 0.4(\text{sys.})$  GeV and of CMS [2] at  $125.3 \pm 0.4(\text{stat.}) \pm 0.5(\text{sys.})$  GeV clearly selects the boundary condition  $\lambda(M_{Pl}) = 0$  as the most interesting one. Using our setup we obtain for the stability bound a

<sup>2</sup>We still show the by now largely historic GFitter bound.

value of<sup>3</sup>

$$m_h > \left[ 127.4 + 2.6 \left( \frac{m_t/\text{GeV} - 173.1}{1.3} \right) - 2.2 \left( \frac{\alpha_s(M_Z) - 0.1193}{0.0028} \right) \right] \text{ GeV} \pm 5 \text{ GeV}, \quad (7.3)$$

where we have shown the dependence on the dominant experimental uncertainties coming from  $\alpha_s(M_Z)$  and  $m_t$  explicitly. As mentioned above, we have estimated the theoretical uncertainty by comparing LO and NLO calculations and our value of 5 GeV might therefore be too an conservative estimate, especially in light of the fact that the earlier publication [252] claims a theory error of 1 GeV while the later publication [255] by partly the same authors quotes 3 GeV.

Clearly the SM is very close to the stability border region, which has garnered a lot of attention and sparked a lot of activity, with the main focus on trying to reduce the theoretical error of the calculation. In the following few paragraphs we will try to give a short summary of the status of the question.

All the ingredients to perform a next-to-next-to leading order computation of the stability bound in the Standard Model have recently been provided: the complete three-loop beta function for the SM gauge couplings has been given in [256], the dominant three-loop terms in the beta-function of  $\lambda$  and  $\lambda_t$  have been provided in [257] and the two-loop QCD and Yukawa contributions to  $\delta_t$  have been given in [254, 258]. While the additional contributions to  $\delta_t$  push the stability window downward, with the dominant contribution given by  $\mathcal{O}(\alpha_s^3)$  which we had already included, the additional contribution to  $\delta_\lambda$  [258] push the stability region upward. The analysis performed in [258], which seems to contain most corrections except for the  $\mathcal{O}(\alpha\alpha_s)$  correction calculated in [254], finds  $m_h > 129.4 \pm 1.8$  GeV and thus disfavors vacuum stability of the SM up to the Planck scale of up to at the  $2\sigma$  level iff  $m_h < 126$  GeV. The analysis performed in [254], which does not include the contribution of order  $\mathcal{O}(y_t^6)$ ,  $\mathcal{O}(y_t^4\alpha_s)$  does not exclude stability up to the Planck scale for the experimental mass range of the Higgs.

It should be noted that the discussion is highly sensitive to the exact value of the top mass parameter. This is important as there is no general consensus on what type of top mass is actually measured via kinematic reconstruction [259]. At the Tevatron, the main method used for the top mass extraction actually “measures” the Pythia mass, which is a Monte-Carlo simulated template mass. Strictly speaking the top pole mass is not a well defined quantity, as the top quark does not exist as free parton. The top mass that the Tevatron has measured is based on the final state of the decay products. On the other hand the running  $\overline{\text{MS}}$  top mass can be extracted directly from the total cross section in the top pair production. In this sense, one can obtain a complementary information of the top mass from the production phase. By converting the  $\overline{\text{MS}}$  mass to the pole mass via matching conditions, the top pole mass value  $168.9_{-3.4}^{+3.5}$  GeV extracted with this method by Langenfeld et al. [260] is found to be lower than the world best average value. This point has also been elaborated on in two subsequent publications [258, 261].

<sup>3</sup>The slight discrepancy to the value of 128.6 GeV obtained in [252] is due to the fact that we have here included the three-loop pure QCD contribution to  $\delta_t$  [253]. This relatively large effect was also reproduced in [254] and casts doubt on their estimate of a theoretical error of 1 GeV.

### 7.3. Radiative Symmetry Breaking in the Minimal Left-Right Symmetric Model

In the introduction, we had mentioned that classical conformal invariance was advocated in [231–233] as a possible consequence of a Planck scale embedding that addresses the hierarchy problem. In the previous section, we had considered the SM, which might be considered to have a softly broken conformal invariance. While it is not possible to have exact conformal invariance due to the logarithmic scale dependence of dimensionless couplings via beta functions, it is, however, desirable to conserve conformal invariance on the classical level. This is not possible within the Standard Model as the large top mass  $m_t > m_Z$  renders the effective potential unstable [239, 246] and the SM thus has to be extended. As new scalar and vector degrees of freedom give positive contributions to the effective potential it is not surprising that e.g for singlet [232, 245, 262–270] and other [271, 272] extensions of the Higgs sector this problem can be circumvented and a successful phenomenology can be achieved.

Here instead of adding singlets to the SM, we discuss conformal invariance in the context of the minimal left-right symmetric model based on the gauge group  $SU(2)_L \times SU(2)_R \times U(1)_{B-L} \times SU(3)_C$  [273, 274] that has been long known as an attractive extension of the SM as it explains parity violation by spontaneous symmetry breaking, has a natural place for neutrino masses and gives an explanation of hypercharge assignments  $Y = T_R^3 + \frac{1}{2}(B-L)$  in terms of baryon minus lepton number  $B-L$ . For simplicity, we restrict ourselves to the simplest version of the minimal LR symmetric model which contains, in addition to a pair of doublets  $\chi_L \sim (2, 1, -1)$ ,  $\chi_R \sim (1, 2, -1)$  that are used to break LR symmetry, the bidoublet  $\Phi \sim (2, 2, 0)$ , which is needed to break electroweak symmetry and provide for fermion masses, as it is able to connect left- and right-handed fermions, which transform as  $(2, 1, B-L)$  and  $(1, 2, B-L)$ , respectively.

As in the last section, we here only present the gist of the discussion and relegate technical details to the publication [20].

#### 7.3.1. Gildener Weinberg Method in the Minimal LR Symmetric Potential

As parity  $P$  is a symmetry of the left-right symmetric model, we use the isomorphism  $P \times SU(2) \times SU(2) \cong \text{Spin}(4)$  to express all fields in terms of representations of  $\text{Spin}(4)$ , which is described by the Clifford algebra of  $\text{SO}(4)$ . In this simplified notation, the bidoublet degrees of freedom are arranged in a complex vector representation of  $\text{SO}(4)$   $\Phi = \begin{pmatrix} 0 & \Phi \\ -\tilde{\Phi}^\dagger & 0 \end{pmatrix}$  and the doublets arrange in a Dirac spinor  $\Psi = (\chi_L, -i\chi_R)^T$ , as do the fermions, which we do not show here as we are primarily concerned with the symmetry breaking aspects.

In the  $\text{Spin}(4)$  notation, the most general scale- and gauge-invariant scalar potential<sup>4</sup> is given by:

$$\begin{aligned}
 V(\Phi, \Psi) = & \frac{\kappa_1}{2} (\bar{\Psi}\Psi)^2 + \frac{\kappa_2}{2} (\bar{\Psi}\Gamma\Psi)^2 + \lambda_1 \left( \text{tr}\Phi^\dagger\Phi \right)^2 + \lambda_2 \left( \text{tr}\Phi\Phi + \text{tr}\Phi^\dagger\Phi^\dagger \right)^2 \\
 & + \lambda_3 \left( \text{tr}\Phi\Phi - \text{tr}\Phi^\dagger\Phi^\dagger \right)^2 + \beta_1 \bar{\Psi}\Psi \text{tr}\Phi^\dagger\Phi + f_1 \bar{\Psi}\Gamma[\Phi^\dagger, \Phi]\Psi,
 \end{aligned}
 \tag{7.4}$$

<sup>4</sup> Here we only consider a simplified potential invariant under the  $Z_4$  symmetry  $\Phi \rightarrow i\Phi$ ,  $\Psi \rightarrow -i\Psi$ . For a discussion of the full potential, see [20].

where  $\Gamma = \Gamma^1\Gamma^2\Gamma^3\Gamma^4$  denotes the chirality operator of Spin(4) and the  $\Gamma^A$  form a representation of the Clifford algebra of Spin(4). As all couplings are real, the Higgs potential is CP conserving. The separate Spin(4) transformations of  $\Psi$  and  $\Phi$  are broken to the diagonal subgroup, unless the coupling  $f_1$  vanishes. Note that the operator multiplying  $\beta_1$  can be rewritten as  $\bar{\Psi}\Psi\text{tr}\Phi^\dagger\Phi = 2\bar{\Psi}\{\Phi^\dagger, \Phi\}\Psi$ . Due to the conformal symmetry, the dimension three term  $\bar{\Psi}\Phi\Psi$  is not allowed and thus there is an accidental symmetry  $\mathcal{A}_\Psi : \Psi \rightarrow e^{i\beta\Gamma}\Psi$ .

As we assume the theory to be weakly coupled, quantum corrections can be taken into account by a loop expansion of the effective potential. We will consider the effective potential up to one loop. In order to discuss symmetry breaking, we have to minimize the potential. However, even the minimization of the one-loop effective potential cannot be done analytically in the case of multiple scalar fields. Instead of resorting to a numerical study, we will use the analytical approximate method of Gildener and Weinberg (GW) [275] which makes essential use of the renormalization group.

GW have noted that for a generic scale invariant potential of the form

$$V_0 = \frac{1}{24} f_{ijkl} \Phi_i \Phi_j \Phi_k \Phi_l \quad (7.5)$$

the renormalization group can be used to enforce a single condition on the scalar couplings of the theory:

$$\min_{N_i N_i=1} (f_{ijkl}(\mu_{GW}) N_i N_j N_k N_l) \Big|_{N_i=n_i} = 0. \quad (7.6)$$

This condition entails that at the scale  $\mu_{GW}$ , the scalar potential has a tree level *flat direction*  $\Phi_i = n_i \phi$ . Barring the possibility of accidental additional flat directions, radiative corrections dominate in this direction in field space while they can be neglected in all other directions [275]. In the  $\overline{\text{MS}}$  scheme, the one-loop effective potential in the flat direction  $\Phi = n \phi$  can be easily calculated [276] to be

$$\delta V(n\phi) = A\phi^4 + B\phi^4 \ln \frac{\phi^2}{\mu_{GW}^2} \quad (7.7)$$

with

$$A = \frac{1}{64\pi^2 \langle \phi \rangle^4} \sum_i n_i M_i^4(n\langle \phi \rangle) \left( \ln \frac{M_i^2(n\langle \phi \rangle)}{\langle \phi \rangle^2} - c_i \right), \quad (7.8a)$$

$$B = \frac{1}{64\pi^2 \langle \phi \rangle^4} \sum_i n_i M_i^4(n\langle \phi \rangle), \quad (7.8b)$$

where  $n_i$  denotes the degrees of freedom,  $M_i$  is the mass and  $c_i = \frac{3}{2}$  for scalars and fermions and  $c_i = \frac{5}{6}$  for gauge bosons. The stationary condition  $\frac{\partial \delta V_{1\text{-loop}}}{\partial \phi} \Big|_{\phi=\langle \phi \rangle} = 0$  results in

$$\ln \frac{\langle \phi \rangle^2}{\mu_{GW}^2} = -\frac{1}{2} - \frac{A}{B} \quad (7.9)$$

and the mass of the excitation in the flat direction – so called *scalon*  $s$ , which is the *pseudo-Nambu Goldstone boson* (pNGB) of broken scale invariance – is given by

$$\begin{aligned} M_S^2 &= n_i n_j \frac{\partial^2 \delta V(n\phi)}{\partial \phi_i \partial \phi_j} \Big|_{n\langle \phi \rangle} = \frac{d^2}{d\phi^2} V(n\phi) \Big|_{\langle \phi \rangle} = 8B \langle \phi \rangle^2 \\ &= \frac{1}{8\pi^2 \langle \phi \rangle^2} (\text{tr} M_S^4 + 3\text{tr} M_V^4 - 4\text{tr} M_D^4). \end{aligned} \quad (7.10)$$

### 7.3. Radiative Symmetry Breaking in the Minimal Left-Right Symmetric Model

From Eq. (7.6), we see that the application of the GW method in the context of the minimal left-right symmetric potential requires the minimization of this very complicated potential on a unit sphere in field space. Parameterizing the scalar fields as

$$\Psi = \frac{1}{\sqrt{2}} \begin{pmatrix} N_1 e^{i\vartheta} \\ N_5 e^{i\vartheta_5} \\ N_2 e^{i\vartheta_2} \\ N_6 e^{i\vartheta_6} \end{pmatrix} \phi \quad \text{and} \quad \Phi = \frac{1}{2} \begin{pmatrix} N_3 e^{i\vartheta_3} & N_7 e^{i\vartheta_7} \\ N_8 e^{i\vartheta_8} & N_4 e^{i\alpha} \end{pmatrix} \phi, \quad (7.11)$$

the GW conditions read

$$\sum_i n_i^2 = 1, \quad V|_{N_i=n_i} = 0 \quad \text{and} \quad \frac{\partial}{\partial N_i} V|_{N_i=n_i} = 0, \quad (7.12)$$

where  $\{n_i\}$  parameterizes a flat direction of the left-right symmetric potential. We restrict ourselves to the case where the electromagnetic gauge group is left unbroken as required by phenomenology, which implies  $n_i = 0$  for  $i = 5, \dots, 8$ . We can further use gauge freedom to set the phases  $\vartheta_2$  and  $\vartheta_3$  to zero, and thus have the VEVs  $v_L = n_1 \frac{\langle \phi \rangle}{\sqrt{2}}$ ,  $v_R = n_2 \frac{\langle \phi \rangle}{\sqrt{2}}$ ,  $\kappa = n_3 \frac{\langle \phi \rangle}{\sqrt{2}}$ ,  $\kappa' = n_4 \frac{\langle \phi \rangle}{\sqrt{2}}$ . A complete classification of solutions of the Gildener-Weinberg conditions (7.12) is given in [20]. In the next section, we first discuss the limit of vanishing vacuum expectation values for the bidoublet and discuss the RG evolution, and then we briefly discuss the general case and sketch some phenomenological consequences.

#### 7.3.2. Spontaneous Breaking of Parity

**LR Symmetry Breaking in the Limit of Vanishing Bidoublet VEVs:** Since phenomenology requires the right-handed VEV  $v_R$  to be much larger than the electroweak scale, it is prudent to neglect the bidoublet in a first step and consider the GW mechanism in the Higgs potential containing only the doublets:

$$V_\Psi = \frac{\kappa_1}{2} (\bar{\Psi}\Psi)^2 + \frac{\kappa_2}{2} (\bar{\Psi}\Gamma\Psi)^2.$$

Then, in a second step, we will treat the bidoublet potential in the LR-broken phase. In unitary gauge, the potential at the minimum reads

$$V_\Psi|_{N_i=n_i} = \frac{1}{8} \phi^4 (\kappa_1 + \kappa_2 (-1 + 2n_1^2))^2, \quad (7.13)$$

where we have used the normalization condition of the VEVs to eliminate  $n_2$ . Stability of this potential requires it to be bounded from below. The term multiplying  $\phi^4$  therefore has to be positive semi-definite in the entire range of  $n_1$ . Inserting the minimum and boundary values  $n_1^2 = 1/2$  and  $n_1^2 = 1$ , respectively, we find the stability conditions  $\kappa_1 \geq 0$  and  $\kappa_+ = \kappa_1 + \kappa_2 \geq 0$ . The GW conditions, after the insertion of the normalization condition<sup>5</sup>

$$0 = \frac{\partial}{\partial N_1} V_\Psi|_{N_i=n_i} = \frac{1}{2} n_1 (\kappa_1 + \kappa_2 (-1 + 2n_1^2)) \quad (7.14a)$$

$$0 = \frac{\partial}{\partial N_2} V_\Psi|_{N_i=n_i} = \frac{1}{2} \sqrt{1 - n_1^2} (\kappa_1 - \kappa_2 (-1 + 2n_1^2)) \quad (7.14b)$$

$$0 = V_\Psi|_{N_i=n_i} = \frac{1}{8} (\kappa_1 + \kappa_2 (-1 + 2n_1^2))^2, \quad (7.14c)$$

<sup>5</sup>We drop the factor  $\phi^n$  in the GW conditions.

allows for three flat directions

$$(i) n_1 = 1, n_2 = 0, \kappa_+ = 0, \quad (ii) n_1 = 0, n_2 = 1, \kappa_+ = 0, \quad (iii) n_1 = n_2 = \frac{1}{\sqrt{2}}, \kappa_1 = 0.$$

The first two solutions correspond to parity breaking and are phenomenologically equivalent, since in the unbroken phase there is no difference between left- and right-handed fields and we can define the direction which acquires a VEV as the right-handed one. Therefore, we do not discuss the second flat direction in the following. If  $\kappa_2$  is negative, there are only maximally left-right symmetry breaking flat directions.

As any GW condition, the conditions (i) and (iii) define a hypersurface in the space of couplings given by  $\kappa_+ = 0$  and  $\kappa_1 = 0$ , respectively. The idea of the radiative symmetry breaking mechanism in the context of Planck scale embeddings is now that one starts with some dimensionless couplings at the Planck scale. These couplings then evolve on logarithmic scales using the renormalization group flow and at some lower energy scale a GW condition is satisfied. Thus the scalar potential obtains a flat-direction and the symmetry is broken with a VEV of this scale.

To see if this appealing physical idea can be realized here, it is essential to study the RG flow of the model to see whether a hypersurface described by a GW condition is reached and which one is reached first. As we are interested in a parity-breaking minimum (i), i.e. a solution for which the GW condition  $\kappa_+ = 0$  is fulfilled, we need  $\kappa_2 < 0$  at the symmetry breaking scale. In Fig. 7.2, the RG flow towards lower energies in the  $\kappa_+ - \kappa_1$  plane is depicted. The gauge boson contributions have the effect of deflecting the couplings away from the point of vanishing couplings and also of increasing the region of parameter space that leads to a maximally symmetry breaking solution.

The logarithmic renormalization group running of the couplings naturally creates a large hierarchy between the LR breaking scale and the Planck scale. In order to illustrate the hierarchy we show a numerical example. If  $\kappa_1(M_{Pl}) = 1$  and  $\kappa_2(M_{Pl}) = -0.68$ , the GW condition is fulfilled at  $\mu_{GW} \approx 5.8$  TeV with  $\kappa_1(\mu_{GW}) = -\kappa_2(\mu_{GW}) = 0.46$ . From the minimum condition Eq. (7.9) we can determine  $\langle \phi \rangle \approx 10.4$  TeV, and find  $v_R = \frac{\langle \phi \rangle}{\sqrt{2}} \approx 7.4$  TeV. Symmetry breaking then results in three heavy gauge bosons of  $SU(2)_R$ , four real components of  $\chi_L$  with mass  $m^2 = 2\kappa_1 v_R^2 \approx (7.1 \text{ TeV})^2$  and a scalon with mass

$$m_s^2 = \frac{3g_1^4 + 6g_1^2 g_2^2 + 9g_2^4 + 64\kappa_2^2}{64\pi^2} v_R^2 \approx (906 \text{ GeV})^2. \quad (7.15)$$

Note that there is no fermionic contribution, as the fermions do not couple directly to the doublets.

**Combined Left-Right and Electroweak Symmetry Breaking:** In the preceding subsection, we only discussed the breaking of left-right symmetry without taking into account the electroweak symmetry breaking that occurs once the bidoublet acquires a VEV. In reference [20], we solved the Gildener-Weinberg conditions (7.6) for the general potential (7.4) and the complete list of possible vacua can be found there. Here we will focus on one phenomenologically preferred flat direction  $v_L = 0, \kappa' = 0$  and

$$\frac{\kappa^2}{v_R^2} = \frac{f_1 - 2\beta_1}{4\lambda_1}, \quad (7.16)$$



### 7.3. Radiative Symmetry Breaking in the Minimal Left-Right Symmetric Model

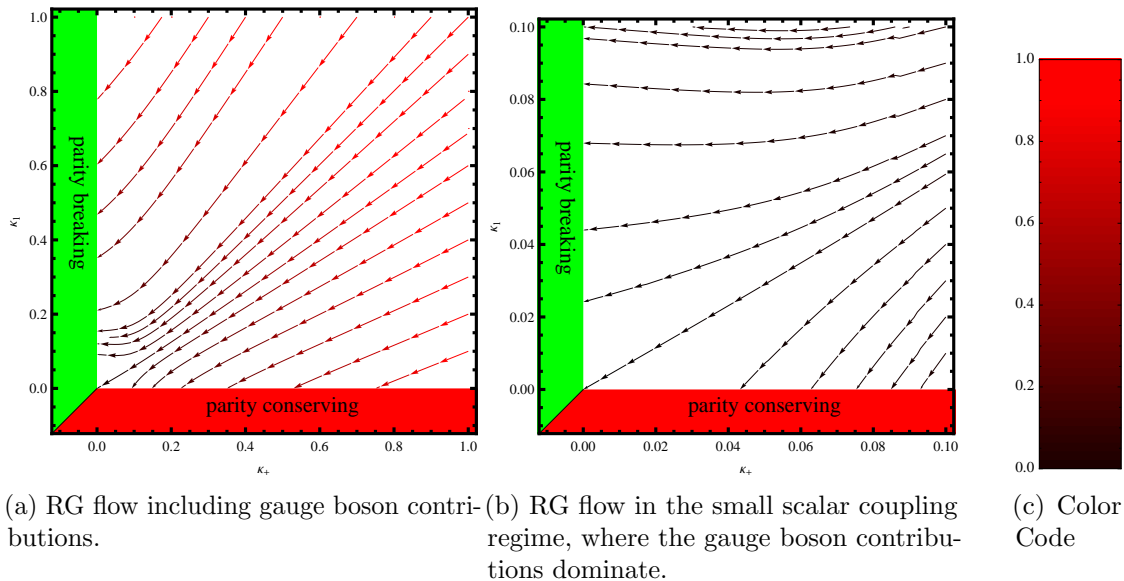


**Figure 7.2:** The RG flow in the plane  $\kappa_+ = \kappa_1 + \kappa_2$ ,  $\kappa_1$  is shown in the limit where the bidoublet can be neglected. The parity breaking (conserving) GW condition is indicated in green (red). In Fig. 7.2a, the RG evolution towards lower energies including gauge bosons contributions is shown. For simplicity, the gauge couplings have been fixed to the values at  $M_Z$ , as they become relevant only at low energy scales. Following the stream lines, it can be seen that even for positive starting values of  $\kappa_2$ , the parity violating minimum might be reached. This region is depicted in Fig. 7.2b. The gauge boson contributions deflect the RG evolution away from the vanishing coupling fixed-point.

characterized by the GW condition on the couplings

$$\text{IIa}_{\mathcal{P}}: \kappa_+ = \frac{(f_1 - 2\beta_1)^2}{8\lambda_1}. \quad (7.17)$$

The relative magnitude of the right-handed breaking scale versus the electroweak breaking scale, which we call little hierarchy in the following, is therefore set by the relative strength of the intermediate couplings  $\beta_1$  and  $f_1$  to the quartic bidoublet coupling  $\lambda_1$ . This is the case for all flat directions with non-vanishing VEVs for both the bidoublet and the doublet. To obtain a reasonable hierarchy between these scales therefore requires some fine-tuning, which is generic in LR-symmetric potentials (see e.g. [277]).

To show that this GW condition can be reached by the renormalization group flow starting from ‘reasonable’ couplings at the Planck scale, it is necessary to study the multi-dimensional parameter space of the model. In [20] we have performed an analysis using an exemplary set of parameters to show that it is indeed possible, but we will not repeat this discussion here and rather discuss some general features of the model.

First of all, the electroweak scale is tied to the left-right symmetry breaking scale via Eq. (7.16) so one would want to break left-right symmetry in the multi-TeV region to avoid introducing a hierarchy problem between the electroweak and right-handed scales. While the direct collider bounds [278–280] constrain the masses for the right-handed gauge bosons to be larger than 2.3 TeV, there are bounds from the flavour sector that push the right-handed scale above 15 TeV [281]. These are due to the fact that the bidoublet contains two Higgs doublets and while one of them corresponds to the usual Higgs with flavour diagonal couplings, the other one has flavour-violating Yukawa couplings and thus mediates FCNCs at tree-level. Here,

we assume these strict bounds to be absent, which can e.g. be achieved by realizing a different mass generation mechanism for the first two generations, e.g. by using vector-like quarks as in the Alternative Left-Right Symmetric Models where the right-handed down quark is not the  $SU(2)_R$  partner of the up quark or in other model building setups [282].

Secondly, we want to comment on the implications of the Higgs mass measurement at 126 GeV. In the Standard Model, we had seen that the Higgs mass value, while being compatible with a survival of the SM up to the Planck scale, is certainly at the lower end of the stability region. In extended models like the one we are considering here, no strict stability bound can be defined as there are additional free couplings that affect the Higgs self-coupling evolution. Here we want to draw attention to the fact that the same model building ingredients that are needed to make radiative symmetry breaking possible in the SM also shift the stability window of the Higgs mass downward. To achieve radiative symmetry breaking, we had mentioned in the introduction that one needs to counteract the negative loop contribution to the effective Higgs mass term by a positive contribution coming from boson loops. In our model the bosons are given by the right-handed gauge bosons and scalars, which are well motivated by other BSM considerations such as neutrino masses, and the same bosons of course also give a positive contribution to the Higgs self-interaction and thus push the stability bounds towards smaller values.

Thirdly, let us sketch some phenomenological consequences of the model. The scalar spectrum is detailed in [20] and assuming a hierarchy  $v_R \sim 5 \text{ TeV} \gg \kappa = 174 \text{ GeV}$  we find the following structure: most of scalars obtain masses of the order of the largest mass scale of the problem except for two of them. The Higgs mass is attached to the electroweak scale and is therefore made lighter if one tunes (7.16) as is to be expected. The only other relatively light scalar is given by the *scalon* introduced in Eq. 7.10. This excitation along the flat direction obtains a mass that is one-loop suppressed and in this setup is given by a mixture of between the SM Higgs and the neutral CP-even component of  $\chi_R$  with a mixing angle of

$$\tan \vartheta = \frac{\kappa}{v_R} \approx 0.02. \quad (7.18)$$

Note that this mixing angle can be independently obtained by comparing left- and right-handed gauge bosons  $\tan \vartheta = \frac{\kappa}{v_R} \approx \frac{m(W_L^\pm)}{m(W_R^\pm)}$  and would therefore be an indication for this type of symmetry breaking. Note that this is not possible in singlet extensions of the SM that realize radiative symmetry breaking. Such extensions, on the other hand, have the advantage that singlets generally are more weakly constrained and the new physics may generally be lighter, which is advantageous as we do not have an explanation of  $v_R \gg \kappa$  here. Quite interestingly, there has been a recent claim [283] by Meissner and Nicolai that an excess of events at 325 GeV with four charged leptons in the final state reported by CDF [284] could be identified with the singlet scalon of their model with a mixing angle of  $\vartheta \approx 0.1$ .

## Chapter 8.

# Summary and Conclusions

In this thesis we have followed a symmetry based approach to the flavour puzzle of the Standard Model. Starting from the observation that mismatched remnant symmetries of the lepton mass matrices are able to completely determine the structure of the leptonic mixing matrix we have performed a comprehensive scan of all possible mixing patterns that may be derived from non-abelian flavour symmetry groups that contain these symmetries. There are two observations to be made: first, it is remarkable that there are only a very limited number of distinct symmetry patterns that may be derived from symmetry groups of order smaller than 50. Of these, the tri-bimaximal mixing configuration

$$\sin^2 \theta_{12} = \frac{1}{3}, \quad \sin^2 \theta_{23} = \frac{1}{2} \quad \text{and} \quad \sin^2 \theta_{13} = 0$$

is the one closest to the experimental data. However, the recent measurement of a non-vanishing value of  $\theta_{13}$  has shown that this symmetric pattern is not exactly realized in nature. Flavour symmetry models with this starting point can still give consistent values for the mixing angles e.g. if one breaks the symmetry generator  $U$  in the neutrino sector. Such models then predict sum rules of deviations from this pattern. For this reason, most of the discussion of this thesis has been concerned with these small flavour groups.

The second observation is that if one widens the scope a bit and also considers larger flavour groups one can find groups such as  $\Delta(600)$  and  $(Z_{18} \times Z_6) \rtimes S_3$  that give a very good description of the experimental data in the lepton sector. Having such new starting points is especially necessary if one wants to explain flavour at a high energy scale, e.g. a GUT scale, as in such models these observables are (among) the only measurable results of such setups and the only way to falsify such models is to measure the mixing angles with higher accuracy. This demonstrates the need for sharp predictions in such models.

Here we follow a different philosophy. Instead of assuming the flavour breaking scale to be at some high energy scale, we ask ourselves if it is possible to instead explain flavour at an accessible energy scale. This approach has its vices and virtues: the biggest virtue certainly is that such models are testable. Models with non-abelian discrete flavour symmetries are inherently baroque: to realize the breaking into different non-commuting subgroups in the charged lepton and neutrino sectors many scalar fields have to be introduced and to realize their VEVs usually further (driving) fields are introduced. While in high-scale models all of these fields are completely unobservable in low-scale models these particles can pop up in collider experiments, searches for lepton flavour violating decays and other experiments. This is of course also in some sense a vice of these models as no new physics has shown up so far and new physics models at the TeV scale become increasingly constrained. However, the flavour symmetry and its breaking pattern may also protect the model from strong bounds that apply to new physics models with generic flavour structure. We will come back to this

point later but let us first mention another not so strong point of low-scale models. Since Yukawa couplings are dimensionless, flavour can be explained (if at all) at any scale be it high or low. This is to be contrasted with the hierarchy problem, which (if the SM is viewed as an effective field theory) has to be solved at the TeV scale. For example the popular lore is that if no stops are found at the LHC (soon) the supersymmetric solution of the hierarchy problem is dead. No analogous statement can be made about flavour models since the Yukawa couplings are only logarithmically scale dependent and thus the flavour scale can always be pushed upwards. Thus it is impossible to predict, whether there ever will be an answer to the flavour puzzle.

If one wants to implement models with discrete flavour symmetries at the electroweak scale one faces an immediate problem having to do with the construction of the theories themselves. To obtain a predictive model one needs at least two different scalar multiplets that break the discrete symmetry group down to two non-commuting subgroups. However, this VEV configuration cannot be obtained without additional model building ingredients. The two options that have been discussed in the literature either require the existence of extra dimensions or continuous R-symmetries in supersymmetry and thus force the flavour symmetry breaking scale to be unobservably high. The essence of these solutions can be distilled, however, and has nothing to do with the scale of symmetry breaking but rather it is due to the fact that the particle content and symmetries are engineered such that there emerges an accidental symmetry in the scalar potential under which the two flavons transform separately. The minimal way to engineer such a symmetry is to extend the flavour group in a non-trivial way. General conditions of how to proceed have been given in Chapter 3 and there a scan was presented for small groups that have these properties and extend popular flavour groups. For the flavour groups  $A_4$ ,  $S_4$  and  $T'$  solutions of size smaller than 1000 were found, while no such solutions exist for  $\Delta(27)$  and  $T_7$ . Since  $A_4$  is the smallest group with three dimensional representations and it can naturally accommodate predictive deviations from TBM (in the trimaximal(TM) mixing form), we concentrated on the smallest semidirect product extension of  $A_4$  that we found in our scan, the flavour group  $Q_8 \times A_4$ .

In Chapter 4 a complete model based on this symmetry group was presented. It was shown that this model can lead to tri-bimaximal mixing at leading order and that the required vacuum configuration can be obtained naturally without the need for fine-tuning of parameters in the scalar potential. The model is also comparably economical, as no driving fields etc. have to be introduced. The relatively large mixing angle  $\theta_{13}$  can be accounted for by next-to-leading order corrections but it was shown that this introduces a large number of free parameters to the model and is thus not very predictive. A more predictive model can be built by introducing another scalar field that realizes the TM mixing. A tree-level seesaw UV completion was presented alongside a possibility to supersymmetrise the model.

In Chapter 5 we have shown how to write down a model that realizes flavour symmetry breaking at the electroweak scale. A complete model of lepton flavour at the electroweak scale was given. The model is also based on the flavour group  $Q_8 \times A_4$ , which allows for natural vacuum alignment at the EW scale, which was not possible before. The SM Higgs is subsumed in a flavour triplet that couples to charged leptons (and quarks) at the renormalizable level, thereby eliminating the need to invoke higher dimensional operators, as is done in models with flavon singlets. Neutrino masses are generated at the one-loop level and are further suppressed by the fact that two small mass insertions are needed in the loop. This TeV seesaw is realized without imposing any new symmetries apart from the flavour symmetries that are kept from the previous model. In the model there are 8 real parameters in the lepton sector to

explain the 12 observables, which gives a predictive framework and in particular a correlation between the atmospheric and reactor angle is predicted, which agrees well with the recent global fits. Furthermore the model automatically includes a WIMP dark matter candidate and its stability and phenomenology have been studied. Constraints from LFV experiments have been shown to be loosened by the flavour symmetry in comparison to flavour generic multi-Higgs doublet models. Finally an extension to the quark sector and collider bounds have been studied. The model survives all direct collider searches, mostly due to the fact that the model has a state that closely mimics the SM Higgs and the bounds coming from LHC for non-coloured particles are not too stringent at the moment. An enhanced  $h \rightarrow \gamma\gamma$  branching ratio can be explained utilizing the multitude of new charged scalars which were introduced to generate neutrino masses.

In Chapter 6 we discussed generalized CP transformations in models with discrete flavour symmetries, a question which we originally stumbled upon motivated by technical necessities of the vacuum alignment mechanism if one wants to promote the flavons in the neutrino sector to EW doublets. Since the issue of CP violation in the lepton sector has come to the forefront of attention due to the large value of  $\theta_{13}$  this question is also of more general importance. We have shown that every generalized CP transformation has to furnish a representation of the automorphism group of the discrete flavour group. This imposes interesting consistency conditions that have had been largely overlooked in the literature. In particular, we have shown that there is no geometrical CP violation in models with the flavour symmetry  $T'$  and that the geometrical phases in models based on  $\Delta(27)$  are the result of an accidental generalized CP transformation.

In the last chapter we have changed perspective and presented speculative attempts to address the naturalness problem of the Higgs sector. The essential idea is that the naturalness problem might disappear when viewed from a Planck scale perspective, which requires the embedding of the SM (or minimal extensions) directly into (quantum) gravity without the existence of intermediate physics scales such as a GUT scale. We have shown the implications for the Higgs mass of certain boundary conditions imposed at the Planck scale. In particular we discussed the vacuum stability of the Higgs potential in light of the recent finding of a Higgs-like particle at 126 GeV and conclude that the possibility that the Higgs self-coupling vanishes at the Planck scale cannot be excluded by the current data. As a further example of a theory that survives up to the Planck scale, we discussed radiative symmetry breaking in the minimal left-right symmetric model. We showed that classical conformal invariance is broken by quantum effects and that the large hierarchy between the Planck and electroweak scales may be explained as a result of the logarithmic running of the dimensionless couplings in the scalar potential.

Let us close by some general remarks about the two issues of the SM Higgs: the flavour puzzle and the naturalness problem. Regarding both issues, all eyes are on the LHC. If there is new physics at the TeV scale, the hope is that it solves the naturalness problem. Precision measurements using kaons and B mesons indicate that new physics, if it exists, most certainly has a non-trivial flavour structure. Even though flavour does not have to be explained at the TeV scale, precision study of the flavour structure of new physics would give important new insights into possible underlying symmetries. If flavour is indeed generated at the TeV scale there would be many new particles that could be discovered and it would be an exciting possibility to sort out which flavour symmetries are realized in nature, if any. If no new physics is discovered at the LHC, precision experiments looking for rare processes could still give important insight. However, as we have argued in Chapter 7, in this case it could be time to

## *Chapter 8. Summary and Conclusions*

take the possibility more seriously that the hierarchy problem is solved at the Planck scale and that there is thus a large desert between the electroweak and Planck scales. One then has to hope that advances in quantum gravity research shed light on the issues discussed in this thesis.

# Appendix A.

## Group Theoretical Details

### A.1. Important Series of Subgroups of $SU(3)$

We here give presentations of important subgroups of  $SU(3)$  that are used in this thesis.

- the series  $\Delta(3n^2)$  is given by the semidirect product  $(Z_n \times Z_n) \rtimes Z_3$  and may be presented as [88, 89, 111]

$$a^3 = c^n = d^n = E, \quad cd = dc, \quad aca^{-1} = c^{-1}d^{-1}, \quad ada^{-1} = c, \quad (\text{A.1})$$

with the special cases  $\Delta(3) \cong Z_3$  and  $\Delta(12) \cong A_4$ .

- the series  $\Delta(6n^2)$  is given by the semidirect product  $(Z_n \times Z_n) \rtimes S_3$  and may be presented by the generators  $a, c, d$  fulfilling (A.1) and an additional generator  $b$  fulfilling [88, 96, 111]

$$b^2 = (ab)^2 = E, \quad bcb^{-1} = d^{-1}, \quad bdb^{-1} = c^{-1}; \quad (\text{A.2})$$

with the special cases  $\Delta(6) \cong S_3$  and  $\Delta(24) \cong S_4$ .

- the series  $T_n$  has the structure  $Z_n \rtimes Z_3$  and may be presented by [111]

$$A^n = B^3 = E, \quad BAB^{-1} = A^a$$

with  $a^3 = 1 \pmod n$ .

### A.2. Clebsch-Gordon Coefficients

In this section, we present the Clebsch-Gordan coefficients, which are relevant for the discussion.

#### A.2.1. $A_4$

The only non-trivial Kronecker product of  $A_4$  is given by

$$\underline{\mathbf{3}} \times \underline{\mathbf{3}} = \underline{\mathbf{1}}_1 + \underline{\mathbf{1}}_2 + \underline{\mathbf{1}}_3 + \underline{\mathbf{3}}_S + \underline{\mathbf{3}}_A, \quad (\text{A.3})$$

where the indices  $S$  and  $A$  indicate whether the representation is in the symmetric or antisymmetric part, respectively. The corresponding Clebsch-Gordan coefficients, which have been

## Appendix A. Group Theoretical Details

$ G $	GAP	
240	108	
288	924	
336	131	
384	618	5809
	5856	18216
	20112	
432	262	
480	964	1041

$ G $	GAP			
240	102	103		
288	400	844	845	846
	847	903		
336	115	116		
384	582	5614	5705	5708
	5713	5714	5728	5733
	18028	18029	18042	18043
	18044	18045	18048	18102
	18117	18120	18130	18143
	20069	20073		
432	240	241		
480	257	961	967	968
	969	970	1020	

$ G $	GAP
288	409
384	5845
480	266

(a)  $G/N \cong A_4$ 
(b)  $G/N \cong S_4$ 
(c)  $G/N \cong T'$

**Figure A.1:** Candidate groups  $G$  of order 201 – 500.  $|G|$  denotes the order of  $G$ . The groups up to order 200 are listed in Tab. 3.3. Details of the groups may be accessed using the computer algebra system GAP by using the command `SmallGroup(Order, GAP)`.

computed using [285], are

$$\begin{aligned}
 (ab)_{\underline{\mathbf{1}}_1} &= \frac{1}{\sqrt{3}} (a_1 b_1 + a_2 b_2 + a_3 b_3) \\
 (ab)_{\underline{\mathbf{1}}_2} &= \frac{1}{\sqrt{3}} (a_1 b_1 + \omega^2 a_2 b_2 + \omega a_3 b_3) & (ab)_{\underline{\mathbf{1}}_3} &= \frac{1}{\sqrt{3}} (a_1 b_1 + \omega a_2 b_2 + \omega^2 a_3 b_3) \\
 (ab)_{A, \underline{\mathbf{3}}} &= \frac{1}{2} \begin{pmatrix} a_2 b_3 - a_3 b_2 \\ a_3 b_1 - a_1 b_3 \\ a_1 b_2 - a_2 b_1 \end{pmatrix} & (ab)_{S, \underline{\mathbf{3}}} &= \frac{1}{2} \begin{pmatrix} a_2 b_3 + a_3 b_2 \\ a_3 b_1 + a_1 b_3 \\ a_1 b_2 + a_2 b_1 \end{pmatrix}
 \end{aligned} \tag{A.4}$$

where  $(a_1, a_2, a_3), (b_1, b_2, b_3) \sim \underline{\mathbf{3}}$ .

### A.2.2. $Q_8 \times A_4$

The product of two triplets  $\underline{\mathbf{3}}_i \times \underline{\mathbf{3}}_i$  is described by the same Clebsch-Gordan coefficients as the one in  $A_4$ . They are shown in Eq. (A.4). The product of two four dimensional representations  $(a_1, a_2, a_3, a_4) \sim \underline{\mathbf{4}}_1$  and  $(b_1, b_2, b_3, b_4) \sim \underline{\mathbf{4}}_1$  contains the singlet

$$(ab)_{\underline{\mathbf{1}}_1} = \frac{1}{2} (a_1 b_1 + a_2 b_2 + a_3 b_3 + a_4 b_4) \tag{A.5}$$

and the triplets:

$$\begin{aligned}
 (ab)_{\underline{\mathbf{3}}_1} &= \frac{1}{2} \begin{pmatrix} -a_4 b_1 + a_3 b_2 - a_2 b_3 + a_1 b_4 \\ -a_3 b_1 - a_4 b_2 + a_1 b_3 + a_2 b_4 \\ a_2 b_1 - a_1 b_2 - a_4 b_3 + a_3 b_4 \end{pmatrix}, & (ab)_{\underline{\mathbf{3}}_2} &= \frac{1}{2} \begin{pmatrix} a_4 b_1 + a_3 b_2 + a_2 b_3 + a_1 b_4 \\ a_3 b_1 + a_4 b_2 + a_1 b_3 + a_2 b_4 \\ a_2 b_1 + a_1 b_2 + a_4 b_3 + a_3 b_4 \end{pmatrix}, \\
 (ab)_{\underline{\mathbf{3}}_3} &= \frac{1}{2} \begin{pmatrix} a_1 b_1 - a_2 b_2 - a_3 b_3 + a_4 b_4 \\ -a_1 b_1 + a_2 b_2 - a_3 b_3 + a_4 b_4 \\ -a_1 b_1 - a_2 b_2 + a_3 b_3 + a_4 b_4 \end{pmatrix}, & (ab)_{\underline{\mathbf{3}}_4} &= \frac{1}{2} \begin{pmatrix} a_4 b_1 - a_3 b_2 - a_2 b_3 + a_1 b_4 \\ -a_3 b_1 + a_4 b_2 - a_1 b_3 + a_2 b_4 \\ -a_2 b_1 - a_1 b_2 + a_4 b_3 + a_3 b_4 \end{pmatrix},
 \end{aligned} \tag{A.6}$$



$$(ab)_{\mathbf{3}_5} = \frac{1}{2} \begin{pmatrix} -a_4b_1 - a_3b_2 + a_2b_3 + a_1b_4 \\ a_3b_1 - a_4b_2 - a_1b_3 + a_2b_4 \\ -a_2b_1 + a_1b_2 - a_4b_3 + a_3b_4 \end{pmatrix}.$$

Another important product is the product of  $a \sim \mathbf{3}_5$  and  $b \sim \mathbf{3}_4$ :

$$(ab)_{\mathbf{3}_1} = \begin{pmatrix} a_2b_3 \\ a_3b_1 \\ a_1b_2 \end{pmatrix}, \quad (ab)_{\mathbf{3}_2} = \begin{pmatrix} a_3b_2 \\ a_1b_3 \\ a_2b_1 \end{pmatrix}, \quad (ab)_{\mathbf{3}_3} = \begin{pmatrix} a_3b_3 \\ a_1b_1 \\ a_2b_2 \end{pmatrix}. \quad (\text{A.7})$$

### A.3. CP Definition for Small Groups

Here we supply a supplement to the discussion in Chapter 6.

$$T_7 \cong Z_7 \rtimes Z_3 \cong \text{SG}(21, 1)$$

The group  $T_7 \cong Z_7 \rtimes Z_3 \cong \text{SG}(21, 1) = \langle A, B | A^7 = B^3 = BAB^{-1}A^5 = E \rangle$  may be represented as [94]

$$\rho(A) = \text{diag}(\eta, \eta^2, \eta^4) \quad \rho(B) = T_3$$

for  $\mathbf{3}_1$  with  $\eta = e^{2\pi i/7}$ .  $T_7$  has a trivial centre and therefore the inner automorphism group  $\text{Inn}(T_7)$  is isomorphic to  $T_7$  itself. However, since  $\rho(A)^* = \rho(A^6) \in \text{Im}\rho$  and  $\rho(B)^* = \rho(B) \in \text{Im}\rho$ , the outer automorphism group is non-trivial. Its generator  $u : (A, B) \rightarrow (A^6, B)$  is thus represented by the unitary matrix on the three dimensional representation and this basis is thus a CP basis. In conclusion, the structure of the automorphism group is described by

$$\begin{aligned} Z(T_7) &\cong Z_1 & \text{Aut}(T_7) &\cong \text{SG}(42, 2) & (\text{A.8}) \\ \text{Inn}(T_7) &\cong T_7 & \text{Out}(T_7) &\cong Z_2. \end{aligned}$$

The outer automorphism exchanges the three-dimensional representations, while leaving the one-dimensional ones fixed, i.e.

$$\underline{\mathbf{1}}_2 \rightarrow \underline{\mathbf{1}}_2, \quad \underline{\mathbf{1}}_3 \rightarrow \underline{\mathbf{1}}_3 \quad \text{and} \quad \underline{\mathbf{3}} \leftrightarrow \underline{\mathbf{3}}^*.$$

$$Z_9 \rtimes Z_3 \cong \text{SG}(27, 4)$$

Similarly to  $\Delta(27)$ , the group  $Z_9 \rtimes Z_3 = \text{SG}(27, 4) = \langle A, B | A^9 = B^3 = BAB^2A^2 = E \rangle$ <sup>1</sup> has a more complicated automorphism group structure. The group is the semi-direct product of  $Z_9$  generated by  $A$  (with  $A^9 = E$ ) with  $Z_3$  generated by  $B$  (with  $B^3 = E$ ) defined by  $BAB^{-1} = A^7$ . The centre of the group is isomorphic to  $Z_3$  and generated by  $A^3$ . Hence, the inner automorphism group has the structure  $Z_3 \times Z_3$ . The outer automorphism group is generated by

$$\begin{aligned} u_1 : (A, B) &\rightarrow (AB, B^2A^6B^2A^3) & (\text{A.9}) \\ u_2 : (A, B) &\rightarrow (AB^4AB^4A^6, B^2A^6B^2A^6) \end{aligned}$$

<sup>1</sup>The possibility of having  $Z_9 \rtimes Z_3$  as a flavour group in the lepton sector has been first mentioned in [95].

## Appendix A. Group Theoretical Details

and the structure of the automorphism group may be summarised as

$$\begin{aligned} Z(G) &\cong Z_3 & \text{Aut}(G) &\cong ((Z_3 \times Z_3) \rtimes Z_3) \rtimes Z_2 \\ \text{Inn}(G) &\cong Z_3 \times Z_3 & \text{Out}(G) &\cong S_3. \end{aligned} \quad (\text{A.10})$$

There is a faithful three dimensional representation given by

$$\rho(A) = \begin{pmatrix} 0 & 1 & 0 \\ 0 & 0 & \omega^2 \\ \omega^2 & 0 & 0 \end{pmatrix}, \quad \rho(B) = \begin{pmatrix} \omega^2 & 0 & 0 \\ 0 & 1 & 0 \\ 0 & 0 & \omega \end{pmatrix}.$$

The generators of the outer automorphisms can be obtained in the same way as before and act on  $(\mathbf{3}, \mathbf{3}^*)$  as

$$U(u_1) = \begin{pmatrix} 0 & \tilde{U} \\ \tilde{U}^* & 0 \end{pmatrix} \quad \text{with} \quad \tilde{U} = \text{diag}(1, 1, \omega^2) \quad (\text{A.11})$$

and

$$U(u_2) = \begin{pmatrix} \tilde{U} & 0 \\ 0 & \tilde{U}^* \end{pmatrix} \quad \text{with} \quad \tilde{U} = \begin{pmatrix} 0 & 1 & 0 \\ 1 & 0 & 0 \\ 0 & 0 & \omega^2 \end{pmatrix}. \quad (\text{A.12})$$

### $\Delta(108) \cong \text{SG}(108, 22)$ (or $\Delta(216) \cong \text{SG}(216, 95)$ )

Recently [205], CP violation has been discussed in the context of  $\Delta(108) = \Delta(3 \times 6^2)$ <sup>2</sup>, which may be represented by a faithful three-dimensional representation as

$$\rho(\mathcal{S}) = S_3, \quad \rho(\mathcal{T}) = T_3, \quad \rho(\mathcal{T}') = \text{diag}(1, \omega, \omega^2). \quad (\text{A.13})$$

The model possesses an accidental  $\mu - \tau$  exchange symmetry, which is generated by  $U_3$ <sup>3</sup>. Including this generator  $U = U_3$ , the group becomes  $\Delta(6 \times 6^2)$ . A generalised CP transformation was defined on the faithful representation  $\ell_R$  as

$$\ell_R \rightarrow iU_3 \ell_R^*,$$

where we have suppressed the Lorentz structure. This is equivalent to the automorphism  $u : (\mathcal{S}, \mathcal{T}, \mathcal{T}') \rightarrow (\mathcal{S}, \mathcal{T}^2, \mathcal{T}')$ , which is outer in  $\Delta(3 \times 6^2)$  and inner in  $\Delta(6 \times 6^2)$ . In [205] this has been consistently applied to all unfaithful representations they consider.

Let us comment on the origin of maximal CP violation in their model, which seems to be in conflict with our general statement that there can be no CP violation. It is related to the breaking of the flavour symmetry in their model. One of the scalar fields breaking the flavour symmetry is the scalar  $\phi$  transforming as

$$\rho(\mathcal{S}) = S_3, \quad \rho(\mathcal{T}) = T_3 \quad \rho(\mathcal{T}') = \mathbb{1}_3, \quad (\text{A.14})$$

and thus transforms only under the subgroup  $\langle \mathcal{S}, \mathcal{T} \rangle \cong A_4$  with the CP transformation  $\phi \rightarrow U_3 \phi^*$ . CP conservation would therefore require  $v_2 = v_3^*$ . However, they have to assume a large hierarchy in the VEVs of  $\phi$  in order to accommodate the hierarchy in the charged lepton sector, which is given by  $m_e : m_\mu : m_\tau = v_1 : v_2 : v_3$ . Hence, the requirement  $|v_2| / |v_3| = m_\mu / m_\tau \ll 1$  is the necessary ingredient for maximal CP violation in the model.

<sup>2</sup> $\Delta(108)$  has been first used in the lepton sector in [286].

<sup>3</sup>The matrices  $S_3$ ,  $T_3$  and  $U_3$  have been defined in Eqs.(2.27), (2.25) and Eq. (2.30).

## A.4. Vacuum Alignment and Scalar Spectrum of EW Model

### A.4.1. Vacuum alignment

The vacuum configuration given in Eq. (5.1) is naturally obtained from the most general potential <sup>4</sup>

$$V = V_\phi(\phi_1, \phi_2) + V_\chi(\chi) + V_{\text{mix}}(\chi, \phi_1, \phi_2)$$

compatible with given symmetries, where  $V_\phi(\phi_1, \phi_2)$  is given in (4.8),  $V_\chi(\chi)$  is given in (5.3) and

$$V_{\text{mix}}(\chi, \phi_1, \phi_2) = \zeta_{13}(\phi_1\phi_1)_{\underline{\mathbf{1}}_1}(\chi^\dagger\chi)_{\underline{\mathbf{1}}_1} + \zeta_{23}(\phi_2\phi_2)_{\underline{\mathbf{1}}_1}(\chi^\dagger\chi)_{\underline{\mathbf{1}}_1} \quad (\text{A.15})$$

compatible with given symmetries. The minimization conditions reduce to the equations

$$\begin{aligned} a(\alpha_+(a^2+b^2) + \alpha_-(a^2-b^2) + \gamma_+(c^2+d^2) + \gamma_-(c^2-d^2) + U_1) + \Gamma bcd &= 0 \\ b(\alpha_+(a^2+b^2) - \alpha_-(a^2-b^2) + \gamma_+(c^2+d^2) - \gamma_-(c^2-d^2) + U_1) + \Gamma acd &= 0 \\ c(\beta_+(c^2+d^2) + \beta_-(c^2-d^2) + \gamma_+(a^2+b^2) + \gamma_-(a^2-b^2) + U_2) + \Gamma abd &= 0 \\ d(\beta_+(c^2+d^2) - \beta_-(c^2-d^2) + \gamma_+(a^2+b^2) - \gamma_-(a^2-b^2) + U_2) + \Gamma abc &= 0 \\ v(M_\chi^2 + \lambda_\chi v^2) &= 0 \end{aligned} \quad (\text{A.16})$$

with

$$U_i = \frac{1}{2}\mu_i^2 + \frac{\sqrt{3}}{12}\zeta_{i3}v^2 \quad \text{for } i = 1, 2,$$

and

$$\begin{aligned} M_\chi^2 &= 2\mu_3^2 + \zeta_{13}(a^2+b^2) + \zeta_{23}(c^2+d^2), & \lambda_\chi &= \frac{2}{3}(\sqrt{3}\lambda_{\chi\underline{\mathbf{1}}_1} + \lambda_{\chi\underline{\mathbf{3}}_1\mathbf{S}}), \\ \xi_+ &= \frac{\xi_1}{2}, & \xi_- &= \frac{\xi_2 + \xi_3}{2\sqrt{3}}, & \gamma_+ &= \frac{\sqrt{3}\gamma_1 + \gamma_4}{4\sqrt{3}}, & \gamma_- &= \frac{\gamma_2 + \gamma_3}{4\sqrt{3}}, & \text{and } \Gamma &= \frac{\gamma_4}{\sqrt{3}}, \end{aligned}$$

with  $\xi = \alpha, \beta$ . Since the number of equations matches the number of VEVs, vacuum alignment is possible. Corrections to the scalar potential only arise on dimension 6 level. These corrections furthermore arise on one-loop level and are thus further suppressed. We therefore neglect VEV shifts arising from these interactions throughout this work.

### A.4.2. Scalar Spectrum

**Scalar Spectrum –  $\phi_i, \chi$ :** Let us first discuss the visible sector, i.e. the flavons  $\phi_1, \phi_2, \chi$  that get VEVs and realize the symmetry breaking the  $\eta$ 's are independent and will be discussed later. The fields can be classified according to remnant symmetries of the potential. There are the obvious symmetries

$$Z_3 : \chi \rightarrow T_3\chi, \quad \phi_i \rightarrow \phi_i, \quad (\text{A.17})$$

<sup>4</sup>We do not have to consider the part involving  $\eta_i$ , because it does not change the minimization conditions of  $\phi_i$  and  $\chi$ , if it does not acquire a VEV.

## Appendix A. Group Theoretical Details

with  $T_3 = \Omega_T \text{diag}(1, \omega^2, \omega) \Omega_T^\dagger$  and

$$Z_2 : \phi_i \rightarrow S_4 \phi_i, \quad \chi \rightarrow \chi, \quad (\text{A.18})$$

with  $S_4 = \Omega_{S_4} \text{diag}(1, 1, -1, -1) \Omega_{S_4}^\dagger$  but there is another accidental symmetry of the potential  $V_\phi$  not part of  $Q_8 \times A_4$ :

$$Z_2 : \phi_i \rightarrow O_4 \phi_i, \quad \chi \rightarrow \chi, \quad (\text{A.19})$$

with<sup>5</sup>  $O_4 = \Omega_{S_4} \text{diag}(1, 1, 1, -1) \Omega_{S_4}^\dagger$ , where

$$\Omega_{S_4} \equiv \frac{1}{\sqrt{2}} \begin{pmatrix} 0 & 1 & 0 & -1 \\ 0 & 1 & 0 & 1 \\ -1 & 0 & 1 & 0 \\ 1 & 0 & 1 & 0 \end{pmatrix}. \quad (\text{A.20})$$

It is useful to go to a basis

$$\tilde{\phi}_i = \Omega_{S_4}^\dagger \phi_i, \quad (H, \varphi', \varphi'')^T = \Omega_T^\dagger \chi, \quad (L_e, L_\mu, L_\tau)^T = \Omega_T^\dagger L \quad (\text{A.21})$$

where these symmetries are represented diagonally. Let us discuss the mass terms in turn:

- the 9 physical scalars contained in  $\chi$  have been discussed following Eq. (5.5) Here we only report the expressions of the dimensionless couplings in terms of masses:

$$\begin{aligned} \lambda_{\chi 1_1} &= M_-^2 + M_+^2 + \frac{3m_h^2}{2} \\ \lambda_{\chi 1_2} &= \frac{1}{2} \left( 3m_1^2 - 3\sqrt{m_1^4 - 2m_1^2 m_2^2 + m_2^4} - 4(M_-^2 - M_+^2)^2 + 3m_2^2 - 2M_-^2 - 2M_+^2 \right) \\ \lambda_{\chi 3_1, S} &= -\sqrt{3} (M_-^2 + M_+^2) \\ \lambda_{\chi 3_1, A} &= -\sqrt{3} \left( m_1^2 + \sqrt{m_1^4 - 2m_1^2 m_2^2 + m_2^4} - 4(M_-^2 - M_+^2)^2 + m_2^2 - M_-^2 - M_+^2 \right) \\ \lambda_{\chi A} &= 6 (M_-^2 - M_+^2) \end{aligned} \quad (\text{A.22})$$

- $(\tilde{\phi}_1)_4$  and  $(\tilde{\phi}_2)_4$  transform as  $(1, -1, -1)$  and have a mass matrix given by

$$\begin{pmatrix} m_{11} & \frac{2(ac(\sqrt{3}\gamma_M - 2\gamma_2) + 2b\gamma_2 d)}{\sqrt{3}} \\ \cdot & m_{11} ((a, b, c, d, \alpha_2) \leftrightarrow (c, d, a, b, \beta_2)) \end{pmatrix}$$

with

$$\begin{aligned} m_{11} &= -4\sqrt{3}a^2\alpha_2 + a \left( \frac{2a\gamma_M(c-d)(c+d)}{(b-a)(a+b)} + \frac{c\Gamma d}{b} \right) - \frac{bc\Gamma d}{2a} \\ &\quad + \frac{1}{12} \left( 48\sqrt{3}\alpha_2 b^2 - 3\Gamma(c^2 + d^2) + 8\sqrt{3}\gamma_2(d^2 - c^2) \right) \end{aligned}$$

<sup>5</sup>The alert reader will recognize this as an outer automorphism  $h_4$  of Eq. (6.30).

#### A.4. Vacuum Alignment and Scalar Spectrum of EW Model

- $(\tilde{\phi}_1)_3$  and  $(\tilde{\phi}_2)_3$  transform as  $(1, -1, 1)$  and have a mass matrix given by

$$\begin{pmatrix} m_{11} & \frac{2(ac\gamma_2 - bd(\gamma_2 - 2\sqrt{3}\gamma_M))}{\sqrt{3}} \\ \cdot & m_{11} ((a, b, c, d, \alpha_2) \leftrightarrow (c, d, a, b, \beta_2)) \end{pmatrix}$$

with

$$m_{11} = 2\sqrt{3}a^2\alpha_2 + \frac{2b^2(\sqrt{3}\alpha_2(a-b)(a+b) + 2\gamma_M(c-d)(c+d))}{b^2 - a^2} - \frac{ac\Gamma d}{b} \\ + \frac{2bc\Gamma d}{a} - \frac{1}{2}\Gamma(c^2 + d^2) + \frac{\gamma_2(c-d)(c+d)}{\sqrt{3}}$$

- the real scalars  $h$ ,  $(\tilde{\phi}_1)_1$ ,  $(\tilde{\phi}_1)_2$ ,  $(\tilde{\phi}_2)_1$  and  $(\tilde{\phi}_2)_2$  transform as  $(1, 1, 1)$  under the remnant symmetry. Here we don't give the full mass matrix but only give the mixing with the Higgs in the limit of small mixings. The mixing matrix with field  $f$  is given by

$$\tan 2\theta_f = \frac{2m_{h,f}}{m_f^2 - m_h^2} \quad (\text{A.23})$$

with

$$m_{h,(\tilde{\phi}_1)_1} = -\frac{bv\zeta_{13}}{\sqrt{3}}, \quad m_{h,(\tilde{\phi}_1)_2} = \frac{av\zeta_{13}}{\sqrt{3}}, \quad m_{h,(\tilde{\phi}_2)_1} = -\frac{dv\zeta_{23}}{\sqrt{3}}, \quad m_{h,(\tilde{\phi}_2)_2} = \frac{cv\zeta_{23}}{\sqrt{3}}.$$

**Scalar Spectrum –  $\eta_i$ :** The relevant part of the scalar potential to calculate the mass insertions needed to calculate neutrino masses for the mass spectrum of  $\eta_i$  has been given in Eqs. (5.12-5.15). To calculate the  $\eta$  mass spectrum the complete interactions

$$\delta V_{\eta_i}^{(2)} = \sum_{i=1,2,3} \lambda_1(\chi^T \sigma_2 \bar{\sigma} \chi)_{\mathbf{1}_1} (\eta_1^T \sigma_2 \bar{\sigma} \eta_3)_{\mathbf{1}_1}^* + \lambda_2 e^{i\alpha_\lambda} (\chi^T \sigma_2 \bar{\sigma} \chi)_{\mathbf{3}_1} (\eta_2^T \sigma_2 \bar{\sigma} \eta_3)_{\mathbf{3}_1}^* \quad (\text{A.24})$$

$$+ \lambda_3(\phi_1 \phi_2)_{\mathbf{1}_1} (\eta_3^\dagger \eta_1)_{\mathbf{1}_1} + \lambda_4(\phi_1 \phi_2)_{\mathbf{3}_1} (\eta_3^\dagger \eta_2)_{\mathbf{3}_1} + \lambda_5(\phi_1 \phi_2)_{\mathbf{3}_2} (\eta_3^\dagger \eta_2)_{\mathbf{3}_2} \quad (\text{A.25})$$

$$+ \lambda_6(\phi_1 \phi_2)_{\mathbf{3}_3} (\eta_3^\dagger \eta_2)_{\mathbf{3}_3} + \lambda_7(\phi_1 \phi_2)_{\mathbf{3}_5} (\eta_1^\dagger \eta_3)_{\mathbf{3}_{5,S}} + \lambda_8(\phi_1 \phi_2)_{\mathbf{3}_5} (\eta_1^\dagger \eta_3)_{\mathbf{3}_{5,A}} \quad (\text{A.26})$$

$$+ l_1^{ij}(\phi_j \phi_j)_{\mathbf{1}_1} (\eta_i^\dagger \eta_i)_{\mathbf{1}_1} + l_2^j(\phi_j \phi_j)_{\mathbf{3}_{2,3}} (\eta_1^\dagger \eta_2)_{\mathbf{3}_{2,3}} + l_3^j(\phi_j \phi_j)_{\mathbf{3}_4} (\eta_2^\dagger \eta_2)_{\mathbf{3}_4} \quad (\text{A.27})$$

$$+ k_1(\chi^\dagger \chi)_{\mathbf{3}_1} (\eta_1^\dagger \eta_2)_{\mathbf{3}_1} + k_2(\chi^\dagger \tau_2 \bar{\sigma} \chi)_{\mathbf{3}_1} (\eta_1^\dagger \sigma_2 \bar{\sigma} \eta_2)_{\mathbf{3}_1} \quad (\text{A.28})$$

$$+ k_3^{(i)}(\chi^\dagger \sigma_2 \bar{\sigma} \chi)_{\mathbf{1}_1} (\eta_i^\dagger \sigma_2 \bar{\sigma} \eta_i)_{\mathbf{1}_1} + k_4^{(i)}(\chi^\dagger \chi)_{\mathbf{1}_1} (\eta_i^\dagger \eta_i)_{\mathbf{1}_1} + \text{h.c.} \quad (\text{A.29})$$

are needed. Let us briefly outline how the various couplings act: The couplings  $k_4^{(i)}$  and  $l_1^{(ij)}$  renormalize  $M_i$ ,  $k_3^{(i)}$  splits masses of charged and neutral components,  $\lambda_1$  and  $\lambda_2$  mix neutral scalar and pseudoscalar components of the various fields. Hence, it also splits the masses of scalar and pseudoscalar of the lightest mass eigenstate,  $k_1$ ,  $l_2^{(i)}$ ,  $l_3^{(j)}$  mix the components of the various  $\eta_i$  and adds flavour breaking effects. Since  $\langle \chi_{\mathbf{1}_{2,3}}^2 \rangle = 0$  such couplings do give contributions to mass terms and are not shown here.  $\lambda_3, \dots, \lambda_8$  break  $Z_4$  and therefore mix components of  $\eta_3$  with components of  $\eta_{1,2}$ .

## A.5. Discrete — Mathematica Package

Discrete is a Mathematica package with several useful model building tools to work with discrete symmetries. It has been published as part of [16] and can be downloaded from <http://projects.hepforge.org/discrete/>. The main features are

- the calculation of arbitrary Kronecker products,
- an interface to the group catalogues within GAP [129], e.g. the SmallGroups [128] library with all discrete groups up to order 2000 (with the exception of groups of order 1024) and many more.
- calculation of Clebsch-Gordan coefficients. They are calculated on demand and are stored internally, in order to improve the performance.
- the possibility to reduce covariants to a smaller set of independent covariants.
- the documentation is integrated in the documentation centre of Mathematica.

It requires a working installation of GAP [129] as well as the GAP package REPSN [287]. GAP including all its packages can be downloaded from <http://www.gap-system.org/>. On Debian-based Linux-distributions, it can be directly installed via the package management.

For a tutorial, we refer the interested reader to [16] and to the documentation and the example notebook within the package.

# Acknowledgements

I would like to take the opportunity to express my gratitude towards everybody who supported me during my Ph.D. studies. In particular I would like to thank

- my advisor Manfred Lindner for his support and guidance; for the opportunity to follow my interests and, last but not least, for giving me the opportunity to attend summer schools and conferences. Arigatō.
- Kher Sham Lim, Manfred Lindner and Michael A. Schmidt for interesting and fruitful collaborations.
- Dennis Dietrich and Kristian McDonald for interesting but less fruitful collaborations.
- Michael A. Schmidt, for enjoyable collaboration across many time zones. Without his encouragement and perseverance this thesis would not have been possible. I am also most grateful for his diligent and swift proof-reading.
- Kher Sham Lim for enjoyable collaborations and for proofreading parts of my thesis.
- James Barry for correction hundreds of commas and other mistakes, especially for saving me from big dessert scenarios.
- my office mates Pei-Hong Gu and Tom Underwood for interesting discussions.
- Werner Rodejohann for advice, and soccer small talk over lunch.
- our secretaries Anja Berneiser and Britta Schwarz, for assistance with administrative tasks
- my fellow Ph.D. and diploma students in the (theory) group for their companionship: Adisorn Adulpravitchai, James Barry, Michael Dürr, Tibor Frossard, Julian Heeck, Kher Sham Lim, Lisa Michaels, Alexander Merle, Vivianna Niro, Dominik Scala, Daniel Schmidt and Juri Smirnov. I especially thank Iwona Mochol and Alexander Dück for exchanging status reports over coffee on how the thesis writing is going.
- all the other members of the group for providing a good research atmosphere: Evgeny Akhmedov, Mayumi Aoki, Alexander Kartavtsev, Joachim Kopp, Shinta Kasuya, Laura Lopez Honorez, Pavel Fileviez Perez, Thomas Schwetz-Mangold, Takashi Shimomura, Yasutaka Takanishi, He Zhang and all the other members of the "particle & astro-particle" group at MPIK.

Furthermore, I would like to express my gratitude towards my family, who have supported me throughout my studies. I especially thank my brother Philipp for proof-reading the thesis, and my sister Franziska, for taking her time obtaining her Ph.D in medicine. Finally and most importantly, I thank my girlfriend Jennifer Bröder for her support and encouragement.





## Bibliography

- [1] **ATLAS Collaboration** Collaboration, G. Aad *et al.*, “Observation of a new particle in the search for the Standard Model Higgs boson with the ATLAS detector at the LHC,” *Phys.Lett.* **B716** (2012) 1–29, [1207.7214 \[hep-ex\]](#).
- [2] **CMS Collaboration** Collaboration, S. Chatrchyan *et al.*, “Observation of a new boson at a mass of 125 GeV with the CMS experiment at the LHC,” *Phys.Lett.* **B716** (2012) 30–61, [1207.7235 \[hep-ex\]](#).
- [3] R. S. Chivukula and H. Georgi, “Composite Technicolor Standard Model,” *Phys.Lett.* **B188** (1987) 99.
- [4] G. D’Ambrosio, G. Giudice, G. Isidori, and A. Strumia, “Minimal flavour violation: An effective field theory approach,” *Nucl.Phys. B* **645** (2002) 155–187.
- [5] K. Babu, “TASI Lectures on Flavor Physics,” [0910.2948 \[hep-ph\]](#).
- [6] C. Froggatt and H. B. Nielsen, “Hierarchy of Quark Masses, Cabibbo Angles and CP Violation,” *Nucl.Phys.* **B147** (1979) 277.
- [7] R. Barbieri, G. Dvali, and L. J. Hall, “Predictions from a U(2) flavor symmetry in supersymmetric theories,” *Phys.Lett.* **B377** (1996) 76–82, [hep-ph/9512388 \[hep-ph\]](#).
- [8] A. Pomarol and D. Tommasini, “Horizontal symmetries for the supersymmetric flavor problem,” *Nucl.Phys.* **B466** (1996) 3–24, [hep-ph/9507462 \[hep-ph\]](#).
- [9] G. Altarelli and F. Feruglio, “Tri-bimaximal neutrino mixing from discrete symmetry in extra dimensions,” *Nucl.Phys. B* **720** (2005) 64–88, [hep-ph/0504165](#).
- [10] X.-G. He, Y.-Y. Keum, and R. R. Volkas, “A(4) flavor symmetry breaking scheme for understanding quark and neutrino mixing angles,” *JHEP* **0604** (2006) 039, [hep-ph/0601001 \[hep-ph\]](#).
- [11] C. S. Lam, “Symmetry of lepton mixing,” *Phys.Lett. B* **656** (2007) 193–198, [0708.3665 \[hep-ph\]](#).
- [12] C. S. Lam, “The Unique Horizontal Symmetry of Leptons,” *Phys. Rev.* **D78** (2008) 073015, [0809.1185 \[hep-ph\]](#).
- [13] C. Lam, “Determining Horizontal Symmetry from Neutrino Mixing,” *Phys.Rev.Lett.* **101** (2008) 121602, [0804.2622 \[hep-ph\]](#).
- [14] M. Holthausen, K. S. Lim, and M. Lindner, “Lepton Mixing from Remnant Symmetries: A Scan of Small Groups.” in preparation.

- [15] M. Holthausen, K. S. Lim, and M. Lindner, “Planck scale Boundary Conditions and the Higgs Mass,” *JHEP* **1202** (2012) 037, [1112.2415 \[hep-ph\]](#).
- [16] M. Holthausen and M. A. Schmidt, “Natural Vacuum Alignment from Group Theory: The Minimal Case,” *JHEP* **1201** (2012) 126, [1111.1730 \[hep-ph\]](#).
- [17] M. Holthausen, “Vacuum Alignment from Group Theory.” to appear in Proceedings of [FLASY12, Second Workshop on Flavor Symmetries and Consequences in Accelerators and Cosmology](#), 30 June 2012 – 4 July 2012. Dortmund, Germany.
- [18] M. Holthausen, M. Lindner, and M. A. Schmidt, “A Complete Model Explaining the Lepton Flavour Structure at the Electroweak Scale.” in preparation.
- [19] M. Holthausen, M. Lindner, and M. A. Schmidt, “CP and Discrete Flavour Symmetries.” in preparation.
- [20] M. Holthausen, M. Lindner, and M. A. Schmidt, “Radiative Symmetry Breaking of the Minimal Left-Right Symmetric Model,” *Phys.Rev.* **D82** (2010) 055002, [0911.0710 \[hep-ph\]](#).
- [21] M. Holthausen, “Radiative Symmetry Breaking in the Minimal Left-Right Symmetric Model.” to appear in Proceedings of 23rd [International Workshop on Weak Interactions and Neutrinos \(WIN’11\)](#), 31 Jan - 5 Feb 2011. Cape Town, South Africa.
- [22] M. Holthausen, “Conformal Symmetry in the Minimal Left-Right Symmetric Model,” Master’s thesis, Heidelberg University, 2009.
- [23] P. Ramond, “Journeys beyond the standard model,”. Reading, Mass., Perseus Books, 1999.
- [24] S. Weinberg, “Baryon and Lepton Nonconserving Processes,” *Phys.Rev.Lett.* **43** (1979) 1566–1570.
- [25] K. Babu and C. N. Leung, “Classification of effective neutrino mass operators,” *Nucl.Phys.* **B619** (2001) 667–689, [hep-ph/0106054 \[hep-ph\]](#).
- [26] P. Minkowski, “ $\mu \rightarrow e\gamma$  at a Rate of One Out of 1-Billion Muon Decays?,” *Phys.Lett.* **B67** (1977) 421.
- [27] T. Yanagida, “Horizontal Gauge Symmetry and Masses of Neutrinos,” in *Proceedings of the Workshop on The Unified Theory and the Baryon Number in the Universe*, O. Sawada and A. Sugamoto, eds., p. 95, KEK, Tsukuba, Japan. 1979.
- [28] S. L. Glashow, “The Future of Elementary Particle Physics,” in *Proceedings of the 1979 Cargèse Summer Institute on Quarks and Leptons*, M. L. vy, J.-L. Basdevant, D. Speiser, J. Weyers, R. Gastmans, and M. Jacob, eds., pp. 687–713. Plenum Press, New York, 1980.
- [29] M. Gell-Mann, P. Ramond, and R. Slansky, “Complex Spinors and Unified Theories,” in *Supergravity*, P. van Nieuwenhuizen and D. Z. Freedman, eds., p. 315. North Holland, Amsterdam, 1979.

- [30] R. N. Mohapatra and G. Senjanovic, “Neutrino Mass and Spontaneous Parity Violation,” *Phys.Rev.Lett.* **44** (1980) 912.
- [31] **Super-Kamiokande Collaboration** Collaboration, Y. Fukuda *et al.*, “Evidence for oscillation of atmospheric neutrinos,” *Phys.Rev.Lett.* **81** (1998) 1562–1567, [hep-ex/9807003](#) [[hep-ex](#)].
- [32] **KamLAND Collaboration** Collaboration, S. Abe *et al.*, “Precision Measurement of Neutrino Oscillation Parameters with KamLAND,” *Phys.Rev.Lett.* **100** (2008) 221803, [0801.4589](#) [[hep-ex](#)].
- [33] **T2K Collaboration**, K. Abe *et al.*, “Indication of Electron Neutrino Appearance from an Accelerator-produced Off-axis Muon Neutrino Beam,” *Phys. Rev. Lett.* **107** (2011) 041801, [1106.2822](#) [[hep-ex](#)].
- [34] **MINOS Collaboration** Collaboration, P. Adamson *et al.*, “Improved search for muon-neutrino to electron-neutrino oscillations in MINOS,” *Phys.Rev.Lett.* **107** (2011) 181802, [1108.0015](#) [[hep-ex](#)].
- [35] **DOUBLE-CHOOZ Collaboration** Collaboration, Y. Abe *et al.*, “Indication for the disappearance of reactor electron antineutrinos in the Double Chooz experiment,” *Phys.Rev.Lett.* **108** (2012) 131801, [1112.6353](#) [[hep-ex](#)].
- [36] **DAYA-BAY Collaboration** Collaboration, F. An *et al.*, “Observation of electron-antineutrino disappearance at Daya Bay,” *Phys.Rev.Lett.* **108** (2012) 171803, [1203.1669](#) [[hep-ex](#)].
- [37] **RENO collaboration** Collaboration, J. Ahn *et al.*, “Observation of Reactor Electron Antineutrino Disappearance in the RENO Experiment,” *Phys.Rev.Lett.* **108** (2012) 191802, [1204.0626](#) [[hep-ex](#)].
- [38] G. L. Fogli, E. Lisi, A. Marrone, D. Montanino, A. Palazzo, and A. M. Rotunno, “Global analysis of neutrino masses, mixings and phases: entering the era of leptonic CP violation searches,” [1205.5254](#).
- [39] D. Forero, M. Tortola, and J. Valle, “Global status of neutrino oscillation parameters after Neutrino-2012,” [1205.4018](#) [[hep-ph](#)].
- [40] M. Gonzalez-Garcia, M. Maltoni, J. Salvado, and T. Schwetz, “Global fit to three neutrino mixing: critical look at present precision,” [1209.3023](#) [[hep-ph](#)].
- [41] C. Kraus, B. Bornschein, L. Bornschein, J. Bonn, B. Flatt, *et al.*, “Final results from phase II of the Mainz neutrino mass search in tritium beta decay,” *Eur.Phys.J.* **C40** (2005) 447–468, [hep-ex/0412056](#) [[hep-ex](#)].
- [42] **KATRIN Collaboration** Collaboration, A. Osipowicz *et al.*, “KATRIN: A Next generation tritium beta decay experiment with sub-eV sensitivity for the electron neutrino mass. Letter of intent,” [hep-ex/0109033](#) [[hep-ex](#)].
- [43] **WMAP Collaboration** Collaboration, E. Komatsu *et al.*, “Seven-Year Wilkinson Microwave Anisotropy Probe (WMAP) Observations: Cosmological Interpretation,” *Astrophys.J.Suppl.* **192** (2011) 18, [1001.4538](#) [[astro-ph.CO](#)].

- [44] M. Gonzalez-Garcia, M. Maltoni, and J. Salvado, “Robust Cosmological Bounds on Neutrinos and their Combination with Oscillation Results,” *JHEP* **1008** (2010) 117, [1006.3795 \[hep-ph\]](#).
- [45] I. Abt, M. F. Altmann, A. Bakalyarov, I. Barabanov, C. Bauer, *et al.*, “A New Ge-76 double beta decay experiment at LNGS: Letter of intent,” [hep-ex/0404039 \[hep-ex\]](#).
- [46] **EXO Collaboration** Collaboration, M. Auger *et al.*, “Search for Neutrinoless Double-Beta Decay in  $^{136}\text{Xe}$  with EXO-200,” *Phys.Rev.Lett.* **109** (2012) 032505, [1205.5608 \[hep-ex\]](#).
- [47] J. Schechter and J. Valle, “Neutrinoless Double beta Decay in  $\text{SU}(2) \times \text{U}(1)$  Theories,” *Phys.Rev.* **D25** (1982) 2951.
- [48] M. Duerr, M. Lindner, and A. Merle, “On the Quantitative Impact of the Schechter-Valle Theorem,” *JHEP* **1106** (2011) 091, [1105.0901 \[hep-ph\]](#).
- [49] **MEG collaboration** Collaboration, J. Adam *et al.*, “New limit on the lepton-flavour violating decay  $\mu^+ \rightarrow e^+ \gamma$ ,” *Phys.Rev.Lett.* **107** (2011) 171801, [1107.5547 \[hep-ex\]](#).
- [50] R. de Adelhart Toorop, F. Feruglio, and C. Hagedorn, “Finite modular groups and lepton mixing,” *Nucl.Phys. B* **858** (2012) 437–467, [1112.1340 \[hep-ph\]](#).
- [51] P. F. Harrison, D. H. Perkins, and W. G. Scott, “A redetermination of the neutrino mass-squared difference in tri-maximal mixing with terrestrial matter effects,” *Phys. Lett.* **B458** (1999) 79–92, [hep-ph/9904297](#).
- [52] P. F. Harrison, D. H. Perkins, and W. G. Scott, “Tri-bimaximal mixing and the neutrino oscillation data,” *Phys. Lett.* **B530** (2002) 167, [hep-ph/0202074](#).
- [53] P. F. Harrison and W. G. Scott, “Symmetries and generalisations of tri-bimaximal neutrino mixing,” *Phys. Lett.* **B535** (2002) 163–169, [hep-ph/0203209](#).
- [54] D. Hernandez and A. Y. Smirnov, “Lepton mixing and discrete symmetries,” *ArXiv e-prints* (2012) , [1204.0445 \[hep-ph\]](#).
- [55] C. Lam, “Finite Symmetry of Leptonic Mass Matrices,” [1208.5527 \[hep-ph\]](#).
- [56] N. Haba, A. Watanabe, and K. Yoshioka, “Twisted flavors and tri/bi-maximal neutrino mixing,” *Phys. Rev. Lett.* **97** (2006) 041601, [hep-ph/0603116](#).
- [57] X.-G. He and A. Zee, “Minimal Modification To The Tri-bimaximal Neutrino Mixing,” *Phys. Lett.* **B645** (2007) 427–431, [hep-ph/0607163](#).
- [58] W. Grimus and L. Lavoura, “A Model for trimaximal lepton mixing,” *JHEP* **0809** (2008) 106, [0809.0226 \[hep-ph\]](#).
- [59] H. Ishimori, Y. Shimizu, M. Tanimoto, and A. Watanabe, “Neutrino masses and mixing from  $S_4$  flavor twisting,” *Phys.Rev.* **D83** (2011) 033004, [1010.3805 \[hep-ph\]](#).
- [60] X.-G. He and A. Zee, “Minimal Modification to Tri-bimaximal Mixing,” *Phys.Rev.* **D84** (2011) 053004, [1106.4359](#).

- [61] S. Antusch, S. F. King, C. Luhn, and M. Spinrath, “Trimaximal mixing with predicted  $\theta_{13}$  from a new type of constrained sequential dominance,” *Nucl.Phys.* **B856** (2012) 328–341, 1108.4278 [hep-ph].
- [62] I. K. Cooper, S. F. King, and C. Luhn, “A4xSU(5) SUSY GUT of Flavour with Trimaximal Neutrino Mixing,” *JHEP* **1206** (2012) 130, 1203.1324 [hep-ph].
- [63] S. F. King and C. Luhn, “Trimaximal neutrino mixing from vacuum alignment in A4 and S4 models,” *JHEP* **1109** (2011) 042, 1107.5332 [hep-ph].
- [64] S. F. King and C. Luhn, “On the origin of neutrino flavour symmetry,” *JHEP* **0910** (2009) 093, 0908.1897 [hep-ph].
- [65] E. Ma and G. Rajasekaran, “Softly broken  $A_4$  symmetry for nearly degenerate neutrino masses,” *Phys. Rev. D* **64** (2001) 113012, hep-ph/0106291.
- [66] E. Ma, “ $A_4$  symmetry and neutrinos with very different masses,” *Phys. Rev. D* **70** (2004) 031901, hep-ph/0404199.
- [67] K. S. Babu, E. Ma, and J. W. F. Valle, “Underlying  $A_4$  symmetry for the neutrino mass matrix and the quark mixing matrix,” *Phys.Lett. B* **552** (2003) 207–213, hep-ph/0206292.
- [68] K. S. Babu and X.-G. He, “Model of Geometric Neutrino Mixing,” hep-ph/0507217.
- [69] G. Altarelli and F. Feruglio, “Tri-bimaximal neutrino mixing,  $A_4$  and the modular symmetry,” *Nucl.Phys. B* **741** (2006) 215–235, hep-ph/0512103.
- [70] S. Pakvasa and H. Sugawara, “Mass of the t Quark in SU(2) x U(1),” *Phys. Lett.* **B82** (1979) 105.
- [71] Y. Yamanaka, H. Sugawara, and S. Pakvasa, “Permutation Symmetries and the Fermion Mass Matrix,” *Phys. Rev.* **D25** (1982) 1895.
- [72] T. Brown, N. Deshpande, S. Pakvasa, and H. Sugawara, “CP Nonconservation and Rare Processes in S(4) Model of Permutation Symmetry,” *Phys. Lett.* **B141** (1984) 95.
- [73] T. Brown, S. Pakvasa, H. Sugawara, and Y. Yamanaka, “Neutrino Masses, Mixing and Oscillations in S(4) Model of Permutation Symmetry,” *Phys. Rev.* **D30** (1984) 255.
- [74] D.-G. Lee and R. N. Mohapatra, “An SO(10) x S(4) scenario for naturally degenerate neutrinos,” *Phys. Lett.* **B329** (1994) 463–468, hep-ph/9403201.
- [75] E. Ma, “Neutrino mass matrix from S(4) symmetry,” *Phys. Lett.* **B632** (2006) 352–356, hep-ph/0508231.
- [76] C. Hagedorn, M. Lindner, and R. Mohapatra, “S(4) flavor symmetry and fermion masses: Towards a grand unified theory of flavor,” *JHEP* **0606** (2006) 042, hep-ph/0602244 [hep-ph].
- [77] Y. Cai and H.-B. Yu, “An SO(10) GUT Model with S4 Flavor Symmetry,” *Phys. Rev.* **D74** (2006) 115005, hep-ph/0608022.

- [78] Y. Koide, “ $S_4$  Flavor Symmetry Embedded into SU(3) and Lepton Masses and Mixing,” *JHEP* **08** (2007) 086, 0705.2275 [hep-ph].
- [79] F. Bazzocchi and S. Morisi, “ $S_4$  as a natural flavor symmetry for lepton mixing,” *Phys. Rev.* **D80** (2009) 096005, 0811.0345 [hep-ph].
- [80] H. Ishimori, Y. Shimizu, and M. Tanimoto, “ $S_4$  Flavor Symmetry of Quarks and Leptons in SU(5) GUT,” *Prog. Theor. Phys.* **121** (2009) 769–787, 0812.5031 [hep-ph].
- [81] F. Bazzocchi, L. Merlo, and S. Morisi, “Phenomenological Consequences of See-Saw in  $S_4$  Based Models,” *Phys. Rev.* **D80** (2009) 053003, 0902.2849 [hep-ph].
- [82] G. Altarelli, F. Feruglio, and L. Merlo, “Revisiting Bimaximal Neutrino Mixing in a Model with  $S_4$  Discrete Symmetry,” *JHEP* **05** (2009) 020, 0903.1940 [hep-ph].
- [83] H. Ishimori, Y. Shimizu, and M. Tanimoto, “ $S_4$  Flavor Model of Quarks and Leptons,” *Prog. Theor. Phys. Suppl.* **180** (2010) 61–71, 0904.2450 [hep-ph].
- [84] W. Grimus, L. Lavoura, and P. O. Ludl, “Is  $S_4$  the horizontal symmetry of tri-bimaximal lepton mixing?,” *J. Phys.* **G36** (2009) 115007, 0906.2689 [hep-ph].
- [85] G.-J. Ding, “Fermion Masses and Flavor Mixings in a Model with  $S_4$  Flavor Symmetry,” *Nucl. Phys.* **B827** (2010) 82–111, 0909.2210 [hep-ph].
- [86] B. Dutta, Y. Mimura, and R. N. Mohapatra, “An SO(10) Grand Unified Theory of Flavor,” *JHEP* **05** (2010) 034, 0911.2242 [hep-ph].
- [87] G. Altarelli and F. Feruglio, “Discrete flavor symmetries and models of neutrino mixing,” *Reviews of Modern Physics* **82** (2010) 2701–2729, 1002.0211 [hep-ph].
- [88] H. Ishimori, T. Kobayashi, H. Ohki, Y. Shimizu, H. Okada, and M. Tanimoto, “Non-Abelian Discrete Symmetries in Particle Physics,” *Progress of Theoretical Physics Supplement* **183** (2010) 1–163, 1003.3552 [hep-th].
- [89] C. Luhn, S. Nasri, and P. Ramond, “Flavor group  $\Delta(3n^2)$ ,” *Journal of Mathematical Physics* **48** (2007) 073501, hep-th/0701188.
- [90] F. Bazzocchi and I. de Medeiros Varzielas, “Tribimaximal mixing in a viable family symmetry unified model with an extended seesaw mechanism,” *Phys. Rev. D* **79** (2009) 093001, 0902.3250 [hep-ph].
- [91] W. Grimus and L. Lavoura, “A model for trimaximal lepton mixing,” *JHEP* **9** (2008) 106, 0809.0226 [hep-ph].
- [92] I. de Medeiros Varzielas, S. F. King, and G. G. Ross, “Neutrino tri-bi-maximal mixing from a non-Abelian discrete family symmetry,” *Phys.Lett. B* **648** (2007) 201–206, hep-ph/0607045.
- [93] C. Luhn, S. Nasri, and P. Ramond, “Tri-bimaximal neutrino mixing and the family symmetry  $Z_7 \rtimes Z_3$ ,” *Phys.Lett. B* **652** (2007) 27–33, 0706.2341 [hep-ph].

- [94] C. Hagedorn, M. A. Schmidt, and A. Y. Smirnov, “Lepton Mixing and Cancellation of the Dirac Mass Hierarchy in SO(10) GUTs with Flavor Symmetries T(7) and Sigma(81),” *Phys.Rev.* **D79** (2009) 036002, 0811.2955 [hep-ph].
- [95] K. M. Parattu and A. Wingerter, “Tribimaximal Mixing From Small Groups,” *Phys.Rev.* **D84** (2011) 013011, 1012.2842 [hep-ph].
- [96] J. A. Escobar and C. Luhn, “The flavor group  $\Delta(6n^2)$ ,” *Journal of Mathematical Physics* **50** (2009) 013524, 0809.0639 [hep-th].
- [97] R. N. Mohapatra, M. K. Parida, and G. Rajasekaran, “High scale mixing unification and large neutrino mixing angles,” *Phys. Rev. D.* **69** (2004) 053007, hep-ph/0301234.
- [98] G.-J. Ding, “Fermion mass hierarchies and flavor mixing from T’ symmetry,” *Phys. Rev. D.* **78** (2008) 036011, 0803.2278 [hep-ph].
- [99] P. H. Frampton and S. Matsuzaki, “T’ predictions of PMNS and CKM angles,” *Phys.Lett. B* **679** (2009) 347–349, 0902.1140 [hep-ph].
- [100] P. H. Frampton and T. W. Kephart, “Flavor symmetry for quarks and leptons,” *JHEP* **9** (2007) 110, 0706.1186 [hep-ph].
- [101] A. Aranda, “Neutrino mixing from the double tetrahedral group T’,” *Phys. Rev. D.* **76** (2007) 111301, 0707.3661 [hep-ph].
- [102] P. D. Carr and P. H. Frampton, “Group Theoretic Bases for Tribimaximal Mixing,” hep-ph/0701034.
- [103] F. Feruglio, C. Hagedorn, Y. Lin, and L. Merlo, “Tri-bimaximal neutrino mixing and quark masses from a discrete flavour symmetry,” *Nucl.Phys. B* **775** (2007) 120–142, hep-ph/0702194.
- [104] M.-C. Chen and K. T. Mahanthappa, “CKM and tri-bimaximal MNS matrices in a  $SU(5) \times T(d)$  model,” *Phys.Lett. B* **652** (2007) 34–39, 0705.0714 [hep-ph].
- [105] B. A. Ovrut, “Isotropy Subgroups of SO(3) and Higgs Potentials,” *J.Math.Phys.* **19** (1978) 418.
- [106] G. Etesi, “Spontaneous symmetry breaking in SO(3) gauge theory to discrete subgroups,” *J.Math.Phys.* **37** (1996) 1596–1602, hep-th/9706029 [hep-th].
- [107] M. Koca, M. Al-Barwani, and R. Koc, “Breaking SO(3) into its closed subgroups by Higgs mechanism,” *J.Phys.A* **A30** (1997) 2109–2125.
- [108] M. Koca, R. Koc, and H. Tutunculer, “Explicit breaking of SO(3) with Higgs fields in the representations  $l = 2$  and  $l = 3$ ,” *Int.J.Mod.Phys. A* **18** (2003) 4817–4827, hep-ph/0410270 [hep-ph].
- [109] J. Berger and Y. Grossman, “Model of leptons from  $SO(3) \rightarrow A_4$ ,” *JHEP* **2** (2010) 71, 0910.4392 [hep-ph].
- [110] A. Adulpravitchai, A. Blum, and M. Lindner, “Non-Abelian discrete groups from the breaking of continuous flavor symmetries,” *JHEP* **9** (2009) 18, 0907.2332 [hep-ph].

- [111] W. Grimus and P. O. Ludl, “Finite flavour groups of fermions,” *J.Phys.* **A45** (2012) 233001, 1110.6376 [hep-ph].
- [112] C. Luhn, “Spontaneous breaking of SU(3) to finite family symmetries – a pedestrian’s approach,” *JHEP* **3** (2011) 108, 1101.2417 [hep-ph].
- [113] A. Merle and R. Zwicky, “Explicit and spontaneous breaking of SU(3) into its finite subgroups,” *JHEP* **2** (2012) 128, 1110.4891 [hep-ph].
- [114] G. Altarelli, F. Feruglio, and Y. Lin, “Tri-bimaximal neutrino mixing from orbifolding,” *Nucl. Phys.* **B775** (2007) 31–44, hep-ph/0610165.
- [115] A. Adulpravitchai, A. Blum, and M. Lindner, “Non-abelian discrete flavor symmetries from  $T^2/Z_N$  orbifolds,” *JHEP* **7** (2009) 53, 0906.0468 [hep-ph].
- [116] H. Abe, K.-S. Choi, T. Kobayashi, H. Ohki, and M. Sakai, “Non-Abelian Discrete Flavor Symmetries on Orbifolds,” *International Journal of Modern Physics A* **26** (2011) 4067–4082, 1009.5284 [hep-th].
- [117] T. Kobayashi, H. P. Nilles, F. Plöger, S. Raby, and M. Ratz, “Stringy origin of non-Abelian discrete flavor symmetries,” *Nucl.Phys. B* **768** (2007) 135–156, arXiv:hep-ph/0611020.
- [118] H. P. Nilles, M. Ratz, and P. K. S. Vaudrevange, “Origin of family symmetries,” *ArXiv e-prints* (2012) , 1204.2206 [hep-ph].
- [119] T. Araki, T. Kobayashi, J. Kubo, S. Ramos-Sánchez, M. Ratz, and P. K. S. Vaudrevange, “(Non-)Abelian discrete anomalies,” *Nucl.Phys. B* **805** (2008) 124–147, 0805.0207 [hep-th].
- [120] M. Honda and M. Tanimoto, “Deviation from tri-bimaximal neutrino mixing in  $A_4$  flavor symmetry,” *Prog. Theor. Phys.* **119** (2008) 583–598, 0801.0181 [hep-ph].
- [121] J. Barry and W. Rodejohann, “Neutrino Mass Sum-rules in Flavor Symmetry Models,” *Nucl.Phys.* **B842** (2011) 33–50, 1007.5217 [hep-ph].
- [122] B. Brahmachari, S. Choubey, and M. Mitra, “ $A_4$  flavor symmetry and neutrino phenomenology,” *Phys. Rev. D* **77** (2008) 073008, 0801.3554 [hep-ph].
- [123] A. de Gouvea and H. Murayama, “Neutrino Mixing Anarchy: Alive and Kicking,” *ArXiv e-prints* (2012) , 1204.1249 [hep-ph].
- [124] A. de Gouvêa and H. Murayama, “Statistical test of anarchy,” *Phys.Lett. B* **573** (2003) 94–100, arXiv:hep-ph/0301050.
- [125] L. Hall, H. Murayama, and N. Weiner, “Neutrino Mass Anarchy,” *Physical Review Letters* **84** (2000) 2572–2575, arXiv:hep-ph/9911341.
- [126] J. R. Espinosa, “Anarchy in the neutrino sector?,” *ArXiv High Energy Physics - Phenomenology e-prints* (2003) , arXiv:hep-ph/0306019.
- [127] G. Altarelli, F. Feruglio, I. Masina, and L. Merlo, “Repressing Anarchy in Neutrino Mass Textures,” *ArXiv e-prints* (2012) , 1207.0587 [hep-ph].



- [128] H.U.Besche, B.Eick, and E.O'Brien, *SmallGroups - library of all 'small' groups, GAP package, Version included in GAP 4.4.12*. The GAP Group, 2002.  
<http://www.gap-system.org/Packages/sgl.html>.
- [129] The GAP Group, *GAP – Groups, Algorithms, and Programming, Version 4.5.5*, 2012.  
<http://www.gap-system.org>).
- [130] Y. Lin, “Tri-bimaximal Neutrino Mixing from A(4) and theta(13) theta(C),” *Nucl.Phys.* **B824** (2010) 95–110, 0905.3534 [hep-ph].
- [131] S. F. King, “Parametrizing the lepton mixing matrix in terms of deviations from tri-bimaximal mixing,” *Phys. Lett.* **B659** (2008) 244–251, 0710.0530 [hep-ph].
- [132] S. Antusch and S. F. King, “Neutrino mixing from the charged lepton sector with sequential right-handed lepton dominance,” *Phys.Lett.* **B591** (2004) 104–112, [hep-ph/0403053](http://arxiv.org/abs/hep-ph/0403053) [hep-ph].
- [133] G. Altarelli, F. Feruglio, and I. Masina, “Can neutrino mixings arise from the charged lepton sector?,” *Nucl.Phys.* **B689** (2004) 157–171, [hep-ph/0402155](http://arxiv.org/abs/hep-ph/0402155) [hep-ph].
- [134] P. H. Frampton, S. T. Petcov, and W. Rodejohann, “On deviations from bimaximal neutrino mixing,” *Nucl.Phys. B* **687** (2004) 31–54, [arXiv:hep-ph/0401206](http://arxiv.org/abs/hep-ph/0401206).
- [135] A. Romanino, “Charged lepton contributions to the solar neutrino mixing and  $\theta_{13}$ ,” *Phys. Rev. D.* **70** (2004) 013003, [arXiv:hep-ph/0402258](http://arxiv.org/abs/hep-ph/0402258).
- [136] S. Antusch and S. F. King, “Charged lepton corrections to neutrino mixing angles and CP phases revisited,” *Phys.Lett.* **B631** (2005) 42–47, [hep-ph/0508044](http://arxiv.org/abs/hep-ph/0508044) [hep-ph].
- [137] R. Mohapatra and W. Rodejohann, “Broken mu-tau symmetry and leptonic CP violation,” *Phys.Rev.* **D72** (2005) 053001, [hep-ph/0507312](http://arxiv.org/abs/hep-ph/0507312) [hep-ph].
- [138] D. Marzocca, S. T. Petcov, A. Romanino, and M. Spinrath, “Sizeable  $\theta_{13}$  from the charged lepton sector in SU(5), (tri-)bimaximal neutrino mixing and Dirac CP violation,” *JHEP* **11** (2011) 9, 1108.0614 [hep-ph].
- [139] S. Antusch and V. Maurer, “Large neutrino mixing angle  $\theta_{13}^{MNS}$  and quark-lepton mass ratios in unified flavor models,” *Phys. Rev. D.* **84** (2011) 117301, 1107.3728 [hep-ph].
- [140] S. King, “Tri-bimaximal-Cabibbo Mixing,” 1205.0506 [hep-ph].
- [141] H. Georgi and C. Jarlskog, “A New Lepton - Quark Mass Relation in a Unified Theory,” *Phys.Lett.* **B86** (1979) 297–300.
- [142] S. Antusch and M. Spinrath, “New GUT predictions for quark and lepton mass ratios confronted with phenomenology,” *Phys.Rev.* **D79** (2009) 095004, 0902.4644 [hep-ph].
- [143] T. Feldmann, C. Pomberger, and S. Recksiegel, “Characterising New Physics Models by Effective Dimensionality of Parameter Space,” *Eur.Phys.J.* **C72** (2012) 1867, 1009.5283 [hep-ph].
- [144] M. A. Luty, “2004 TASI lectures on supersymmetry breaking,” [hep-th/0509029](http://arxiv.org/abs/hep-th/0509029) [hep-th].

- [145] F. Riva, “Low-Scale Leptogenesis and the Domain Wall Problem in Models with Discrete Flavor Symmetries,” *Phys.Lett.* **B690** (2010) 443–450, 1004.1177 [hep-ph].
- [146] H. Nagao and Y. Shimizu, “Realisability of SUSY discrete flavour symmetry in our universe,” *ArXiv e-prints* (2012) , 1206.0627 [hep-ph].
- [147] F. Feruglio, C. Hagedorn, and L. Merlo, “Vacuum Alignment in SUSY A4 Models,” *JHEP* **1003** (2010) 084, 0910.4058 [hep-ph].
- [148] G. Giudice and R. Rattazzi, “Theories with gauge mediated supersymmetry breaking,” *Phys.Rept.* **322** (1999) 419–499, hep-ph/9801271 [hep-ph].
- [149] S. Antusch, S. F. King, M. Malinsky, and G. G. Ross, “Solving the SUSY Flavour and CP Problems with Non-Abelian Family Symmetry and Supergravity,” *Phys.Lett.* **B670** (2009) 383–389, 0807.5047 [hep-ph].
- [150] C. Csaki, C. Delaunay, C. Grojean, and Y. Grossman, “A Model of Lepton Masses from a Warped Extra Dimension,” *JHEP* **0810** (2008) 055, 0806.0356 [hep-ph].
- [151] A. Kadosh and E. Pallante, “An  $A_4$  flavor model for quarks and leptons in warped geometry,” *JHEP* **8** (2010) 115, 1004.0321 [hep-ph].
- [152] A. Kadosh and E. Pallante, “CP violation and FCNC in a warped  $A_4$  flavor model,” *JHEP* **1106** (2011) 121, 1101.5420 [hep-ph].
- [153] K. S. Babu and S. Gabriel, “Semidirect Product Groups, Vacuum Alignment and Tribimaximal Neutrino Mixing,” *Phys. Rev.* **D82** (2010) 073014, 1006.0203.
- [154] J. Barry and W. Rodejohann, “Deviations from tribimaximal mixing due to the vacuum expectation value misalignment in  $A_4$  models,” *Phys. Rev. D* **81** (2010) 093002, 1003.2385 [hep-ph].
- [155] Y. Shimizu, M. Tanimoto, and A. Watanabe, “Breaking Tri-bimaximal Mixing and Large  $\theta_{13}$ ,” *Prog. Theor. Phys.* **126** (2011) 81–90, 1105.2929 [hep-ph].
- [156] S. Antusch, J. Kersten, M. Lindner, M. Ratz, and M. A. Schmidt, “Running neutrino mass parameters in see-saw scenarios,” *JHEP* **0503** (2005) 024, hep-ph/0501272.
- [157] M. Lattanzi and J. W. F. Valle, “Decaying warm dark matter and neutrino masses,” *Phys. Rev. Lett.* **99** (2007) 121301, 0705.2406 [astro-ph].
- [158] J. Schechter and J. W. F. Valle, “Neutrino masses in  $SU(2) \times U(1)$  theories,” *Phys. Rev. D* **22** (1980) 2227–2235.
- [159] J. Schechter and J. W. F. Valle, “Neutrino decay and spontaneous violation of lepton number,” *Phys. Rev. D* **25** (1982) 774–783.
- [160] M. Malinsky, J. Romao, and J. Valle, “Novel supersymmetric  $SO(10)$  seesaw mechanism,” *Phys.Rev.Lett.* **95** (2005) 161801, hep-ph/0506296 [hep-ph].
- [161] E. Ma and G. Rajasekaran, “Softly broken  $A_4$  symmetry for nearly degenerate neutrino masses,” *Phys. Rev. D* **64** (2001) 113012, hep-ph/0106291.

- [162] E. Ma, “Quark and Lepton Flavor Triality,” *Phys.Rev.* **D82** (2010) 037301, [1006.3524 \[hep-ph\]](#).
- [163] R. de Adelhart Toorop, F. Bazzocchi, L. Merlo, and A. Paris, “Constraining Flavour Symmetries At The EW Scale I: The A4 Higgs Potential,” *JHEP* **1103** (2011) 035, [1012.1791 \[hep-ph\]](#).
- [164] R. de Adelhart Toorop, F. Bazzocchi, L. Merlo, and A. Paris, “Constraining Flavour Symmetries At The EW Scale II: The Fermion Processes,” *JHEP* **1103** (2011) 040, [1012.2091 \[hep-ph\]](#).
- [165] E. Ma, “Verifiable radiative seesaw mechanism of neutrino mass and dark matter,” *Phys. Rev.* **D73** (2006) 077301, [hep-ph/0601225](#).
- [166] J. Kubo, E. Ma, and D. Suematsu, “Cold dark matter, radiative neutrino mass,  $\mu \rightarrow e\gamma$ , and neutrinoless double beta decay,” *Phys.Lett. B* **642** (2006) 18–23, [hep-ph/0604114](#).
- [167] F. Feruglio, C. Hagedorn, Y. Lin, and L. Merlo, “Lepton Flavour Violation in Models with A(4) Flavour Symmetry,” *Nucl.Phys.* **B809** (2009) 218–243, [0807.3160 \[hep-ph\]](#).
- [168] F. Borzumati and A. Masiero, “Large Muon and electron Number Violations in Supergravity Theories,” *Phys.Rev.Lett.* **57** (1986) 961.
- [169] F. Feruglio, C. Hagedorn, Y. Lin, and L. Merlo, “Lepton Flavour Violation in a Supersymmetric Model with A(4) Flavour Symmetry,” *Nucl.Phys.* **B832** (2010) 251–288, [0911.3874 \[hep-ph\]](#).
- [170] E. Ma and M. Raidal, “Neutrino mass, muon anomalous magnetic moment, and lepton flavor nonconservation,” *Phys.Rev.Lett.* **87** (2001) 011802, [hep-ph/0102255 \[hep-ph\]](#).
- [171] L. Lavoura, “General formulae for  $f_1 \rightarrow f_2$  gamma,” *Eur. Phys. J.* **C29** (2003) 191–195, [hep-ph/0302221](#).
- [172] **Particle Data Group** Collaboration, J. Beringer *et al.*, “Review of Particle Physics (RPP),” *Phys.Rev.* **D86** (2012) 010001.
- [173] **Muon G-2 Collaboration** Collaboration, G. Bennett *et al.*, “Final Report of the Muon E821 Anomalous Magnetic Moment Measurement at BNL,” *Phys.Rev.* **D73** (2006) 072003, [hep-ex/0602035 \[hep-ex\]](#).
- [174] F. Jegerlehner and A. Nyffeler, “The muon g-2,” *Phys.Rept.* **477** (2009) 1–110, [0902.3360 \[hep-ph\]](#).
- [175] E. Ma and M. Raidal, “Erratum: Neutrino Mass, Muon Anomalous Magnetic Moment, and Lepton Flavor Nonconservation [Phys. Rev. Lett. 87, 011802 (2001)],” *Physical Review Letters* **87** (2001) 159901, [arXiv:hep-ph/0102255](#).
- [176] B. Grzadkowski, M. Iskrzyński, M. Misiak, and J. Rosiek, “Dimension-six terms in the Standard Model Lagrangian,” *JHEP* **10** (2010) 85, [1008.4884 \[hep-ph\]](#).
- [177] K. Ichiki, M. Oguri, and K. Takahashi, “WMAP Constraints on Decaying Cold Dark Matter,” *Phys. Rev. Lett.* **93** (2004) 071302, [astro-ph/0403164](#).

- [178] Y. Gong and X. Chen, “Cosmological Constraints on Invisible Decay of Dark Matter,” *Phys. Rev.* **D77** (2008) 103511, 0802.2296 [astro-ph].
- [179] S. Palomares-Ruiz, “Model-Independent Bound on the Dark Matter Lifetime,” *Phys. Lett.* **B665** (2008) 50–53, 0712.1937 [astro-ph].
- [180] M. Cirelli, P. Panci, and P. D. Serpico, “Diffuse gamma ray constraints on annihilating or decaying Dark Matter after Fermi,” *Nucl. Phys.* **B840** (2010) 284–303, 0912.0663 [astro-ph.CO].
- [181] H. Davoudiasl, D. E. Morrissey, K. Sigurdson, and S. Tulin, “Baryon Destruction by Asymmetric Dark Matter,” 1106.4320.
- [182] T. Hambye, F. S. Ling, L. Lopez Honorez, and J. Rocher, “Scalar Multiplet Dark Matter,” *JHEP* **07** (2009) 090, 0903.4010 [hep-ph].
- [183] K. Griest and D. Seckel, “Three exceptions in the calculation of relic abundances,” *Phys.Rev.* **D43** (1991) 3191–3203.
- [184] S. Andreas, T. Hambye, and M. H. G. Tytgat, “WIMP dark matter, Higgs exchange and DAMA,” *JCAP* **0810** (2008) 034, 0808.0255 [hep-ph].
- [185] E. Aprile *et al.*, “Dark Matter Results from 100 Live Days of XENON100 Data,” *Phys.Rev.Lett.* **107** (2011) 131302, 1104.2549.
- [186] K. Griest, “Cross-Sections, Relic Abundance and Detection Rates for Neutralino Dark Matter,” *Phys.Rev.* **D38** (1988) 2357.
- [187] K. Griest, M. Kamionkowski, and M. S. Turner, “Supersymmetric Dark Matter Above the W Mass,” *Phys.Rev.* **D41** (1990) 3565–3582.
- [188] J. Baglio, A. Djouadi, and R. Godbole, “The apparent excess in the Higgs to di-photon rate at the LHC: New Physics or QCD uncertainties?,” *Phys.Lett.* **B716** (2012) 203–207, 1207.1451 [hep-ph].
- [189] T. Plehn and M. Rauch, “Higgs Couplings after the Discovery,” 1207.6108 [hep-ph].
- [190] “Coupling properties of the new Higgs-like boson observed with the ATLAS detector at the LHC,” Tech. Rep. ATLAS-CONF-2012-127, CERN, Geneva, Sep, 2012.
- [191] **CMS Collaboration** Collaboration, S. Chatrchyan *et al.*, “Search for a light charged Higgs boson in top quark decays in pp collisions at  $\sqrt{s} = 7$  TeV,” *JHEP* (2012) , 1205.5736 [hep-ex].
- [192] **ATLAS Collaboration** Collaboration, G. Aad *et al.*, “Search for charged Higgs bosons decaying via  $H^+ \rightarrow \tau \nu$  in top quark pair events using pp collision data at  $\sqrt{s} = 7$  TeV with the ATLAS detector,” *JHEP* **1206** (2012) 039, 1204.2760 [hep-ex].
- [193] M. Carena, I. Low, and C. E. Wagner, “Implications of a Modified Higgs to Diphoton Decay Width,” *JHEP* **1208** (2012) 060, 1206.1082 [hep-ph].

- [194] G. Bhattacharyya, P. Leser, and H. Pas, “Exotic Higgs boson decay modes as a harbinger of  $S_3$  flavor symmetry,” *Phys.Rev.* **D83** (2011) 011701, 1006.5597 [hep-ph].
- [195] Q.-H. Cao, S. Khalil, E. Ma, and H. Okada, “Observable  $T_7$  Lepton Flavor Symmetry at the Large Hadron Collider,” *Phys.Rev.Lett.* **106** (2011) 131801, 1009.5415.
- [196] Q.-H. Cao, A. Damanik, E. Ma, and D. Wegman, “Probing Lepton Flavor Triality with Higgs Boson Decay,” *Phys.Rev.* **D83** (2011) 093012, 1103.0008 [hep-ph].
- [197] G. Bhattacharyya, P. Leser, and H. Pas, “Novel signatures of the Higgs sector from  $S_3$  flavor symmetry,” *Phys.Rev.* **D86** (2012) 036009, 1206.4202 [hep-ph].
- [198] P. J. Fox, R. Harnik, J. Kopp, and Y. Tsai, “LEP Shines Light on Dark Matter,” *Phys.Rev.* **D84** (2011) 014028, 1103.0240 [hep-ph].
- [199] M. Chen and K. T. Mahanthappa, “Group theoretical origin of CP violation,” *Phys.Lett. B* **681** (2009) 444–447, 0904.1721 [hep-ph].
- [200] A. Meroni, S. Petcov, and M. Spinrath, “A SUSY  $SU(5)_xT$  Unified Model of Flavour with large  $\theta_{13}$ ,” 1205.5241 [hep-ph].
- [201] G. Branco, J. Gerard, and W. Grimus, “Geometrical T Violation,” *Phys.Lett.* **B136** (1984) 383.
- [202] I. de Medeiros Varzielas and D. Emmanuel-Costa, “Geometrical CP Violation,” *Phys.Rev.* **D84** (2011) 117901, 1106.5477 [hep-ph].
- [203] I. d. M. Varzielas, D. Emmanuel-Costa, and P. Leser, “Geometrical CP Violation from Non-Renormalisable Scalar Potentials,” *Phys.Lett.* **B716** (2012) 193–196, 1204.3633 [hep-ph].
- [204] I. d. M. Varzielas, “Geometrical CP violation in multi-Higgs models,” *JHEP* **1208** (2012) 055, 1205.3780 [hep-ph].
- [205] P. Ferreira, W. Grimus, L. Lavoura, and P. Ludl, “Maximal CP violation in lepton mixing from a model with  $\Delta(27)$  flavour symmetry,” 1206.7072 [hep-ph].
- [206] T. Lee, “A Theory of Spontaneous T Violation,” *Phys.Rev.* **D8** (1973) 1226–1239.
- [207] G. C. Branco, “Spontaneous CP Violation in Theories with More Than Four Quarks,” *Phys.Rev.Lett.* **44** (1980) 504.
- [208] G. Ecker, W. Grimus, and W. Konetschny, “Quark Mass Matrices in Left-Right Symmetric Gauge Theories,” *Nucl.Phys.* **B191** (1981) 465.
- [209] G. Ecker, W. Grimus, and H. Neufeld, “Spontaneous CP violation in left-right symmetric gauge theories,” *Nucl.Phys.* **B247** (1984) 70–82.
- [210] H. Neufeld, W. Grimus, and G. Ecker, “Generalized CP Invariance, Neutral Flavor Conservation and the Structure of the Mixing Matrix,” *Int.J.Mod.Phys.* **A3** (1988) 603–616.

- [211] W. Grimus and M. N. Rebelo, “Automorphisms in gauge theories and the definition of CP and P,” *Phys.Rept.* **281** (1997) 239–308, [arXiv:hep-ph/9506272](#).
- [212] P. Harrison and W. Scott, “ $\mu$  -  $\tau$  reflection symmetry in lepton mixing and neutrino oscillations,” *Phys.Lett.* **B547** (2002) 219–228, [hep-ph/0210197](#).
- [213] W. Grimus and L. Lavoura, “A Nonstandard CP transformation leading to maximal atmospheric neutrino mixing,” *Phys.Lett.* **B579** (2004) 113–122, [hep-ph/0305309](#) [[hep-ph](#)].
- [214] A. S. Joshipura, B. P. Kodrani, and K. M. Patel, “Fermion Masses and Mixings in a  $\mu$ - $\tau$  symmetric SO(10),” *Phys.Rev.* **D79** (2009) 115017, [0903.2161](#) [[hep-ph](#)].
- [215] W. Grimus and L. Lavoura, “ $\mu$ - $\tau$  Interchange symmetry and lepton mixing,” [1207.1678](#).
- [216] G. C. Branco, P. M. Ferreira, L. Lavoura, M. N. Rebelo, M. Sher, and J. P. Silva, “Theory and phenomenology of two-Higgs-doublet models,” *Phys.Rept.* **516** (2012) 1–102, [1106.0034](#) [[hep-ph](#)].
- [217] M. Gronau, A. Kfir, and R. Loewy, “Basis Independent Tests of CP Violation in Fermion Mass Matrices,” *Phys.Rev.Lett.* **56** (1986) 1538.
- [218] J. Bernabeu, G. Branco, and M. Gronau, “CP Restrictions on Quark Mass Matrices,” *Phys.Lett.* **B169** (1986) 243–247.
- [219] G. C. Branco, L. Lavoura, and M. N. Rebelo, “Majorana Neutrinos and CP violation in the leptonic sector,” *Phys. Lett.* **B180** (1986) 264.
- [220] P. M. Ferreira and L. Lavoura, “Seesaw neutrino masses from an  $S_4$  model with two equal vacuum expectation values,” *ArXiv e-prints* (2011) , [1111.5859](#) [[hep-ph](#)].
- [221] A. C. B. Machado, J. C. Montero, and V. Pleitez, “Three-Higgs-doublet model with A symmetry,” *Phys.Lett. B* **697** (2011) 318–322, [1011.5855](#) [[hep-ph](#)].
- [222] G. Isidori, Y. Nir, and G. Perez, “Flavor Physics Constraints for Physics Beyond the Standard Model,” *Ann.Rev.Nucl.Part.Sci.* **60** (2010) 355, [1002.0900](#) [[hep-ph](#)].
- [223] W. Skiba, “TASI Lectures on Effective Field Theory and Precision Electroweak Measurements,” *ArXiv e-prints* (2010) , [1006.2142](#) [[hep-ph](#)].
- [224] R. Barbieri and A. Strumia, “The ‘LEP paradox’,” *ArXiv High Energy Physics - Phenomenology e-prints* (2000) , [arXiv:hep-ph/0007265](#).
- [225] S. Weinberg, “Implications of Dynamical Symmetry Breaking,” *Phys.Rev.* **D13** (1976) 974–996.
- [226] S. Weinberg, “Implications of Dynamical Symmetry Breaking: An Addendum,” *Phys.Rev.* **D19** (1979) 1277–1280.
- [227] E. Gildener, “Gauge Symmetry Hierarchies,” *Phys.Rev.* **D14** (1976) 1667.

- [228] L. Susskind, “Dynamics of Spontaneous Symmetry Breaking in the Weinberg-Salam Theory,” *Phys.Rev.* **D20** (1979) 2619–2625.
- [229] e. ’t Hooft, Gerard, e. Itzykson, C., e. Jaffe, A., e. Lehmann, H., e. Mitter, P.K., and others”, “Recent Developments in Gauge Theories. Proceedings, Nato Advanced Study Institute, Cargese, France, August 26 - September 8, 1979”, “*NATO Adv.Study Inst.Ser.B Phys.*”, “**59**”, (1980,) ”1–438” ,.
- [230] W. A. Bardeen, “On naturalness in the standard model,”. Presented at the 1995 Ontake Summer Institute, Ontake Mountain, Japan, Aug 27 - Sep 2, 1995.
- [231] K. A. Meissner and H. Nicolai, “Effective Action, Conformal Anomaly and the Issue of Quadratic Divergences,” *Phys. Lett.* **B660** (2008) 260–266, [0710.2840 \[hep-th\]](#).
- [232] K. A. Meissner and H. Nicolai, “Conformal symmetry and the standard model,” *Phys. Lett.* **B648** (2007) 312–317, [hep-th/0612165](#).
- [233] K. A. Meissner and H. Nicolai, “Conformal invariance from non-conformal gravity,” *Phys. Rev.* **D80** (2009) 086005, [0907.3298 \[hep-th\]](#).
- [234] K. A. Meissner and H. Nicolai, “Renormalization Group and Effective Potential in Classically Conformal Theories,” [0809.1338 \[hep-th\]](#).
- [235] M. Shaposhnikov and D. Zenhausern, “Quantum scale invariance, cosmological constant and hierarchy problem,” *Phys. Lett.* **B671** (2009) 162–166, [0809.3406 \[hep-th\]](#).
- [236] R. Foot, A. Kobakhidze, K. L. McDonald, and R. R. Volkas, “A solution to the hierarchy problem from an almost decoupled hidden sector within a classically scale invariant theory,” *Phys. Rev.* **D77** (2008) 035006, [0709.2750 \[hep-ph\]](#).
- [237] N. Cabibbo, L. Maiani, G. Parisi, and R. Petronzio, “Bounds on the Fermions and Higgs Boson Masses in Grand Unified Theories,” *Nucl.Phys.* **B158** (1979) 295–305.
- [238] P. Q. Hung, “Vacuum Instability and New Constraints on Fermion Masses,” *Phys.Rev.Lett.* **42** (1979) 873.
- [239] M. Lindner, “Implications of Triviality for the Standard Model,” *Zeit. Phys.* **C31** (1986) 295.
- [240] L. J. Hall and Y. Nomura, “A Finely-Predicted Higgs Boson Mass from A Finely-Tuned Weak Scale,” *JHEP* **1003** (2010) 076, [0910.2235 \[hep-ph\]](#).
- [241] C. Froggatt and H. B. Nielsen, “Standard model criticality prediction: Top mass 173 +- 5-GeV and Higgs mass 135 +- 9-GeV,” *Phys.Lett.* **B368** (1996) 96–102, [hep-ph/9511371 \[hep-ph\]](#).
- [242] M. Shaposhnikov and C. Wetterich, “Asymptotic safety of gravity and the Higgs boson mass,” *Phys.Lett.* **B683** (2010) 196–200, [0912.0208 \[hep-th\]](#).
- [243] J. Casas, J. Espinosa, and M. Quiros, “Improved Higgs mass stability bound in the standard model and implications for supersymmetry,” *Phys.Lett.* **B342** (1995) 171–179, [hep-ph/9409458 \[hep-ph\]](#).

- [244] J. Casas, J. Espinosa, and M. Quiros, “Standard model stability bounds for new physics within LHC reach,” *Phys.Lett.* **B382** (1996) 374–382, [hep-ph/9603227](#) [[hep-ph](#)].
- [245] M. Sher, “Electroweak Higgs Potentials and Vacuum Stability,” *Phys. Rept.* **179** (1989) 273–418.
- [246] M. Lindner, M. Sher, and H. W. Zaglauer, “Probing Vacuum Stability Bounds at the Fermilab Collider,” *Phys. Lett.* **B228** (1989) 139.
- [247] G. Isidori, V. S. Rychkov, A. Strumia, and N. Tetradis, “Gravitational corrections to standard model vacuum decay,” *Phys.Rev.* **D77** (2008) 025034, [0712.0242](#) [[hep-ph](#)].
- [248] M. Chaichian, R. Gonzalez Felipe, and K. Huitu, “On quadratic divergences and the Higgs mass,” *Phys.Lett.* **B363** (1995) 101–105, [hep-ph/9509223](#).
- [249] M. Veltman, “The Infrared - Ultraviolet Connection,” *Acta Phys.Polon.* **B12** (1981) 437.
- [250] R. Decker and J. Pestieau, “Lepton Selfmass, Higgs Scalar and Heavy Quark Masses,” *Lett.Nuovo Cim.* **29** (1980) 560.
- [251] M. Baak, M. Goebel, J. Haller, A. Hoecker, D. Ludwig, *et al.*, “Updated Status of the Global Electroweak Fit and Constraints on New Physics,” [1107.0975](#) [[hep-ph](#)].
- [252] J. Ellis, J. R. Espinosa, G. F. Giudice, A. Hoecker, and A. Riotto, “The probable fate of the Standard Model,” *Phys.Lett. B* **679** (2009) 369–375, [0906.0954](#) [[hep-ph](#)].
- [253] K. Melnikov and T. v. Ritbergen, “The Three loop relation between the MS-bar and the pole quark masses,” *Phys.Lett.* **B482** (2000) 99–108, [hep-ph/9912391](#) [[hep-ph](#)].
- [254] F. Bezrukov, M. Y. Kalmykov, B. A. Kniehl, and M. Shaposhnikov, “Higgs boson mass and new physics,” [1205.2893](#) [[hep-ph](#)].
- [255] J. Elias-Miró, J. R. Espinosa, G. F. Giudice, G. Isidori, A. Riotto, and A. Strumia, “Higgs mass implications on the stability of the electroweak vacuum,” *Phys.Lett. B* **709** (2012) 222–228, [1112.3022](#) [[hep-ph](#)].
- [256] L. N. Mihaila, J. Salomon, and M. Steinhauser, “Gauge Coupling Beta Functions in the Standard Model to Three Loops,” *Phys.Rev.Lett.* **108** (2012) 151602, [1201.5868](#) [[hep-ph](#)].
- [257] K. G. Chetyrkin and M. F. Zoller, “Three-loop  $\beta$ -functions for top-Yukawa and the Higgs self-interaction in the standard model,” *JHEP* **6** (2012) 33, [1205.2892](#) [[hep-ph](#)].
- [258] G. Degrandi, S. Di Vita, J. Elias-Miro, J. R. Espinosa, G. F. Giudice, *et al.*, “Higgs mass and vacuum stability in the Standard Model at NNLO,” *JHEP* **1208** (2012) 098, [1205.6497](#) [[hep-ph](#)].
- [259] A. Hoang, “What Top Mass is Measured at the LHC ?.” Talk given at “[Strong interactions: From methods to structures](#)”, Bad Honnef, February 12 - 16, 2011.
- [260] U. Langenfeld, S. Moch, and P. Uwer, “Measuring the running top-quark mass,” *Phys.Rev.* **D80** (2009) 054009, [0906.5273](#) [[hep-ph](#)].



- [261] S. Alekhin, A. Djouadi, and S. Moch, “The top quark and Higgs boson masses and the stability of the electroweak vacuum,” *Phys.Lett.* **B716** (2012) 214–219, [1207.0980 \[hep-ph\]](#).
- [262] R. Hempfling, “The Next-to-Minimal Coleman-Weinberg Model,” *Phys. Lett.* **B379** (1996) 153–158, [hep-ph/9604278](#).
- [263] J. A. Casas, V. Di Clemente, and M. Quiros, “The standard model instability and the scale of new physics,” *Nucl. Phys.* **B581** (2000) 61–72, [hep-ph/0002205](#).
- [264] H. Nishino and S. Rajpoot, “Broken scale invariance in the standard model,” [hep-th/0403039](#).
- [265] J. R. Espinosa and M. Quiros, “Novel effects in electroweak breaking from a hidden sector,” *Phys. Rev.* **D76** (2007) 076004, [hep-ph/0701145](#).
- [266] W.-F. Chang, J. N. Ng, and J. M. S. Wu, “Shadow Higgs from a scale-invariant hidden U(1)s model,” *Phys. Rev.* **D75** (2007) 115016, [hep-ph/0701254](#).
- [267] R. Foot, A. Kobakhidze, and R. R. Volkas, “Electroweak Higgs as a pseudo-Goldstone boson of broken scale invariance,” *Phys. Lett.* **B655** (2007) 156–161, [0704.1165 \[hep-ph\]](#).
- [268] R. Foot, A. Kobakhidze, K. L. McDonald, and R. R. Volkas, “Neutrino mass in radiatively-broken scale-invariant models,” *Phys. Rev.* **D76** (2007) 075014, [0706.1829 \[hep-ph\]](#).
- [269] T. Hambye and M. H. G. Tytgat, “Electroweak Symmetry Breaking induced by Dark Matter,” *Phys. Lett.* **B659** (2008) 651–655, [0707.0633 \[hep-ph\]](#).
- [270] K. A. Meissner and H. Nicolai, “Neutrinos, Axions and Conformal Symmetry,” *Eur. Phys. J.* **C57** (2008) 493–498, [0803.2814 \[hep-th\]](#).
- [271] S. Iso, N. Okada, and Y. Orikasa, “Classically conformal  $B-L$  extended Standard Model,” *Phys. Lett.* **B676** (2009) 81–87, [0902.4050 \[hep-ph\]](#).
- [272] S. Iso, N. Okada, and Y. Orikasa, “The minimal B-L model naturally realized at TeV scale,” *Phys.Rev.* **D80** (2009) 115007, [0909.0128 \[hep-ph\]](#).
- [273] R. N. Mohapatra and J. C. Pati, “Left-Right Gauge Symmetry and an Isoconjugate Model of CP Violation,” *Phys. Rev.* **D11** (1975) 566–571.
- [274] G. Senjanovic and R. N. Mohapatra, “Exact Left-Right Symmetry and Spontaneous Violation of Parity,” *Phys. Rev.* **D12** (1975) 1502.
- [275] E. Gildener and S. Weinberg, “Symmetry Breaking and Scalar Bosons,” *Phys. Rev.* **D13** (1976) 3333.
- [276] S. R. Coleman and E. Weinberg, “Radiative Corrections as the Origin of Spontaneous Symmetry Breaking,” *Phys. Rev.* **D7** (1973) 1888–1910.
- [277] N. G. Deshpande, J. F. Gunion, B. Kayser, and F. I. Olness, “Left-right symmetric electroweak models with triplet Higgs,” *Phys. Rev.* **D44** (1991) 837–858.

- [278] **ATLAS Collaboration** Collaboration, G. Aad *et al.*, “Search for heavy neutrinos and right-handed W bosons in events with two leptons and jets in pp collisions at  $\sqrt{s} = 7$  TeV with the ATLAS detector,” *Eur.Phys.J.* **C72** (2012) 2056, [1203.5420 \[hep-ex\]](#).
- [279] **ATLAS Collaboration** Collaboration, G. Aad *et al.*, “Search for a heavy gauge boson decaying to a charged lepton and a neutrino in 1 fb<sup>-1</sup> of pp collisions at  $\sqrt{s} = 7$  TeV using the ATLAS detector,” *Phys.Lett.* **B705** (2011) 28–46, [1108.1316 \[hep-ex\]](#).
- [280] **CMS Collaboration** Collaboration, “Search for a heavy neutrino and right-handed W of the left-right symmetric model in pp collisions at  $\sqrt{s} = 7$  TeV,”.
- [281] F. Xu, H. An, and X. Ji, “Neutron Electric Dipole Moment Constraint on Scale of Minimal Left-Right Symmetric Model,” *JHEP* **1003** (2010) 088, [0910.2265 \[hep-ph\]](#).
- [282] D. Guadagnoli and R. N. Mohapatra, “TeV Scale Left Right Symmetry and Flavor Changing Neutral Higgs Effects,” *Phys.Lett.* **B694** (2011) 386–392, [1008.1074 \[hep-ph\]](#).
- [283] K. A. Meissner and H. Nicolai, “A 325 GeV scalar resonance seen at CDF?,” [1208.5653 \[hep-ph\]](#).
- [284] **CDF Collaboration** Collaboration, T. Aaltonen *et al.*, “Search for high-mass resonances decaying into  $ZZ$  in  $p\bar{p}$  collisions at  $\sqrt{s} = 1.96$  TeV,” *Phys.Rev.* **D85** (2012) 012008, [1111.3432 \[hep-ex\]](#).
- [285] P. M. van Den Broek and J. F. Cornwell, “Clebsch-Gordan coefficients of symmetry groups,” *Physica Status Solidi (B)* **90** (1978) 211–224.
- [286] I. de Medeiros Varzielas, S. King, and G. Ross, “Tri-bimaximal neutrino mixing from discrete subgroups of SU(3) and SO(3) family symmetry,” *Phys.Lett.* **B644** (2007) 153–157, [hep-ph/0512313 \[hep-ph\]](#).
- [287] V. Dabbaghian, *REPSN - for constructing representations of finite groups*, GAP package, Version 3.0.2. The GAP Group, 2011. <http://www.gap-system.org/Packages/repsn.html>.